Advanced Characterisation of Hot Mix Asphalt with Recycled Crushed Glass

by

Theresa Bernadette George

Thesis presented in partial fulfillment of the requirement for the degree of Master of Engineering in Civil Engineering in the Faculty of Engineering at Stellenbosch University

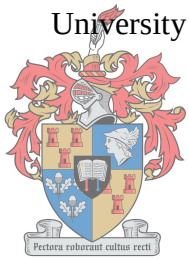

Department of Civil Engineering
Stellenbosch University
Private Bag
X1 Matieland
7602 South
Africa

Supervisor: Prof. K.J. Jenkins
Co-Supervisors: Dr. J.K. Anochie-Boateng
Assoc. Prof. ir. M.F.C. van de Ven

December 2018

DECLARATION

By submitting this dissertation, I declare that the entirety of the work contained therein is my own, original work, that I am the sole author thereof (save to the extent explicitly otherwise stated), that reproduction and publication thereof by Stellenbosch University will not infringe any third party rights and that I have not previously in its entirety or in part submitted it for obtaining any qualification.

Signature:

Date:

ABSTRACT

Over the last few decades, the use of glass in pavement applications has been implemented by various countries in the international community. South Africa, however, on average generates roughly 900 000 tonnes of domestic waste glass each year and has made little use of this readily available raw material. More recently, with national policies mandating the reuse, recycling and minimisation of domestic waste, in addition with several economic and environmental benefits, it is expected that the use of alternative materials, e.g. recycled glass, in road construction will increase.

Depending on the application, the uses of recycled glass in road construction vary widely. This study investigates the engineering performance of Hot Mix Asphalt (HMA) incorporating locally available recycled crushed glass for use in the wearing course of South African pavements. The study contributes to current research at the Council for Scientific and Industrial Research (CSIR) which aims to optimise the design, construction and maintenance of roads through the use of cost-effective and sustainable materials that include waste materials.

A continuously-graded asphalt mix with a glass replacement ratio of 15% and 50/70 penetration grade bitumen was designed for a traffic level of 3 to 30 million E80s. The mix design was conducted according to the current method for traditional asphalt mixes in South Africa. The results indicate that the glass-asphalt mix conforms to the South African mix design criteria.

Furthermore, the moisture susceptibility of the glass-asphalt mix was evaluated with and without the use of anti-stripping additives. The standard Tensile Strength Ratio parameter supported with a microscopic imaging technique and an analytical modelling method were used to evaluate and quantify the resistance of the glass-asphalt mix to moisture damage. Analysis of the results reveal that an antistripping additive is essential to meet moisture susceptibility criteria and alleviate stripping for the investigated source and grading of glass particles, at a glass content of 15%.

The study also assesses and compares the stiffness and permanent deformation properties of the glass-asphalt mix to a traditional continuously-graded asphalt wearing course mix, typically used for road construction in South Africa. Selected mathematical models were used to

effectively characterise the deformation and stiffness behaviour of the mixes. The glass-asphalt mix shows increased stiffness and improved resistance to permanent deformation at elevated temperatures.

Additionally, a multi-layer linear-elastic analysis is used to assess the influence of temperature and loading frequency variation on the structural capacity of the glass-asphalt and HMA surfacing layers. The analysis reveals that the structural capacity of both surfacing layers are comparable at intermediate temperatures, for both high and low loading frequencies.

The findings of this study reveal that improved performance could potentially be achieved with the use of recycled crushed glass in continuously-graded asphalt wearing course mixes in South Africa.

DEDICATION

To my husband for his continuous love and support

ACKNOWLEDGEMENTS

I wish to express my gratitude to the following organisations and individuals who assisted and supported me during this research study:

1. Prof. K.J. Jenkins, Supervisor - Stellenbosch University; for his guidance and support during the study.
2. Dr. J.K. Anochie-Boateng, Co-supervisor and Project Leader of the CSIR's project on glass-asphalt development; for his guidance and support during the study.
3. Assoc. Prof. ir. M.F.C. van de Ven, Co-supervisor - TU Delft; for his guidance and support during the study.
4. The Council for Scientific and Industrial Research (CSIR) through its R&D office for funding this research through Parliamentary Grant (PG) Funding - PG project B1iE201:002.
5. CSIR Pavement Materials and Testing Laboratory staff, in particular Mr. Nnditsheni Mpofu and Mr. Ngwako Maake, for their assistance during the study.
6. My colleagues in the Pavement Design and Construction research group for valuable discussions held during the study.
7. Mr. Benoit Verhaeghe, Pavement Design and Construction competency area manager - CSIR; for his assistance and support during the study.
8. Dr. Martin Mgangira, Pavement Design and Construction research group leader - CSIR; for his support during the study.
9. Much Asphalt, AfriSam and Consol for providing me with the necessary raw materials required to conduct the study.
10. My family, most especially my husband and my mom, for helping me with Zion.
11. My husband for his continuous support throughout my Masters study.
12. Above all, my Heavenly Father, for His wisdom, strength and guidance throughout my Masters study.

LIST OF ABBREVIATIONS

AASHTO	- American Association of State Highway and Transportation Officials
AMPT	- Asphalt Mixture Performance Tester
ASTM	- American Society of Testing Materials
BD	- Bulk Density
CSIR	- Council for Scientific and Industrial research
FAA	- Fine Aggregate Angularity
GHG	- Greenhouse Gas Emissions
HMA	- Hot Mix Asphalt
HWTT	- Hamburg Wheel Tracking Test
ITS	- Indirect Tensile Strength
LVE	- Linear-Viscoelastic
MPS	- Maximum Particle Size
MVD	- Maximum Voidless Density
NEM: WA	- National Environmental Management: Waste Act
NEMA	- National Environmental Management Act
NMPS	- Nominal Maximum Particle Size
NWMS	- National Waste Management Strategy
PRO	- Producer Responsibility Organisation
R&D	- Research and Development
RTFOT	- Rolling Thin Film Oven Test
SANRAL	- South African National Roads Agency Limited
SANS	- South African National Standards
SAPDM	- South African Pavement Design Method
SEM	- Scanning Electron Microscopy
SHRP	- Strategic Highway Research Program
TGRC	- The Glass Recycling Company
TSR	- Tensile Strength Ratio
VFB	- Voids Filled with Binder
VIM	- Voids in Mix
VMA	- Voids in Mineral Aggregate
XRD	- X-Ray Diffraction
XRF	- X-Ray Fluorescence

TABLE OF CONTENTS

LIST OF TABLES

LIST OF FIGURES

1. INTRODUCTION

1.1 Background

The National Environmental Management: Waste Act (Act 59 of 2008) commits National Government to, amongst others, promote "waste minimisation, reuse, recycling and recovery of waste" in South Africa. However, national waste information obtained in 2011 indicates that an estimated 70% (approx. 650,000 tonnes) of waste glass generated in South Africa was landfilled, while only 30% was recycled**.** This data highlights that a substantial amount of waste glass could, therefore, potentially be diverted from landfill and recovered to be recycled or reused.

Additionally, considerable quantities of recycled crushed glass fines (less than 5 mm), accumulate as stockpiles at glass packaging manufacturing plants in Gauteng and the Western Cape provinces of South Africa. These processed glass fines, which are unusable in the glass packaging manufacturing process, are stockpiled and earmarked for disposal to landfill; thereby contributing to the waste glass that is currently being landfilled. This further adds undue pressure on rapidly depleting landfill airspace and has led to the necessity for adopting sustainable practices. Waste glass that is recovered to be recycled or re-used is a key component in this.

The pavement industry, amongst others, can provide a number of alternative uses for this recovered waste glass. One such use is where crushed waste glass can be used as a material substitute in asphalt pavements, which will provide a more cost effective and environmentally friendly solution to disposal and will add value to this otherwise waste material.

The use of crushed glass in Hot Mix Asphalt (HMA) paving applications has been widely implemented in the United States and Canada since the early 1970's. Other countries that have reported using crushed glass in asphalt paving applications include United Kingdom, Australia, New Zeland, Japan and Taiwan (Yamanaka et al., 2001; Su & Chen, 2002; Dane County Department of Public Works, 2003; Arnold et al., 2008; Australian government Department of Sustainability, Environment, Water Population and Communities, 2011; Andela & Sorge, n.d.).

Early applications of crushed glass in asphalt pavements in the United States incorporated glass particles greater than 12.5 mm with quantities in excess of 25%. The application of coarse glass particles (≥ 5 mm) in large quantities was considered to be a major contributing factor to the stripping and ravelling problems reported in early glass-asphalt pavement applications.

More recently, 10 to 15% crushed glass has been specified for use in asphalt wearing courses in the United States; while some countries, e.g. New Zealand, utilise as little as 5% glass content in asphalt base courses. Various studies have shown that improved performance, in terms of permanent deformation, has been obtained for HMA pavements incorporating up to 15% crushed glass using both fine and coarse graded glass particles with a maximum particle size of up to 9.5 mm**.** Furthermore, recommendations on the inclusion of antistripping additives and their relevance in resisting moisture induced damage in glass-asphalt mixes have been based specifically on the grading of the glass particles utilised in combination with specific types of coarse and fine aggregates common to a particular region or country.

In South Africa, however, minimal research has been conducted on the viability of using recycled crushed glass in asphalt pavement applications. Research is, therefore, needed to characterise the performance of locally available recycled crushed glass in asphalt pavements in South Africa. In this regard, the interaction of the glass particles in combination with conventional materials typically used for asphalt production in South Africa, and its effect on asphalt mix performance, requires investigation.

Investigations in this regard will contribute towards developing innovations to address "waste minimisation, re-use, recycling and recovery of waste", whilst simultaneously developing solutions to maintain or otherwise improve the performance of asphalt pavements in South Africa. In addition, recycling waste glass for use as a secondary material in pavement applications will contribute towards stimulating a regional secondary resources economy with potential for industrial development and creation of sustainable jobs.

1.2 Problem Statement

There is currently a gap in existing knowledge on the engineering performance of recycled crushed glass in South African asphalt mixes. Nominal research has been conducted in South Africa on the suitability of locally available recycled crushed glass as a substitute for asphalt aggregates currently used and the associated engineering performance properties of asphalt mixes incorporating recycled crushed glass.

Furthermore, current entrenched asphalt mix design methods and specifications in South Africa have limited the use of alternative material design practices resulting in the use of expensive materials, e.g. highly modified bituminous binder, to achieve the required pavement performance. In many cases, such materials are specified too easily before exploring other pioneering material design alternatives.

Therefore, there is a need to investigate the effectiveness of recycled crushed glass as a substitute material in South African asphalt mixes that will maintain or otherwise improve pavement performance. The findings of the investigation can further be documented as guidelines and incorporated into future mix design methods and specifications for South Africa.

1.3 Research Goal and Objectives

1.3.1. Research Goal

The goal of this study is to determine the influence of recycled crushed glass on the engineering performance of a continuously-graded asphalt wearing course mix.

1.3.2. Research Objectives

To achieve the research goal, the following objectives were developed:

- Mix design and production of a medium continuously-graded asphalt wearing course mix consisting of 15% recycled crushed glass.
- Evaluate the stripping potential of the glass-asphalt mix with and without the use of local anti-stripping additives.
- Compare the stiffness and deformation properties of the glass-asphalt mix and a traditional asphalt wearing course mix commonly used for road construction in South Africa.

- Characterise the deformation and linear visco-elastic behaviour of the glass-asphalt mix using selected mathematical models.

1.4 Research Scope

The scope of this study includes the following:

- Review of available literature on the utilisation of crushed glass in HMA.
- Conduct survey to identify possible sources of crushed waste glass in South Africa.
- Procurement of constituent materials for glass-asphalt mix design and production.
- Development (design and production) of glass-asphalt mix.
- Conduct series of laboratory tests to determine the physical and engineering properties of glass-asphalt mix.
- Data processing and analysis of laboratory test results for performance evaluation and comparison.

1.5 Outline of Dissertation

This dissertation is presented as follows:

Chapter 1 provides the background and need for the study and highlights the objectives and scope of the study undertaken.

Chapter 2 provides a literature review on studies conducted on the utilisation of crushed glass in HMA and its effect on the laboratory as well as in-situ performance properties of glass-asphalt mixes. An overview on the global utilisation of crushed glass in asphalt pavement applications is also provided.

Chapter 3 presents the design and production of a continuously-graded glass-asphalt mix and discusses the volumetric properties of the mix in relation with criteria set out for traditional continuously-graded asphalt mixes in South Africa. A review on the physical characteristics of the locally available recycled crushed glass material is also presented.

Chapter 4 presents the selection of the optimum glass-asphalt mix based on an evaluation on the degree of moisture susceptibility of the mix with and without the addition of selected

antistripping additives. The moisture damage evaluation is discussed relative to South African standard requirements.

Chapter 5 presents a comparison of the stiffness and permanent deformation properties of the glass-asphalt mix and a traditional asphalt mix. Furthermore, an evaluation on the use of selected constitutive models namely, Kelvin, Burger's and Huet-Sayegh to effectively characterise the linear visco-elastic behaviour of the glass-asphalt mix over a wide range of temperatures and loading frequencies is presented. Similarly, the use of selected mathematical models namely, power model, Wilshire and Evans model, polynomial model and Francken model, to effectively evaluate the permanent deformation behaviour of the glass-asphalt mix is presented.

Chapter 6 presents a multi-layer linear-elastic analysis of the glass-asphalt surfacing layer within a typical pavement structure of ES10 and ES30 design structural capacity. The effects of temperature and loading frequency variation on the stress-strain behaviour as well as the structural capacity of the glass-asphalt surfacing layer overlying a high and low strength supporting base layer is assessed.

Chapter 7 provides the conclusions and recommendations of the study.

2. LITERATURE STUDY

2.1 Introduction

2.1.1 Domestic Waste Glass

According to the National Waste Information Baseline Report (Department of Environmental Affairs, 2012), more than 900,000 tonnes of domestic waste glass is assessed to have been produced in South Africa in 2011. This comprises of approximately 4% of the general waste stream in South Africa for the 2011 year (Department of Environmental Affairs, 2012). See Figure 2-1. Of this waste, approximately 30% was recycled and the remaining 70% disposed at landfill (Department of Environmental Affairs, 2012). A substantial amount of domestic waste glass could, therefore, potentially be diverted from landfill and recovered to be recycled or reused.

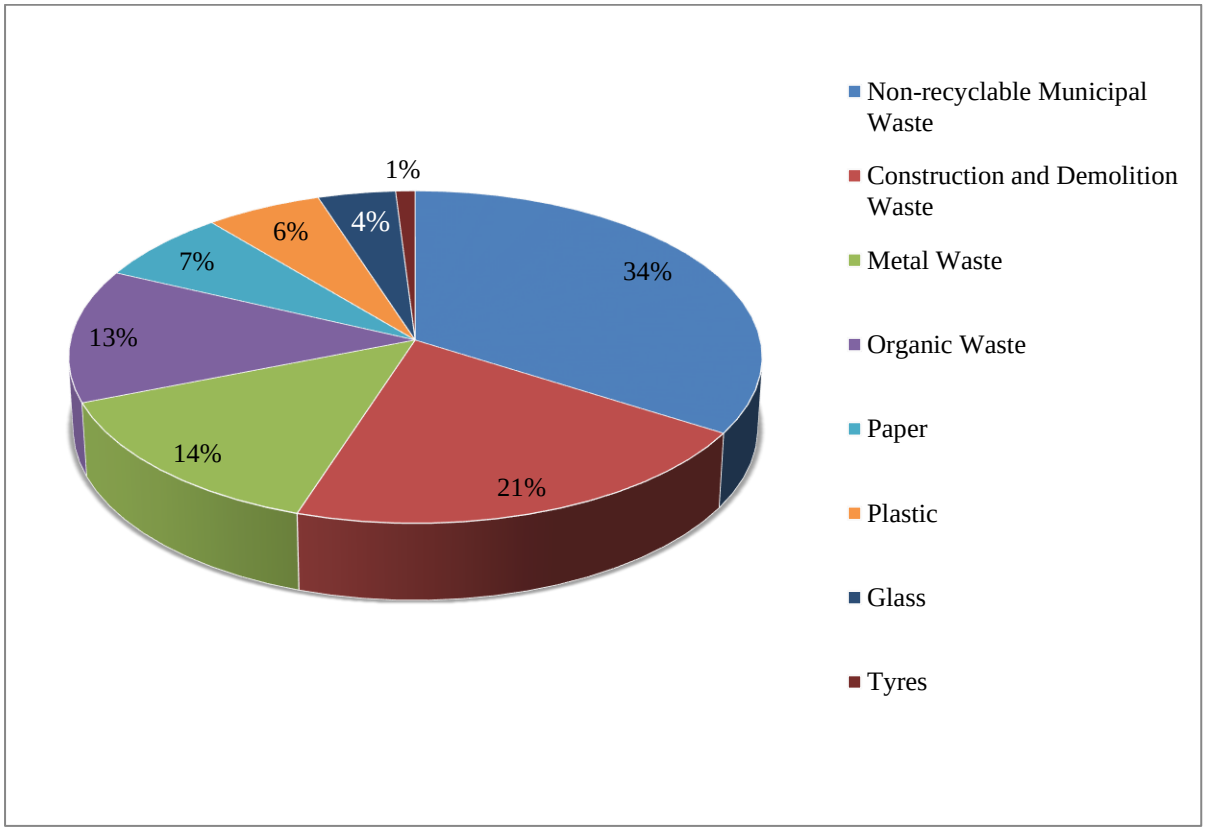

Figure 2-1: General waste composition, 2011 (percentage by mass) (Department of Environmental Affairs, 2012)

2.1.2 Domestic Waste Glass Management in South Africa

The legislative framework for waste management in South Africa stems from Section 24 of the Constitution, which commits "to secure an environment that is not harmful to the health and well-being of the people of South Africa" (Department of Environmental Affairs, 2012). The legislation which has been promulgated through Parliament to establish and promote this is the National Environmental Management Act (No. 107 of 1998) (NEMA) and the National Environmental Management: Waste Act (No. 59 of 2008) (NEM: WA).

The NEM: WA establishes, amongst others, the following objectives with regards to waste management in South Africa (Department of Environmental Affairs, 2012):

- "Minimise the consumption of natural resources,
- Avoid and minimise the generation of waste,
- Reduce, re-use, recycle and recover waste".

Furthermore, the NEMA and NEM: WA have led to the development of the National Waste Management Strategy (NWMS) (2011), which directs local municipalities to develop alternative waste management processes, as one of their main objectives, to ensure diversion of waste sent to landfills (Department of Environmental Affairs, 2012).

A few municipalities have begun to address this objective by promoting separation of waste at source initiatives, which makes use of different waste collection bags for general waste and recyclable waste, which can then be collected for recycling. One of the leaders in implementing this initiative is the Ethekwini municipality in KwaZulu Natal, who to date have 1 million homes involved and contributing to the initiative, and hence seem well established for improving their waste glass collection figures.

In spite of the fact that recycling is enacted within South Africa, most recycling exercises are generally determined by the industry through the foundation of industry bodies or Producer Responsibility Organisations (PRO). PRO's are non-profit organisations supported by the industry to advance the recovery and recycling of waste materials in South Africa.

One such PRO is The Glass Recycling Company (TGRC), which is responsible for promoting / supporting and enabling the recovery and recycling of waste glass. The TGRC is supported by the Department of Environmental Affairs, and since its establishment in 2006, South Africa

has seen a considerable increase in the recycling rate of glass packaging, which has increased from just 18% in 2005/06 to 41.1% in 2015/16.

Some of the initiatives implemented by the TGRC include the installation of over 2000 glass banks, which are placed in various locations in communities and are intended for members of the public to have easy access to waste glass deposit points where glass can be deposited for recycling. The TGRC also provides an SMS service for members of the public who are interested in finding their nearest glass bank.

Another initiative by the TGRC allows members of the public, who are mostly from previously disadvantaged backgrounds, to establish buy-back centres, where glass can be collected for recycling. Equipment to establish such centres is provided by the TGRC and the buy-back centres in turn provide a source of income to jobless members of the public who form the majority of waste glass collectors.

In addition to the initiatives mentioned, South Africa has also established a glass returnable deposit system, which is a large scale initiative and sees a mandatory deposit fee being charged on consumers who purchase returnable glass bottles. This fee is reimbursed to consumers upon return of the bottles to retail outlets, and the retailers in turn send the returned bottles back to the bottle supplier, who may then clean and re-use or recycle the returned bottles.

Notwithstanding the objectives from the NEM: WA as well as recycling initiatives undertaken by industry bodies, the shortage of landfill airspace as well the ever increasing cost of raw materials warrants development and expansion of the recycling industry in South Africa. Furthermore the various green economy policies and strategies also have a positive spin off on job creation within the country.

2.1.3 Sources of Recycled Crushed Glass in South Africa

A survey of the major consumers in the waste glass market in South Africa was conducted during the course of this study. At present there is only one well established market for recovered domestic waste glass in the country; which is the glass packaging industry. The survey population thus included two leading glass packaging manufacturing companies as well as other major collectors of domestic waste glass.

Numerous established collectors of domestic waste glass in the Gauteng province were contacted telephonically to enquire about their waste glass collection operations. It was indicated by all the facilities that the collected waste glass is merely sold as is collected (broken or whole bottles) and is not processed i.e. colour sorted, crushed, cleaned etc. Furthermore, it was indicated that majority of the collected waste glass is sold to two of South Africa's leading glass manufacturing companies - Nampak Wiegand Glas and Consol. These companies are the only two glass manufacturers in South Africa that utilise recycled waste glass to manufacture new glass containers. Nampak Wiegand Glass has one plant located in Gauteng and Consol has two plants located in Gauteng and in the Cape Peninsula.

Other than the above two manufacturers, it is believed that there are a large number of small organisations involved in the recycling of waste glass in South Africa. An example of one such organisation is a company in Cape Town, whose primary business is the recycling of float glass into crushed glass for use in aggregate applications. Since companies of this nature are only capable of low production rates of glass aggregate, a stable supply of sufficiently sized stockpiles cannot be guaranteed. It was, therefore, decided to contact only Nampak Wiegand Glass and Consol to get an indication of their recycling processes.

It was indicated by the glass manufacturing companies that the plants utilise state-of-the-art technology that is able to automatically separate the waste glass according to colour and size, remove any deleterious materials from the waste glass and cleans it as a final step, making it ready for further use downstream in the production of new glass products.

Both companies have, however, indicated that a significant amount of the processed glass in the form of fines (less than 5mm) that cannot be used in the glass packaging manufacturing process accumulates as stockpiles at their processing plants. In addition, the recycled crushed glass fines were observed to be relatively free of contaminants such as paper, plastic, dirt debris as well as materials such as lead, arsenic, or similar toxic or hazardous metals.

Nampak Wiegand Glass and Consol have indicated that availability of this material is approximately 1,000 and 3,000 tons per month respectively. Furthermore, it was indicated by Consol that approximately R 3 million per annum is accounted for the disposal and transportation of the waste glass to landfill sites (Moloi, 2015). Figure 2-2 illustrates the recycling process implemented at the Consol manufacturing plant.

An alternative application can be proposed whereby the waste glass can be used as an aggregate substitution in pavement construction which will provide a more cost effective and environmentally friendly solution to disposal. The possibility of using waste glass in pavement applications can be seen a sustainable alternative to natural aggregates, especially since good quality aggregates are scarce and glass cullet (crushed glass) as a raw material has no associated financial costs currently in South Africa.

1. Off-loading and stockpiling of glass bottles

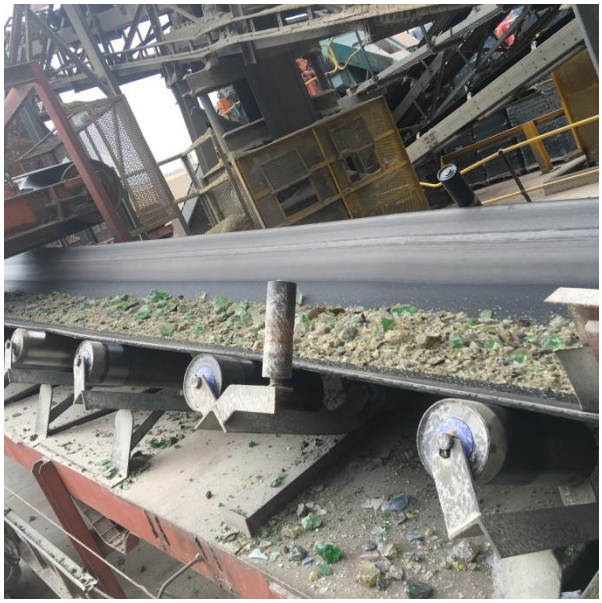

2. Glass bottle insertion and primary crushing

3. Primary Separation: Conveyor equipped with separation technology

4. Secondary separation

5. Secondary crushing and particle size separation

Particle size separation: Large-coarse crushed glass (to be used in bottle manufacturing)

Particle size separation: Medium-coarse crushed glass (to be used in bottle manufacturing)

Particle size separation: Fine crushed glass (discarded as unusable and transported to landfill)

Figure 2-2: Waste glass recycling operations at Consol

2.1.4 Global Utilisation of Crushed Glass in Pavement Applications

Figure 2-3 shows the geographical distribution of the countries indicating experience with waste glass in pavement applications. A selected few reported cases of the mentioned application in the various countries are described below.

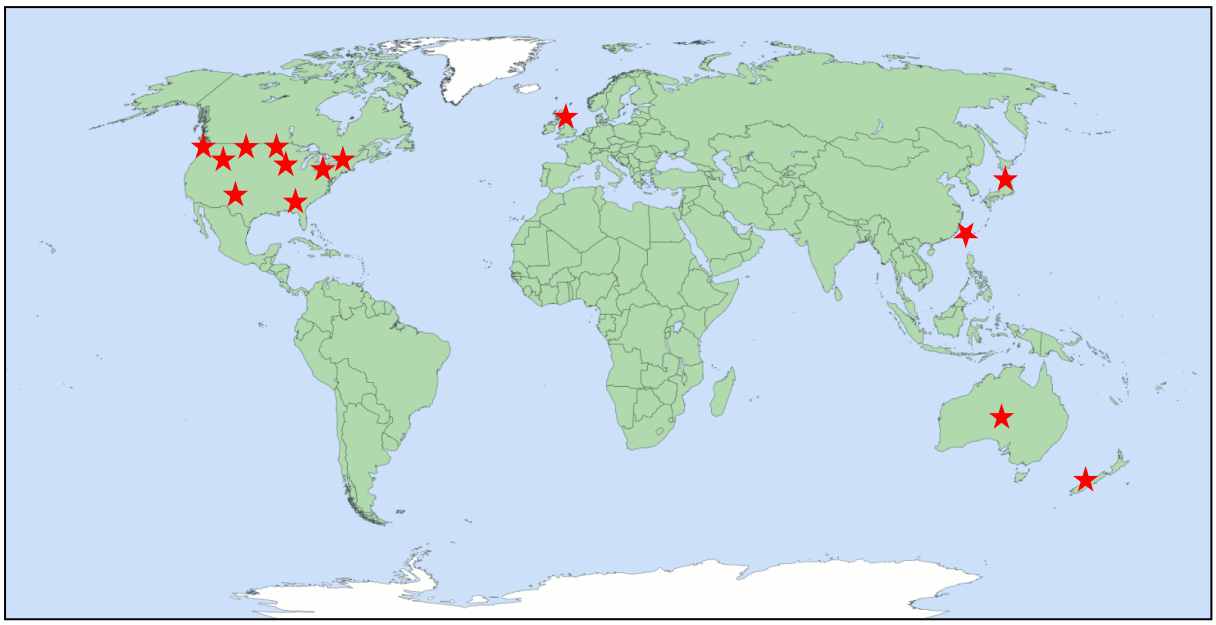

Figure 2-3: Countries using waste glass in pavement applications

United States of America (USA)

The United States Department of Transportation (USDOT) has reported the use of crushed glass in asphalt paving applications across nine states since early 1993. This accounts for approximately 2.4 million tonnes of glass that was utilised in the production of glass-asphalt in the US since (Dane County Department of Public Works, 2003).

A brief summary on the utilisation of glass-asphalt has been provided by the following states (Dane County Department of Public Works, 2003):

- Since 1971, Baltimore, Maryland, has produced glass-asphalt consisting of 30 to 40% crushed glass with a maximum particle size (MPS) of up to 9.5 mm.
- The New York DOT specifies the use of up to 30% crushed glass for various asphalt paving applications. New York City is using up to 30% crushed glass with a MPS of 9.5 mm in both the surfacing and binder course layers without the use of antistripping additives. The performance of glass-asphalt pavements in the city have been reported to have performed

"as well as, if not better than, conventional pavements." Brooklyn is utilising 10% recycled crushed glass (obtained from a glass recycling facility) in asphalt surfacing layers. Since 1994, Brooklyn, New York, has reported the use of crushed glass in asphalt paving applications for more than six years.

- Pennsylvania has utilised approximately 100,000 tonnes of crushed glass as an aggregate substitute in asphalt in 1992.
- Menasha, Wisconsin, has utilised crushed glass bottles in the production of glass-asphalt with a glass replacement ratio of 10%. In 1992, a glass-asphalt pavement incorporating 7.5% crushed glass with a MPS of 9.5 mm was constructed. The addition of an antistripping additive was also used. Following a year post construction no moisture damage or skid related concerns were reported. Furthermore, the pavement produced a noticeable reflection resulting from the reflection of light off the glass pavement.
- Los Angeles has initiated a program that utilises crushed glass for the production of 50,000 tonnes of glass-asphalt per year. The glass-asphalt incorporates 10% by weight of crushed glass with a MPS of 2.38 mm. In addition, health and safety tests conducted on the use of the crushed glass concluded no associated safety hazards.
- The New Jersey DOT specification includes criteria for the allowable use of crushed glass in asphalt.

Australia

In 2003, Pioneer Road Services Western Australia (WA), with the assistance of Main Roads WA, carried out the first glass-asphalt trial sections in Australia. The glass-asphalt trials demonstrated improved skid resistance and braking time than traditional asphalt pavements (Pioneer Road Services Pty Ltd, n.d.).

In 2010, Waverley Council, in partnership with New South Wales Department of Environment Climate Change and Water, New South Wales Roads and Traffic Authority, Institute of Public Works Engineering Australia and the Packaging Stewardship Forum, provided the first pavement test section in New South Wales with the aim of demonstrating the suitability of crushed glass as an alternative material in the construction of pavements in New South Wales. Two sections, each 100-metre in length, consisting of crushed glass were constructed. The first pavement section used crushed glass in asphalt and the second section used crushed glass

in concrete (Australian Government: Department of Sustainability, Environment, Water, Population and Communities, 2011).

New Zealand

Due to the geographical layout of New Zealand, councils in the South Island of the country find it uneconomical to ship recovered waste glass to the glass recycling plant, which is located in Auckland, on the North Island. This has led to large stockpiles being generated at these South Island councils, and one solution which is currently being used to divert this waste glass by crushing it and using it in combination with other aggregate materials as basecourse aggregate (Arnold et al., 2008).

The New Zealand Transport Agency currently makes provision in the Transit New Zealand (2006) specification for inclusion of crushed glass, up to 5% by mass, in the asphalt basecourse of pavements. The specification further stipulates that crushed glass less than 9.5 mm may be used. The basis for this change to the Transit New Zealand (2006) specification was based on international practices, where crushed glass quantities of up to 15 percent by weight were regarded as acceptable. The reason however that New Zealand conservatively restricted their quantities to 5% and not 15% was due to the fact that basecourses in New Zealand pavements are only covered by a chipseal as opposed to other countries, particularly in the Northern Hemisphere, where the basecourses are covered by at least 100 mm of asphalt wearing course.

Taiwan

Field studies are currently being carried out in Taiwan to examine the potential for using recycled crushed glass as an aggregate substitute material in Hot Mix Asphalt. In 2002, the Taiwan Highway Engineering Department constructed three asphalt pavement test sections, one with an area of 140 m^2 and two with an area of 510 m^2. The smaller test section was constructed using 10% glass content while the two larger test sections were constructed using varying percentages of recycled crushed glass i.e. at 0, 5, 10, and 15%. Furthermore, in order to resist the effects of stripping of the binder from the glass particles, all test sections, consisting of recycled glass, incorporated 2% lime.

A year post construction of the test sections, it was reported that the section consisting of 10% recycled glass demonstrated comparable performance to that of the section without recycled glass (Su & Chen, 2002).

Japan

It has been reported that recycled crushed glass has been widely utilised in Japan over the past decade as road-paving materials (Chang et al., 2001). Approximately 60 000 tons per annum is utilised in various applications including aggregates for pavements (specifically asphalt pavements), subgrades, backfill materials, etc. (Yamanaka et al., 2001).

United Kingdom (UK)

In 2001 various test resurfacing projects using Hot Mix Asphalt, containing 10% recycled crushed glass, were carried out in London (Heindrich et al., 2007).

In 2003, 35,000 tons of glass-asphalt was used in the resurfacing of a highway in the UK. The project made use of glass-asphalt as both a base and binder course asphalt for several miles of the highway. Following the completion of the project, performance monitoring tests conducted on the pavement section revealed that the performance of the glass-asphalt pavement was equivalent to the performance of pavements constructed using traditional aggregates (Andela & Sorge, n.d.).

The glass trade association of Britain, British Glass, funded studies on the use of crushed glass in asphalt. The studies involved the construction of pavement trial sections that were tested for wear and skid resistance, the results of which indicated that the use of crushed glass in asphalt yielded good resistance to wearing and skid resistance. The successful results obtained from the trials allowed for a section of pavement consisting of glass-asphalt, consisting of 17% crushed glass, to be constructed in the City of Westminster (Dane County Department of Public Works, 2003).

Recently, the resurfacing of a major route in Cheshire, carrying more than 120 000 vehicles per day with a speed of 110 km/hour, was carried out using glass-asphalt. This was conducted following the successful implementation of several glass-asphalt pavement test sections across the UK (Khatib, 2009).

2.1.5 Material Properties of Recycled Crushed Glass

2.1.5.1 Physical Properties

Appearance

The engineering properties of recycled crushed glass are influenced, in part, by the amount of deleterious materials present in the recovered waste glass that is sent for recycling. Such materials include paper, foil, plastic, metal, cork, wood etc. The amount of these materials that is present is largely dependent on the collection and sorting methods of recovered waste glass. Some specifications in the United States have specified a maximum permissible limit of 10% deleterious materials by volume of waste glass while other specifications stipulate up to 5% by volume (Nebraska State Recycling Association, 1997, Washington State Department of Trade and Economic Development, 1993).

Shape Characteristics

Recycled crushed glass consists of mostly angular particles and may consist of some flat and elongated particles, with the level of angularity and the presence of flat and elongated particles largely dependent on the level of crushing. Additional crushing will result in the generation of smaller particles that are, to some degree, less angular and contain less flat and elongated particles (Federal Highway Administration, n.d.). Additional crushing of the waste glass material can also remove sharp edges and the associated safety risks pertaining to manual handling of recycled crushed glass.

Surface Texture

The relatively smooth surface texture of the glass particles may result in insufficient adhesion between the binder and the glass aggregate surface. This can be explained by the ability of the bitumen to wet the glass aggregate. Wetting describes the degree to which a liquid in contact with a solid substrate spreads out.

When bitumen spreads over and wets an aggregate, the surface tension of the individual phases reduces and a new interfacial relationship develops. This change in energy is known as the work of adhesion and is a measure of the strength of contact between two phases. A high work of adhesion indicates good wetting.

The mathematical expression for the work of adhesion (W_a) is equal to the sum of the surface tension of the individual bitumen (γ_B) and aggregate (γ_A) phases minus the interfacial tension between these phases(γ_{AB}), expressed in Equation 2-1 (Masson & Lacasse, 2000) :

$$\boldsymbol{W_a = \gamma_B + \gamma_A - \gamma_{AB}}$$
Equation 2-1

With

γ_A, γ_B = surface tension of bitumen and aggregate

γ_{AB} = bitumen-aggregate interfacial tension

The bitumen-aggregate interfacial tension (γ_{AB}) can be obtained from the contact angle created by the bitumen when in contact with an aggregate surface. This is explained by three-phase bitumen-aggregate-water system, as illustrated in Figure 2-4, where θ is the contact angle between the aggregate-bitumen interface and the tangent of the water-bitumen interface. Based on this, γ_{AB} can be expressed as follows (Masson & Lacasse, 2000):

$$\boldsymbol{\gamma_{AB} = \gamma_{WA} - \gamma_{WB} cos\theta}$$ Equation 2-2

Taking Equation 2-1 and 2-2 into consideration, it can be understood that a contact angle greater than 90° will result in a negative work of adhesion which implies that the bitumen will not wet the aggregate surface. On the other hand, a contact angle smaller than 90° will result in a positive work of adhesion, implying that the bitumen will spread and wet the aggregate.

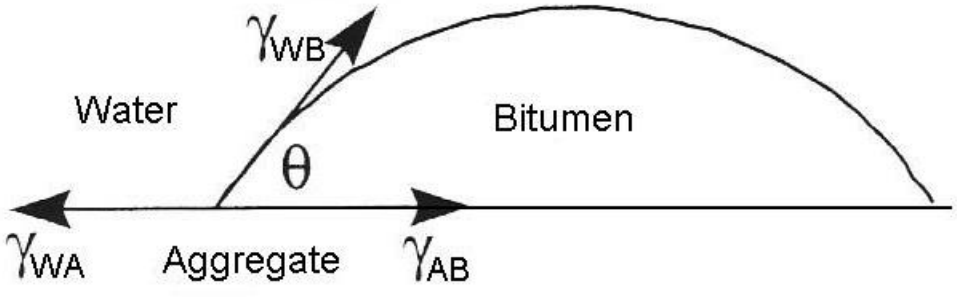

Figure 2-4: Schematic representation of the bitumen-aggregate-water phase system (Masson & Lacasse 2000)

In the case of most siliceous aggregates, which includes crushed glass, that have smooth surface texture, higher contact angles are expected thus reducing wetting of the glass particles,

resulting in less adhesion. This concept however addresses adhesion in terms of mere physical contact between the glass aggregate and the bitumen.

Specific Gravity and Relative Density

A study conducted by Dames and Moore (1993) indicated that the specific gravity of coarse crushed glass (i.e. > 5mm) ranges from 1.96 to 2.41 and 2.49 to 2.52 for fine crushed glass (i.e. < 5mm). It should be noted that the level of variance in the above values is influenced by the degree of purity of the crushed glass sample. The specific gravity of crushed glass is much less than that of crushed natural aggregates which range from 2.60 to 2.83 (Nebraska State Recycling Association, 1997).

Grading

The particle size distribution (grading) of recycled crushed glass can vary from one plant to the other and is determined by the plant specific methods used to process the waste glass. Figure 2- 5 represents the typical particle size distribution of the recycled crushed glass from the Consol glass manufacturing plant. Samples of the same were collected in 2015 as well as at the start of the current study (2016). It can be observed that the particle size distribution of both samples is very similar. Variations in grading are therefore not accounted for and the source may be considered suitable for use in pavement applications in South Africa.

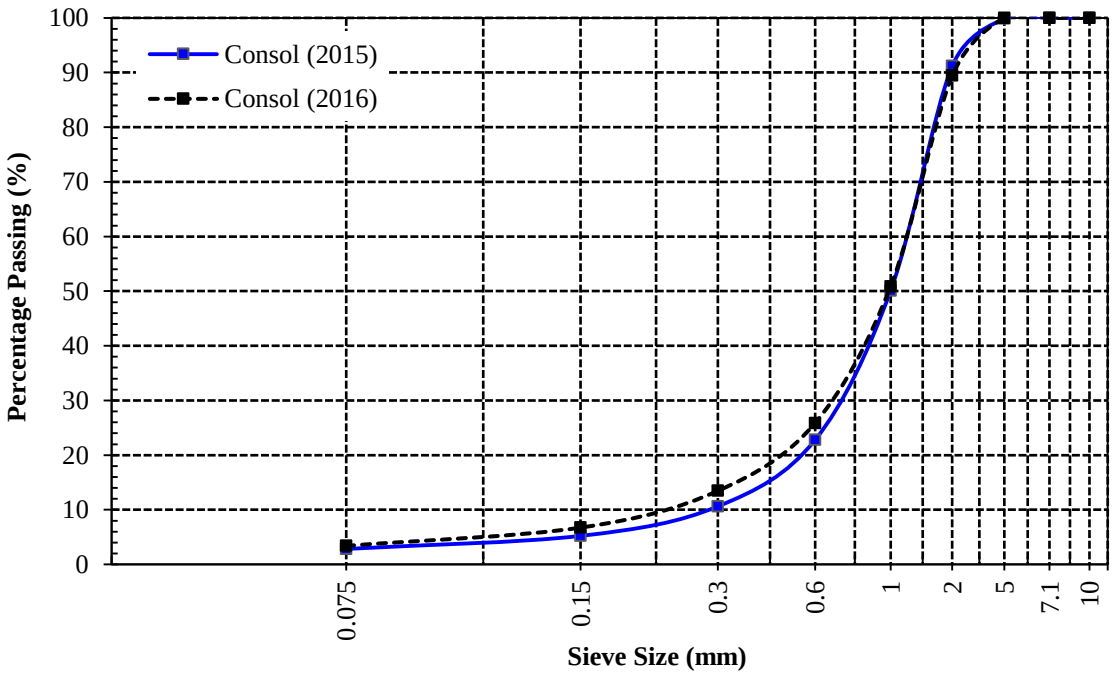

Figure 2-5: Particle size distribution of recycled crushed glass from Consol

Permeability

The permeability of recycled crushed glass varies with grading (which is known to be dependent on the level of crushing) as well as quantities utilised, and increases with an increase in the recycled crushed glass content, particle size and level of contamination (Nebraska State Recycling Association, 1997). The coefficient of permeability of coarse recycled crushed glass typically ranges from 10^{-1} to 10^{-2} cm/sec which is comparable to the coefficient of permeability of coarse sand (Federal Highway Administration, n.d.).

Thermal Conductivity

A common characteristic of glass is its thermal insulation (heat retention) properties. Studies conducted at the Colorado School of Mines in the mid 1970's have reported that due to the low thermal conductivity of glass, pavements consisting of crushed glass take a longer time to cool down than pavements consisting of natural aggregates (Federal Highway Administration, n.d.). More recently, studies conducted by the Washington State Department of Trade and Economic Development (1993), comparing the thermal conductivity of crushed glass with natural gravelly sand is indicated in Table 2-1. The results also indicated that crushed glass demonstrates higher thermal insulation properties than natural aggregate materials.

This may be advantageous during the construction of glass-asphalt pavements, especially in cold weather conditions, since the higher thermal insulation properties of the crushed glass material will assist in allowing glass-asphalt mix to retain heat longer during pavement paving.

Table 2-1: Thermal Conductivity Test Results (Washington State Department of Trade and Economic Development, 1993)

Material	Apparent Thermal Conductivity Watts/Meter - °K	
	Sample 1	Sample 2
Crushed Glass	0.315	0.260
Gravelly Sand	0.463	0.638

Reflection and Glare

Crushed glass has high reflective properties, which can be used to increase the visibility of pavement surfaces, and can assist in differentiating the pavement from its surroundings. Increased reflection, however, may result in glare which can potentially decrease visibility for road users. Although there are no studies, to date, which identify the exact quantities or particle

size of crushed glass that lead to glare, increased reflection has been has been noticed in pavements consisting of crushed greater than 15% (Federal Highway Administration, n.d.).

Leachability

Although glass is an inert material, domestic waste glass collection methods could introduce the presence of contaminants which may affect its chemical characteristics. Typical contaminants such as lead foil wrappers, for example, may increase the levels of lead in recycled crushed glass samples. However, waste glass collection and processing methods, which include removal of contaminants and cleaning, influences the degree of lead concentration. Large concentrations of contaminants that may however be contained in recycled crushed glass samples will most likely have an adverse effect on the environment due to leaching of heavy metals, such as lead, into the soil.

2.1.5.2 Chemical Properties

Mineralogical Composition

Majority of glass bottles and window glass are manufactured from soda-lime glass, which constitutes a significant portion of the glass produced in South Africa. Table 2-2 lists the typical chemical composition of this type of glass. For comparative purposes, the chemical composition of the recycled crushed glass used in this dissertation is also indicated. The chemical composition was obtained by means of X-ray fluorescence (XRF) analysis on a sample of the recycled crushed glass. The analysis was conducted at the Council for Geoscience in Pretoria.

Table 2-2: Typical chemical composition of soda-lime glass (Federal Highway Administration, n.d.)

Constituent	Soda-Lime	Recycled Crushed Glass Investigated
SiO_2	70 - 73	71.72
Al_2O_3 [1]	1.7 - 2.0	2.48
Fe_2O_3	0.06 - 0.24	0.65
Cr_2O_3 [2]	0.1	0.11
Cao	9.1-9.8	10.02
MgO	1.1 - 1.7	0.47
BaO	0.14 - 0.18	0.03
Na_2O	13.8 - 14.4	12.85
K_2O	0.55 - 0.68	0.50
PbO	--	0.03
B_2O_3	--	--

1. Higher levels of amber-coloured glass
2. Only present in green glass

The predominant compound present in most aggregates is either silica or calcium carbonate. An aggregate is said to be either acidic if the silica (SiO2) content is greater than 65%, neutral with SiO2 content between 52 and 65% and basic if SiO2 content is less than 52% (Rice 1958, Belošoviè & Žideková 1996). As seen in Table 2-2, SiO2 constitutes 71.7% of the glass particles investigated in this study, and is hence considered an acidic "aggregate". The acid-base composition of typical aggregates is presented in Figure 2-6 (Angelo & Anderson, 2003).

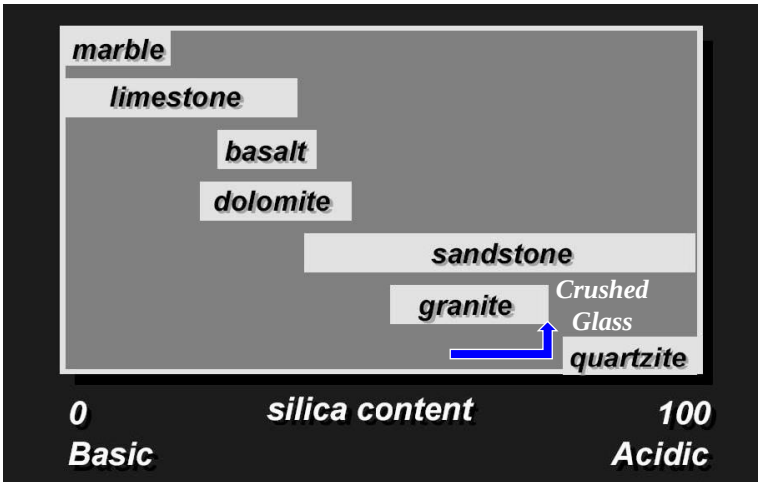

Figure 2-6: Acid-base composition of typical aggregates

Chemical Reaction with Bitumen and Water

The acidic components of bitumen such as carboxylic acids, anhydrides, 2-quinolone types and sulfoxides are considered to be the most strongly absorbed bitumen functional groups on the aggregate surface. While they are considered to be minor components in bitumen, a significantly high concentration of these components is present in the absorbed bitumen due to reaction with hydroxyl groups at the aggregate surface. This is said to be the general trend with different types of aggregates.

Although these acidic components are relatively polar and adhere strongly to dry aggregate, they tend to be removed easily from the aggregate in the presence of water. Highly siliceous aggregates, which includes crushed glass, are considered to be poor adherents to the polar groups of bitumen in the presence of water. This is due to the formation of stronger hydrogen bonds between water molecules and silanols (SiOH) than the bond between bitumen polar groups and SiOH groups.

Although this behaviour is common with siliceous aggregates, Cheng et al. (2002) have demonstrated that irrespective of the strength of the physical or chemical bond between bitumen and aggregate, the bond between water and aggregate is substantially higher. Table 2- 3 presents the outcome of their investigation. It can be observed that the calculated bond strength (ergs/cm^2) between water and aggregate (both siliceous and calcareous) is approximately 30% higher than between all bitumen types and the same aggregates. This observation highlights the damaging effects of water on the adhesive bond (physical or chemical) between aggregate (siliceous or calcareous) and bitumen.

The use of antistripping additives is said to modify the physical and chemical properties of the aggregate and bitumen, thereby improving the durability and strength of the interfacial bond between the two surfaces.

Table 2-3: Adhesive bond energy per unit area of sample (ergs/cm^2) (Cheng et al., 2002)

Bitumen	Georgia Granite	Texas Limestone	Colorado Limestone
AAD-1	153	141	124
AAM-1	198	205	179
Rubber asphalt	212	189	166
Aged Rubber Asphalt	171	164	145
Water	256	264	231

Surface Potential

The diffusion of dissociated bitumen polar groups into the bitumen-aggregate interface and their absorption onto the aggregate surface, explains the bitumen-aggregate bonding mechanism. Since the process of dissociation is rapid, it is most likely diffusion and absorption that controls the rate of adhesion (Bagampadde et al. 2003). The degree of absorption is determined by the charges present on the aggregate and bitumen surfaces, which can be determined by measuring the zeta potential of both surfaces.

Figure 2-7 presents the classification of aggregates based on their silica and alkaline or alkaline earth oxide content, according to surface charge. It can be seen that most siliceous (acidic) aggregates, which includes crushed glass, possess a negative surface charge in the presence of water. Furthermore, studies conducted by Labib (1992) have indicated that for different types of bitumen with varying composition and viscosity, the surface charge is negative for a wide pH range. This is expected since the bitumen functional groups absorbed onto the aggregate surface are mainly from the acid components. As a result, the development of repulsive forces

between the negatively charged siliceous glass aggregate and bitumen surfaces can occur which can contribute towards the detachment of bitumen from the glass aggregate surface.

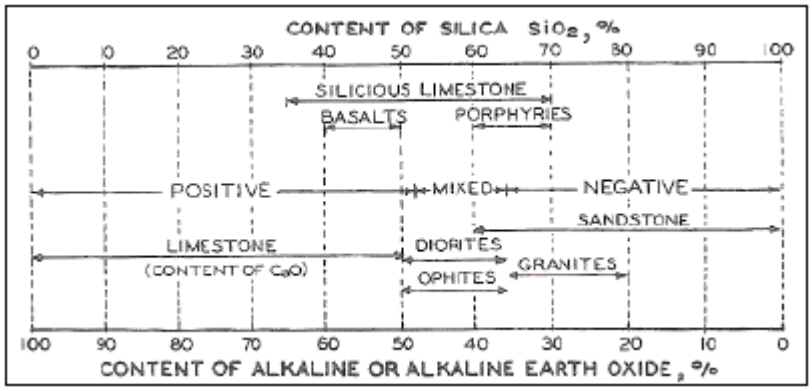

Figure 2-7: Classification of aggregates based on surface charge (Mertens & Wright, 1959)

2.2 Crushed Glass in Hot-Mix-Asphalt

Crushed glass may be used within a specified percentage, as a fine aggregate substitute, in Hot Mix Asphalt (HMA) pavements. The term "glasphalt or glass-asphalt" has at times been used to describe these pavements. Even though HMA pavements which have incorporated crushed glass have shown good performance, the following areas of concern have been identified (Federal Highway Administration, 1998):

1) Reduced adhesion at the bitumen and glass interface.
2) Potential loss of skid resistance
3) Breakage of larger sized glass particles
4) Increased susceptibility to stripping and ravelling

To avoid the above mentioned concerns, quantities of crushed glass should be limited to 15% in the surface course of HMA pavements (Federal Highway Administration, 1998). HMA pavements incorporating quantities in excess of 15% in the surface course may potentially experience stripping of the bitumen from the glass particles, which can ultimately lead to deterioration of the pavement. There is, however, the possibility of including larger quantities of up to 25% when using crushed glass as part of the base or binder course (layer between surface and base course) in HMA pavements.

In addition, the particle size of crushed glass is an important factor to take into consideration. Various research studies have established that using small crushed glass with a maximum

particle size of 10 mm can address the potential problems mentioned above, while other studies have indicated that crushed glass should be smaller than 5 mm to have a marked effect on improved asphalt performance (Hughes, 1990; VTRC, 1998; Wu et al., 2003).

The incorporation of crushed glass in HMA also provides an added advantage over traditional aggregates due to the low absorption properties of glass. This may allow asphalt mixes to utilise less bitumen without possibly having an impact on field performance. Although this may be beneficial from an economic and environmental perspective, the low absorptive properties may contribute towards stripping of the binder from the glass particles. However, to counter this effect the use of anti-stripping additives has been recommended for inclusion in glass-asphalt mixes. Hydrated lime and amine based liquid antistripping additives are most commonly used. The chemical interaction of these antistripping additives with siliceous glass "aggregates" are explained below.

Hydrated Lime

As previously mentioned, the hydrogen bonds formed between carboxylic acids in bitumen and silanols of siliceous glass particles are easily removed in the presence of water, thereby contributing to poor adhesion between the bitumen and glass aggregate surface. Through the addition of hydrated lime ($Ca(OH)_2$), the absorption of these water-sensitive carboxylic acids can be prevented by converting them into insoluble salts. Insoluble calcium organic salts are formed when the Ca^{2+} ions from the lime react with the carboxylic acids and 2-quinolenes from the bitumen. The formation of these strong bonds contribute to improved adhesion (Petersen, 2002).

Schmidt and Graf (1972) have indicated that improved adhesion achieved by hydrated lime is not entirely due to the reaction between the Ca^{2+} ions from the lime and the carboxylic acids and 2-quinolenes from the bitumen but can also be due to the migration of Ca^{2+} ions to the surface of the aggregate, where hydrogen, sodium, potassium, or other cations are replaced. This results in calcium rich bonding sites for bitumen acidic groups.

Additionally, studies conducted by Robert et al. (1996) have revealed that hydrated lime forms strong bonds with most siliceous aggregates through the formation of a calcium silicate crust on the surface of the aggregate which has adequate porosity for binder penetration.

Liquid Antistripping Additive

Amine based liquid anti-stripping additives are known to improve the adhesion of bitumen with siliceous aggregates. This is attributed to hydrogen bonding between the polar amine end group and the silanols of the siliceous aggregate and anchoring of the hydrocarbon chain of the amine in the bitumen. The long hydrocarbon chain of the amines forms a bridge between the siliceous aggregate and the bitumen surface, resulting in a strong adhesive bond between the two surfaces (Tarrer & Wagh, 1991). Two typical amine groups, i.e. primary and tertiary, are schematically presented in Figure 2-8.

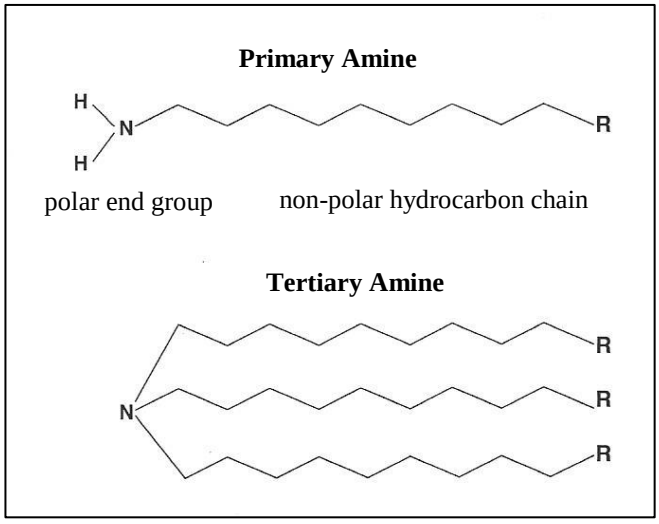

Figure 2-8**: Schematic representation of typical amine groups**

Numerous studies on the utilisation of crushed glass in HMA and the effect on the volumetric and mechanical performance properties as well as insitu performance (in some studies) have been conducted by various researchers and are described in detail below.

Hughes (1990) investigated the technical feasibility of utilising crushed glass as a substitute aggregate in HMA. The crushed glass utilised in the study was obtained from a contractor in New York who at the time had constructed a significant number of glass asphalt pavements. The maximum particle size (MPS) of the glass utilised was 10 mm. The particle size distribution of the glass material is indicated in Figure 2-9 and represents a similar grading to that of coarse sand. It should be noted that for comparative purposes, the particle size distribution of the glass material used in this dissertation is also shown. Comparatively, a much finer grading can be observed with 100% passing the 5 mm sieve as opposed to 70% passing the 5 mm sieve in Hughes' study.

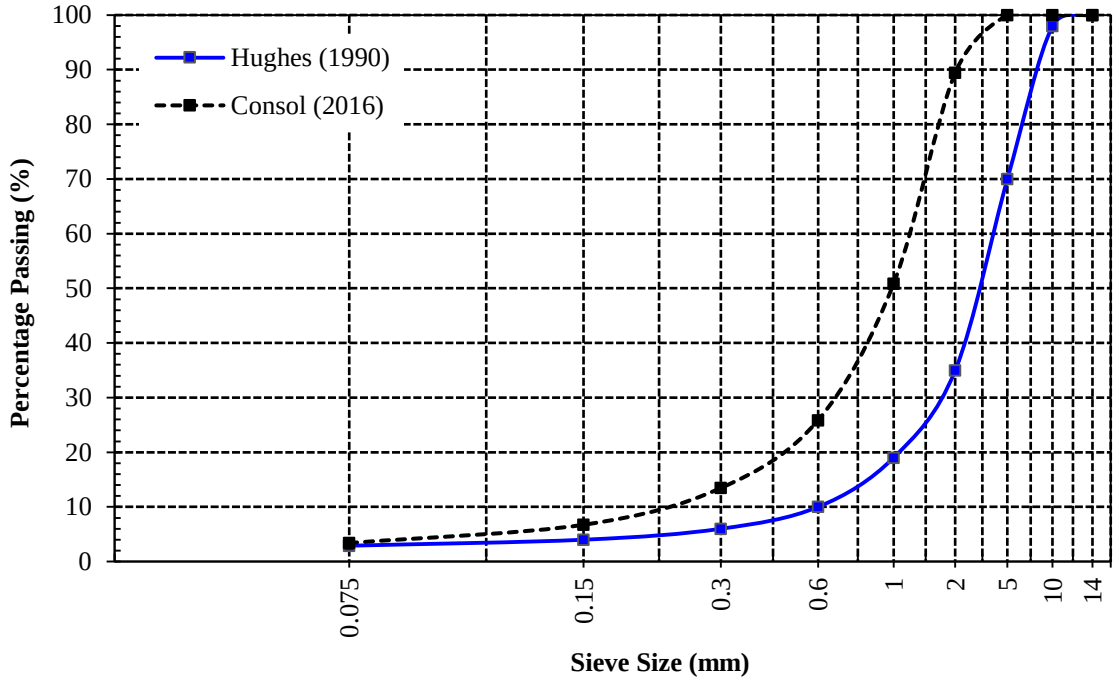

Figure 2-9: Particle size distribution of crushed glass utilised in HMA

The combined grading of the individual aggregates and filler material used to produce an asphalt mix is referred to as the design grading. The design grading of the glass-asphalt mix used in Hughes' study was a 10 mm nominal maximum particle size (NMPS) medium continuously graded asphalt mix. NMPS is defined in Sabita Manual 35/TRH8 (2016) as "one sieve size larger than the largest sieve to retain a minimum of 15 percent of the aggregate particles".

The investigation entailed a comparison of the volumetric properties of the asphalt mix consisting of 5% and 15% glass with the volumetric properties of the same asphalt mix without glass (control mix). It was indicated that the control mix that was selected for the study is typically used as a wearing course in asphalt pavements in the state of Virginia. The proportion of glass that was incorporated into the mix substituted a portion of the sand as well as a portion of the fine and coarse aggregates utilised in the study. The design grading of the glass-asphalt mixes were similar to the design grading of the control mix. An optimum binder content of 5.75% for the control mix was determined at 5% air voids at a 75-blow compactive effort. The same optimum binder content was used for the two glass-asphalt mixes (i.e. at 5% and 15% glass content).

The volumetric properties that were obtained as part of the investigation are indicated in Figure 2-10. The voids in the mineral aggregate (VMA) and the voids filled with binder (VFB) in the asphalt mixes were obtained at the determined optimum binder content of 5.75%. The results revealed that with the addition of 15% crushed glass, a decrease in the voids in the mix (VIM) and VMA and an increase in the VFB in comparison with the control mix were observed. It was indicated that the highly angular particle shape and smooth texture of the glass particles were contributing factors to the observed volumetric properties. Due to the highly angular particle shape and smooth texture of the crushed glass and the observed effect on the volumetric properties it was recommended that the optimum binder content for the target percentage of crushed glass to be incorporated in the mix be determined.

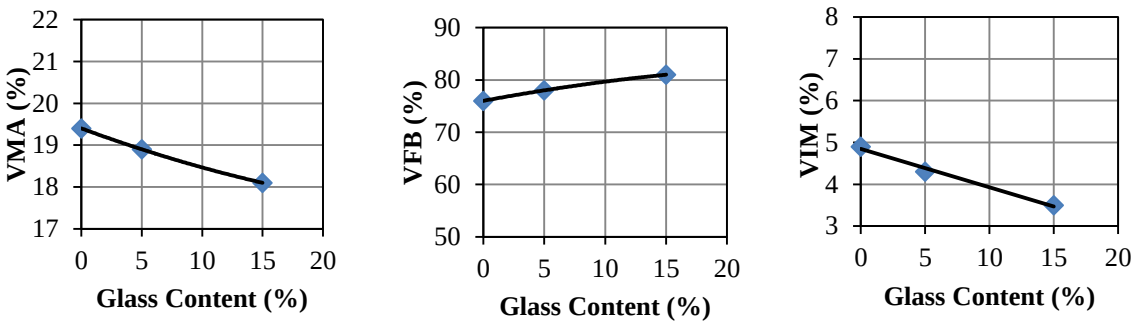

Figure 2-10: Volumetric properties for asphalt mix containing glass at 5.75% binder content (Hughes, 1990)

The study also included an assessment of the mixes to resist moisture damage. The parameter used to assess the moisture damage was the tensile strength ratio (TSR) which is a ratio of the indirect tensile strength of a set of specimens conditioned by moisture to the tensile strength of a set of unconditioned specimens. TSR values range from 0 (which indicates no resistance to moisture damage) to 1.0 (which indicates no susceptibility to moisture damage).

One percent (1%) hydrated lime was used in the glass-asphalt mixes as an antistripping additive to help prevent the loss of adhesion between the bitumen and the glass particles in the presence of moisture. The control mix, however, did not include an antistripping additive.

The moisture damage test revealed that the addition of 5% of crushed glass had a minor effect on both the conditioned strength and the TSR values in comparison with the control mix. The TSR of the glass-asphalt mix constituting 15% crushed glass was approximately 0.9. Though

the conditioned strength and the TSR values were not considerably affected by the percentage composition of crushed glass, some detachment of the binder from the glass particles was observed. The inclusion of more coarse crushed glass in the mix was believed to contribute towards this observation.

Based on the study conducted by Hughes (1990), it was recommended that a maximum of 15% crushed glass may be used in asphalt mixes provided that the crushed glass adheres with grading controls to be 100% passing the 9.5mm sieve and not more than 6% passing the 0.075mm sieve. Furthermore, it was recommended that moisture damage tests should be conducted on glass-asphalt mixes in particular and must produce a TSR value of 0.9 or higher. This is a more severe requirement for resistance to moisture damage than for mixes not using crushed glass, however, it was suggested to be reasonable due to the propensity of glass to suffer moisture damage.

The Virginia Transportation Research Council (VTRC) (1998) conducted an extensive laboratory study to determine the maximum amount of crushed glass that can be used in HMA without compromising on the stripping resistance. Stripping in a mix occurs due to the loss of adhesion between the binder and the aggregate in the presence of moisture. The study was conducted based on the interest that was expressed by the Virginia Department of Transportation (VDOT) on the utilisation of crushed glass in asphalt pavements.

Asphalt mixes, each containing hydrated lime and a chemical antistripping additive, were produced at varying crushed glass contents (0, 5, 12 and 20%). Recycled crushed glass with a MPS of 10 mm, obtained from a glass recycling plant in Fairfax, Virginia, was used in the asphalt mixes due to its availability from the same source of glass used in a number of test sections in Virginia, which also did not require additional crushing.

The TSR parameter was used to evaluate the stripping resistance of the glass-asphalt mixes. A TSR value of 0.90 was used to determine the maximum crushed glass content that could safely be used in asphalt mixes. The VDOT usually specifies a minimum TSR value of 0.85; however, 0.90 was specified in order to ensure a higher resistance to stripping in the glass-asphalt mix.

The design grading used to manufacture the glass-asphalt mixes was a 14 mm NMPS fine continuously-graded mix. It was indicated that a constant design grading was maintained for all the mixes i.e. at 0, 5, 12 and 20% crushed glass content.

It was observed from the results that the mixes with no additives produced TSR values in the 0.7 to 0.8 range. However, with the addition of the antistripping additives the mixes consisting of both additives produced TSR's of approximately 0.85 or above. This was, however, only relevant for the mixes containing up to 12% crushed glass content.

Furthermore, the results revealed that the mixes with hydrated lime indicated the least variance (approximately 0.05) in TSR values with increasing crushed glass content. This behaviour indicated that the stripping resistance of the mix may be maintained at a certain level with the addition of hydrated lime as opposed to the chemical additive which showed a decline in the TSR results as the glass content increased.

In addition, a comparison of the mixes consisting of 20% crushed glass showed that the mix containing the chemical additive had a significantly lower average wet (conditioned) strength than that of the mix with hydrated lime. However, the mixes consisting of lower glass content did not show any significant variance in average wet strength.

The study, therefore, concluded that up to 15% of crushed glass in asphalt, with hydrated lime serving as an anti-stripping additive, is acceptable to prevent stripping of glass-asphalt. It should be noted that the findings of the study was centred on the assumption that the TSR, as a performance indicator, reliably predicts field stripping. Furthermore it was indicated that the proposed acceptable crushed glass content may vary with different mix types as well as well as for different grading of crushed glass.

Based on the above results, the VDOT has recommended that standards in Virginia specifying a maximum glass content of 15% in HMA be maintained.

Wu et al. (2003) conducted a comprehensive laboratory study to determine the optimal percentage of crushed glass that can be incorporated into an asphalt mix. The investigation was conducted on four asphalt mixes consisting of 0, 5, 10, 15 and 20% of crushed glass. The glass material utilised in the study was obtained by manually crushing reclaimed beer bottles.

The investigation included a preliminary study to determine the MPS of crushed glass that can be incorporated into the asphalt mixes which would ensure maximum adhesion between the glass particles and the bitumen in the presence of moisture. The Hamburg Wheel Tracking Test (HWTT) was used to assess the moisture susceptibility of the asphalt mixes with a maximum glass particle size of 10 mm in comparison with a maximum glass particle size of 5 mm. The HWTT measures the collective effect of rutting and moisture damage by means of a rubber wheel that traverses in both directions across an asphalt specimen which is submerged in a water bath at a specified test temperature.

It was observed after the HWTT that there were much more uncovered surface areas in the mixes with a maximum glass particle size of 10 mm (Mix A) as opposed to the mixes with a maximum glass particle size of 5 mm (Mix B) - see Figure 2-11. This may be due to the larger number of fractured faces of the fine crushed glass particles as opposed to the coarse glass particles, which in turn increases the physical area of contact and hence improves adhesion at the bitumen aggregate interface. The larger number of fractured faces may also prevent an abrupt plane of stress transfer, where the stresses are rather transferred across or into the bitumen, resulting in less stripping.

Furthermore, the HWTT results revealed that the dynamic stability of the Mix A was considerably lower than Mix B. The dynamic stability is measured as the number of passes per mm rut depth obtained from the HWTT. Based on the above observations, the preliminary study therefore concluded that the utilisation of crushed glass with a MPS of 10 mm was not viable. A maximum glass particle size of 5 mm was hence adopted for the primary investigation.

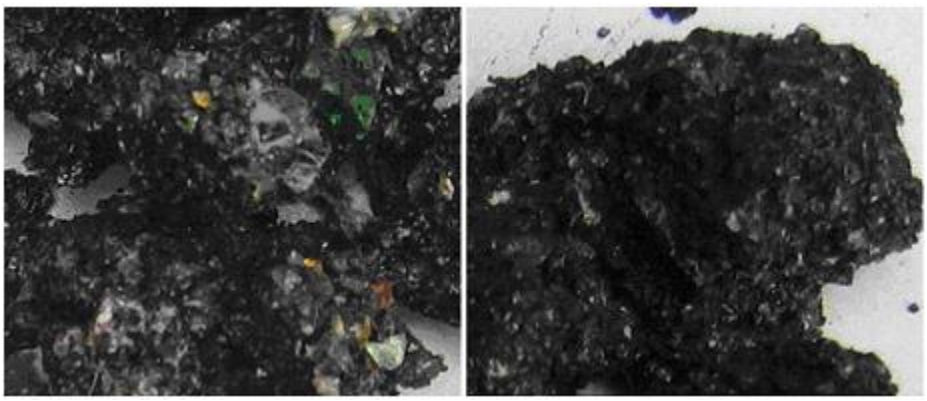

Figure 2-11: 10 mm (left) and 5 mm (right) maximum glass particle size in asphalt mix (Wu et al., 2003)

The particle size distribution of the manually crushed reclaimed beer bottles that was used in the primary investigation is indicated in in Figure 2-12. It should be noted that for comparative purposes, the particle size distribution of the glass material used in this dissertation is also indicated. It can be observed that the grading of the crushed glass material is relatively similar except between a particle size of 1mm and 5 mm, where the glass used in Wu et al.'s study is 20% coarser.

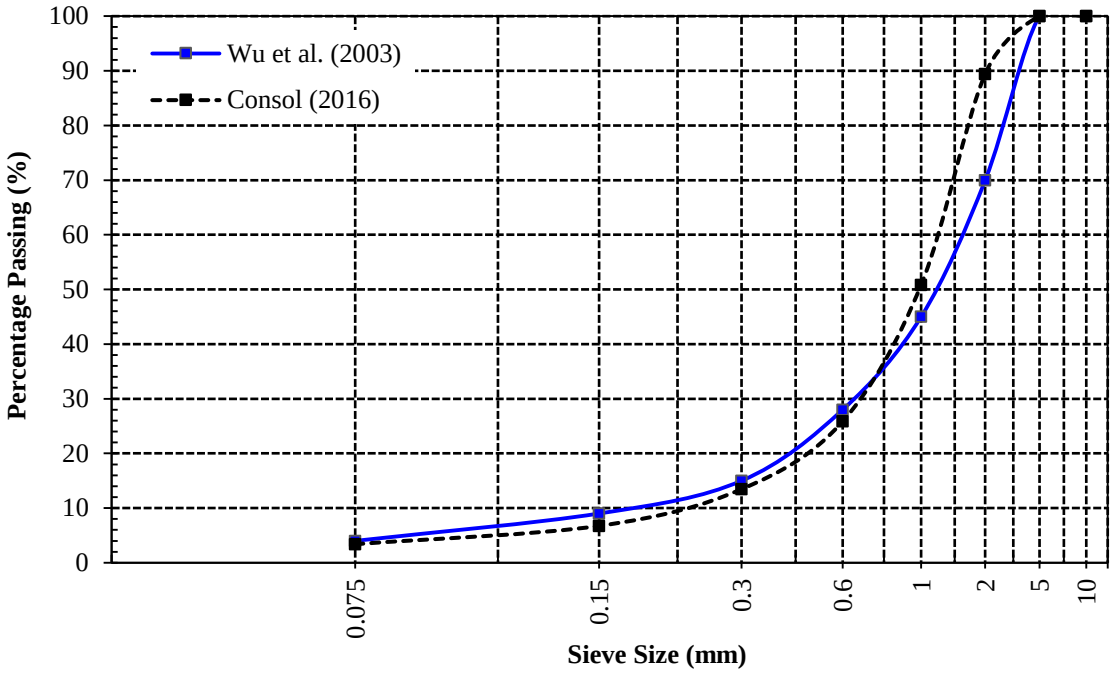

Figure 2-12: Particle size distribution of crushed glass used in HMA

Similar to the preliminary study, the HWTT was conducted on the asphalt mixes constituting 0, 5, 10, 15 and 20% of crushed glass. The determining parameters that were investigated to select the optimal mix were based on the permanent rutting deformation and stripping weight loss of the asphalt mixes obtained from the HWTT. The stripping weight loss is measured by comparing the weight of the mixes before testing (unconditioned samples) in comparison with the weight of the mixes after the HWTT. It should be noted that the test temperature was selected at 45°C due to the samples dispersing at the specified high temperature of 60°C.

The design grading used to manufacture the glass-asphalt mixes was a 14 mm NMPS medium continuously-graded glass-asphalt mix. It was indicated that the design grading was similar for all the crushed glass contents. The optimum binder content of the mix with no glass (control mix) was determined to be 4.8% at 4.13% air voids. Similar to Hughes's (1990) study; the

same binder content was used for the different glass-asphalt mixes (i.e. at 5%, 10%, 15% and 20% crushed glass content).

The HWTT revealed an increase in permanent rutting deformation and stripping weight loss with increasing crushed glass content, as indicated in Table 2-4.

Table 2-4: Hamburg wheel tracking test results (Wu et al., 2003)

Glass Replacement (%)	Rutting Deformation (mm)	Stripping Weight (g)	Remarks
0	9.80	15.60	*sample was broken at a rut depth of 13.7mm
5	10.6	23.40	
10	13.6	49.50	
15	15.0	88.70	
20	13.7	230.3	

Furthermore, it was observed that the asphalt samples with higher crushed glass content (i.e. at 15%) had reached a maximum rut depth of 15 mm after a much shorter period of time. The obtained rut depth with respect to loading times is illustrated in Figure 2-13. In addition, it was revealed that the start of asphalt stripping of the glass-asphalt mixes occurred at less than 1500 loading repetitions. The addition of crushed glass, therefore, proved to have a negative effect on the moisture susceptibility of the asphalt mixes particularly at higher contents (i.e. at 15 and 20%). Based on the above observations, it was identified that a more conservative optimum crushed glass content was achieved using a 10% replacement ratio.

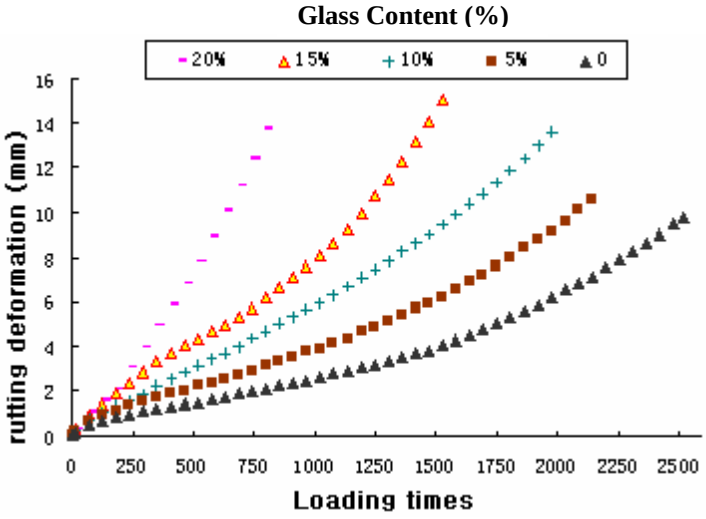

Figure 2-13: Rut depth with respect to loading repetitions (Wu et al., 2003)

The study consequently proceeded to investigate the effect of the addition of antistripping agents namely, hydrated lime and a liquid anti-stripping agent namely, coconut ethanolamine,

on the permanent rutting deformation and moisture susceptibility of the selected optimal mix (i.e. at 10% crushed glass content).

Trial tests conducted on the optimal mix, firstly with 2% hydrated lime and secondly with 0.4% (by mass of bitumen) of the liquid anti-stripping agent, demonstrated a substantial improvement in resistance to rutting deformation as well as moisture damage in comparison with the same mix without an anti-stripping agent. It was also interesting to note that the rutting deformation results were comparable to the mix without glass. Furthermore, the results indicated that the liquid anti-stripping agent was more effective than the hydrated lime in resisting rutting deformation and moisture damage.

Figure 2-14 shows the internal state of the broken glass-asphalt sample (i.e. at 10% crushed glass content) tested before and after the addition of the liquid anti-stripping agent. It can be seen that some aggregate surfaces are not coated with bitumen in the sample without the anti-stripping agent (left) as opposed to the sample with the anti-stripping agent where no exposed aggregate surfaces are displayed (right).

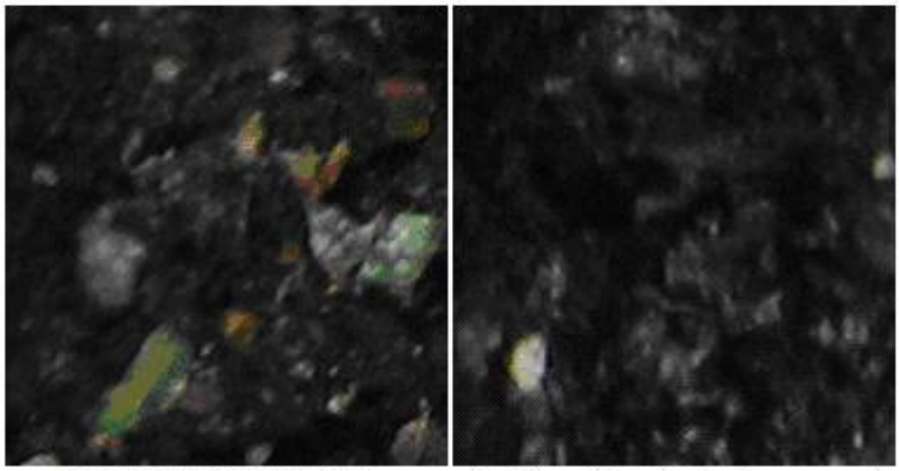

Figure 2-14: Glass asphalt mix prior to (left) and post (right) use of liquid anti-stripping agent (Wu et al., 2003)

Based on the study conducted by Wu et al. (2003) it was recommended that large glass particles (i.e. larger than 5 mm) should be avoided when utilised as an aggregate replacement in asphalt mixes. The following areas of concern were addressed:

- An increase in the size of the aggregate particles results in a smaller surface area causing weaker adhesive bonds between the glass particles and the bitumen.

- The smooth surface texture of large glass particles contributes to the formation of weak adhesive bonds between the glass particles and the bitumen.
- Large glass particles may cause significant abrasion of car tyres as well as reduction in skid resistance caused due to the breakage of the large glass particles by traffic loading.

It was hence recommended that smaller glass particles (less than 5 mm) should be utilised in asphalt mixes since the presence of more fragmentised and textured surfaces of smaller particles aid in promoting adhesion between bitumen and glass particles.

Su & Chen (2002) conducted a study to determine the feasibility of utilising recovered domestic waste glass with the aim of using it as an aggregate substitute in HMA. The investigation entailed a comprehensive laboratory study whereby four glass contents i.e. 0, 5, 10 and 15% by weight of total aggregate were utilised as a partial aggregate replacement to develop four asphalt mixes.

The glass that was utilised was manually crushed and thereafter pulverised to a MPS of 5 mm. The particle size distribution of the crushed glass is indicated in Figure 2-15. For comparative purposes, the particle size distribution of the glass material used in this dissertation is also indicated. A different approach was adopted in replacing the aggregate with the crushed glass. The approach involved substituting each percentage composition of crushed glass of a specific particle size with the same content and particle size of the virgin aggregate.

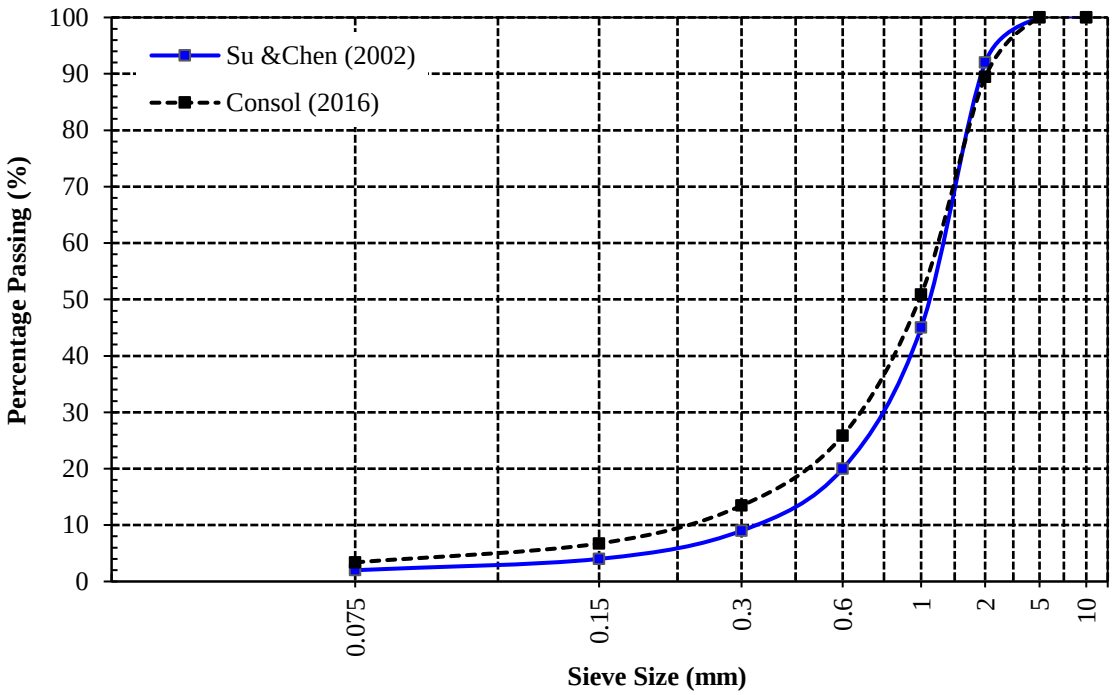

Figure 2-15: Particle size distribution of crushed glass used in HMA

In addition to the above, lime at varying contents (0-3%) were added to each mix to assess the effect of the varying contents of lime on the stability of the mixes. Stability is a measure of the resistance of an asphalt mix to permanent deformation and is measured by the maximum load supported by a test specimen when loaded diametrically at 50.8 mm/minute at 60°C (Pavement Interactive, n.d.). The obtained stability values at the varying lime contents are illustrated in Figure 2-16. The addition of 2% lime was observed as the optimum amount of lime to be included in order to achieve maximum stability of the mix.

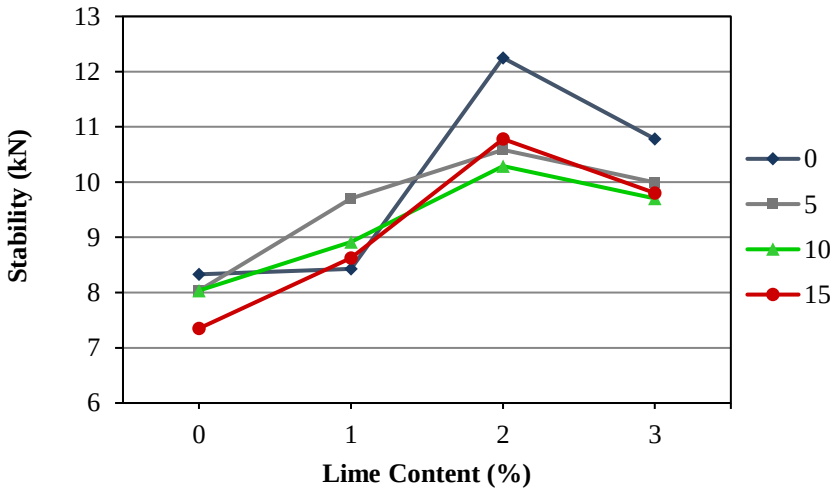

Figure 2-16: Stability values of glass asphalt mixes with lime (Su & Chen, 2002)

The design grading used to manufacture the glass-asphalt mixes was a 20 mm NMPS fine continuously-graded glass-asphalt mix. It was indicated that the design grading was similar for the four glass-asphalt mixes. As opposed to the investigations carried out by Hughes (1990) and Wu et al. (2003), the optimum binder content for each percentage composition of glass was determined, as depicted in Figure 2-17.

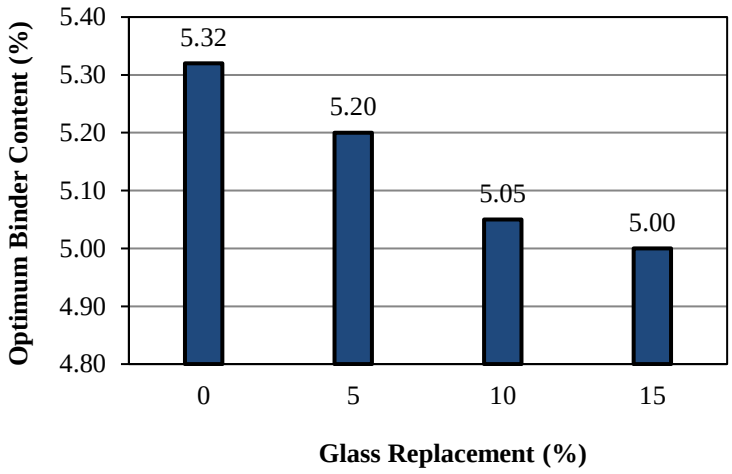

Figure 2-17: Optimum binder content of glass-asphalt mixes (Su & Chen, 2002)

The tests that were conducted on the asphalt mixes included both laboratory and field tests, of which the latter was conducted on three different test sites, funded by the Highway Engineering Department in Taiwan. The test pavements were constructed with the investigated amounts of glass (i.e. 0, 5, 10 and 15%) at the respective optimum binder content's (i.e. 5.32, 5.20, 5.05 and 5.00 %). The reported outcome of both the laboratory and field tests is provided below.

Laboratory test observations:

- The optimum binder content varied with respect to the glass content incorporated within the mix. Furthermore, the optimum binder content decreased as the glass content within the mixes increased. This phenomenon was attributed to the smooth surface texture of the glass particles, resulting in a lower rate of binder absorption.
- Due to the lower binder absorption rate, it was observed that the film of binder that coated the glass particles was relatively thin which resulted in weak bonds between the binder and the glass particles, resulting in durability issues.
- The above durability concern was improved with the addition of 2% lime.

Field test observations:

- The stability values of all the glass-asphalt filed specimens were found to be “profoundly greater” than the minimum criteria as specified in the Marshal Test procedure, i.e. 6.68 kN.
- It was identified that the light reflection intensities when tested at night increased on the test sections with increased amounts of crushed glass. As expected the light reflection was significantly higher than that of asphalt pavements without crushed glass, as shown in Figure 2-18.
- The investigation on skid resistance revealed improved resistance along the longitudinal and transverse profile of the asphalt pavements as the crushed glass content increased.
- It was specifically highlighted that the asphalt pavement that constituted 10% of crushed glass after one year of service indicated no ravelling of the glass particles as well as no rutting of the glass-asphalt pavement.

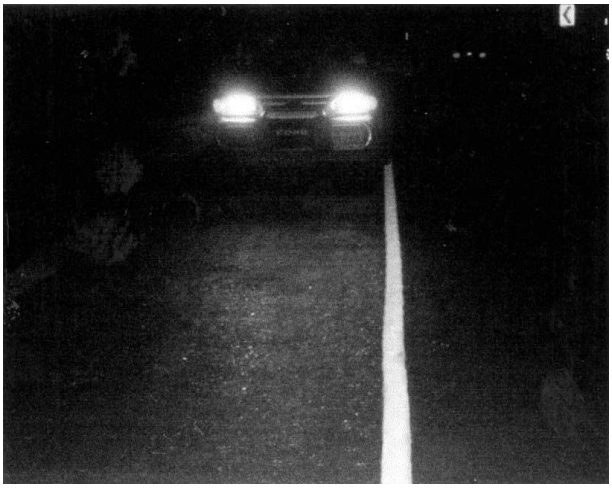

Figure 2-18: Light reflection properties of glass particles demonstrated on asphalt test pavement (Su & Chen, 2002)

Arabani (2010) conducted a study to investigate the effect of varying contents of crushed glass on the stiffness modulus of asphalt mixes at different temperatures. The stiffness modulus is a performance-related parameter used to predict the strength of pavements subjected to dynamic loading. The stiffness moduli of the mixes were determined by the indirect tensile stiffness modulus (ITSM) test. A repeated load was applied along the vertical diameter of the test specimen at a frequency of 1Hz with a load duration of 0.1 seconds and a rest period of 0.9 seconds. The resulting recoverable horizontal tensile strain was measured for determination of the stiffness modulus.

Five asphalt mixes were prepared consisting of 0, 5, 10, 15 and 20% crushed glass and the optimum binder content of the mixes ranged between 5.5% and 6%. In addition, 2% hydrated lime was used in the mixes as an antistripping agent.

The crushed glass used in the study was collected from a glass production company in Iran. The MPS of the glass utilised was 5 mm. The particle size distribution of the crushed glass is indicated in Figure 2-19. It can be observed that the grading of the crushed glass used in this dissertation is approximately 10 to 30% finer for a particle size between 1 mm and 2 mm.

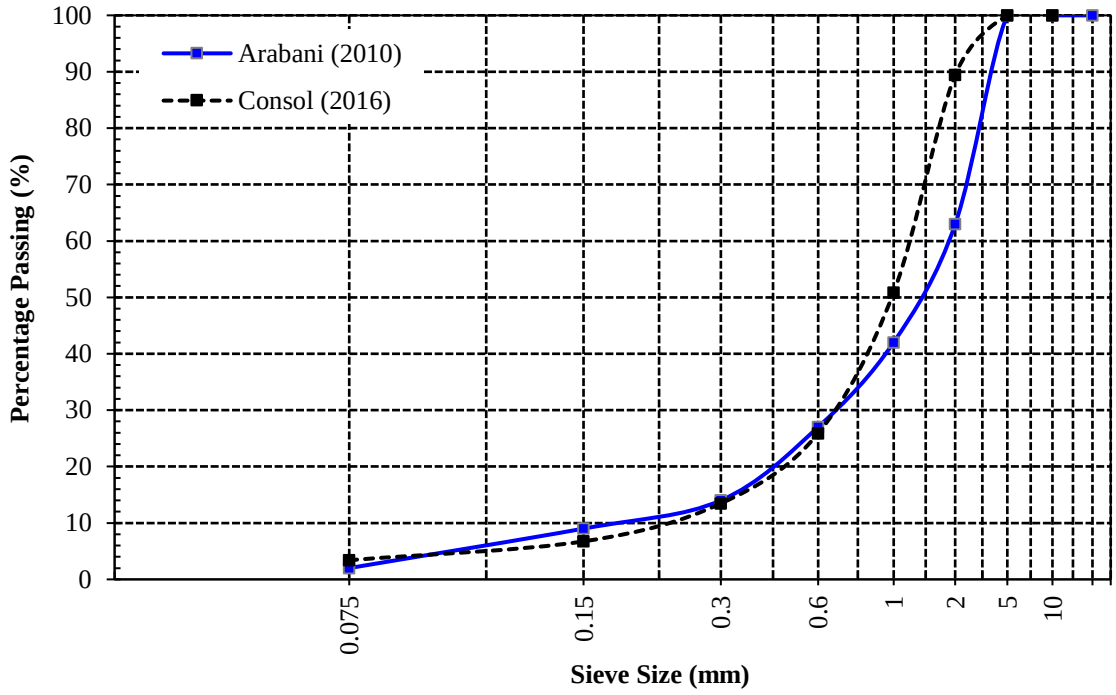

Figure 2-19: Particle size distribution of crushed glass utilised in HMA

It was specified that the design grading of the glass-asphalt mix was obtained within the limits indicated in Table 2-5 and was similar for all crushed glass contents (i.e. 0, 5, 10 15 and 20%).

Table 2-5: Design grading of glass-asphalt mix (Arabani, 2010)

Sieve Size (mm)	Percentage of Weight Passing (%)
0.075	2-10
0.3	5-21
2	28-58
5	44-74
14	90-100
20	100

The obtained stiffness moduli of the glass-asphalt mixes for the varying proportions of crushed glass as well at three different test temperatures (i.e. 5, 25 and 40 °C) are presented in Figure 2-20.

It was observed that the glass-asphalt mixes demonstrated improved stiffness modulus with an increase in crushed glass content, whereby the maximum stiffness occurred at 15%. However, at crushed glass content above 15%, the stiffness modulus of the glass-asphalt mix decreased. It was indicated that above the optimum crushed glass content (i.e. 15%), the stiffness modulus of the mix decreases due to the addition of a large number of smooth glass particles as well as higher quantities of glass in the mix that do not absorb the bitumen adequately resulting in a more fragile structure.

It was also observed that at different temperatures, the stiffness modulus remained relatively constant. It was, therefore, suggested that the stiffness modulus of glass-asphalt mixes are at its maximum at 15% crushed glass content at any specific temperature. In addition, the stiffness modulus of the glass-asphalt mixes indicated lower sensitivity to variations in temperature when compared to the asphalt mix without glass. When the test temperature was increased from 5°C to 40°C, the stiffness modulus of the asphalt mix without crushed glass reduced by approximately 70%, while the stiffness modulus of the glass-asphalt mix (i.e. with 15% crushed glass content) only experienced a reduction of approximately 50%.

It was indicated that the increased stiffness modulus of the glass-asphalt mixes (excluding the mix with 20% crushed glass) in comparison with the asphalt mix without crushed glass was attributed to the highly angular glass particles; allowing for better interlock between the aggregates and the glass particles.

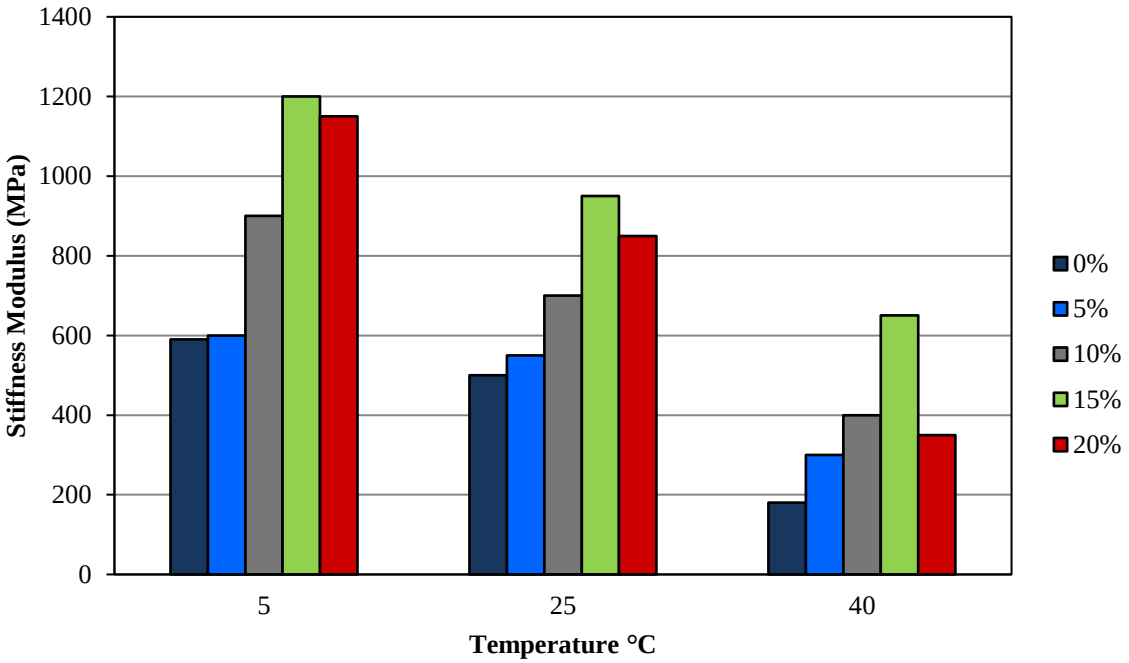

Figure 2-20: Variations of stiffness modulus with temperature at different crushed glass content (Arabani, 2010)

Lachance-Tremblay et al. (2014) conducted a study to assess and compare the performance of asphalt mixes consisting of five different contents of crushed glass (5, 10, 15, 20, and 25%) with an asphalt mix (control mix) without crushed glass. The control mix selected for the study is standardised by the Quebec Ministry of transportation (MTQ) and is commonly used in surfacing courses in Quebec. The following performance characteristics of the asphalt mixes were studied: 1) resistance to rutting, 2) low temperature cracking resistance and 3) stripping susceptibility.

In this experimental investigation, similar to the study conducted by Su & Chen (2002), two different sizes of crushed glass i.e. 0 to 0.315 mm and 0.63 to 2.5 mm were used as a substitute to the natural aggregates used (See Figure 2-21).

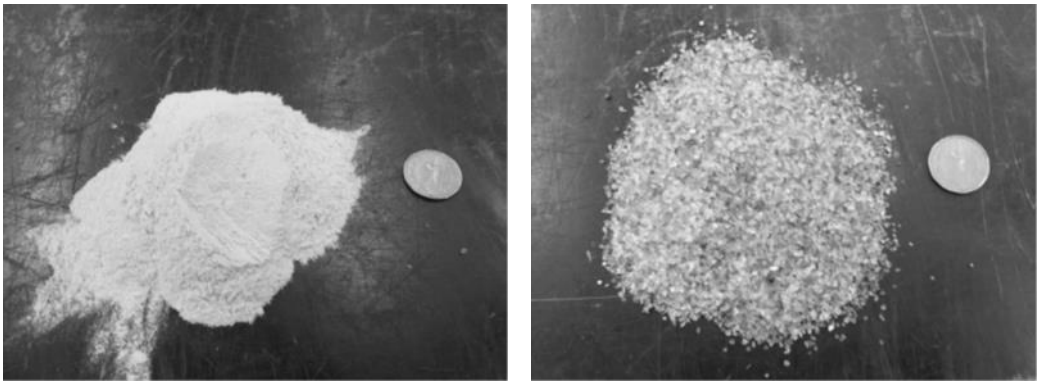

a) 0 to 0.315 mm **b) 0.63 to 2.5 mm**

Figure 2-21: Different sizes of crushed glass used (Lachance-Tremblay et al., 2014)

The design grading used to manufacture the glass-asphalt mixes was a 14 mm NMPS medium continuously-graded glass-asphalt mix. It was indicated that the design grading was similar for all contents of crushed glass (i.e. 5, 10, 15, 20, and 25%) and was designed to represent a similar design grading to that of the control mix.

The asphalt mix with 10% crushed glass was selected as the optimal mix on which the performance testing was carried out. This mix was selected based on the voids content being very similar to the reference mix at 100 gyrations. The optimum binder content of the mix was determined to be 4.53% at 5.5% air voids.

The rutting resistance of the selected glass and reference asphalt mix was evaluated with the "French Wheel Tracking Rutting test" using the "MLPC French rutting tester". The rut depth of the glass-asphalt mix after 30,000 cycles was approximately 1% lower than the control mix but was still below the maximum allowable rutting depth (i.e. 10% rut depth at 30 000 cycles).

The cracking resistance of the glass and reference asphalt mix at low temperatures was assessed by conducting the "thermal stress restrained specimen test (TSRST)". It was observed that the average failure stress and failure temperature of both asphalt mixes were the same. Additionally, it was observed that in both cases the average failure temperature was very close to the low temperature performance grade of the binder used in the investigation, i.e. -34°C. The addition of 10% crushed glass, therefore, did not have an effect on the low temperature performance of the asphalt mix.

The “stripping susceptibility test” was used to measure the resistance of the two mixes to moisture damage. The glass-asphalt mix demonstrated slightly inferior resisting to moisture damage than the reference mix. It should be mentioned, however, that no anti-stripping agent was added to the glass-asphalt mixes.

Details on the testing procedure and test specifications of the French Wheel Tracking Rutting test, TSRST and the stripping susceptibility test are not provided but can be referred to in the LC 26-410 (equivalent, EN 12697-22), AASHTO TP10-93 and LC 26-001 (equivalent, ASTM D1075) standards respectively.

Based on the study conducted by Lachance-Tremblay et al. (2014) it was concluded that the addition of 10% crushed glass can be utilised in asphalt mixes without compromising the overall performance of the asphalt mix. It was, however, recommended that special attention must be taken to consider the size of the crushed glass particles as well as to note that a decrease in resistance to rutting as well as moisture damage may occur due to the lack of adhesion between the bitumen and the surface of the crushed glass particles. As in previous studies conducted, it was indicated that this occurrence may be improved with the addition of an anti-stripping additive.

Anochie-Boateng and George (2016) conducted a study to compare the performance properties of a continuously-graded asphalt mix containing crushed glass with that of a traditional asphalt wearing course mix used on South African Roads. The performance of the asphalt mix was evaluated based on stiffness, permanent deformation and fatigue properties. The asphalt mix consisted of 15% crushed glass with the addition of 3% hydrated lime constituting the filler component in the mix, and serving as an antistripping additive to promote better adhesion between the bitumen and the glass particles. The crushed glass, utilised in the study, was collected from the same source as the crushed glass utilised in this dissertation. The particle size distribution of the crushed glass used for both studies is indicated in Section 2.1.5. The MPS of the glass utilised was 5 mm.

In order to conduct a comparative analysis on the performance of the two mixes, the same component materials as that of the traditional asphalt mix was utilised in the study. The traditional mix, however, did not incorporate an antistripping additive but consisted of 1% plant

fines (i.e. baghouse fines obtained from the asphalt manufacturing plant) as the filler component in the mix.

The design grading used to manufacture the glass-asphalt mix was a 10 mm NMPS medium continuously-graded glass-asphalt mix. The grading was designed to represent a similar design grading to that of the traditional asphalt mix. The optimum binder content of the glass-asphalt mix was 5.1% and was determined at 4% air voids. A similar optimum binder content (5.0%) was obtained for the traditional mix that did not contain crushed glass.

The dynamic modulus test was used to evaluate the stiffness properties of the glass-asphalt mix in comparison with the traditional mix. It was observed that at a test frequency of 10Hz and a test temperature of 20°C, the stiffness of the glass-asphalt mix improved by 25%. It was indicated that the above test conditions best simulate South African field pavement conditions.

The flow number test was used to evaluate the permanent deformation properties of the glass-asphalt mix and the traditional mix. It is known that asphalt mixes with a higher flow number demonstrates improved resistance to rutting (permanent deformation) than an asphalt mix with a lower flow number. The flow number results hence revealed that the glass-asphalt mix has higher rutting resistance at the tested conditions i.e. temperature of 50°C and stress levels of 276 kPa and 483 kPa than the traditional mix.

The observed behaviour has been attributed, in part, to the increased angularity of the glass particles which in turn increases the interlock between the glass particles and the aggregate, thereby contributing towards the improved permanent deformation resistance of the glass-asphalt mix. In addition, the incorporation of 3% hydrated lime in the glass-asphalt mix was also indicated to have contributed towards the improved stiffness properties of the glass-asphalt mix in comparison with the traditional mix, which incorporated 1% plant filler.

The fatigue properties of the two mixes were evaluated using the four-point beam fatigue test. Fatigue failure in asphalt layers occurs when the number of applied load repetitions surpasses the ability of the asphalt layer to resist the associated tensile strains. It was observed that the glass-asphalt mix, at a test frequency of 10Hz and a test temperature of 20°C, showed a significant reduction in fatigue life at the lower strain levels while comparable fatigue life was indicated at the higher strain levels.

Anochie-Boateng and George (2016) concluded that there is potential to utilise crushed glass as an aggregate substitute in asphalt wearing course mixes. This conclusion was drawn based on the improved performance obtained in stiffness and permanent deformation as well as the comparable fatigue life at high strain levels when compared to the traditional mix investigated in the study. Furthermore, the observed performance was based on the specified design grading for the glass-asphalt mix and the traditional mix as well as the component materials utilised to produce both mixes.

2.3 Summary

The literature study highlights the global use of crushed glass in HMA since the early 1970's. Countries that have reported using crushed glass in asphalt paving applications include United States, Canada, United Kingdom, Australia, New Zeland, Japan and Taiwan. Although large quantities of recycled crushed glass are available for exploitation in South Africa, the local use of this material in South African pavements has, however, not been utilised thus far and hence forms the basis for investigation in this study.

The literature study also highlights various favourable properties of crushed glass material for incorporation as an aggregate substitute in asphalt pavement applications. Such properties include the highly angular shape characteristics, low specific gravity, high thermal insulation properties as well as the high reflective properties of crushed glass material.

The smooth surface texture of glass material has, however, been emphasised as a contributory factor towards reduced adhesion at the bitumen and glass interface resulting in an increased susceptibility to stripping and ravelling in glass-asphalt pavements in comparison with traditional asphalt pavements. To avoid these concerns, various studies have limited the use of crushed glass up to 15% in the surface course with control limits set on the grading of the glass particles used. Few studies have also reported on the incorporation of various antistripping additives which have shown a marked improvement on the moisture susceptibility of glass-asphalt mixes and as such have been known to alleviate the common stripping related concerns. In addition, certain studies have indicated improved performance in terms of rutting and stiffness in HMA pavements incorporating up to 15% crushed glass above which reduced performance has been reported.

It was, however, noted that the studies reported have drawn conclusions and proposed recommendations on the use of crushed glass in asphalt mixes that are typical to a specific country or state while utilising the crushed glass material in combination with different types of coarse and fine aggregates common to a particular region. In addition the crushed glass material has in some cases been manually engineered to obtain a specific particle size distribution while in other cases the material has been used as obtained from their local glass manufacturing plants or material recovery facilities, which varies from one study to the other. Such variations including variations that arise from the use of different types of raw materials e.g. binder, filler material, antistripping additives etc. as well as different testing methodologies

and specifications (applicable to a specific country or state) may have an influence on the observed performance reported in the various investigations detailed in the literature study.

3. GLASS-ASPHALT MIX DESIGN

3.1. Introduction

Chapter 3 presents the design and production of a 10 mm nominal maximum particle size, medium continuously-graded glass-asphalt mix that consists of 15% recycled crushed glass as a partial substitute to the traditional fine aggregate in the mix. This percentage composition of recycled crushed glass was selected based on the findings from various studies (highlighted in Chapter 2) indicating an optimum crushed glass replacement ratio of 10 to 15%.

Three of the above glass-asphalt mixes were produced; with the first mix (referred to as GA Mix1) containing 1% hydrated lime which constitutes the filler component and acts as an antistripping additive. The second mix (referred to as GA Mix 2) consists of 1% "plant filler" (baghouse fines from asphalt manufacturing plant) as the filler component and contains a liquid antistripping additive. The third mix (referred to as GA Mix 3) comprises of the same filler component as GA Mix 2 (1% plant filler) and does not contain an antistripping additive. All three glass-asphalt mixes utilises the same aggregate materials. The incorporation of 1% hydrated lime was selected based on the maximum specified amount allowed for inclusion in continuously-graded asphalt mixes in South Africa (Sabita, 2016).

The glass-asphalt mixes are designed as a surfacing course with a design traffic level between 3 and 30 million Equivalent Standard Axle Loads (ESALs) and represents a similar design aggregate grading to the South African National Roads Agency Limited (SANRAL) medium continuously-graded asphalt mix (herein after referred to as the standard mix). It has been indicated that the standard asphalt mix is commonly used as a surfacing course on South African roads. Furthermore, to maintain consistency, the same aggregates as well as the same binder i.e. 50-70 penetration grade binder, utilised in the standard mix, was used to prepare the glass-asphalt mixes.

The glass-asphalt mix design and production makes use of standard design practices for traditional asphalt mixes in South Africa and is conducted in accordance with Sabita Manual 35/TRH 8 (2016) – "Design and Use of Asphalt in Road Pavements".

3.2. Raw Materials

3.2.1. Aggregate

The same aggregates from the same sources as the standard mix were utilised in this study. The aggregate materials and sources are provided in Table 3-1. The aggregate sources are all located in the Gauteng province.

Table 3-1: Aggregate Material and Sources

Aggregate Fractions	Aggregate Source
Andesite 9.5 mm	AfriSam Eikenhof
Andesite 6.7 mm	
Andesite Crusher dust (CD)	
Granite Crusher sand (CS)	AfriSam Jukskei
Mine sand	Benoni Summit

As indicated in Chapter 2, the recycled crushed glass was sourced from the Consol manufacturing plant located in Gauteng. Physical characterisation of the recycled crushed glass particles is discussed in detail in Section 3.7.

The aggregates and glass material were dried in an oven at a temperature of 105°C for a duration of 16 hours, after which the materials were split down by riffling to the approximate quantities required by the mix. Wet sieve analysis was conducted on the individual aggregate fractions as well as on the glass material. Photographs of the glass material retained on each standard sieve is presented in Figure 3-1. The sieve analysis was conducted in accordance with South African National Standard (SANS) 3001-AG1 (2014). The results are presented in Table 3-3 and illustrated graphically in Figure 3-2.

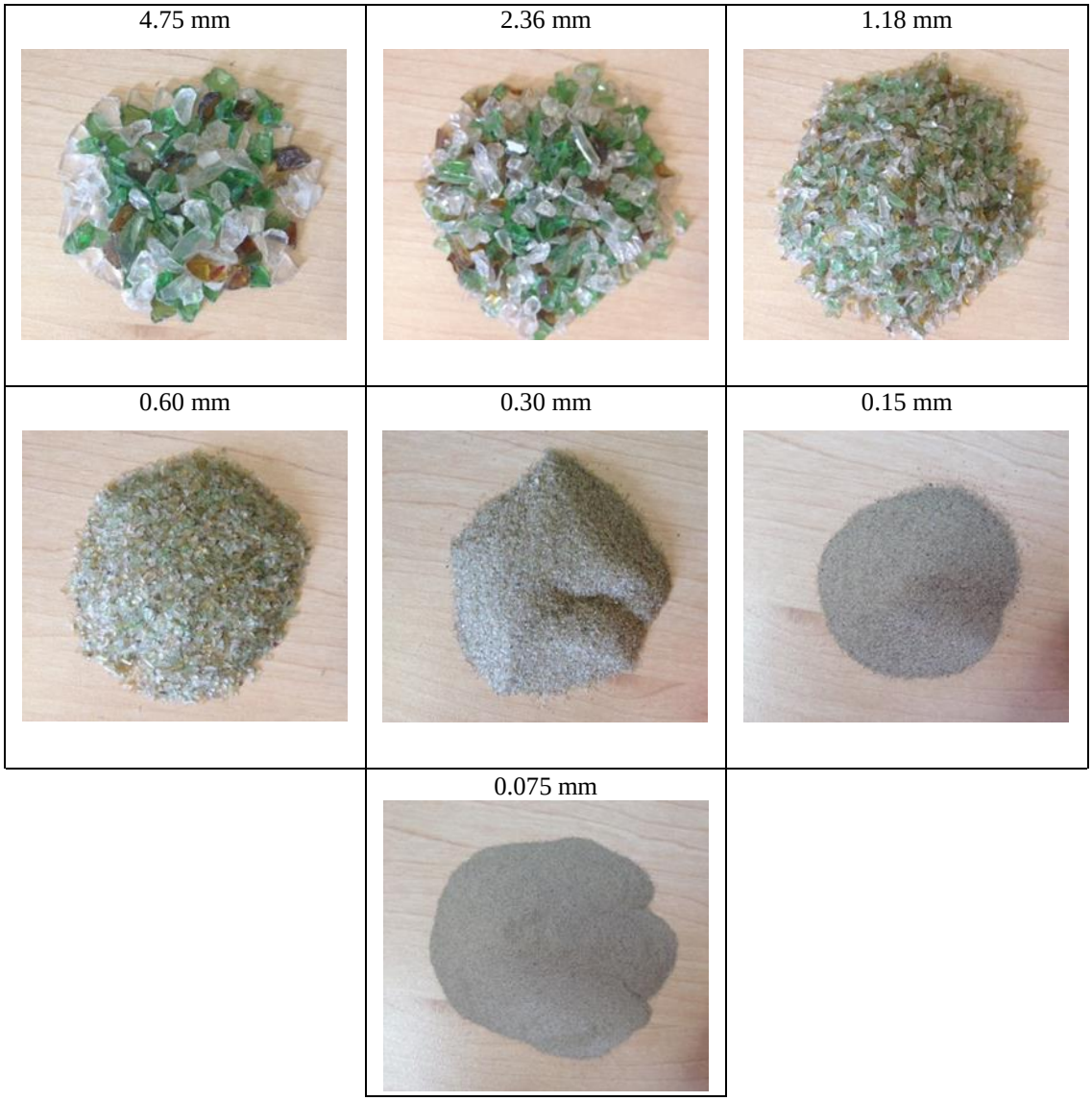

Figure 3-1: Photographs of recycled crushed glass particles retained on standard sieve size

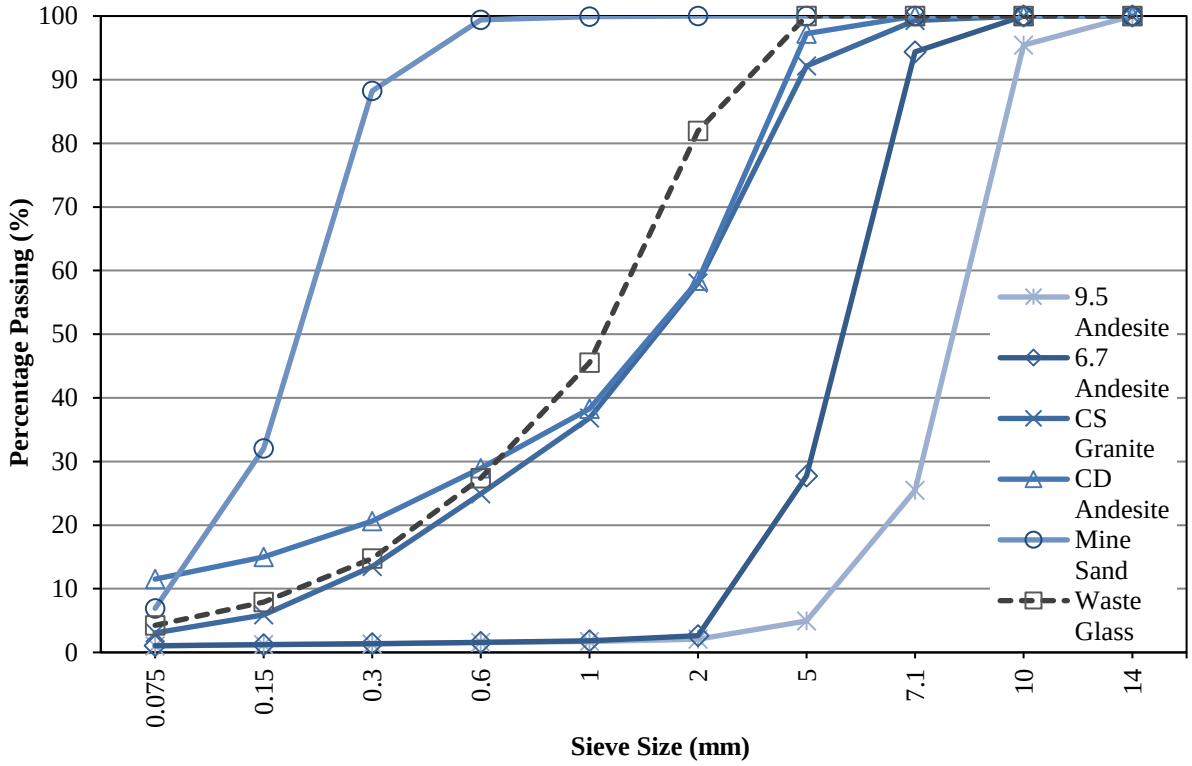

Figure 3-2: Particle size distribution of individual aggregate fractions

3.2.2. Filler

Hydrated lime, supplied by Lime Distributors (Pty) Ltd., and baghouse fines (referred to as plant filler and comprising mainly of SiO_2), obtained from the Much Asphalt plant in Eikenhof, were used as the mineral filler component in GA Mix 1 and GA Mix 2, 3 respectively. The hydrated lime and plant filler has a particle size range between 1.5 and 75 µm and 0.4 and 75 µm respectively.

3.2.3. Bituminous Binder

A 50-70 penetration grade binder, manufactured by the National Petroleum Refiners of South Africa (Pty) Ltd. (Natref), was obtained from the Much Asphalt plant in Benoni. The properties of the binder were determined as per the relevant standard test method indicated in Table 3-2. Tests were conducted on the original binder as well as on the binder subjected to the Rolling Thin Film Oven Test (RTFOT – to simulate ageing that occurs during manufacture and laying of the mix). The tests were conducted at the Advanced Materials Testing Laboratory at the CSIR.

Based on the results presented in Table 3-2, it can be seen that the properties of the binder comply with the requirements as specified in SANS 4001 BT1 (2016).

Table 3-2: Properties of the 50-70 Penetration Grade Binder

Properties	Unit	Test Results	Requirement	Test Method
Penetration	dmm	65	50-70	EN 1426
Softening Point	°C	47.4	46-56	ASTM D36M
Viscosity				
at 60°C	Pa.s	256	>120	ASTM D4402M
at 135°C	mPa.s	493	220-500	ASTM D4402M
Flash Point	°C	328	≥230	ASTM D92
Spot Test	% xylene	Negative up to 30	Negative up to 30	AASHTO T102
After RTFOT-ageing				
Mass Change	%m/m	0.096	0.3 max	ASTM D2872
Viscosity at 60°C	Pa.s	658		ASTM D4402M
% original	% original	257	300 max	ASTM D4402M
Softening Point	°C	53.4	48 min	ASTM D36M
Increase	°C	6	7 max	ASTM D36M
Penetration	dmm	43		EN 1426
% original	% original	66	55 min	EN 1426

3.2.4. Antistripping Additives

Hydrated lime and a liquid additive, namely WETFIX BE, were applied as antistripping additives. Much Asphalt among other asphalt manufacturing companies in South Africa has indicated use of the above mentioned liquid additive as an adhesion promoter in Hot Mix Asphalt. A dosage amount of 0.5% of WETFIX BE (by volume of binder), as recommended by the supplier, was added to the binder.

The application process of the liquid additive to the binder involved heating the original binder to approximately 150°C (mixing temperature), maintaining the same temperature on a hot plate while blending in the liquid additive, using a high shear blender, for one hour. The blended binder was thereafter maintained at the same temperature and immediately incorporated into the mix.

3.3. Aggregate Design

The design grading of the standard mix was used as the target grading in this study for the glass-asphalt mix designs. Table 3-3 indicates the percentage incorporation (percentage blend) of each aggregate fraction and the filler required to achieve the target grading. The target

grading was achieved by adjusting the percentage blends in order to minimize the sum of the least squared difference between the glass-asphalt design grading and the target grading. This optimization technique was conducted using the "Solver" function in Microsoft Excel™. The objective was to obtain a similar particle size distribution to that of the standard mix.

It should be noted that for comparative analysis, the aggregate designs for all three glass-asphalt mixes (GA Mix 1, 2 and 3) are the same. The crusher sand aggregate in the standard mix is partially substituted with 15% waste glass material in GA Mix 1, 2 and 3. Although the type of filler varies in all three mixes - with GA Mix 1 containing 1% hydrated lime and GA Mix 2, 3 containing 1% plant filler - the design grading is not affected due to a similar particle size distribution of both filler components.

As previously stated, GA Mix 2, in addition, contains a liquid antistripping additive which is incorporated with the binder as described in Section 3.2.4 above. The hydrated lime in GA Mix 1 was selected to replace the 1% of plant filler in the standard mix so as to achieve the desired bonding effect between the glass and the binder.

As specified in Sabita Manual 35/TRH 8 (2016), the design grading has been plotted on a 0.45 power chart as illustrated in Figure 3-3. In this approach, the sieve size values are raised to the power of 0.45 before being plotted. The maximum density line in Figure 3-3 represents the grading at 0% voids. It can be observed that the grading represents a coarse grading between 0.075 mm and 5 mm (i.e. when design grading lies below the maximum density line) and a fine grading between 7.1 mm and 14 mm (i.e. when design grading lies above the maximum density line).

Furthermore, it can be observed that the design grading falls within the grading control points specified for a 10 mm nominal maximum particle size (NMPS) continuously graded asphalt mix (Sabita, 2016). NMPS is defined in Sabita Manual 35/TRH8 (2016) as "one sieve size larger than the largest sieve to retain a minimum of 15 percent of the aggregate particles".

Table 3-3: Aggregate design for GA Mix 1, 2 and 3

.		AGGREGATE						FILLER		AGGREGATE DESIGN				
		GA Mix 1, 2 & 3						GA Mix 1	GA Mix 2&3	GA Mix 1, 2 & 3			Grading Spec.	
		9.5 Andesite	6.7 Andesite	CD Andesite	CS Granite	Mine Sand	Recycled crushed glass	HL	PF	Design Grading	Target Grading	Standard Deviation	Min	Max
% Blend		**28%**	**17%**	**22%**	**11%**	**6%**	**15%**	**1%**	**1%**				(%)	(%)
		PERCENTAGE PASSING (%)												
Sieve Size (mm)	14	100	100	100	100	100	100	100	100	**100**	100	0.0	**100**	
	10	95	100	100	100	100	100	100	100	**99**	97	1.2	**80**	**100**
	7.1	25	94	100	99	100	100	100	100	**78**	75	2.2		**85**
	5	5	28	97	92	100	100	100	100	**60**	59	0.4		
	2	2	3	58	58	100	82	100	100	**40**	42	1.7	**32**	**67**
	1	2	2	38	37	100	46	100	100	**27**	30	2.1		
	0.6	2	2	29	25	99	27	100	100	**21**	21	0.1		
	0.3	1	1	21	13	88	15	100	100	**15**	14	0.8		
	0.15	1	1	15	6	32	8	100	100	**9**	9	0.3		
	0.075	1.0	1.1	11.5	3.1	6.9	4.3	99.0	99.0	**5.4**	5.8	0.3	**4**	**10**

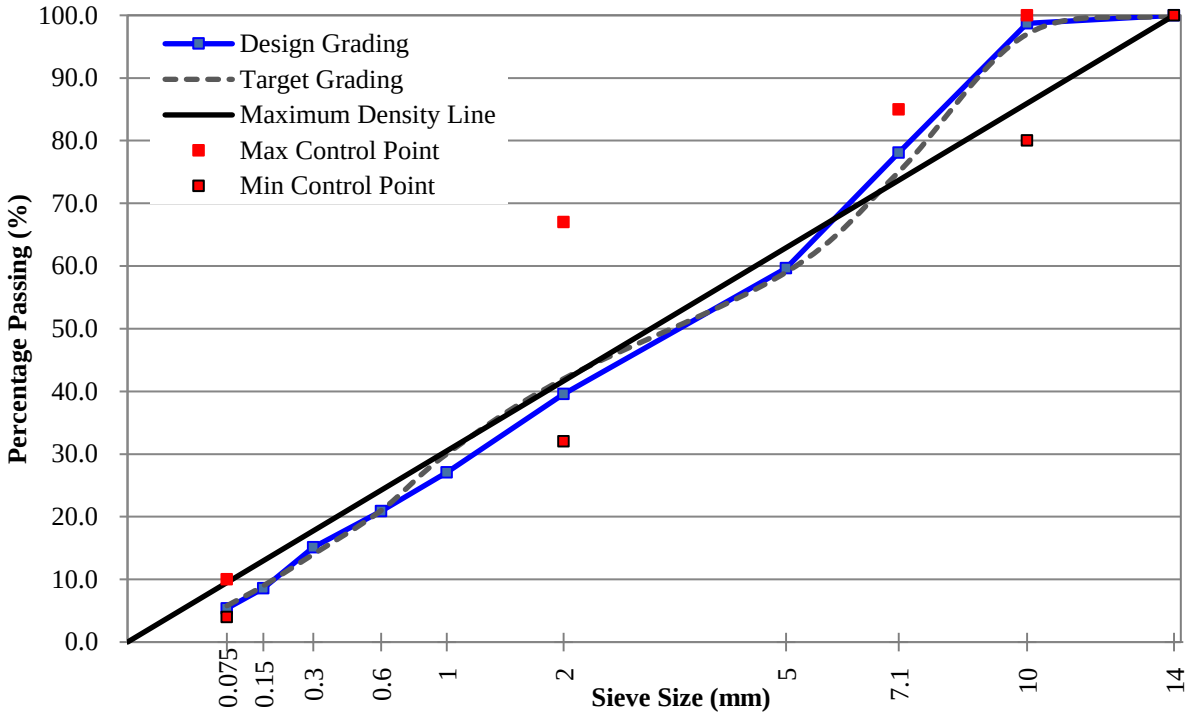

Figure 3-3: Design grading of 10 mm NMPS GA Mix 1, 2 & 3

3.4. Minimum Binder Content

In accordance with Sabita Manual 35/TRH8 (2016), the minimum binder content for GA Mix 1, 2 and 3 was determined in accordance with Equation 3-1:

$$B_{ppc} = K * \propto * \sqrt[5]{SA} \qquad \text{Equation 3-1}$$

Where:

1. B_{ppc}= mass of binder expressed as a percentage of the total dry mass of aggregate, including filler
2. K = richness modulus (K) is a measure of the thickness of the binder film coating the aggregate. Minimum K values are provided in Sabita Manual 35/TRH 8 (2016) as 2.9 for sand skeleton mixes and 3.4 for stone skeleton mixes
3. α = correction coefficient for the bulk density of the aggregate (BD_A), determined as follows:

$$\propto = \frac{2.65}{BD_A}$$

The BD of the aggregate sample was calculated by determining the ratio between the mass of the aggregate sample to the volume of water the aggregate sample displaces in accordance with

SANS 3001-AG20 (2014) for the aggregates retained on the 5 mm sieve and SANS 3001-AG21 (2014) for the aggregate passing 5 mm sieve.

The BD_A in GA Mix 1, 2 and 3 was obtained by multiplying the BD_A by the percentage blend of aggregate in the mix as indicated in Table 3-4 and 3-5.

Table 3-4: Bulk density of aggregate in GA Mix 1

Aggregate	**BD_A** (ton/m^3)	**% Blend**	**BD_A in Mix** (ton/m^3)
9.5 Andesite	2.877	28%	0.806
6.7 Andesite	2.886	17%	0.491
CD Andesite	2.770	22%	0.609
CS Granite	2.619	11%	0.288
Mine Sand	2.642	6%	0.159
Recycled crushed glass	2.451	15%	0.368
Hydrated Lime	2.440	1%	0.024
Total BD_A in Mix (ton/m^3)			**2.744**

Table 3-5: Bulk density of aggregate in GA Mix 2 & 3

Aggregate	**BD_A** (ton/m^3)	**% Blend**	**BD_A in Mix** (ton/m^3)
9.5 Andesite	2.877	28%	0.806
6.7 Andesite	2.886	17%	0.491
CD Andesite	2.770	22%	0.609
CS Granite	2.619	11%	0.288
Mine Sand	2.642	6%	0.159
Recycled crushed glass	2.451	15%	0.368
Plant Filler	2.770	1%	0.028
Total BD_A in Mix (ton/m^3)			**2.748**

4. SA= specific surface area of blended aggregates (m²/kg)

As per Sabita Manual 35/TRH8 (2016), the specific surface area (SA) is estimated based on the design aggregate grading of the asphalt mix and specified SA factors. The aggregate SA is determined by multiplying the SA factors by the percentage passing the various sieve sizes as determined by Equation 3-2. The results for GA Mix 1, 2 and 3 are presented in Table 3-6.

$$\boldsymbol{SA = (2 + 0.02a + 0.04b + 0.08c + 0.14d + 0.3e + 0.6f + 1.6g) * 0.20482} \qquad \text{Equation 3-2}$$

Where:

a = percentage passing 5 mm sieve;

b = percentage passing 2 mm sieve;

c = percentage passing 1 mm sieve;

d = percentage passing 0.60 mm sieve;

e = percentage passing 0.30 mm sieve;

f = percentage passing 0.15 mm sieve, and

g = percentage passing 0.075 mm sieve.

Table 3-6: Aggregate specific surface area for GA Mix 1, 2 and 3

Sieve Size (mm)	% Passing
5	60
2	40
1	27
0.6	21
0.30	15
0.15	09
0.075	5.4
Total Surface Area (SA)	**5.60**

A minimum K value of 2.9, recommended for medium dense-graded asphalt mixes (Sabita, 2016), as well as the determined specific surface area and bulk relative density of the aggregates in the mix were used to determine the minimum binder content for GA Mix 1, 2 and 3 as per Equation 3-1. The obtained results are presented in Table 3-7.

Table 3-7: Determination of minimum binder content

Glass-Asphalt Mix	Calculation	Minimum Binder Content
GA Mix 1	$B_{ppc} = 2.9 * \frac{2.65}{2.744} * \sqrt[5]{5.60}$	4.0%
GA Mix 2 and 3	$B_{ppc} = 2.9 * \frac{2.65}{2.748} * \sqrt[5]{5.60}$	3.9%

3.5. Volumetric Properties

The following properties were determined at four trial binder contents as specified in Sabita Manual 35/TRH8 (2016). The minimum binder content is selected as the first trial binder content and thereafter increases by increments of 0.5%.

3.5.1. Maximum Voidless Density (MVD)

The MVD of an asphalt mix is the relative density which does not include the air voids. Hence, if an asphalt sample did not include any air voids, theoretically, the relative density would be at a theoretical maximum for the remaining aggregate and binder.

The MVD is calculated by determining the ratio of the weight of an asphalt sample (which is a loose sample that has not been compacted) to its volume, which is measured by the amount of water it displaces.

In this study, two loose glass-asphalt samples were prepared from the design aggregate grading to determine the MVD at each trial binder content. The MVD was obtained in accordance with SANS 3001-AS11 (2011). Results for GA Mix 1, 2 and 3 are summarised in Table 3-8 and presented in detail in Appendix A – Table A1.

Table 3-8: MVD results at each trial binder content for GA Mix 1, 2 and 3

Binder Content (%)	MVD 1 (ton/m^3)	MVD 2 (ton/m^3)	Average MVD (ton/m^3)
GA Mix 1			
4.0	2.615	2.617	2.616
4.5	2.591	2.593	2.592
5.0	2.575	2.577	2.576
5.5	2.560	2.554	2.557
GA Mix 2			
3.9	2.621	2.620	2.620
4.4	2.593	2.597	2.595
4.9	2.579	2.583	2.581
5.4	2.559	2.563	2.561
GA Mix 3			
3.9	2.615	2.620	2.617
4.4	2.599	2.597	2.598
4.9	2.580	2.575	2.578
5.4	2.556	2.561	2.559

3.5.2. Bulk Density (BD), Voids in Mix (VIM) and Optimum Binder Content

Three specimens were compacted at each trial binder content in accordance with AASHTO T312 (2015). Mixing, compaction and specimen preparation is provided in detail in Section 3.6. The specimens were compacted to the specified dimensions of approximately 150 mm diameter by 115 $\pm$ 5 mm height at 100 gyrations as indicated in Table 3-9. Sabita Manual

35/TRH 8 (2016) specifies a laboratory compaction requirement of 100 gyrations for a design traffic level of 3 to 30 million ESAL's.

BD tests were thereafter conducted on the compacted specimens in accordance with SANS 3001-AS10 (2011). The BD of an asphalt specimen is the density of the specimen (mass per unit volume) relative to the density of water at 23°C. The BD of an asphalt specimen is calculated by determining the ratio between the weight of the specimen to the volume of water the specimen displaces. The BD results are summarised in Table 3-9 and presented in detail in Appendix A – Table A2.

The laboratory measured MVD values (See Section 3.5.1) and BD values were used to determine the voids of the compacted specimens as determined in Table 3-9. The voids of the compacted specimens (VIM) of GA Mix 1, 2 and 3 were hence plotted against each trial binder content as presented in Figures 3-3 to 3.5.

The VIM versus binder content graphs was used to determine the optimum binder content of the three glass-asphalt mixes. Sabita Manual 35/TRH 8 (2016) requires the optimum binder content to be established at 4% air voids. An optimum binder content of 5.4% for GA Mix 1, 2 and 3 was determined graphically at 4% air voids on the VIM versus binder content graph as presented in Figures 3-3 to 3.5. The obtained optimum binder content was then used to determine the volumetric properties of the mixes. It can be seen from Figures 3-4 to 3.6, that the BD of GA Mix 1, 2 and 3 was determined at approximately 2.46 at the optimum binder content of 5.4%.

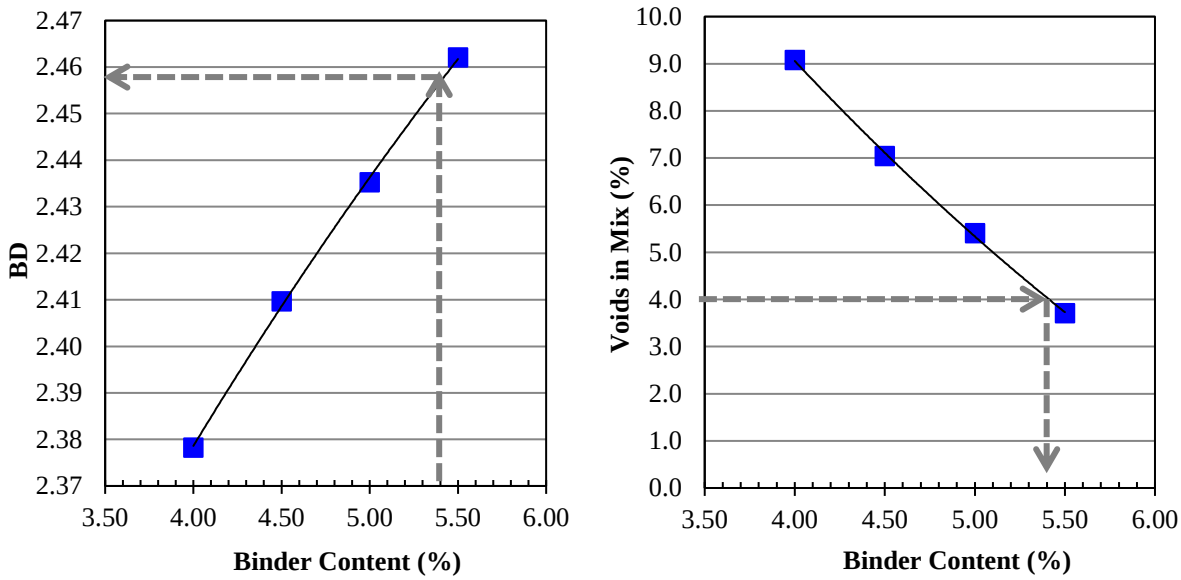

Figure 3-4: Bulk density and voids in GA Mix 1 after 100 gyrations

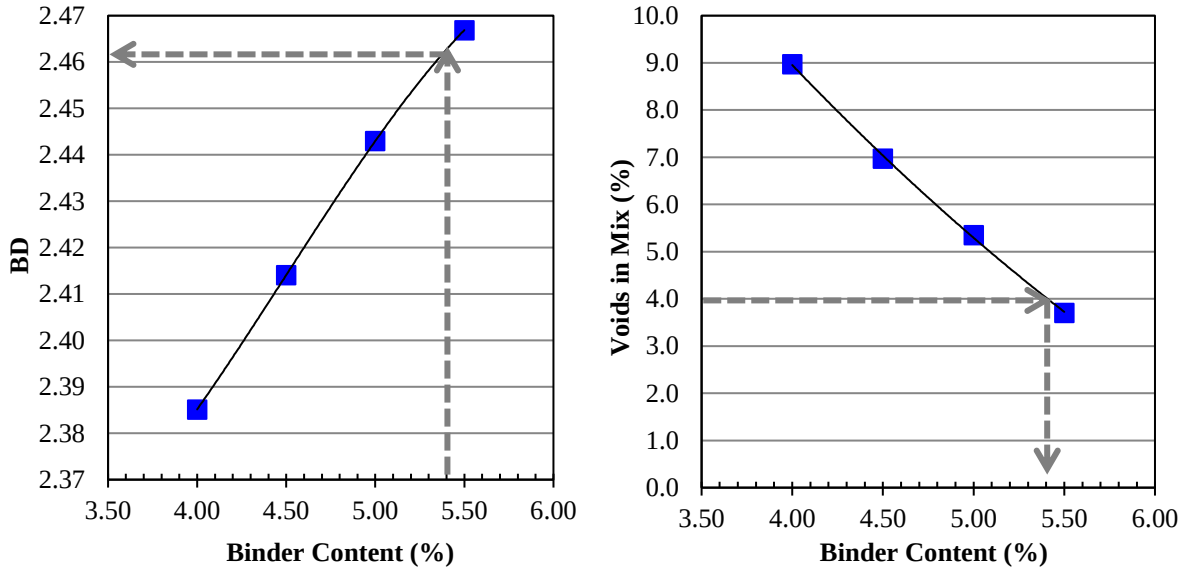

Figure 3-5: Bulk density and voids in GA Mix 2 after 100 gyrations

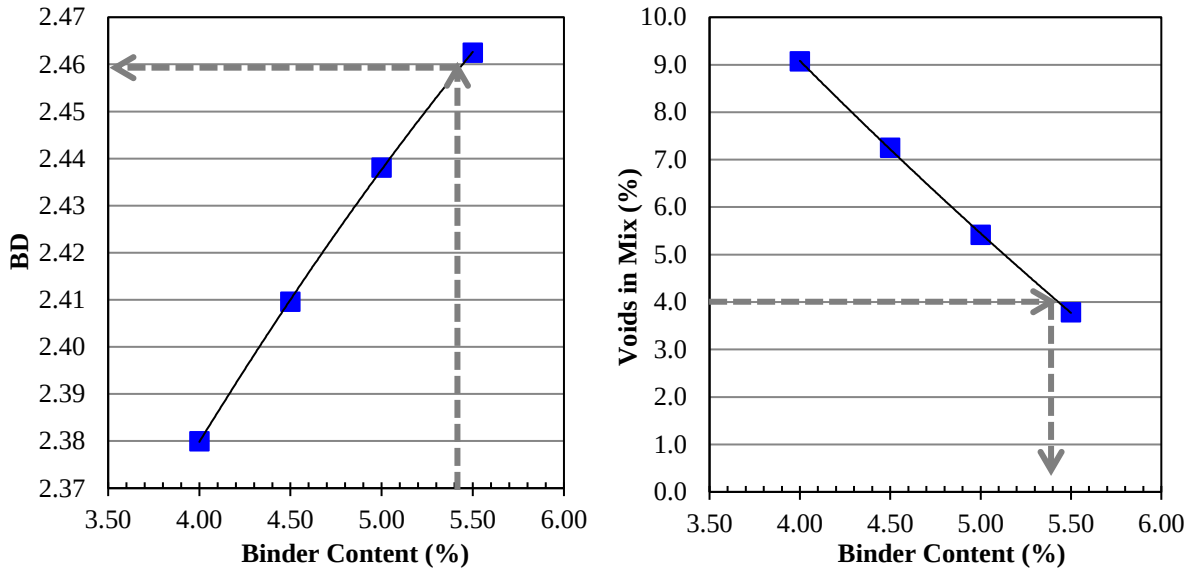

Figure 3-6: Bulk density and voids in GA Mix 3 after 100 gyrations

Table 3-9: Bulk density and voids in GA Mix 1, 2 and 3 after 100 gyrations

Binder Content (%)	Sample No.	Height (mm)	Diameter (mm)	BD (ton/m^3)	Avg.BD (ton/m^3) (A)	Avg. MVD (ton/m^3) (B)	Voids (%) (B-A)/(B)
GA Mix 1							
4.0	15036G 16	121.3	149.9	2.375	2.378	2.616	9.1
	15036G 17	121.4	149.9	2.381			
4.5	15036G 07	119.2	149.9	2.408	2.410	2.592	7.0
	15036 gg1	119.5	149.9	2.411			
5.0	15036G 08	117.6	150.0	2.436	2.438	2.576	5.4
	15036G 19	116.9	150.0	2.440			
5.5	15036G 12	116.7	149.9	2.459	2.462	2.557	3.7
	15036G 13	116.2	150.0	2.465			
GA Mix 2							
3.9	15036G PF AS04	121.3	149.9	2.386	2.385	2.620	9.0
	15036G PF AS05	120.9	150.1	2.384			
4.4	15036G PF AS07	119.7	149.9	2.420	2.414	2.595	7.0
	15036G PF AS09	119.9	149.9	2.409			
4.9	15036G PF AS01	117.6	149.8	2.445	2.443	2.581	5.4
	15036G PF AS02	118.0	149.8	2.441			
5.4	15036G PF AS10	117.4	149.9	2.462	2.467	2.561	3.7
	15036G PF AS11	116.5	149.9	2.470			
	15036G PF AS12	116.4	149.9	2.469			
GA Mix 3							
3.9	15036G PF18	120.7	149.9	2.383	2.380	2.617	9.1
	15036G PF20	121.0	150.0	2.377			
4.4	15036G PF13	119.6	149.9	2.408	2.410	2.598	7.2
	15036G PF14	119.2	149.9	2.411			

4.9	15036G PF01	117.6	149.9	2.440	2.439	2.578	5.4
	15036G PF02	117.9	149.9	2.437			
5.4	15036G PF09	116.7	150.0	2.459	2.462	2.559	3.8
	15036G PF10	116.2	150.0	2.465			

3.5.3. Voids in Mineral Aggregate (VMA)

VMA is defined as the volume of voids between the bitumen coated aggregated particles (i.e. air voids) and the volume of effective binder (binder not absorbed) as illustrated in Figure 3-7. The VMA is therefore the volume that is available for filling with binder, plus any inter-particle voids that may be unfilled after the binder has been added.

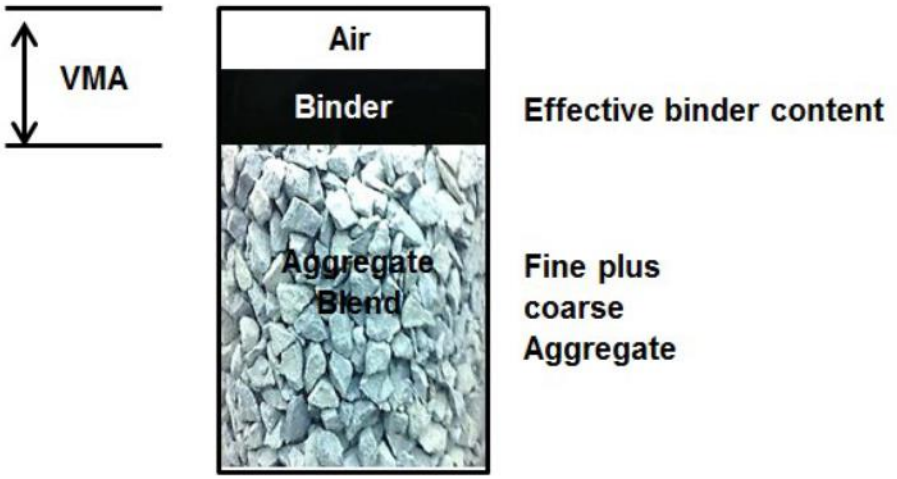

Figure 3-7: Illustration of voids in mineral aggregate (VMA)

As specified in Sabita Manual 35/TRH 8 (2016), the effective binder (B_{EF}) for GA Mix 1, 2 and 3 was determined in accordance with SANS 3001-AS11 (2011) and is presented in Table 3 -10. The following were considered in the calculations:

- The bulk density of the binder (BD_B) was determined in accordance with ASTM D70. The BD_B was determined to be 1030 kg/m^3
- The bulk density of the aggregate (BD_A) was determined to be 2744 kg/m^3 for GA Mix 1 and 2748 kg/m^3 for GA Mix 2 & 3 (See Table 3-4 and 3-5).
- The density of water (ρ_w) was considered to be 997.1 kg/m^3

Table 3-10: Effective binder content for GA Mix 1, 2 and 3

BC	M_B	M_A	V_B	V_A	V_T	V_{DA}	B_{ABS}	M_{BABS}	M_{BEF}	B_{EF}
	Mass of binder in mix	Mass of aggregate in mix	Volume of binder in mix	Volume of aggregate in mix	Total volume of binder and aggregate in	De-aired volume of mix	Binder absorbed by aggregate	Mass of binder absorbed in	Mass of effective binder in mix	% of effective binder in mix
(%)	(g)	(g)	(cm^3)	(cm^3)	(cm^3)	(cm^3)	(%)	(g)	(g)	(%)
GA Mix 1										
4.0	49.55	1189.30	48.11	433.42	481.53	474.98	0.57	6.75	42.81	3.43
4.5	56.37	1196.28	54.73	435.96	490.69	484.66	0.52	6.22	50.15	3.98
5.0	62.33	1184.22	60.51	431.57	492.08	485.31	0.59	6.98	55.35	4.41
5.5	69.42	1192.78	67.40	434.69	502.09	495.09	0.60	7.21	62.21	4.90
GA Mix 2										
3.9	49.42	1186.18	47.98	431.65	479.64	472.92	0.58	6.92	42.51	3.42
4.4	55.58	1179.57	53.96	429.25	483.21	477.33	0.51	6.05	49.53	3.99
4.9	61.65	1171.26	59.85	426.22	486.07	479.04	0.62	7.24	54.40	4.38
5.4	68.52	1177.38	66.53	428.45	494.98	487.97	0.61	7.22	61.30	4.89
GA Mix 3										
3.9	49.53	1188.77	48.09	432.59	480.68	474.48	0.54	6.39	43.14	3.46
4.4	56.04	1189.26	54.41	432.77	487.18	480.74	0.56	6.63	49.41	3.94
4.9	61.87	1175.44	60.06	427.74	487.81	481.40	0.56	6.60	55.26	4.44
5.4	69.20	1189.05	67.19	432.70	499.88	493.18	0.58	6.90	62.30	4.92

It can be observed from Table 3-10 that the binder absorption (B_{ABS}) for GA Mix 1, 2 and 3 is on average 0.57%. Lower binder absorption is expected for glass-asphalt mixes as opposed to conventional asphalt mixes. This is primarily due to the lower absorptive properties of the crushed glass particles as opposed to traditional aggregates. This in turn will result in a higher effective binder content in glass-asphalt mixes.

The B_{EF} (see Table 3-10), BD and VIM (see Table 3-9) of GA Mix 1, 2 and 3 were then utilised to calculate the VMA as per the following equations set out in Sabita Manual 35/TRH 8 (2016):

$$\boldsymbol{Volume\ of}\ \mathbf{B_{EF}}\ (\%) = \frac{\mathbf{B_{EF}} * \mathbf{BD}}{\boldsymbol{BD_B}} \qquad \text{Equation 3-3}$$

$$\boldsymbol{VMA}\ (\%) = \boldsymbol{Volume\ of}\ \mathbf{B_{EF}} + \boldsymbol{VIM} \qquad \text{Equation 3-4}$$

The determined volume of B_{EF} and VMA values are presented in Appendix A – Table A2. The results were plotted at each trial binder content and the VMA was determined at the obtained

optimum binder content (5.4%) and thereafter assessed against the minimum VMA criteria (15%) as presented in Figure 3-8. It can be observed that GA Mix 1, 2 and 3 meets the minimum criteria with a VMA value a tad greater than 15.5%. In South Africa, the minimum VMA criteria for a 10 mm NMPS continuously-graded asphalt mix at 4% design voids is 15% (Sabita, 2016).

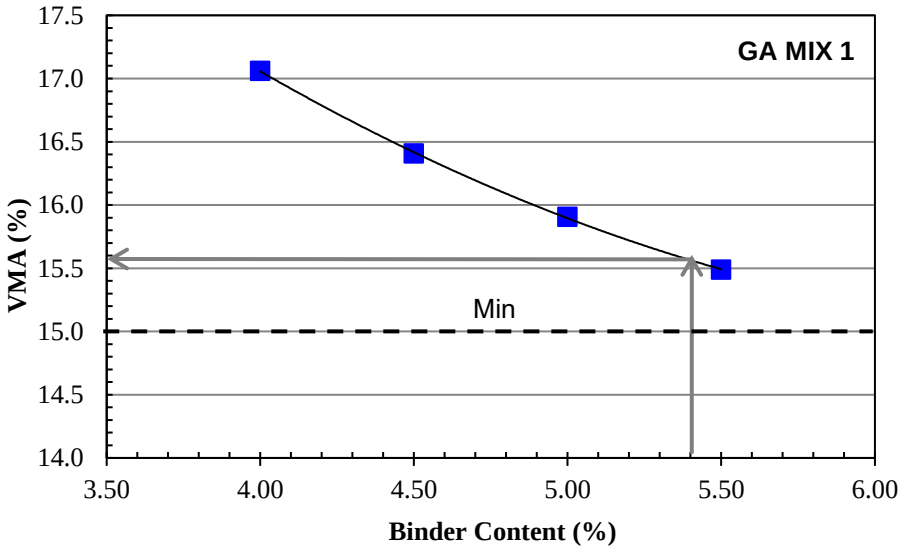

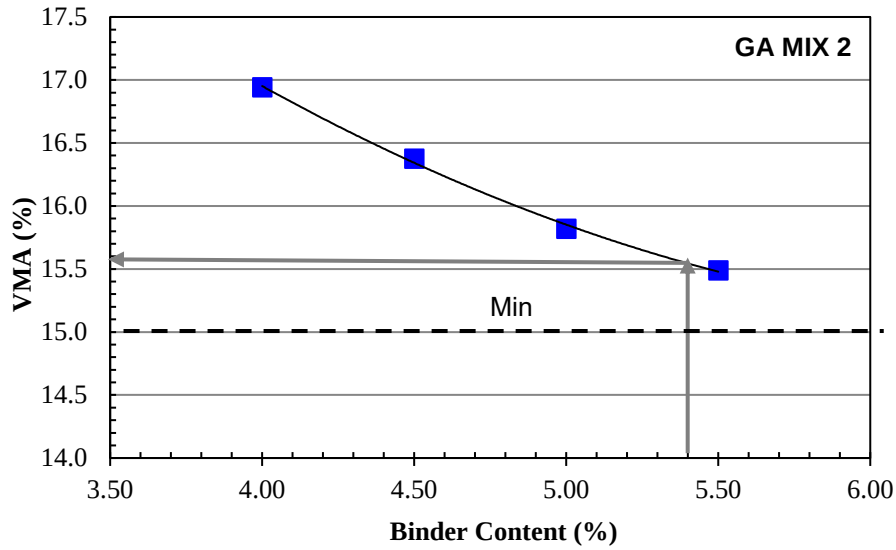

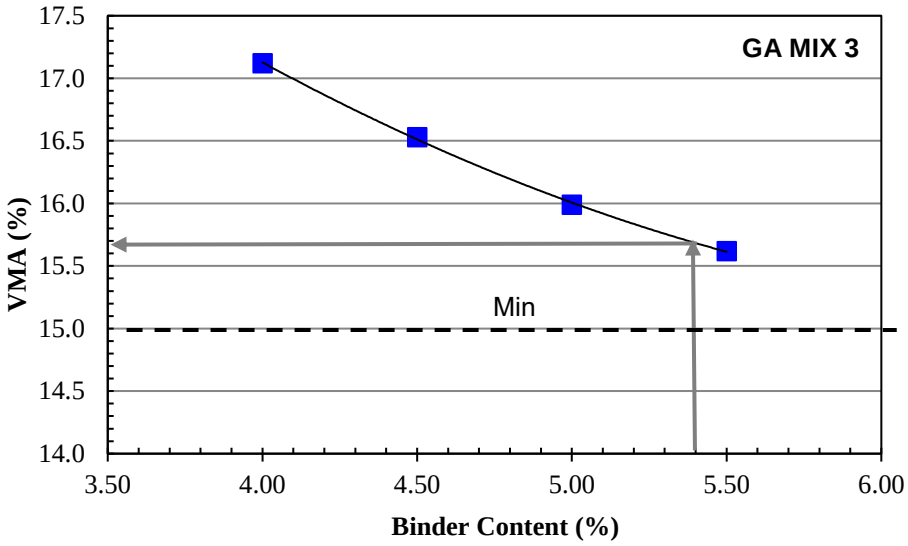

Figure 3-8: Voids in mineral aggregate for GA Mix 1, 2 and 3

3.5.4. Voids Filled with Binder (VFB)

VFB is the percentage of voids between aggregate particles (i.e. VMA) in the mix that is filled with binder. The VFB for GA Mix 1, 2 and 3 was determined as per Equation 3-5 (Sabita, 2016):

$$\boldsymbol{VFB = 100 * \left(\frac{Volume\ of\ B_{EF}}{VMA}\right)} \qquad \text{Equation 3-5}$$

The determined VFB values are presented in Appendix A – Table A2. The results were plotted at each trial binder content and the VFB was determined at the obtained optimum binder content (5.4%) and thereafter assessed against the VFB requirements set out in Sabita manual 35/TRH 8 (2016) as presented in Figure 3-9. The lower and upper VFB limit specified in Sabita manual 35/TRH8 is 65% and 75% respectively for a design traffic level between 3 and 30 million ESALs. It can be observed that GA Mix 1, 2 and 3 meets both of the standard requirements with a VFB of approximately 74%.

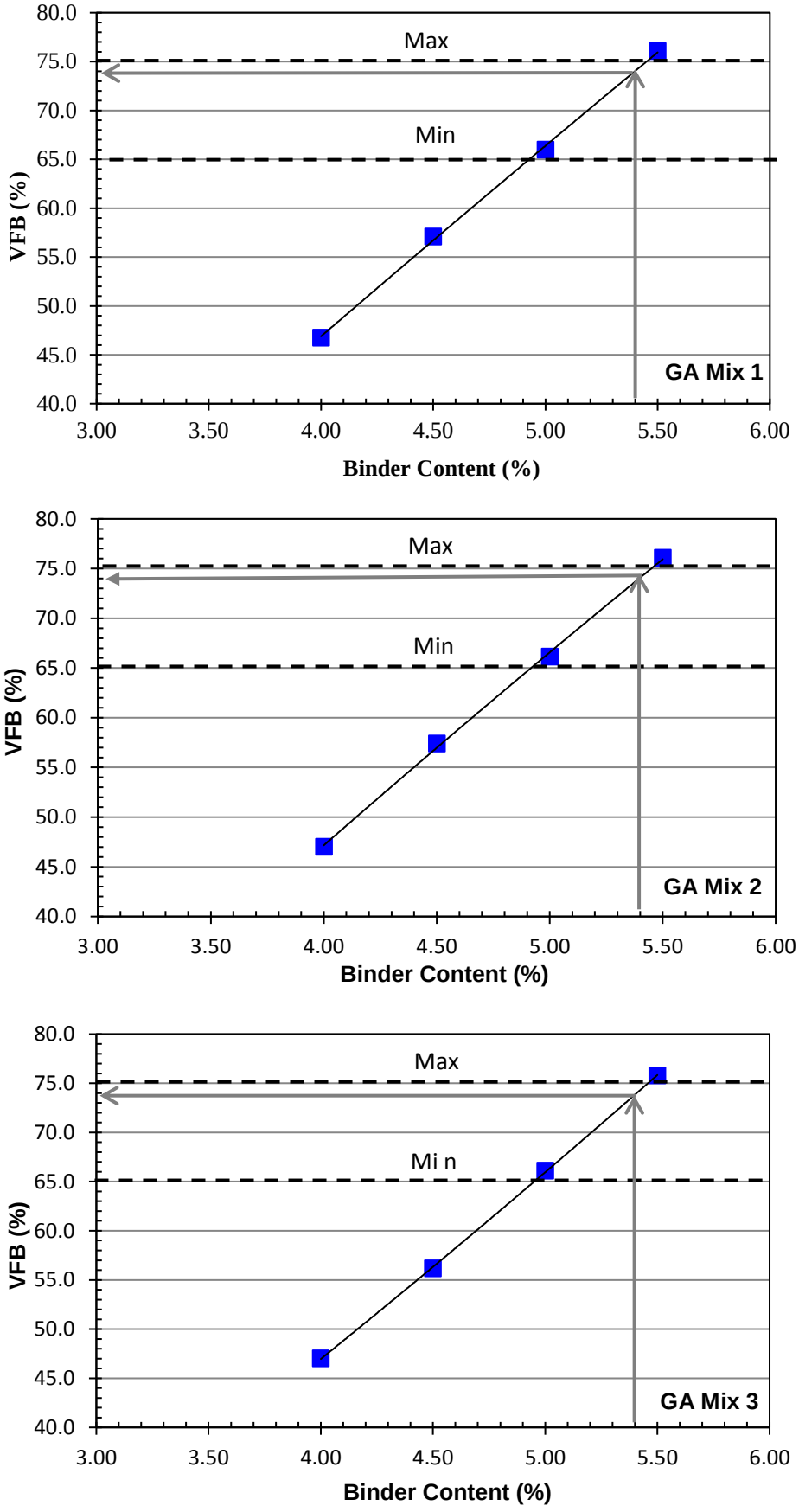

Figure 3-9: Voids filled with binder for GA Mix 1, 2 and 3

3.6. Mixing, Ageing, Compaction and Specimen Preparation

3.6.1. Mechanical Mixing

A heated mechanical mixer was used to prepare the asphalt mix. The constituent aggregates was placed in the mixer (preheated to 165°C) as well as the binder and mixed together at a temperature of 150°C for nearly 15 minutes until the aggregates appeared to be well coated with the binder. The aggregates were incorporated as per the design aggregate grading.

3.6.2. Short-term Oven Ageing

The mixture was then placed in an oven for short-term ageing. The prepared mix is short-term aged to simulate the ageing process that occurs during the asphalt production phase and the transportation phase. The short-term ageing was performed on loose mixtures before compaction. The mix was aged at 135ºC (compaction temperature) for 4 hours in open pans in a standard forced ventilation laboratory oven.

3.6.3. Gyratory Compaction

Gyratory compacted specimens were produced for the mix designs, Modified Lottman test, Hamburg wheel tracking test, flow number and dynamic modulus tests. Specimens were compacted using a computer controlled Industrial Process Controls Ltd (IPC) gyratory compactor. The gyratory compaction procedure that was followed was in accordance with the CSIR test protocol development for SAPDM (Anochie-Boateng et al., 2010) and AASHTO T312 (2015). The mass of the mix required to achieve the desired height and voids was calculated using the procedure stipulated in AASHTO T312 (2015) and the CSIR protocol respectively. The hot mix material was placed in the mould after the ageing period and rodded around the sides to prevent segregation of the mix. The filled mould was then placed into the gyratory compactor for compaction.

3.6.4. Specimen Preparation

Specimens were compacted to specified dimensions for the above mentioned tests. Following compaction, the specimens were subjected to a cooling period of roughly 10 minutes in the moulds, following which they were removed from the mould. The extruded specimens were then allowed to cool overnight after which, the bulk relative density of the compacted specimens were determined. For the performance tests (i.e. flow number and dynamic modulus tests), a 100 mm diameter specimen was cored from the centre of a 150 mm diameter

compacted specimen and the top and bottom were cut to produce a specimen that was 150 mm in height. The bulk relative density of the cored specimen was once again determined as before.

3.7. Physical Characterisation of Aggregate and Recycled Crushed Glass

3.7.1. Bulk Density (BD)

BD is defined as the ratio of the mass of a unit volume of aggregate, including the water permeable voids, to the mass of an equal volume of gas-free distilled water at 25°C.

The BD of the aggregates and recycled crushed glass was conducted in accordance with SANS 3001-AG20 for the aggregates greater than 5 mm (i.e. 9.5 mm andesite and 6.7 mm andesite) and SANS 3001-AG21 for the aggregates less than 5 mm (i.e. fine aggregates including the crushed glass material). The BD results are presented in Table 3-11.

It can be observed that the BD of the glass material is comparatively lower than the conventional aggregates which range from 2.64 to 2.89. The use of this material in road construction may thus prove to be more cost-effective than the conventional aggregates.

Table 3-11: Bulk Density of aggregates and recycled crushed glass

Aggregate	BD (ton/m^3)
9.5 Andesite	2.877
6.7 Andesite	2.886
CD Andesite	2.770
CS Granite	2.619
Mine Sand	2.642
Recycled crushed glass	2.451

3.7.2. Water Absorption

Absorption, which is also determined by SANS 3001-AG20 (for the aggregates greater than 5 mm) and SANS 3001-AG21 (for the aggregates less than 5 mm), is a measure of the amount of water that an aggregate can absorb into its pore structure. Aggregate absorption is measured by the increase in mass due to water in the pores of the material and is indicative of the amount of binder the aggregate will absorb in an asphalt mix. Improved adhesion is achieved through mechanical interlocking of the binder into the pores of the aggregate surface.

It can be observed from the results indicated in Table 3-12 that the aggregates utilised in the study are not highly absorptive as the maximum allowable absorption specified for coarse (> 5mm) and fine aggregates (< 5mm) is 1% and 1.5% respectively (Sabita, 2016). The fine aggregates (i.e. CD andesite and CS granite) are, however, more absorptive than the coarser aggregates while the fine crushed glass material indicates much less absorption in comparison with the conventional fine aggregates.

Although better adhesion may be obtained with the more absorptive conventional aggregates, glass-asphalt mixes may require less binder to coat the glass particles than the more absorptive aggregates in conventional asphalt mixes; a factor that may be more desirable from an economical point of view.

Table 3-12: Aggregate and recycled crushed glass absorption

Aggregate	Water Absorption (%)
9.5 Andesite	0.7
6.7 Andesite	0.6
CD Andesite	2.0
CS Granite	1.0
Mine Sand	0.5
Recycled crushed glass	0.5

3.7.3. Fine Aggregate Angularity (FAA)

The fine aggregate angularity of a fine aggregate sample is estimated by means of the FAA test which measures the loose uncompacted void content of the fine aggregates. The loose uncompacted void content is a measure of the angularity of the fine aggregate and assumes a higher angularity with a higher void content and similarly a lower angularity with a lower void content.

The FAA test was performed on the crushed waste glass as well as on the conventional fine aggregates. The test was conducted in accordance with ASTM C1252 – "Uncompacted Void Content of Fine Aggregate" at the Advanced Materials Testing Laboratory at the CSIR and SRT Laboratories. The obtained results are compared in Table 3-13.

It can be observed that the uncompacted void content of the recycled crushed glass is significantly higher than the conventional fine aggregates which indicates a higher angularity.

This can be desirable in glass-asphalt mixes because angular particles interlock better with each other which aids in resisting deformation of the mix. This is, however, not seen in rounded particles, where the interlock between particles is not adequate to generate the inter-particle friction necessary to resist deformation.

According to AASHTO M323 (2013) Superpave mix design specifications, a minimum uncompacted void content of 45% is specified for a design traffic level of 30 million ESALs. Many agencies in the USA, however, have their own requirements for FAA evaluation which may differ from the mentioned mix design specifications. Since mix design specifications in South Africa do not specify requirements for FAA, it was decided to use the criteria set out in the Superpave mix design specifications. Based on an uncompacted void content of 45% as a minimum criterion in relation with the "CSIR" results, it can be observed that the crushed fine aggregates as well as the recycled crushed glass meets the minimum criteria. This is consistent with typical test values for crushed materials which typically range from 43% to 52% uncompacted voids (Pavement Interactive, n.d.). It is also interesting to note that the mine sand has an angularity as high as the recycled crushed glass. This is quite surprising; as the mine sand is natural (uncrushed and more rounded) sand which should typically range from 38% to 46% uncompacted voids (Pavement Interactive, n.d.).

Table 3-13: Angularity of fine aggregates and recycled crushed glass

Aggregate	Uncompacted Void Content (%) - SRT	Uncompacted Void Content (%) - CSIR
CD Andesite	39.7	44.6
CS Granite	38.3	45.0
Mine Sand	48.3	50.5
Recycled crushed glass	51.3	50.9

3.7.4. Sand Equivalency

As stipulated in Sabita Manual 35/TRH 8 (2016), the sand equivalency test was conducted in accordance with SANS 3001-AG5. The sand equivalency test was conducted on the fine aggregate and recycled crushed glass material to determine the relative proportions of plastic fines or clay-like materials present in the aggregate. Aggregates in an asphalt mix can be coated by these materials which can result in inadequate bonding between the binder and the aggregate.

The sand equivalent values for the aggregates and recycled crushed glass were determined by pouring a representative sample of aggregate passing the 5 mm sieve and a small amount of specified flocculating solution into a graduated cylinder. The clay-like materials coating the aggregates were then loosed by agitating the sample. Also, from within the sample, irrigation was carried out using the same flocculating solution which would suspend the clay-like materials higher than the aggregate. On passing the specific sedimentation time, it was possible to determine the height of fine aggregate and flocculated clay. The sand equivalent value was then calculated using the ratio of the height of aggregate over the height of clay. The height of the aggregate and clay can be seen in Figure 3-10. A cleaner aggregate, which means less plastic fines or clay-like material, are present if the sand equivalent values are high.

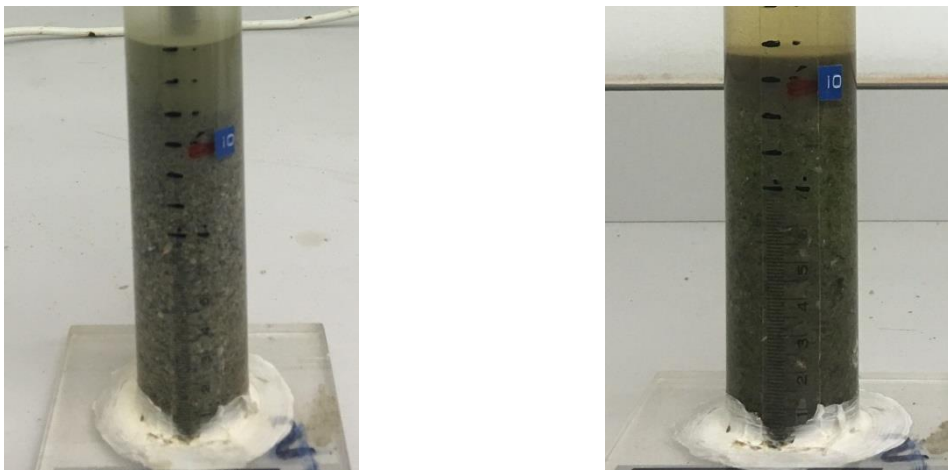

Figure 3-10: Sand equivalency of fine granite aggregates and recycled crushed glass material

The sand equivalent values obtained for the fine aggregates and recycled crushed glass are indicated in Table 3-14. Sabita Manual 35/TRH 8 (2016) specifies a minimum sand equivalent value of 50%. It can be observed that the fine aggregates as well as the recycled crushed glass meet the minimum specification criteria. Furthermore, the recycled crushed glass indicates the presence of much less clay-like materials than the conventional fine aggregates. This also shows that the crushed glass fines obtained from Consol are relatively free of such materials that are likely to cause instability or moisture damage of the glass-asphalt mix.

Table 3-14: Sand equivalent values for fine aggregate and recycled crushed glass

Aggregate	Sand Equivalent (%)	Min. Sand Equivalent (%)
CD Andesite	76	50
CS Granite	84	
Mine Sand	71	
recycled crushed glass	89	

3.7.5. X-Ray Diffraction (XRD) Analysis of Waste Glass Material

XRD analysis was conducted on the entire grading of the recycled crushed glass material in order to identify the percentage composition of amorphous (non-crystalline) silica, i.e. glass, present in the sample. This provides an indication of the relative degree of "cleanliness or purity" of the recycled crushed glass obtained from Consol.

Table 3-15 indicates the percentage composition of amorphous silica versus crystalline silica present in the sample of recycled crushed glass. The form of crystalline silica identified in the recycled crushed glass sample is quartz which is the most common form of crystalline silica and is a mineral found in most rocks, sands and soils.

It can be observed that on average more than 90% of the recycled crushed glass sample comprises of amorphous silica. The source of recycled crushed glass, therefore, demonstrates a high degree of purity and may hence be considered favourable for application in glass-asphalt mixes. Furthermore, it can be noted that the amorphous content is similar for the sample of recycled crushed glass collected from the same source in 2015. It can therefore be noted that consistency in sample quality can be achieved from the same source hence marking the source suitable for continuous use in glass-asphalt mixes in the country.

Furthermore, amorphous forms of silica do not present the serious health hazards associated with the crystalline forms and may therefore also be considered favourable from a health and safety perspective.

Table 3-15: XRD test results

	Amorphous Silica (%) (Glass) - 2015	**Amorphous Silica (%) (Glass)** - 2017	**Crystalline Silica (%) (Quartz)** - 2017
-0.075 mm	89.05	83.67	14.36
0.075 mm	89.62	86.75	12.57
0.150 mm	87.51	89.05	9.47
0.300 mm	90.59	91.66	6.69
0.600 mm	96.71	95.82	2.75
1.180 mm	97.94	97.56	1.37
2.360 mm	98.60	97.19	1.27
4.750 mm	--	97.04	1.05

3.8. Morphology of recycled crushed glass material

The microscopic morphology of the fine recycled crushed glass was examined by Scanning Electron Microscopy (SEM). The SEM examinations indicated that the crushed glass consists mainly of fine angular particles with a broad particle size range, as shown in Figure 3-11. The observed angularity is consistent with the high FAA test results obtained for the recycled crushed glass. Also, due to the crushed fine grading of the glass material, reduced quantities of elongated particles and very few particles with sharp edges can be observed.

Furthermore, the SEM images reveal that the surfaces of the crushed glass particles are not entirely smooth as one would expect, but rather fine to coarse textured features, less than 1 µm, can be observed on the surfaces, as shown in Figure 3-12. However, these textured features may not be sufficient for proper adhesion of bitumen on the glass surface due to a lack of anchoring points. Moreover and as expected, it can be observed that porous features are not visible on the surface of the glass particles; which is in line with the non-absorptive properties of glass.

Figure 3-11: Fine angular crushed glass particles (Scale: 200 µm, Mag: 20x)

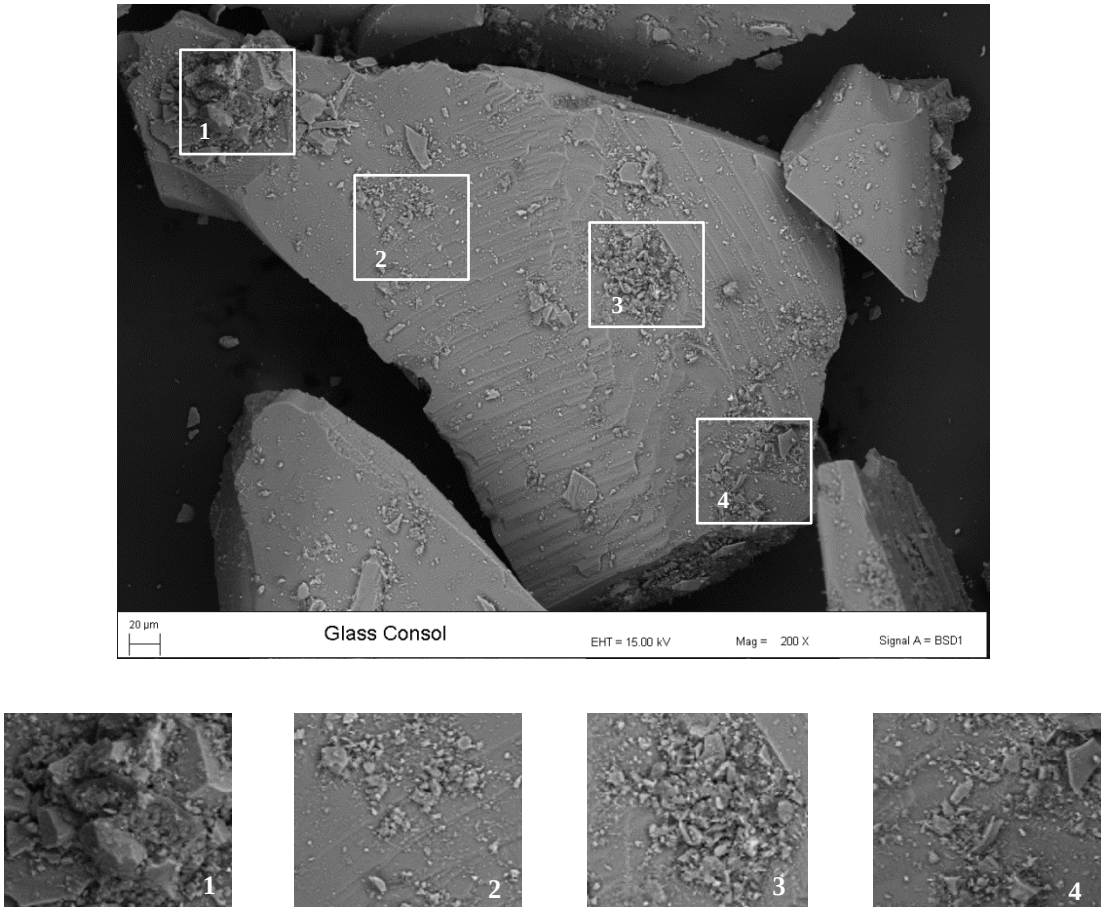

Figure 3-12: Textured features on surface of fine crushed glass particles (Scale: 20 µm, Mag: 200x)

The high angularity of the material was also observed through a SEM analysis conducted by Anochie-Boateng and George (2016) for the same source and grading of recycled crushed glass in an asphalt mix. The SEM analysis demonstrated high angularity and in turn increased interlock between the constituent particles in comparison with a traditional asphalt mix without the crushed glass material, as presented in Figure 3-13.

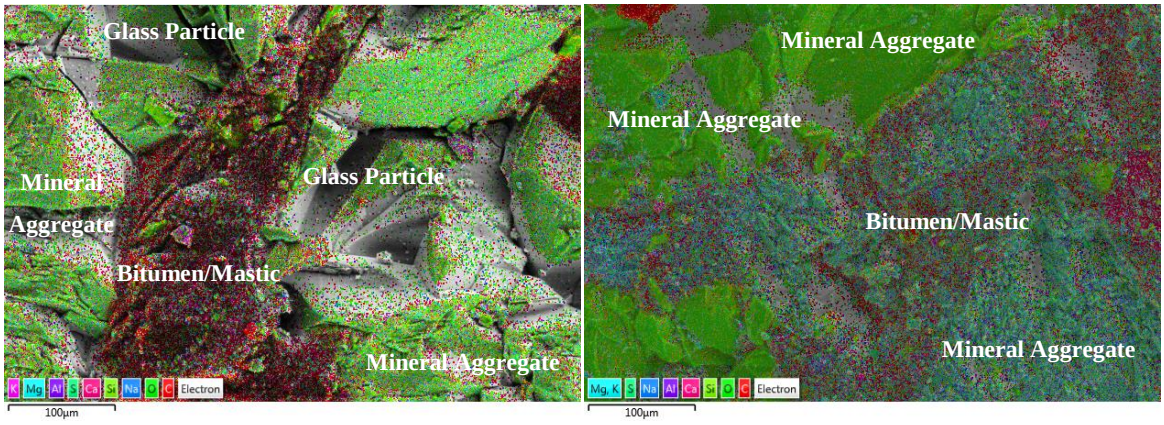

a **b**

Figure 3-13: SEM of a) glass-asphalt mix and b) conventional asphalt mix (Anochie-Boateng & George, 2016)

3.9. Summary

It should be noted that the above conclusions pertain to only the recycled crushed glass and aggregates evaluated in this study as well as the specified design aggregate grading used to manufacture the glass-asphalt mixes.

Chapter 3 presents the design and production of three 10 mm NMPS medium continuously-graded glass-asphalt mixes (i.e. GA Mix 1, 2 and 3) that consists of 15% recycled crushed glass and consisting of various filler material and antistripping additives, as summarised in Table 3- 16.

Table 3-16: Design and Production of Glass-Asphalt Mixes

Glass-Asphalt Mix	Filler Material	Antistripping Additive
GA Mix 1	1% Hydrated lime	Hydrated lime
GA Mix 2	1% Plant filler	Liquid antistripping agent
GA Mix 3	1% Plant filler	None

The glass-asphalt mixes are designed as a surfacing course for a design traffic level between 3 and 30 million ESALs and represents a similar design aggregate grading to the standard SANRAL 10 mm NMPS medium continuously-graded asphalt mix using the same component materials (i.e. traditional aggregates and binder).

The following can be summarised based on the mix design results presented in this chapter for GA Mix 1, 2 and 3:

- The optimum binder content for the glass-asphalt mixes designed with the selected aggregate fractions is 5.4%.
- The design aggregate grading for the glass-asphalt mixes satisfies the aggregate control points specified in Sabita Manual 35/TRH 8 (2016).
- All the volumetric properties of the glass-asphalt mixes comply with the criteria set out in Sabita Manual 35/TRH 8 (2016).
- The physical characterisation of the recycled crushed glass material utilised in this study presents mostly viable and favourable properties for incorporation as an aggregate substitute in asphalt mixes; although the relatively smooth surface texture may demonstrate adhesion related concerns regarding bonding between the binder and the recycled crushed glass material.

4. SELECTION OF OPTIMUM GLASS-ASPHALT MIX

4.1. Introduction

Various glass-asphalt field projects implemented in the USA have identified the primary mechanism of failure in glass-asphalt pavements to be stripping (Virginia Transportation Research Council, 1998). Stripping occurs due to the loss of adhesion between the binder and the aggregate in the presence of moisture. The non-porous, relatively smooth surface texture as well as the hydrophilic (strong affinity for water) nature of glass makes glass-asphalt pavements more susceptible to moisture induced damage (i.e. stripping) than conventional asphalt pavements. The degree of moisture susceptibility is, however, largely dependent on the quantity as well as the grading of glass particles introduced into a surface course mix. Furthermore, the incorporation of antistripping additives may alleviate or control the stripping related problems associated with glass-asphalt.

In this chapter, the optimum glass-asphalt mix is selected based on an evaluation on the degree of moisture susceptibility of GA Mix 1, 2 and 3 relative to South African standard requirements. The Hamburg wheel tracking test (HWTT) and the Modified Lottman test were conducted to assess the above. It should be noted that the HWTT results were only utilised to assess moisture susceptibility and not the permanent deformation (rutting) properties of the mixes. An assessment on the permanent deformation properties of the optimum glass-asphalt mix can be referred to in Chapter 5.

4.2. Moisture Susceptibility Evaluation of Glass-Asphalt Mixes Using Modified Lottman Test

The Modified Lottman test, conducted in accordance with ASTM D4867M (2009) – "Effect of Moisture on Asphalt Concrete Paving Mixtures", is the standard test adopted in South Africa to evaluate the durability of asphalt mixes (Sabita, 2016). It should be noted that ASTM D4867M (2009) specifies the use of this test to dense graded (continuously graded) mixes.

In this study, the test was performed to assess the moisture susceptibility of GA Mix 1, 2 and 3. Six test specimens were compacted to a dimension of 150 mm diameter by 62.5 mm height using the Superpave Gyratory Compactor. The specimens were compacted to achieve a target air void content of approximately 7 $\pm$ 0.5% and divided into two subsets (three test specimens

each) such that the average air void content of each subset was approximately equal. The air void contents obtained for the two subsets are presented in Tables 4-4 to 4-6.

One subset was maintained dry (referred to as "dry subset") while the other (referred to as "wet subset") underwent a partial saturation and freeze-thaw conditioning process. Although the freeze cycle is optional in ASTM D4867M (2009) and may not be applicable to South African field conditions, it was decided to include the freeze cycle since the asphalt mix contains glass particles, which makes it more prone to moisture damage than traditional aggregates. In addition the glass particles require additional treatment with anti-stripping additives. The aim is to therefore simulate conditioning that is more severe than conditioning expected in the field.

The wet subset was partially saturated at 25°C using a vacuum chamber. A partial vacuum of 20 inches Hg was applied to the wet subset for five minutes in order to obtain a degree of saturation between 55 and 80% as specified in ASTM D4867M (2009). The degree of saturation obtained for each subset is calculated as indicated in Tables 4-4 to 4-6.

The vacuum-saturated samples were thereafter placed in a freezer at -18°C for 15 hours and then placed in a 60°C water bath for a 24 hour period. The wet subset is considered conditioned after this freeze-thaw cycle. Both wet and dry subsets were subsequently brought to a constant temperature (25°C) in a water bath for 60 minutes and 20 minutes respectively prior to indirect tensile strength (ITS) testing.

For this study, the UTM-25 machine was utilised as the loading apparatus. The test specimens were placed in the loading apparatus and the loading strips were then centrally positioned on the vertical diametrical plane as illustrated in Figure 4-1. A diametrical load at 50 mm/min at 25°C was applied until the maximum load required to break the specimens was reached. The maximum load was used to determine the ITS for each subset as per Equation 4-1. The results are summarised in Tables 4-4 to 4-6 and presented in detail in Appendix B – Table B1, B2 and B3.

$$S_t = \frac{2*P}{\pi*t*D}$$ Equation 4-1

Where:

S_t = indirect tensile strength (kPa)

P = maximum load (kN)

t = specimen height immediately before tensile strength test (m)

D = specimen diameter (m)

The Modified Lottman test was conducted at the CSIR Pavement Materials and Testing Laboratory. The testing setup utilised in this study is illustrated in Figure 4-1.

Saturated at 20 inches Hg

Conditioned 24h in 60°C water

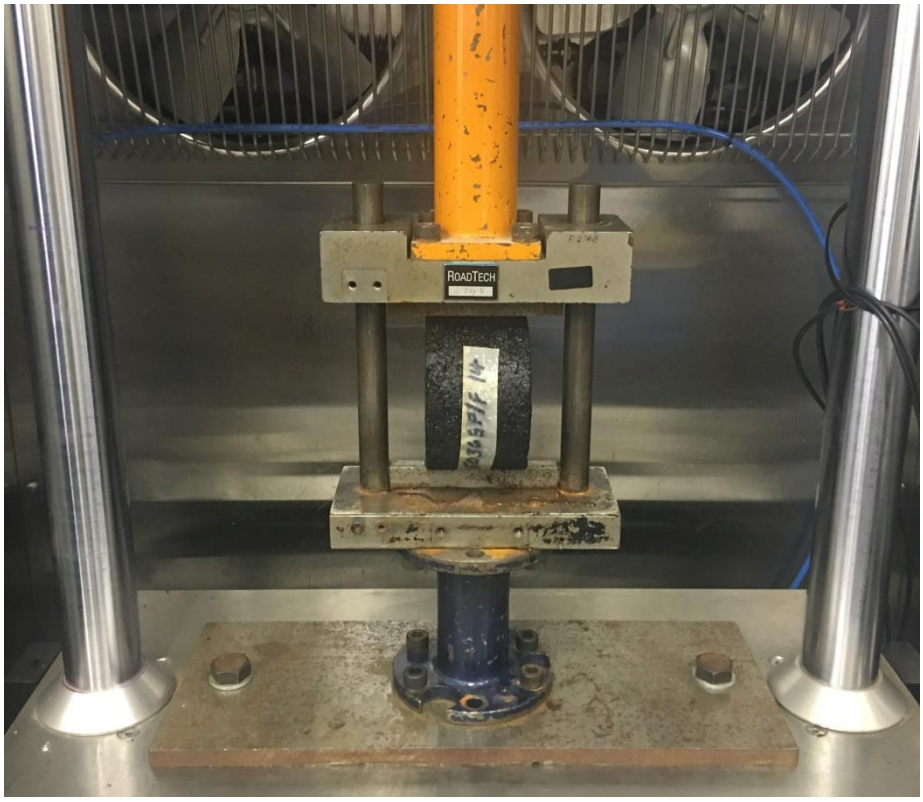

ITS testing at 50 mm/min load application

Figure 4-1: Modified Lottman testing as per ASTM D4867M

4.2.1. Analysis of Results as per ASTM D4867M

The stripping potential of the compacted specimens is evaluated by the tensile strength ratio (TSR). The TSR is determined by the ratio of the average ITS of the wet subset to the ITS of the dry subset (ASTM D4867M-09, 2009).

4.2.1.1. Indirect Tensile Strength (ITS)

The ITS is a measure of the tensile properties of an asphalt mix which is associated with the cracking resistance of the mix. A higher ITS indicates increased resistance to cracking and is also associated with increased toughness and durability as well as increased resistance to rutting between 10°C and 30°C .

In South Africa, the minimum ITS criteria is 800 kPa at 25°C. However, a few studies have shown that ITS values lower than 1000 kPa may have a tendency to demonstrate reduced rutting resistance in the field while ITS values greater than 1700 kPa may demonstrate brittleness and low flexibility (Anochie-Boateng & George, 2016).

The average ITS results of the wet (conditioned) and dry (unconditioned) subsets are reported in Figure 4-2. The dry ITS results for all three glass-asphalt mixes meet the minimum criteria (i.e. 800 kPa) while only GA Mix 1 exceeds 1000 kPa. It should be noted, however, that the dry subset has been conditioned for 20 minutes prior to testing and may hence present more conservative ITS results.

It can also be observed from the results that the incorporation of hydrated lime in GA Mix 1 contributed towards the enhanced dry strength in comparison with GA Mix 2 and 3. It is also apparent from the percentage reduction in strength of the conditioned subset of GA Mix 1 (11%) in comparison with GA Mix 2 (20%) that the role of the hydrated lime as an antistripping additive in the presence of water was considerably more effective than the liquid antistripping additive. Although a larger reduction in dry strength was noted for GA Mix 2 in comparison with GA Mix 3, the percentage reduction in strength of the conditioned subset of GA Mix 2 (20%) was not as pronounced as in the case of GA Mix 3 (24%); which was expected due to the absence of an antistripping additive in GA Mix 3.

It is interesting to note that GA Mix 2, which contains a liquid antistripping additive, indicated the lowest dry strength in comparison with GA Mix 1 and 3. The liquid additive may thus have an adverse effect on the strength of asphalt mixes, although the moisture susceptibility may improve. This observation is in line with the general notion that such liquid additives cause early pavement failures such as rutting (Nazirizad et al., 2015) even although they are known to improve moisture susceptibility.

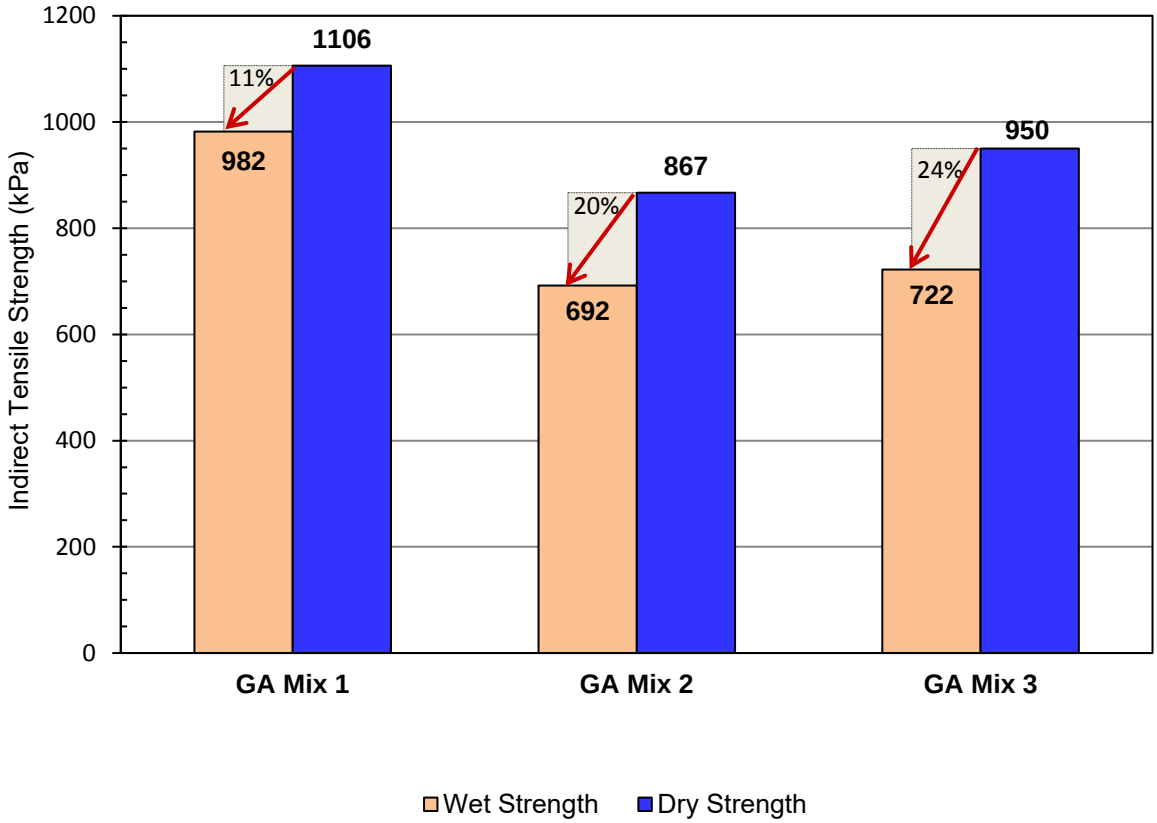

Figure 4-2: Average ITS results for GA Mix 1, 2 and 3

4.2.1.2. Tensile Strength Ratio (TSR)

The TSR results of GA Mix 1, 2 and 3 are reported in Figure 4-3. In South Africa a minimum TSR of 0.8 for asphalt wearing courses is specified (Sabita, 2016). The VDOT has, however, specified a minimum TSR of 0.9 for glass asphalt pavements in Virginia due to the higher tendency of stripping associated with glass asphalt (Virginia Transportation Research Council, 1998).

With respect to the specification for asphalt wearing courses in South Africa, it can be seen that GA Mix 1 and GA Mix 2 meets the minimum TSR criteria. Based on the TSR as a reliable

indicator of moisture susceptibility; the stripping resistance of GA Mix 1 (TSR=0.89) is more pronounced than GA Mix 2 (TSR=0.8), which only just meets the minimum criteria. GA Mix 3, however, does not meet the minimum criteria and is expected to demonstrate the least resistance to stripping. This expected behaviour is once again attributed to the absence of an antistripping additive in the mix making GA Mix 3 most susceptible to moisture damage.

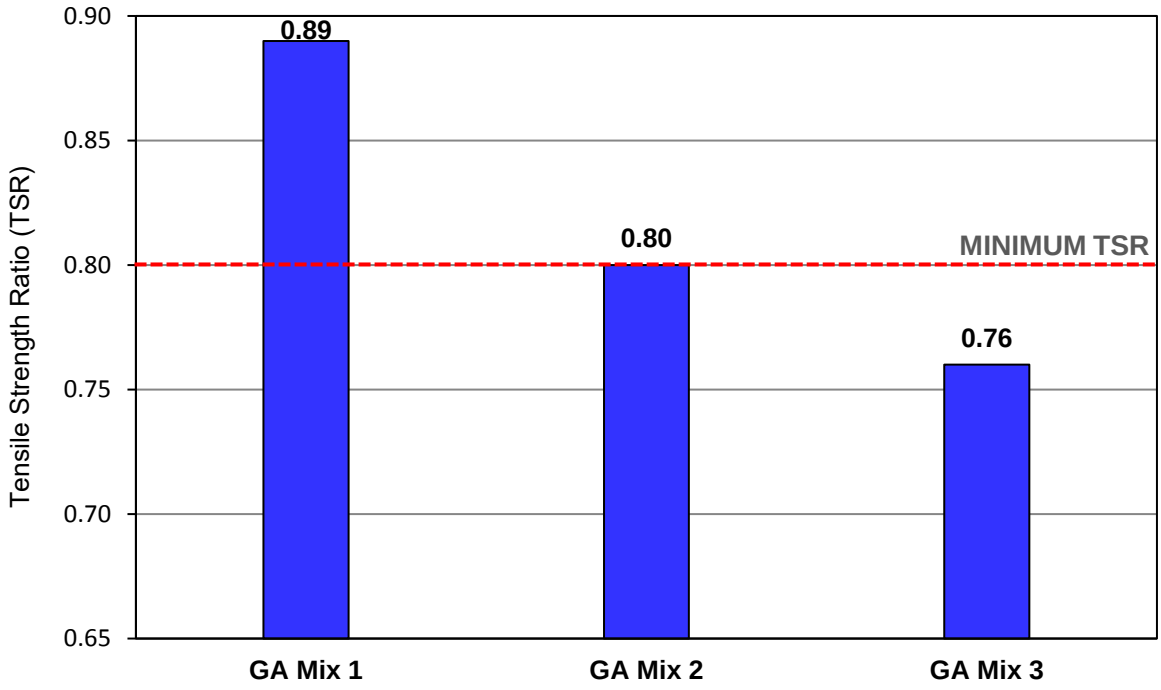

Figure 4-3: TSR results for GA Mix 1, 2 and 3

Table 4-1: Summary of Modified Lottman results for GA Mix 1

Dry Subset			
	15036L16	15036L17	15036L18
BD (ton/m^3)	2.400	2.382	2.395
MVD (ton/m^3)	2.570	2.570	2.570
% Air void	6.6	7.3	6.8
Average % air void		6.9	
Dry Strength (kPa)	1186	1072	1059
Average Strength (kPa)		**1106**	
Wet Subset			
	15036L19	15036L20	15036L21
BD (ton/m^3)	2.400	2.391	2.396
MVD (ton/m^3)	2.57	2.57	2.57
% Air void	6.6	7.0	6.8
Average % air void		6.8	
Wet Strength (kPa)	1046	924	976
Average Strength (kPa)		**982**	
TENSILE STRENGTH RATIO (TSR)		**0.89**	

Table 4-2: Summary of Modified Lottman results for GA Mix 2

Dry Subset			
	15036MA3	15036MA4	15036MA5
BD (ton/m^3)	2.390	2.388	2.390
MVD (ton/m^3)	2.569	2.569	2.569
% Air void	7.0	7.1	7.0
Average % air void	7.0		
Dry Strength (kPa)	865	813	922
Average Strength (kPa)	**867**		
Wet Subset			
	15036MA1	15036MA2	15036MA6
BD (ton/m^3)	2.388	2.386	2.391
MVD (ton/m^3)	2.569	2.569	2.569
% Air void	7.0	7.0	6.9
Average % air void	7.0		
Wet Strength (kPa)	686	700	691
Average Strength (kPa)	**692**		
TENSILE STRENGTH RATIO (TSR)	**0.80**		

Table 4-3: Summary of Modified Lottman results for GA Mix 3

Dry Subset			
	15036M17	15036M18	15036M19
BD (ton/m^3)	2.400	2.396	2.394
MVD (ton/m^3)	2.566	2.566	2.566
% Air void	6.5	6.6	6.7
Average % air void	6.6		
Dry Strength (kPa)	990	931	929
Average Strength (kPa)	**950**		
Wet Subset			
	15036M14	15036M15	15036M16
BD (ton/m^3)	2.399	2.395	2.399
MVD (ton/m^3)	2.566	2.566	2.566
% Air void	6.5	6.7	6.5
Average % air void	6.6		
Wet Strength (kPa)	702	716	747
Average Strength (kPa)	**722**		
TENSILE STRENGTH RATIO (TSR)	**0.76**		

4.2.1.3. Visual Estimation of Moisture Damage

ASTM D4867M specifies a visual assessment to be conducted on the fractured (tested) specimens. This assessment entails breaking the tested specimens open and reporting on the visually estimated degree of moisture damage.

As per the above specification requirement, the wet and dry tested subsets for GA Mix 1, 2 and 3 were visually inspected for moisture damage. A brief description of the moisture susceptibility evaluation made during visual inspection of the wet subset for each mix is provided below. It should be noted that little to no stripping was observed for the dry subset for all three mixes.

- **GA Mix 1:** Little to no stripping was observed. The aggregate and glass particles appeared to be well coated with the bitumen.
- **GA Mix 2:** Minor stripping of the glass particles in particular was visible.
- **GA Mix 3:** Major stripping was observed as indicated by numerous exposed surface areas of aggregate and glass particles.

4.2.2. Moisture Damage Evaluation Using Image Analysis Techniques

In addition to the above visual assessment, image analysis techniques were implemented in this study to assess the degree of stripping that had occurred in each mix. This method will eliminate visual judgment and biased interpretation associated with the current standard of visual inspection and reporting.

One fractured specimen from the wet subset of each mix was examined under a stereo microscope at a 6x zoom magnification. In order to obtain a representative area, several sections of dimension 22.05 mm (width) by 14.68 mm (height) each spanning over the cross-sectional area of the fractured specimen were examined under the microscope. It should be noted that the outer edges of the fractured specimen were not included due to aggregate breakage that had occurred on the outer edges. Aggregate breakage is primarily caused from loading during testing and or during the breaking open of the specimen post testing. The microscopic sections were captured by a digital camera (fitted to the microscope) and the resulting images were analysed using ImageJ, an open-source image processing and analysis

software. The stereo microscope and camera setup utilised in this study is illustrated in Figure 4-4.

The colour images were processed (using ImageJ) into binary images comprising of white and black pixels as indicated in Figures 4-5 to 4-7. As seen, the exposed aggregate and glass particles are characterised by white pixels while the bitumen coated particles are represented by black pixels. In ImageJ, the binary images were used to quantify the degree of stripping by measuring the area of white pixels as a ratio to the area of sum of white and black pixels for each mix. The results of this analysis are reported in Tables 4-1 to 4-3.

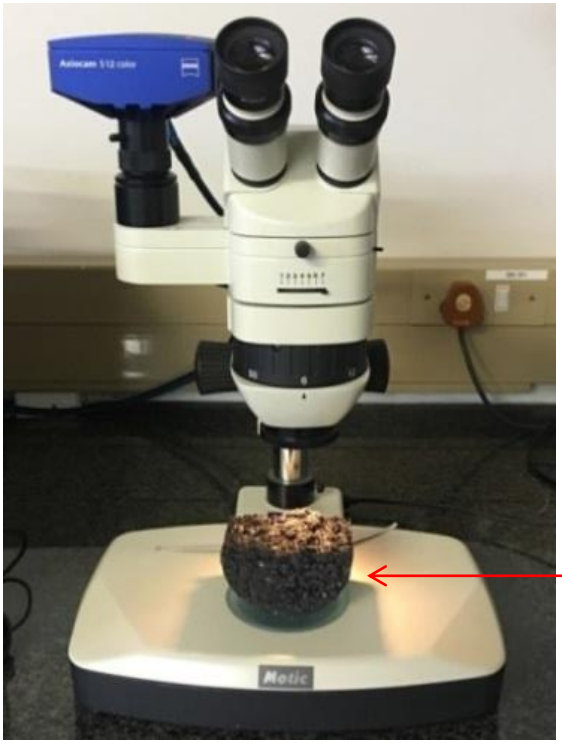

Figure 4-4: Stereo microscope and camera setup at National Metrological Institute of South Africa

Top Right Section: Processed Image

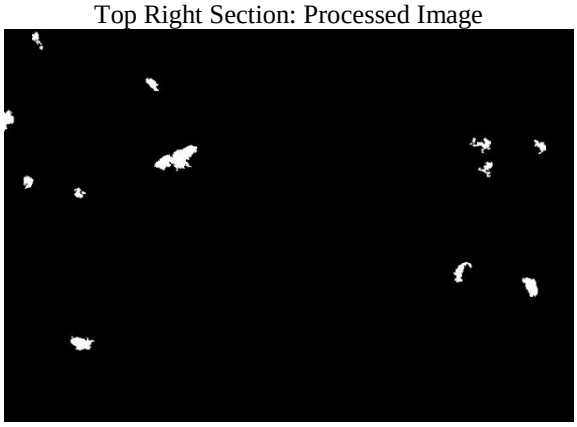

Top Right Section: Microscopic Image

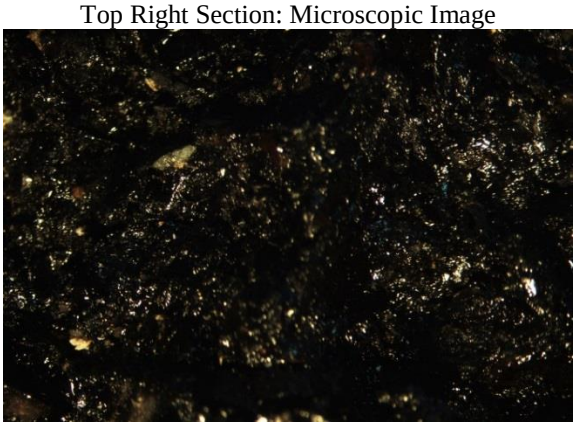

Bottom Right Section: Processed Image

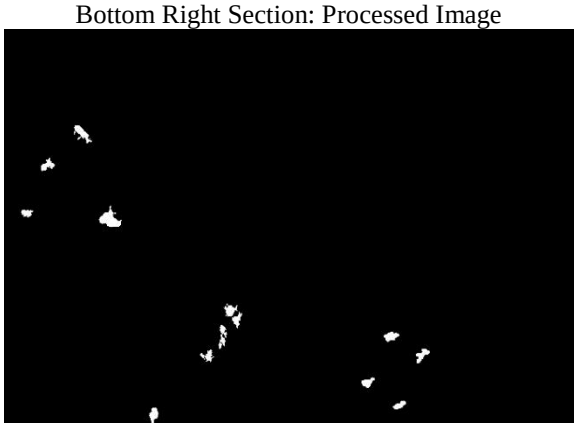

Bottom Right Section: Microscopic Image

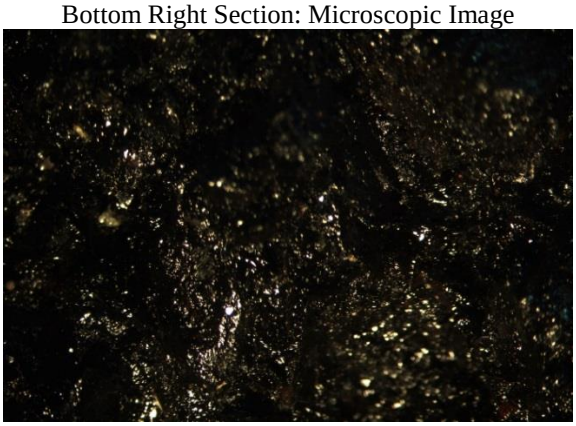

Top Middle Section: Processed Image

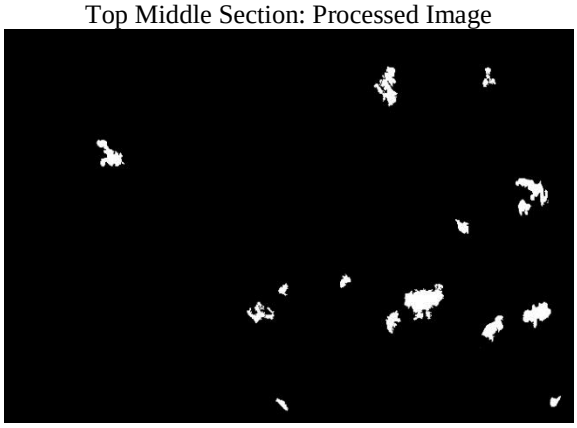

Top Midde Section: Microscopic Imge

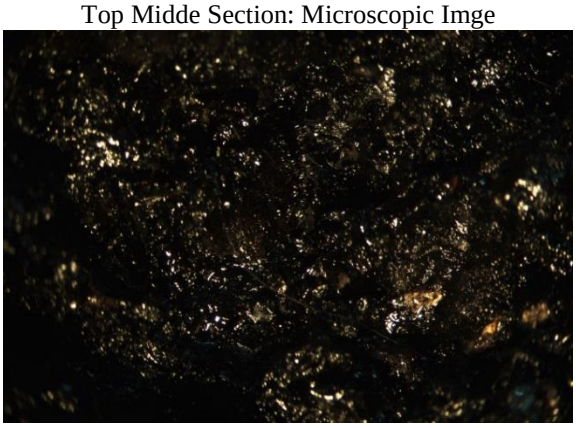

Bottom Middle Section: Processed Image

Bottom Middle Section: Microscopic Image

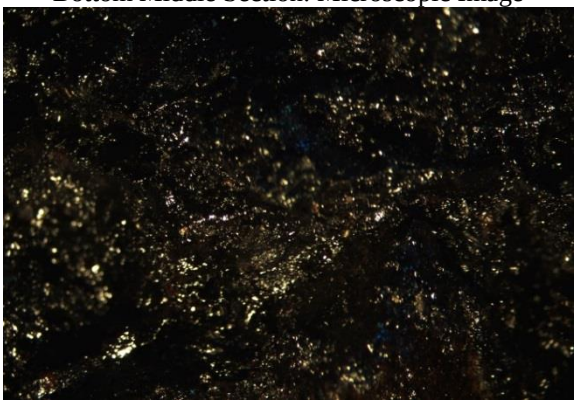

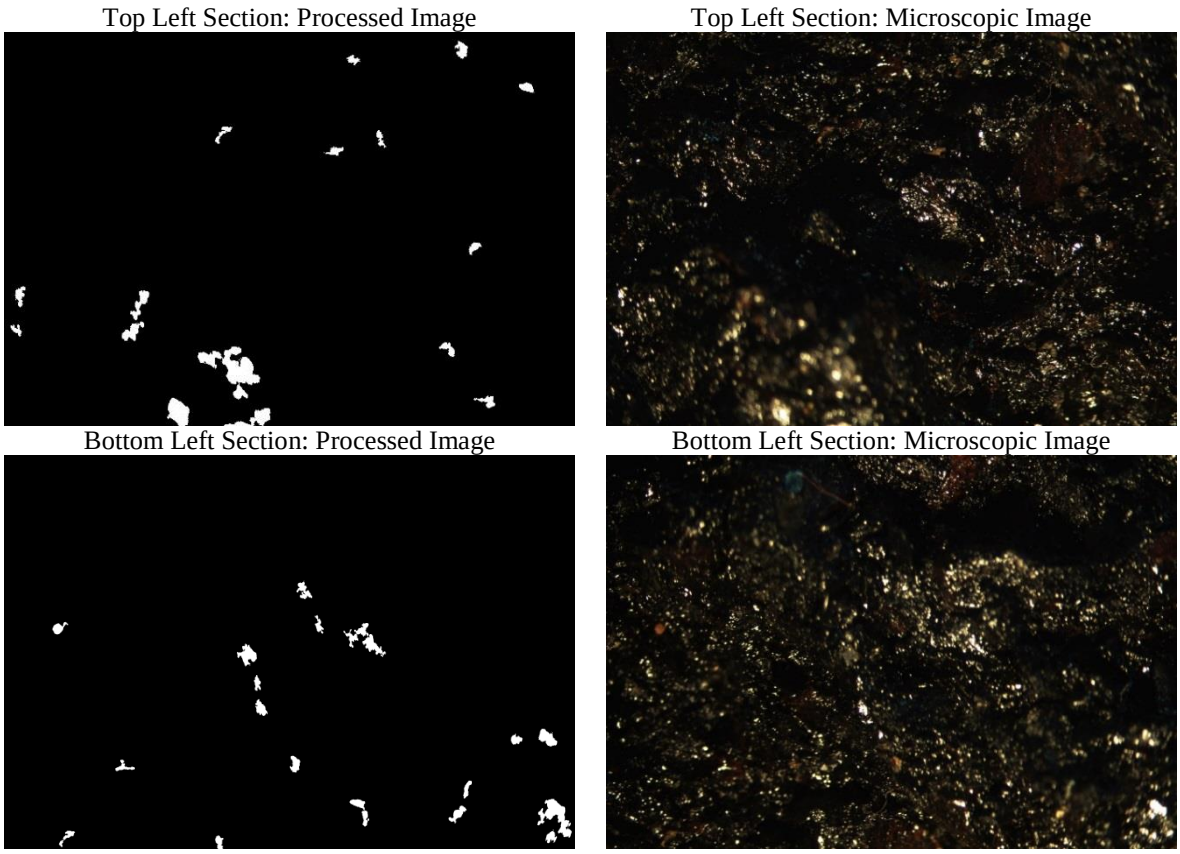

Figure 4-5: Microscopic analysis of GA Mix 1 after Modified Lottman test

Table 4-4: Exposed aggregate surface area for GA Mix 1

Section	White Pixels (mm^2)	Total Pixels (mm^2)	Area of White Pixels (%)	Total Area of White Pixels (%)
Top Right	2.60	323.34	0.80	5.86
Bottom Right	1.85	323.34	0.57	
Top Middle	5.13	323.34	1.59	
Bottom Middle	0.64	323.34	0.20	
Top Left	4.88	323.34	1.51	
Bottom Left	3.86	323.34	1.19	

Top Right Section: Processed Image

Top Right Section: Microscopic Image

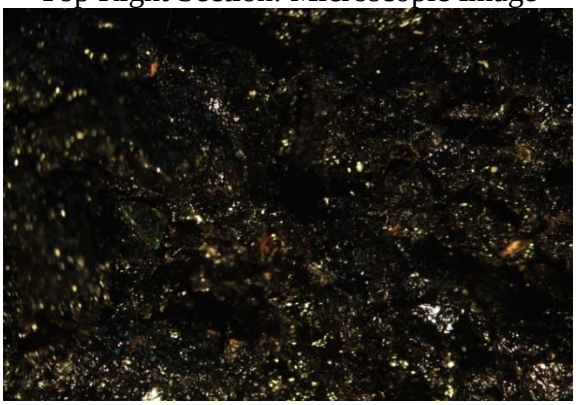

Bottom Right Section: Processed Image

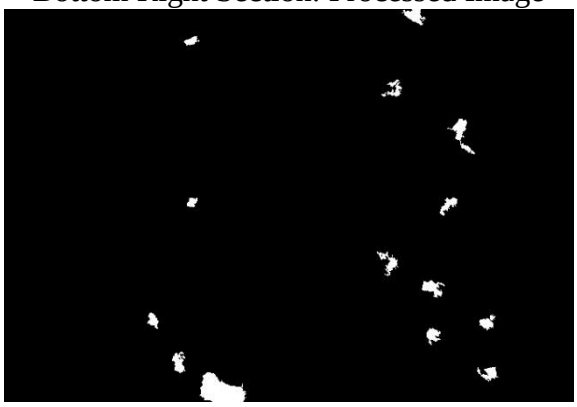

Bottom Right Section: Microscopic Image

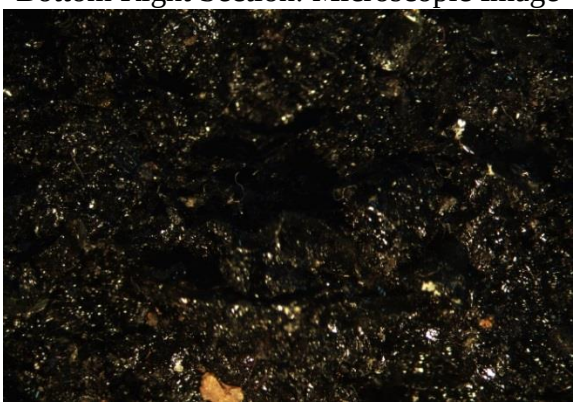

Top Middle Section: Processed Image

Top Middle Section: Microscopic Image

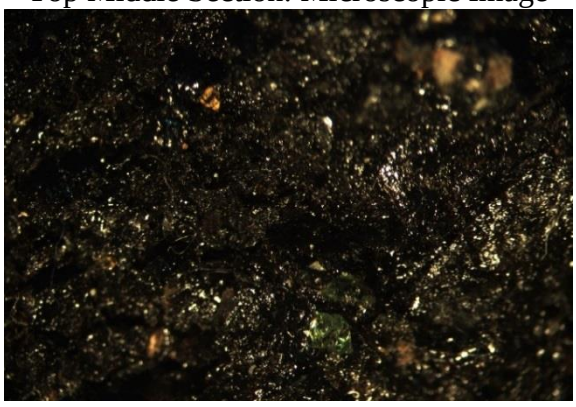

Bottom Middle Section: Processed Image

Bottom Middle Section: Microscopic Image

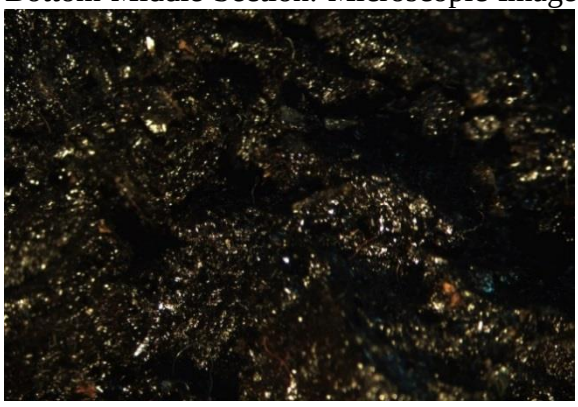

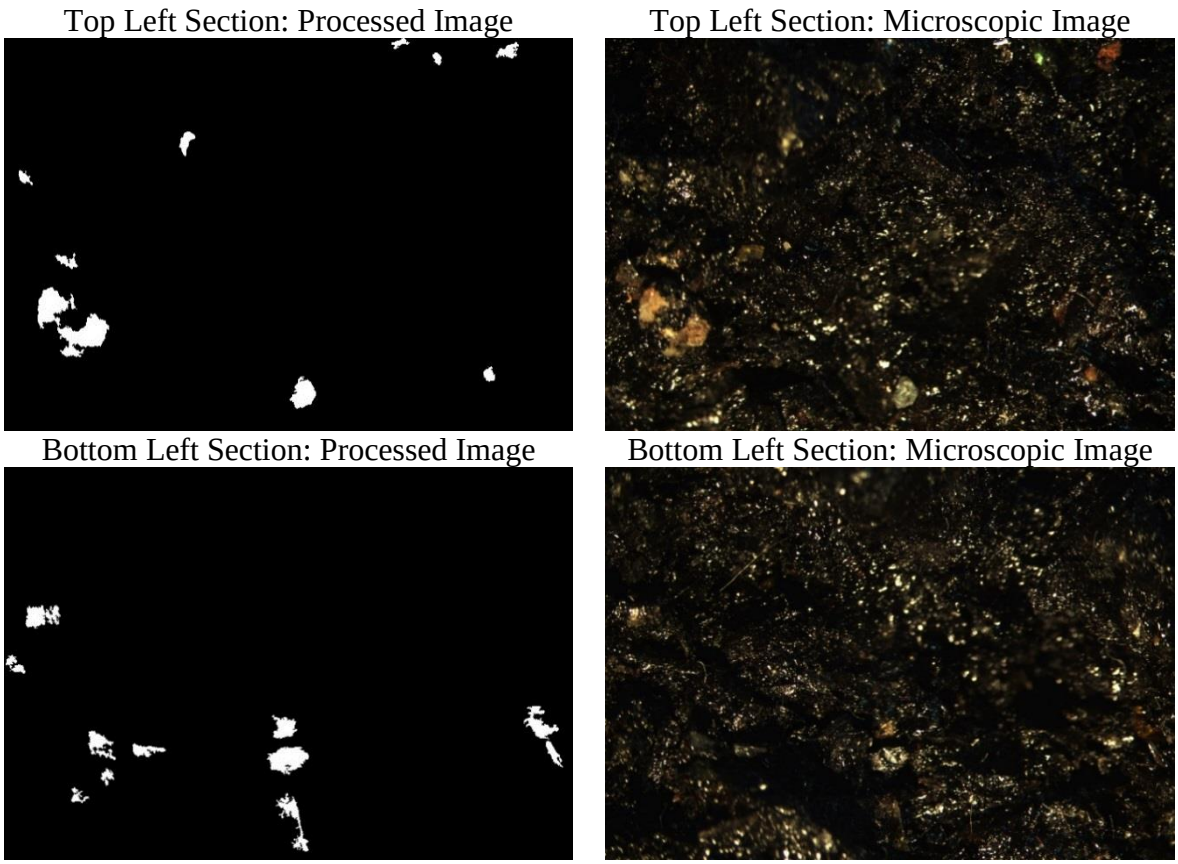

Figure 4-6: Microscopic analysis of GA Mix 2 after Modified Lottman test

Table 4-5: Exposed aggregate surface area for GA Mix 2

Section	White Pixels (mm^2)	Total Pixels (mm^2)	Area of White Pixels (%)	Total Area of White Pixels (%)
Top Right	2.08	323.34	0.64	9.59
Bottom Right	4.06	323.34	1.26	
Top Middle	13.25	323.34	4.10	
Bottom Middle	1.35	323.34	0.42	
Top Left	4.89	323.34	1.51	
Bottom Left	5.36	323.34	1.66	

Top Right Section: Processed Image

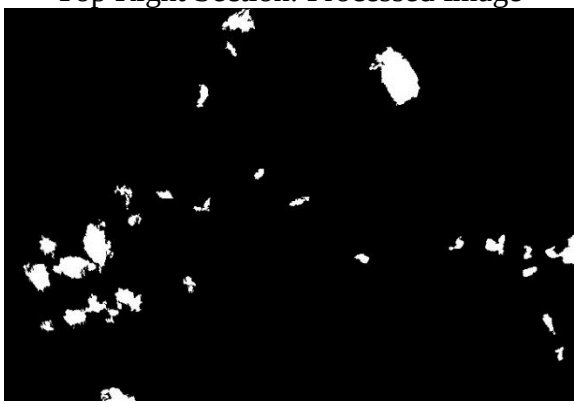

Top Right Section: Microscopic Image

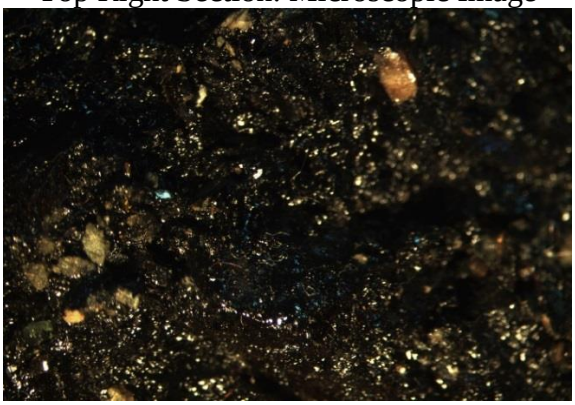

Bottom Right Section: Processed Image

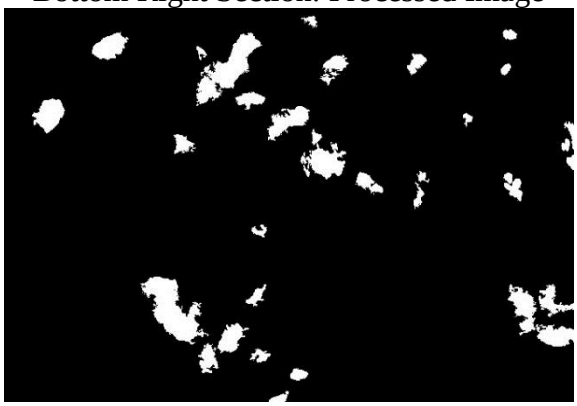

Bottom Right Section: Microscopic Image

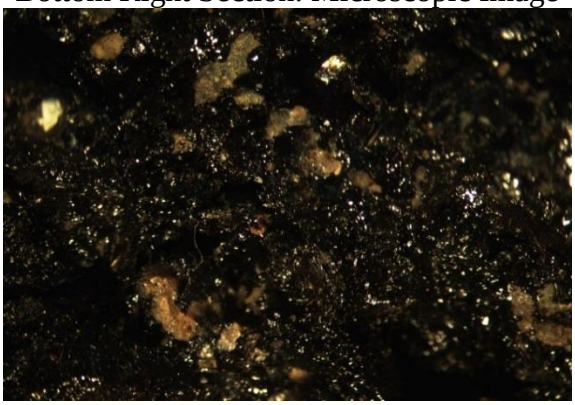

Top Middle Section: Processed Image

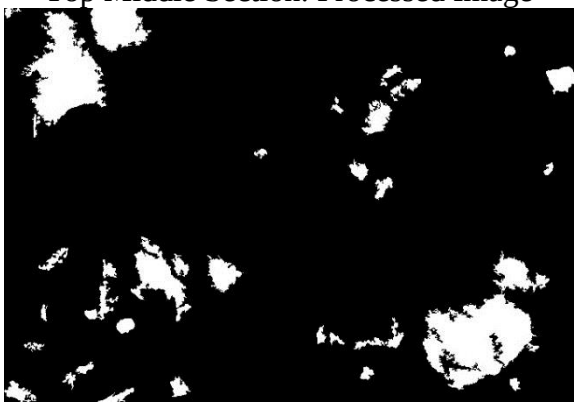

Top Middle Section: Microscopic Image

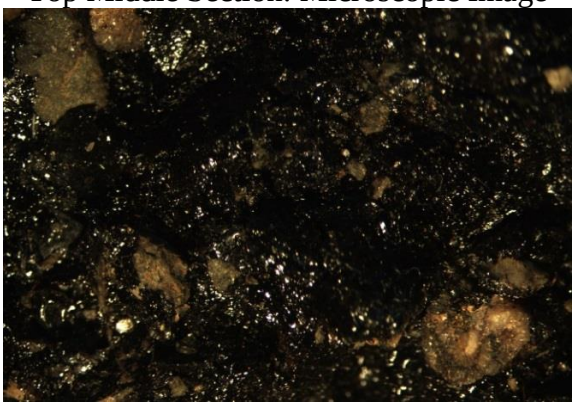

Bottom Middle Section: Processed Image

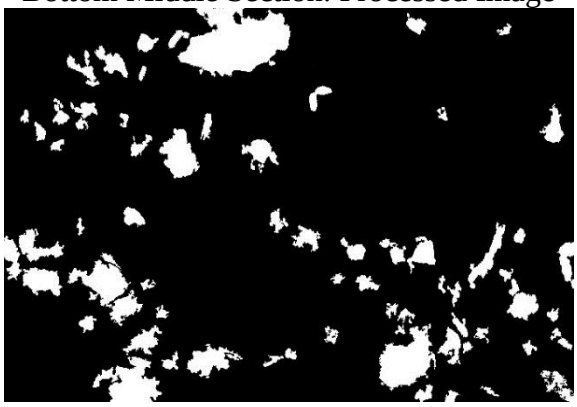

Bottom Middle Section: Microscopic Image

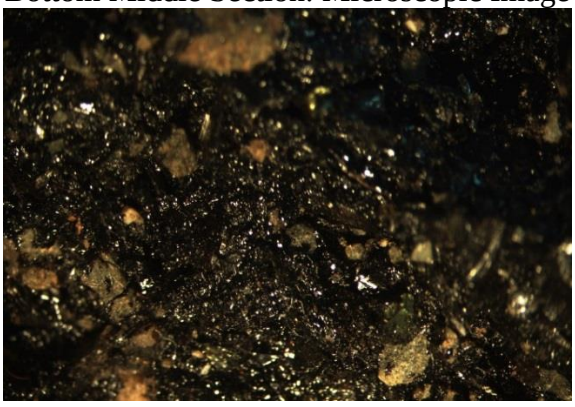

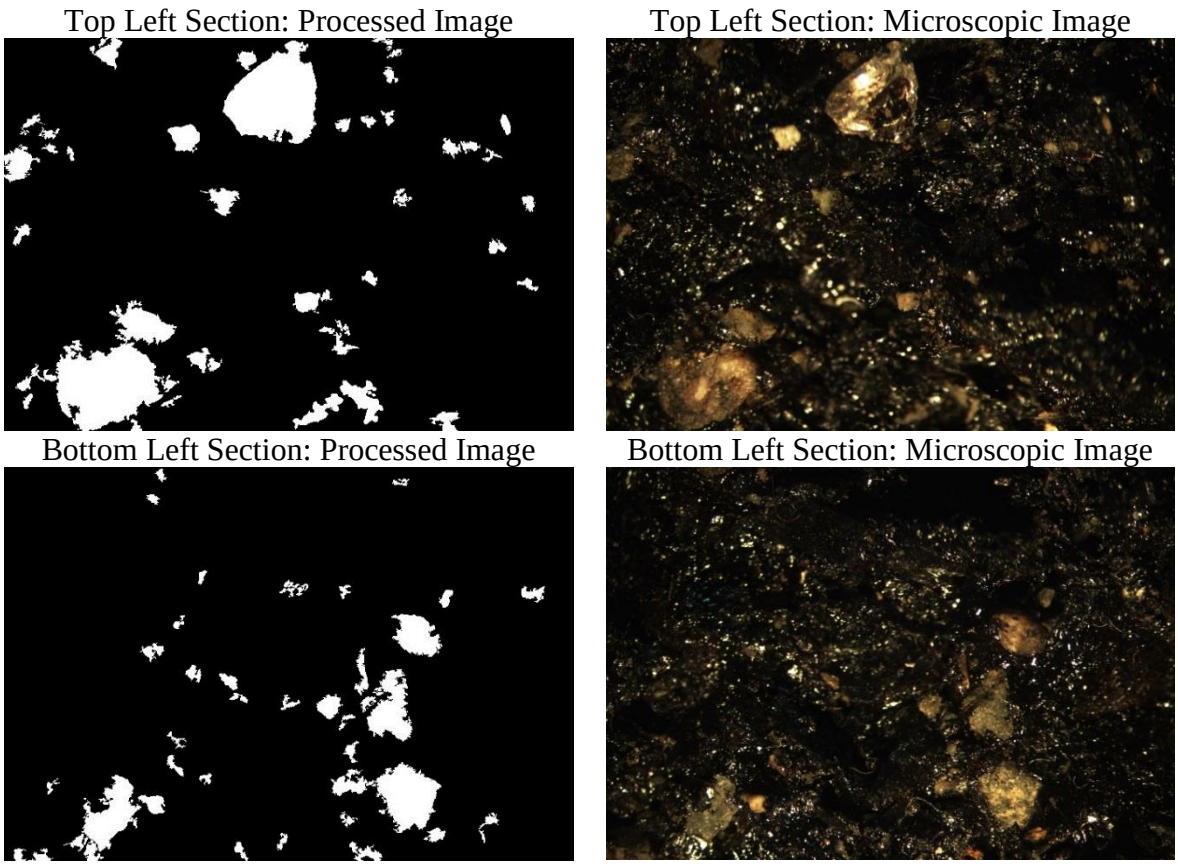

Figure 4-7: Microscopic analysis of GA Mix 3 after Modified Lottman test

Table 4-6: Exposed aggregate surface area for GA Mix 3

Section	White Pixels (mm^2)	Total Pixels (mm^2)	Area of White Pixels (%)	Total Area of White Pixels (%)
Top Right	10.39	323.34	3.2	46.9
Bottom Right	18.34	323.34	5.7	
Top Middle	30.93	323.34	9.6	
Bottom Middle	38.76	323.34	12.0	
Top Left	33.21	323.34	10.3	
Bottom Left	19.64	323.34	6.1	

The highly reflective properties of the glass particles can be observed in Figures 4-5 to 4-7. The reflection is indicated by the even and consistent distribution of bright speckles in all three mixes. To avoid processing and analysis of these reflections, particles up to and including 0.15 mm for all three mixes were excluded from the images using the "particle analyser" function in ImageJ.

The images show a clear variation in the degree of stripping with the addition of both antistripping additives. A significant reduction in the area of white pixels (stripped areas) can

be observed for GA Mix 1 and 2 in comparison with GA Mix 3. The total area of white pixels reduces from approximately 47% (GA Mix 3) to less than 10% (GA Mix 1 and 2). These results confirm the effectiveness of antistripping additives in improving the moisture susceptibility of glass-asphalt mixes. Moreover, the addition of hydrated lime appears to reduce the stripped areas slightly more than the liquid antistripping additive; although a major distinction is not apparent from the microscopic images.

It is hence recommended that such image analysis techniques be implemented in order to provide a more accurate representation of the degree of stripping. Furthermore, the degree of stripping obtained from the microscopic images follow a similar trend to the degree of moisture damage obtained from the TSR parameter and this technique can thus be used as a tool to validate the TSR results. This method can also be useful to traditional asphalt mixes.

It should be noted, however, due to the lengthy time involving image processing and analysis, only one fractured specimen from the wet subset of each mix was examined under the microscope. To obtain a better representation of the degree of stripping, it is recommended that all three fractured specimens from the wet subset be analysed.

4.3. Moisture Susceptibility Evaluation of Glass-Asphalt Mixes Using Hamburg Wheel Tracking Test

The Hamburg Wheel Tracking Test (HWTT) is currently used in South Africa as a standard laboratory test to evaluate the combined effects of moisture induced damage and rutting potential of asphalt mixes (Sabita, 2016). The HWTT is conducted according to AASHTO T 324 -**"**Standard Method of Test for Hamburg Wheel Track Testing of Compacted Hot Mix Asphalt (HMA)**"**.

The specimen setup as stipulated in the specification allows for testing to be conducted on either a slab specimen or a pair of cylindrical specimens. For this study, a pair of cylindrical specimens for each mix (i.e. GA Mix 1, GA Mix 2 and GA Mix 3) was compacted to a dimension of 150 mm diameter by 60 mm height using the Superpave Gyratory Compactor. The specimens for each mix were compacted at the determined optimum binder content of 5.4% to a target air void content of approximately 7 $\pm$ 0.5% as summarised in Table 4-7.

Table 4-7: Determination of air void content for GA Mix 1, 2 and 3

Mix	Sample No.	BD (ton/m^3)	MVD (ton/m^3)	Air Voids (%)
GA Mix 1	5877-1-1	2.389	2.570	7.0
	5877-1-2	2.388		7.1
GA Mix 2	5877-2-1	2.387	2.569	7.1
	5877-2-2	2.390		7.0
GA Mix 3	5877-3-1	2.393	2.566	6.7
	5877-3-2	2.391		6.8

The above pair of compacted specimens, for each mix, was mounted together and then submerged in the water bath of the Hamburg wheel tracking device at 50°C for 30 minutes prior to testing. The adjoined specimens were thereafter subjected to a moving wheel load of 703 N which covers a distance of 230 mm in one direction along the surface of the cylindrical specimens. The HWTT was conducted at the CSIR Pavement Materials and Testing Laboratory.

During testing, the rut depth was measured along the surface of the adjoined cylindrical specimens using a profilometer and the maximum rut depth obtained at the recorded number of wheel passes was used as the output data for analysis and reporting of the HWTT results.

It should be noted that the HWTT for GA Mix 1, 2 and 3 was terminated at 16 000, 12 000 and 14 000 wheel passes respectively, as the onset of tertiary flow and moisture damage (discussed in more detail in Section 4.3.1 and 4.3.2) had occurred well before this point and further testing would result in the steel wheel damaging the specimen mount of the equipment.

As mentioned in Section 4.1; in this study the HWTT results were only utilised to assess moisture susceptibility and not the permanent deformation (rutting) properties of the mixes.

4.3.1. Current HWTT Analysis Methodology as per AASHTO T 324

As illustrated in Figure 4-8, a typical HWTT output curve can be divided into three main phases (NCHRP Project 20-07/Task 361, 2015) as described below:

a) Post compaction phase: the specimen is consolidated within the post compaction phase which takes place when the mix is densified by the wheel load and a significant decrease in the air voids occurs. This phase is assumed to take place during the first 1000 wheel passes (NCHRP Project 20-07/Task 361, 2015).

b) Creep phase: the creep phase occurs primarily as a result of the permanent deformation of the asphalt mix under loading and is represented by an approximately constant rate of increase in rut depth with wheel pass.
c) Stripping phase: the stripping phase starts after water penetrates through the binder-aggregate interface and the bond between the two components start to degrade resulting in an accelerated increase in rut depth with wheel pass. The rut depth accumulated in this phase is a contribution mainly from moisture damage (stripping) as well as from further permanent deformation under loading.

AASHTO T 324 (2014) requires the following test parameters to be determined from the aforementioned phases in order to quantify the resistance of a mix to moisture damage (stripping):

- Creep slope ("first portion" in Equation 4-2)
- Stripping slope ("second portion" in Equation 4-2)
- Stripping Inflection Point (SIP): The SIP is the graphical point on the HWTT curve at which the creep slope intersects the stripping slope. This point on the curve is representative of the number of wheel passes where the rut depth suddenly increases, primarily due to the stripping of the binder from the aggregate (NCHRP Project 20-07/Task 361, 2015). The SIP is therefore hypothesised to represent the onset of stripping (Aschenbrener & Currier, 1993) and is indicative of the resistance of an asphalt mix to moisture damage. The SIP, with respect to the number of wheel passes, is defined in AASHTO T 324 (2014) as per Equation 4-2.

$$\boldsymbol{SIP} = \frac{\boldsymbol{Intercept\ (second\ portion) - Intercept\ (first\ portion)}}{\boldsymbol{Slope\ (first\ portion) - Slope (second\ portion)}} \qquad \text{Equation 4-2}$$

The above test parameters are graphically illustrated in Figure 4-8.

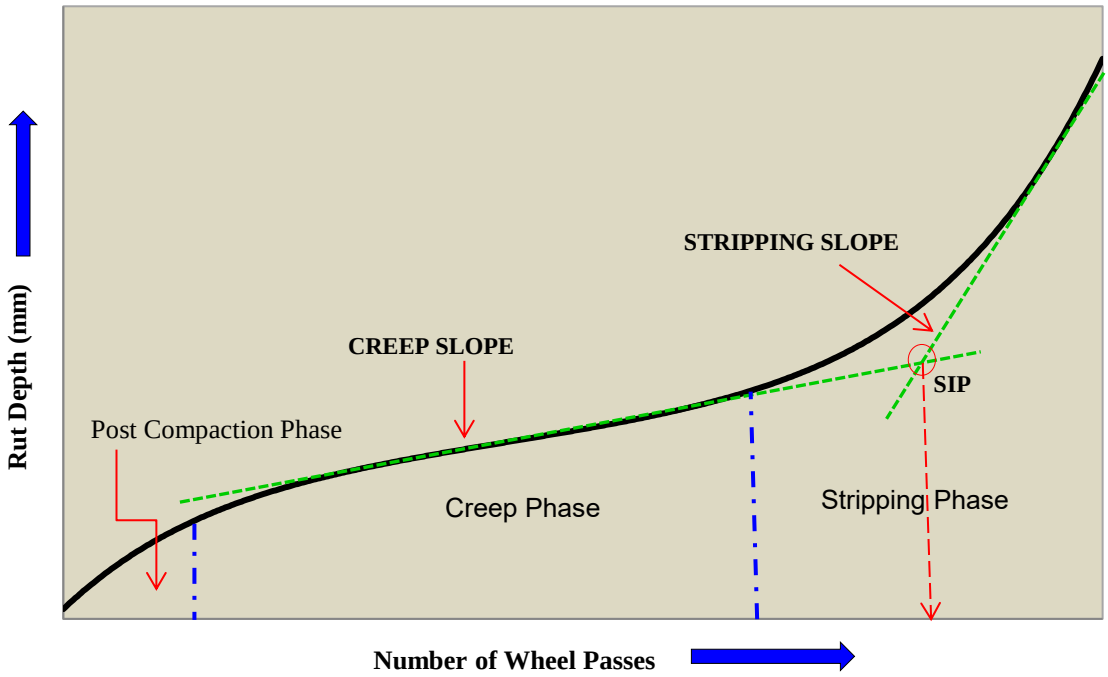

Figure 4-8: Typical HWTT output curve with test parameters

Currently, the SIP at a certain number of wheel passes is widely used as the main HWTT parameter to evaluate the moisture susceptibility of asphalt mixes. Extensive research conducted by the Colorado Department of Transportation (CDOT) has indicated that asphalt mixes with SIP values greater than 10 000 passes demonstrated good pavement performance while for pavements that lasted 1 year, the SIP values was less than 3 000 passes (Aschenbrener, 1995) . It should be noted that the compliance criteria for stripping in South Africa allows for a minimum of 10 000 passes to the SIP (Sabita, 2016). This criterion has been adopted from research work conducted in the USA (Sabita, 2016).

Although the SIP has been increasingly used to evaluate moisture susceptibility, it has been noted that analysis and reporting of the SIP and the aforementioned test parameters (i.e. creep slope and stripping slope) are not clearly and consistently defined as well as not standardised in AASHTO T 324 (Schram & Williams, 2014).

Visually selecting the “first portion” and “second portion” and manually plotting straight lines from the creep phase and stripping phase for the determination of the resultant slopes and intercepts is vague and may thus introduce variation during SIP calculations. Moreover, the post compaction phase is assumed to occur within the first 1000 cycles.

4.3.2. Proposed New HWTT Analysis Methodology

To improve the evaluation of mix moisture susceptibility, a new analysis approach is proposed in this dissertation by curve fitting the HWTT results for the complete output of rut depth against wheel pass. This approach entails the introduction of a new SIP parameter to evaluate and quantify the resistance of GA Mix 1, 2 and 3 to moisture damage (stripping). In addition, the new approach is compared with the current analysis procedure in AASHTO T 324 in order to assess the ability of the new approach to effectively evaluate the moisture susceptibility performance of the three asphalt mixes in the HWTT. A detailed discussion of the new analysis methodology is presented in Section 4.3.2.1.

4.3.2.1. Data Analysis Methodology

The new analysis approach makes use of a 6-degree polynomial function to fit the HWTT output data for rut depth versus number of wheel passes (for GA Mix 1, 2 and 3) as per Equation 4-3.

$$\boldsymbol{RD_N = aN^6 + bN^5 + cN^4 + dN^3 + eN^2 + fN + C} \qquad \text{Equation 4-3}$$

Where:

RD_N = Rut depth at certain number of wheel passes (mm)

N = Number of wheel passes

a, b, c, d, e, f and C = 6-degree polynomial coefficients

It is apparent from the fitted curves illustrated in Figures 4-9 to 4-11 that all three mixes experienced the post-compaction phase, creep phase and stripping phase during the test. The three phases of the fitted curves were analysed by assessing the rate of change of deformation (rut depth) occurring over the respective number of wheel passes. To assess the rate of change of deformation, the first derivative of Equation 4-3 was determined as per Equation 4-4.

$$\boldsymbol{\frac{dRD}{dN} = 6aN^5 + 5bN^4 + 4cN^3 + 3dN^2 + 2eN + f} \qquad \text{Equation 4-4}$$

The calculated rate of change of deformation is represented graphically by the secondary axis in Figures 4-9 to 4-11. It can be observed that the rate of change of deformation in the post compaction phase (Phase 1) decreases rapidly within the first 2 000 cycles and thereafter

reaches an approximately constant rate of change of deformation represented by the creep phase (Phase 2).

It is therefore important to note that it may not be reasonable to assume that Phase 1 occurs within 1000 cycles as the number of cycles accumulated in this phase varies depending on when the rate of deformation stabilises (represented by Phase 2). This variance may be attributed to differences in air void content, method of compaction, workability of the mix, mix type, performance grade of the binder etc. for a particular mix.

Following the creep phase, it can be observed that there is a rapid increase in the rate of change of deformation. It is apparent from Figures 4-9 to 4-11 that this accelerated increase in the rate of change of deformation occurs where the mix transitions from the creep phase to the stripping phase (Phase 3). Graphically, this transition is represented at the point where the curvature of the fitted HWTT curve changes from negative to positive.

To determine the point at which the curvature changes from negative to positive, the second derivative of Equation 4-3 is determined as per Equation 4-5.

$$\frac{d^2RD}{dN^2} = 30aN^4 + 20bN^3 + 12cN^2 + 6dN + 2e \qquad \text{Equation 4-5}$$

The new SIP parameter (SIP_{New}) is determined by setting Equation 4-5 to zero and solving for the number of wheel passes ("N"). This was performed using the "Goal Seek" function in Excel.

The SIP_{New} parameter is used in this study as an indicator to evaluate moisture susceptibility. The corresponding number of wheel passes at this inflection point signifies the maximum number of wheel passes that can be resisted by the asphalt mix in the HWTT before adhesive failure at the binder-aggregate interface occurs. As such, mixes with higher SIP_{New} values is expected to be less moisture susceptible in comparison with those with lower SIP_{New} values.

The results presented in Figures 4-9 to 4-11 are provided in Table B4, B5 and B6 in Appendix B.

4.3.2.2. Moisture Susceptibility Evaluation

The HWTT results for all three glass-asphalt mixes were evaluated using the SIP $_{New}$ parameter as a moisture susceptibility indicator. A SIP $_{New}$ of 10 636, 10 101 and 9 731 wheel passes were obtained for GA Mix 1, 2 and 3 respectively. The results are presented graphically in Figures 4-9 to 4-11.

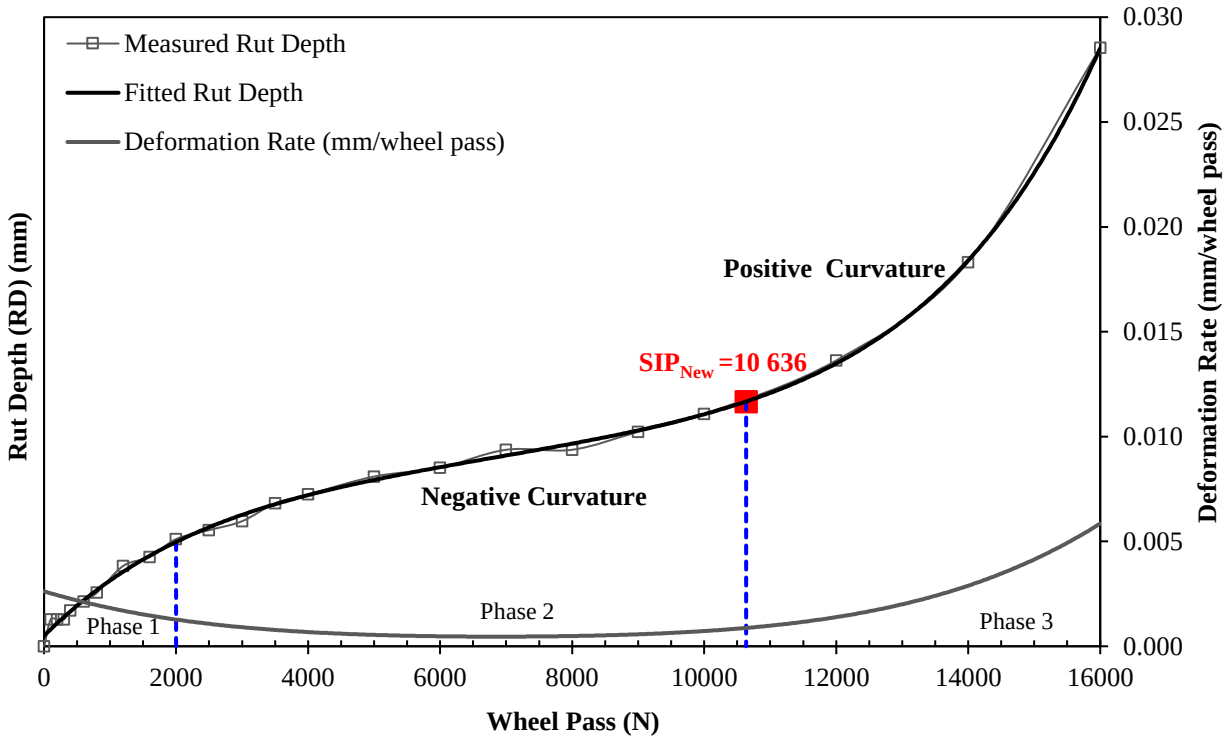

Fitted HWTT curve equation (R^2 = 0.999):
RD = 3.90E-25N^6 + 8.33E-20N^5 - 3.16E-15N^4 + 5.26E-11N^3 - 4.71E-07N^2 + 2.62E-03N + 0.42

Figure 4-9: Determination of SIP $_{New}$ from HWTT results (GA Mix 1)

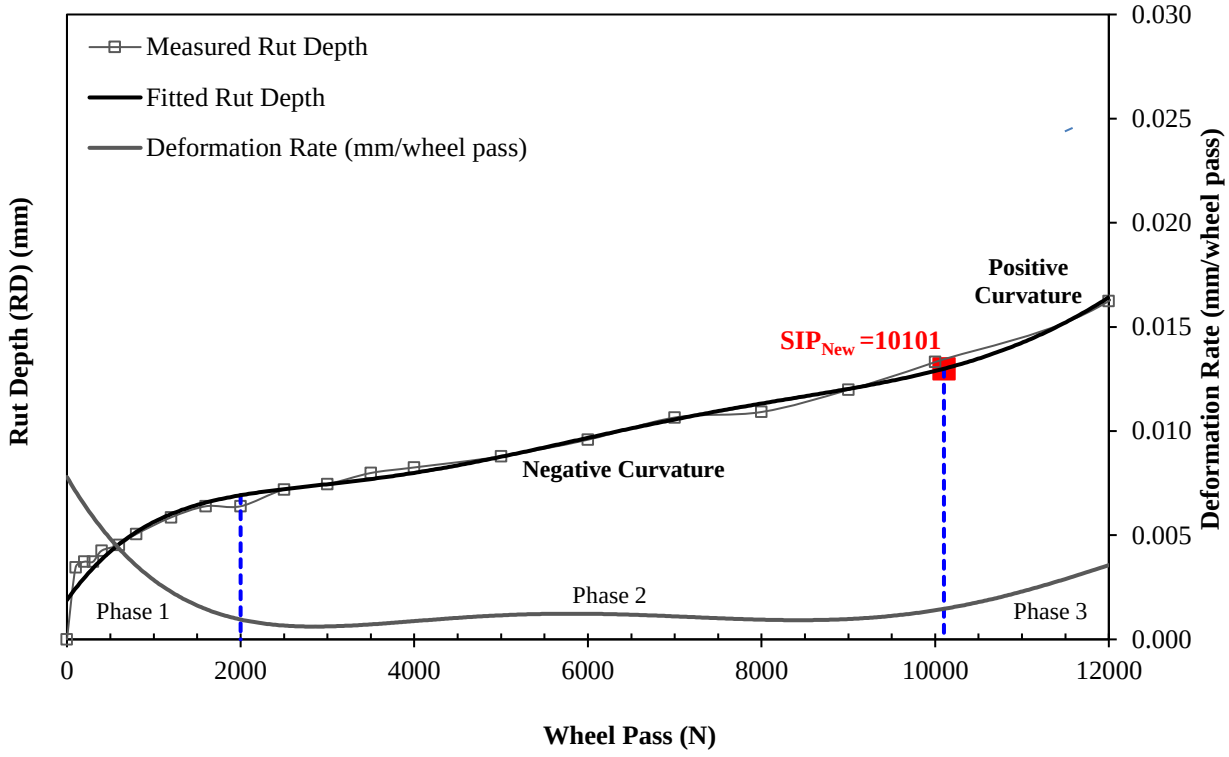

Fitted HWTT curve equation (R^2 = 0.993):
RD = -1.23E-22N6 + 5.69E-18N5 - 1.00E-13N4 + 8.45E-10N3 - 3.55E-06N2 + 7.79E-03N + 2.52

Figure 4-10: Determination of SIP New from HWTT results (GA Mix 2)

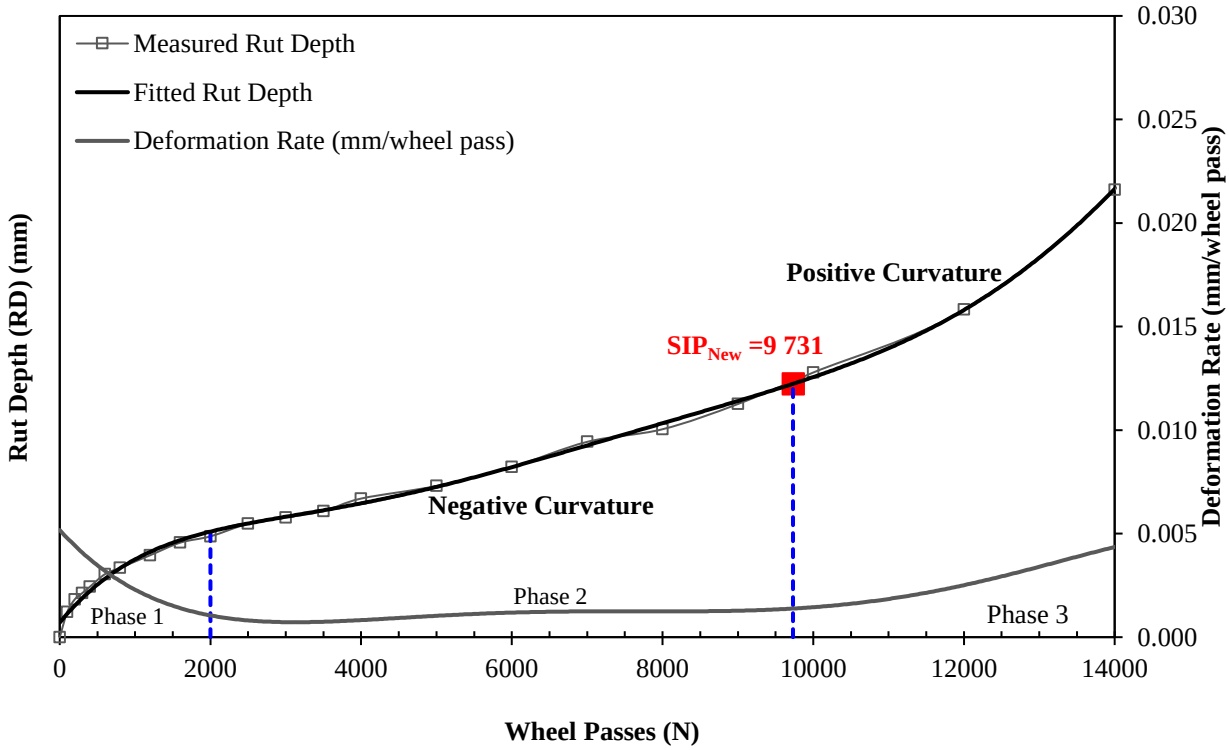

Fitted HWTT curve equation (R^2 = 0.999):
y = -5E-23x6 + 2E-18x5 - 5E-14x4 + 4E-10x3 - 2E-06x2 + 0.0052x + 0.82

Figure 4-11: Determination of SIP New from HWTT results (GA Mix 3)

Based on the calculated SIP_{New} values for all three mixes; it is apparent that the incorporation of hydrated lime as an antistripping additive was most effective in improving mix moisture susceptibility. Furthermore, the effect of adding hydrated lime was more beneficial in improving moisture susceptibility than the liquid antistripping additive.

As expected, GA Mix 3, with a SIP_{New} of less than 10 000 wheel passes, demonstrated the least resistance to moisture damage. This behaviour may be attributed to poor bonding between the glass particles and the binder due to the absence of an antistripping additive in the mix.

Based on the findings of studies conducted by CDOT (Aschenbrener, 1995), a stripping inflection point of greater than 10 000 wheel passes was used in this study as a criterion for characterising good pavement performance. As such, GA Mix 1 is expected to demonstrate good performance to moisture susceptibility while GA Mix 2 only just meets the minimum criterion. On the basis of the determined SIP_{New} of GA Mix 3, the mix is most likely to indicate excessive maintenance problems before the design life of the pavement is reached.

In addition, visual inspections of the tested specimens were conducted in order to identify if the observations were consistent with the moisture susceptibility evaluation using the SIP_{New} parameter. Photographs of the tested specimens are provided in Figure 4-12.

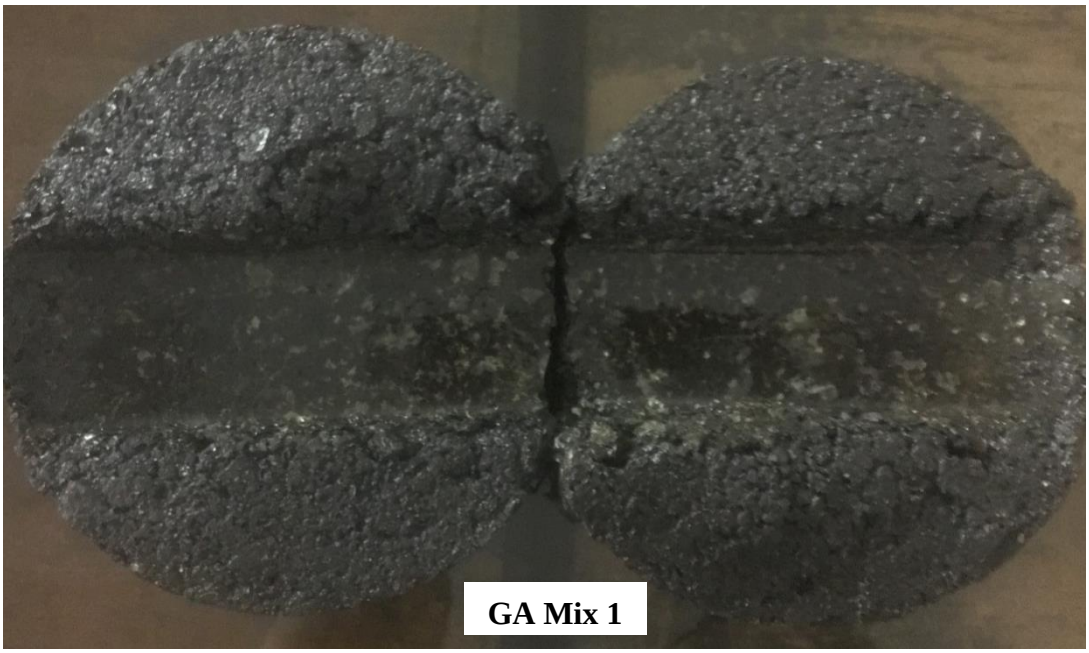

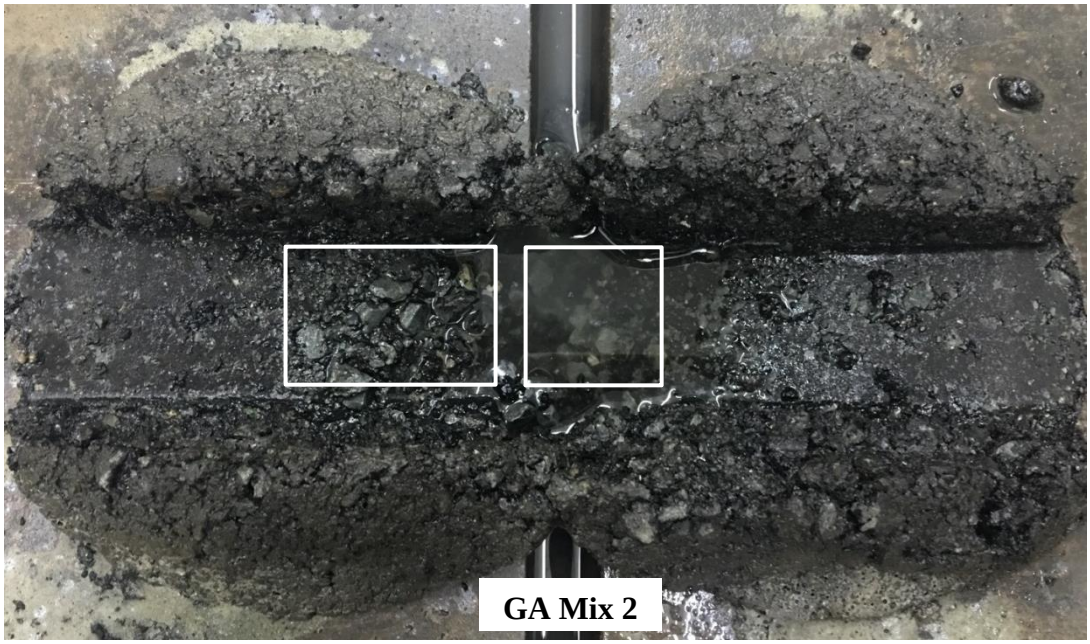

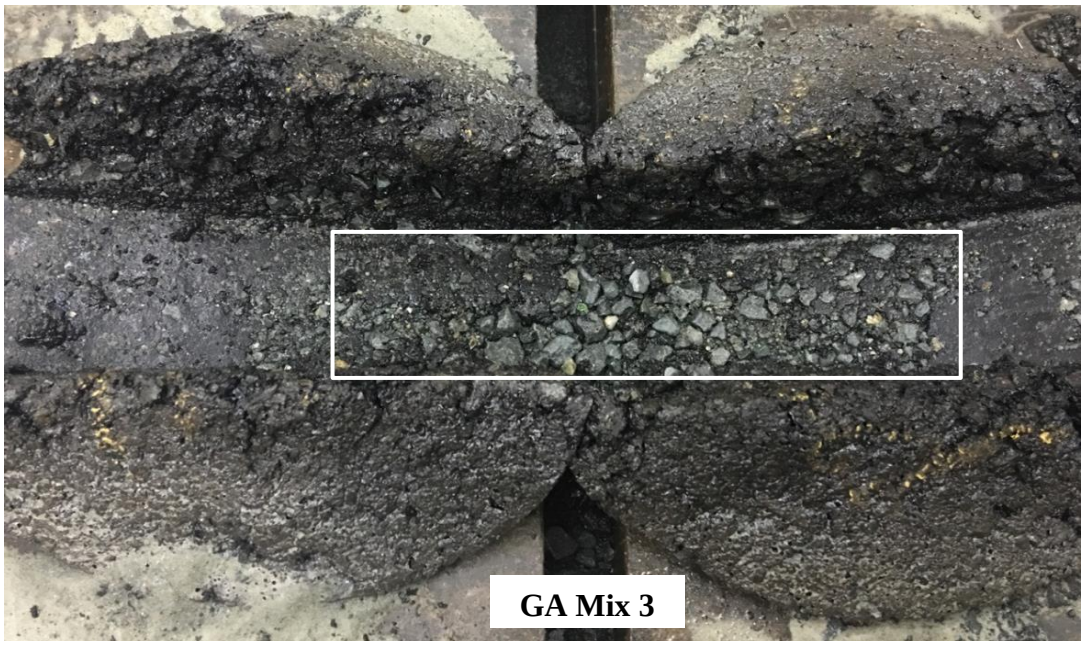

Figure 4-12: Photographs of tested HWTT specimens

It can be observed in Figure 4-12 that stripping of the binder from the aggregates was not evident in GA Mix 1 as the aggregates and the glass particles appear to be in tact with the binder after the full 16 000 load applications. Although an antistripping additive was incorporated in GA Mix 2, signs of minor stripping were observed. In comparison with GA Mix 2, much more uncovered surface areas of both aggregates and glass particles were visible on the tested specimens of GA Mix 3.

Based on the above, the SIP $_{New}$ parameter appears to be in general agreement with the visual observations made for all three glass-asphalt mixes.

4.3.2.3. Comparison of Test Parameters

It was interesting to compare the above approach used to quantify the stripping inflection point with the current analysis procedure described in AASHTO T 324 in order to assess its capability to accurately evaluate the moisture susceptibility of the three glass-asphalt mixes.

In the current AASTO T 324, quantification of the SIP is defined in Equation 4-2. However, AASHTO T 324 does not define how to identify the "first portion" (creep phase) and the "second portion" (stripping phase) in order to plot the respective slopes.

To maintain consistency with the analysis methodology described in Section 4.3.2; the "first portion" was identified after the post compaction phase, where the first derivative of the curve-fit was approximately constant. The number of cycles and rut depth in this portion of the fitted curve was used to calculate the slope and intercept of the straight line plotted through the creep phase.

The start of the "second portion" was identified where the first derivative of the curve-fit rapidly increased (i.e. where the curvature of the fitted curve changed from negative to positive). The stripping slope was obtained by drawing a tangential line at the location of the maximum value of the first derivative in this portion of the fitted curve.

The intersection of the two straight lines was then used to calculate the stripping inflection point (SIP $_{Current}$) for GA Mix 1, 2 and 3 based on Equation 4-2.

The results are summarised in Table 4-8 and graphically presented in Figures 4-13 to 4-15.

Table 4-8: Determination of SIP as per AASHTO T 324

GA Mix 1	GA Mix 2	GA Mix 3
$\text{SIP} = \frac{\text{Intercept (second portion)} - \text{Intercept (first portion)}}{\text{Slope (first portion)} - \text{Slope(second portion)}}$, (AASHTO T324, 2014)		
$\text{SIP} = \frac{(-69.86 - 3.76)}{(0.00054 - 0.00585)}$	$\text{SIP} = \frac{(-20.81 - 6.87)}{(0.00102 - 0.00356)}$	$\text{SIP} = \frac{(-35.69 - 3.27)}{(0.00110 - 0.00435)}$
SIP = 13 864	SIP = 10 893	SIP = 11976

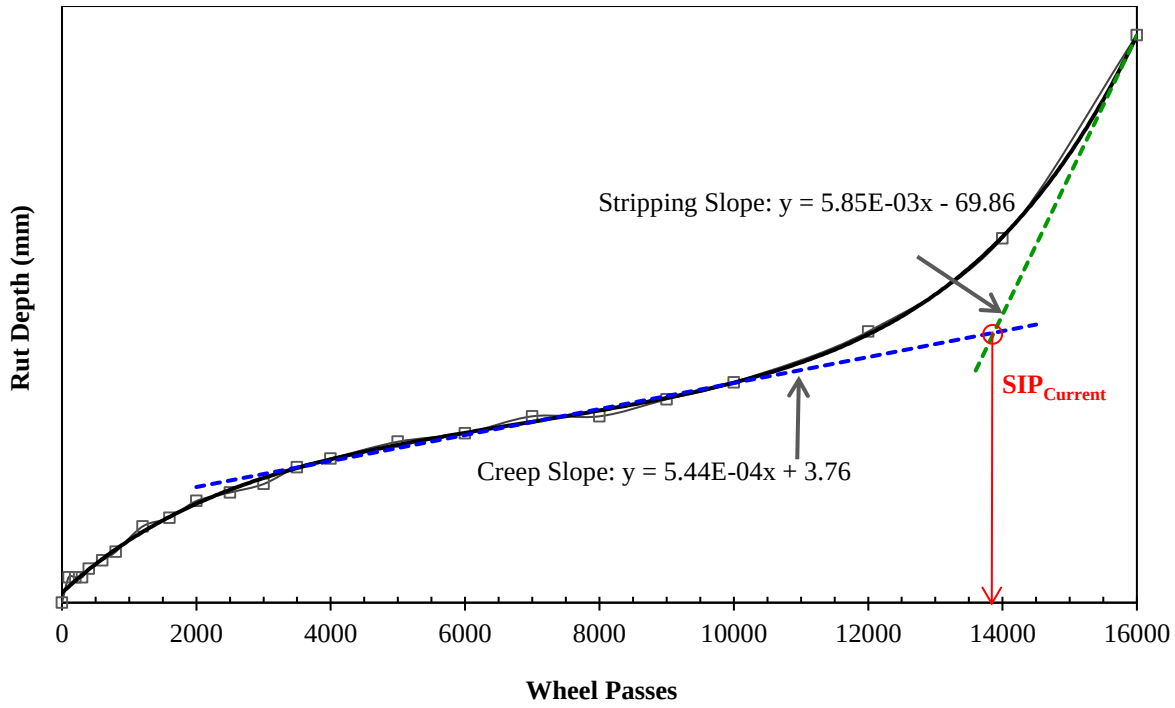

Figure 4-13: Determination of SIP $_{Current}$ from HWTT results (GA Mix 1)

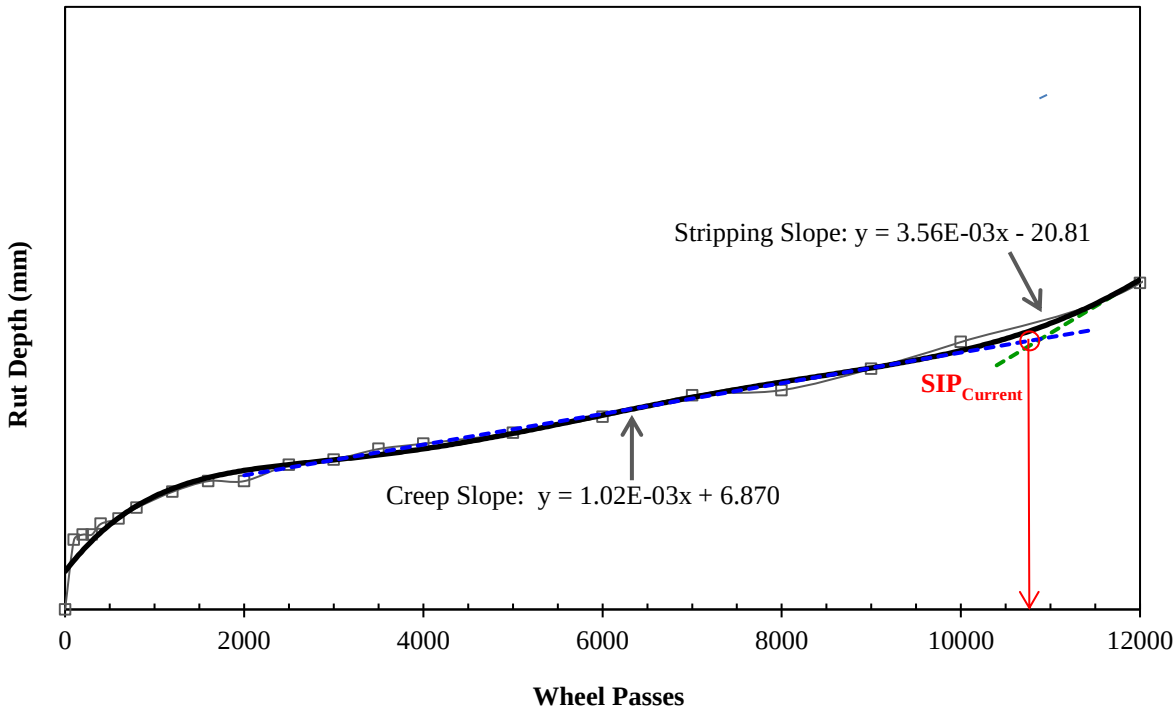

Figure 4-14: Determination of SIP $_{Current}$ from HWTT results (GA Mix 2)

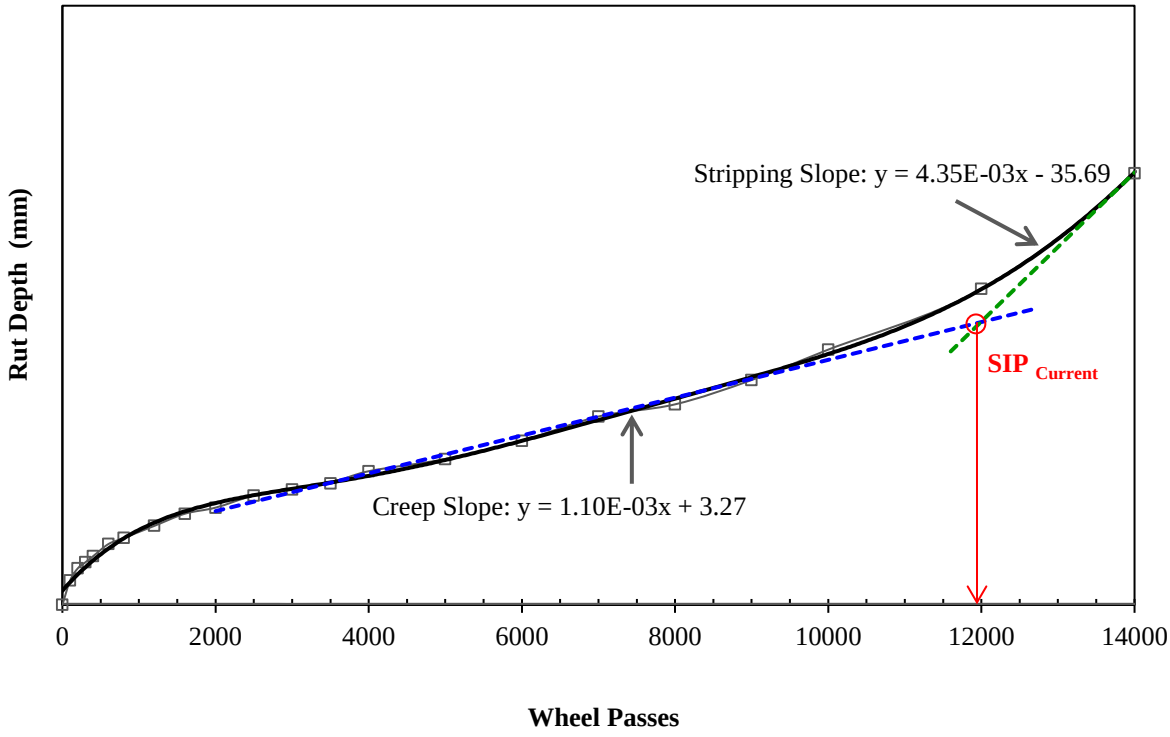

Figure 4-15: Determination of SIP $_{Current}$ from HWTT results (GA Mix 3)

From the above results, it can be observed that the calculated SIP $_{Current}$ value for GA Mix 3 (11 976 wheel passes) is higher than the SIP $_{Current}$ value for GA Mix 2 (10 893 wheel passes). This is quite surprising as GA Mix 3 does not incorporate an antistripping agent but appears to have a greater resistance to stripping than GA Mix 2 as indicated by a higher SIP $_{Current}$ value.

As previously mentioned, the absence of an antistripping additive, particularly in glass-asphalt mixes, may speed up water penetration through the interface between the glass particles and the binder, subsequently causing early adhesive failure and stripping in the mix as visually confirmed in GA Mix 3. As such, it is unlikely that GA Mix 3 will demonstrate better pavement performance in terms of stripping resistance which further validates inconsistency of the calculated SIP $_{Current}$ value relative to the SIP criterion for good pavement performance (i.e. >10 000 wheel passes).

Moreover, it is interesting to note that the above evaluation on moisture susceptibility of the three glass-asphalt mixes is consistent with the moisture susceptibility evaluation conducted using the TSR parameter, obtained from the Modified Lottman test.

A summary of the moisture susceptibility parameters evaluated in Section 4.2 and 4.3 (i.e. TSR parameter, total area of white/black pixels and the SIP $_{New}$ parameter) is presented in Figure 4-16 and Table 4-9.

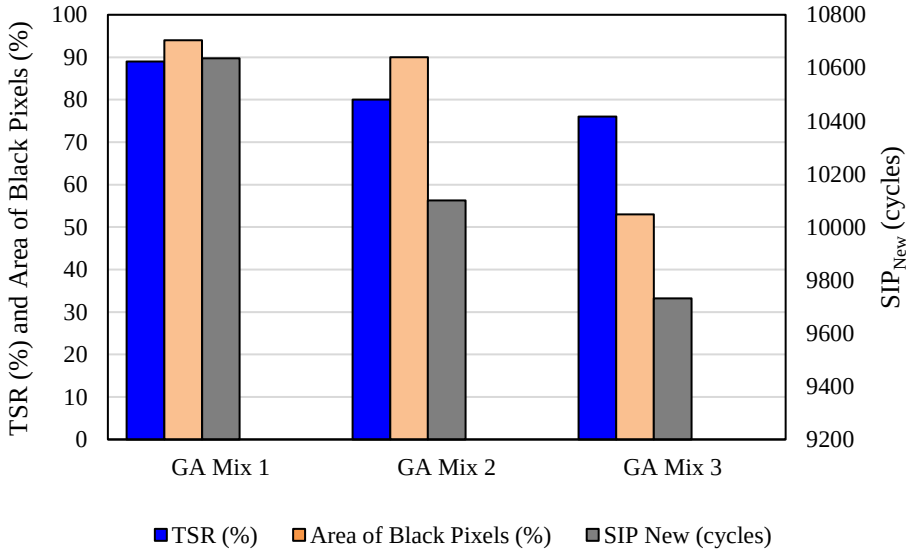

Figure 4-16: Moisture susceptibility evaluation of GA Mix 1, 2 and 3

4.4. Summary

Chapter 4 presents the assessment on moisture susceptibility of three glass-asphalt mixes studied (i.e. GA Mix 1, GA Mix 2, and GA Mix 3) as a basis for selection of the optimum-glass asphalt mix. The HWTT and the Modified Lottman test were conducted to assess the above.

A summary of the performance ranking of GA Mix 1, 2 and 3 in terms of moisture susceptibility is presented in Table 4-9. A ranking of 1 to 3 indicates least to most moisture susceptible. The ranking parameters were obtained from the Modified Lottman test (i.e. TSR and microscopic image analysis) and the HWTT (i.e. SIP New parameter) evaluated in Section 4.2 and 4.3.

Table 4-9: Moisture susceptibility ranking for GA Mix 1, 2 and 3

Glass-Asphalt Mix	Performance Ranking	TSR [1]	Microscopic Image Analysis	SIP_{New} [2]
			(%)	(Passes)
GA Mix 1	1	0.89 (1)	5.86 (1)	10 636 (1)
GA Mix 2	2	0.80 (2)	9.59 (2)	10 101 (2)
GA Mix 3	3	0.76 (3)	46.9 (3)	9 731 (3)

[1] Min. TSR criteria (South Africa) = 0.8
[2] Min. SIP criteria (South Africa) = 10 000 passes

Based on the TSR results obtained from the Modified Lottman test, GA Mix 1 and 2 meet the minimum TSR compliance criteria (i.e. 0.8) with GA Mix 1 indicating better resistance to stripping than GA Mix 2. GA Mix 3, however, does not meet the minimum TSR criteria and is expected to demonstrate the least resistance to stripping.

A similar trend is obtained from the microscopic image analysis conducted on the Modified Lottman test specimens of each glass-asphalt mix whereby a significant reduction in the area of white pixels (stripped areas) was obtained for GA Mix 1 and 2 in comparison with GA Mix 3, with GA Mix 1 indicating a smaller area of stripping than GA Mix 2.

The proposed new SIP parameter, obtained from the HWTT, proved to be more effective in evaluating mix moisture susceptibility than the current method of evaluation. In this regard, GA Mix 1 and 2 appear to be the least susceptible to moisture damage, as indicated by a SIP_{New} value of greater than 10 000 passes, while GA mix 3 does not meet the SIP compliance criterion.

It is evident from the above that all parameters appear to effectively rank GA Mix 1 as least susceptible to moisture damage. Although GA Mix 2 meets the minimum TSR and SIP_{New} criteria for moisture susceptibility, it is evident that the hydrated lime in GA Mix 1 is more effective than the liquid antistripping additive in GA Mix 2 in resisting stripping. Furthermore, it can be observed that GA Mix 3, which does not contain an antistripping additive, is ranked as most susceptible to moisture damage and additionally does not meet the moisture susceptibility criteria. Based on these rankings, GA Mix 1 was selected as the optimum glass-asphalt mix on which further investigation regarding the engineering performance properties were conducted.

5. PERFORMANCE EVALUATION OF OPTIMUM GLASS-ASPHALT MIX

5.1. Introduction

Chapter 5 compares the performance properties of the optimum glass-asphalt mix (GA Mix 1) and a traditional asphalt mix in terms of permanent deformation and stiffness. The traditional asphalt mix (referred to as Reference Mix) was designed to represent a similar design aggregate grading to the glass-asphalt mix using the same component materials (i.e. traditional aggregates, filler (hydrated lime) and binder). The Reference Mix is discussed in Section 5.2.

As part of the performance evaluation of GA Mix 1 and the Reference Mix, mathematical models that effectively describe the permanent deformation and stiffness behaviour of both mixes are also discussed.

5.2. Reference Mix

5.2.1. Design Aggregate Grading

As mentioned in Chapter 3, both mixes have been designed to represent a similar design aggregate grading to the SANRAL 10 mm NMPS medium continuously-graded asphalt mix (standard mix). Similar to GA Mix 1, the same aggregates and binder (i.e. 50-70 penetration grade binder) used in the standard mix were utilised in the Reference Mix. As mentioned in Chapter 3, the filler material used in the standard mix comprised of baghouse fines (plant filler), however, for comparative purposes the same filler material used in GA Mix 1 was used in the Reference Mix.

The design grading of the Reference Mix has been plotted on a 0.45 power chart as illustrated in Figure 5-1. It can be observed that a similar particle size distribution to GA Mix 1 has been obtained for the Reference Mix. This was achieved using the same optimisation technique in Microsoft Excel™ described in Section 3.3. Table 5-4 indicates the percentage blend of each aggregate fraction and filler incorporated in the design grading of the Reference Mix.

It can be observed that the design grading falls within the grading control points specified for a 10 mm nominal maximum particle size (NMPS) continuously graded asphalt mix (Sabita, 2016).

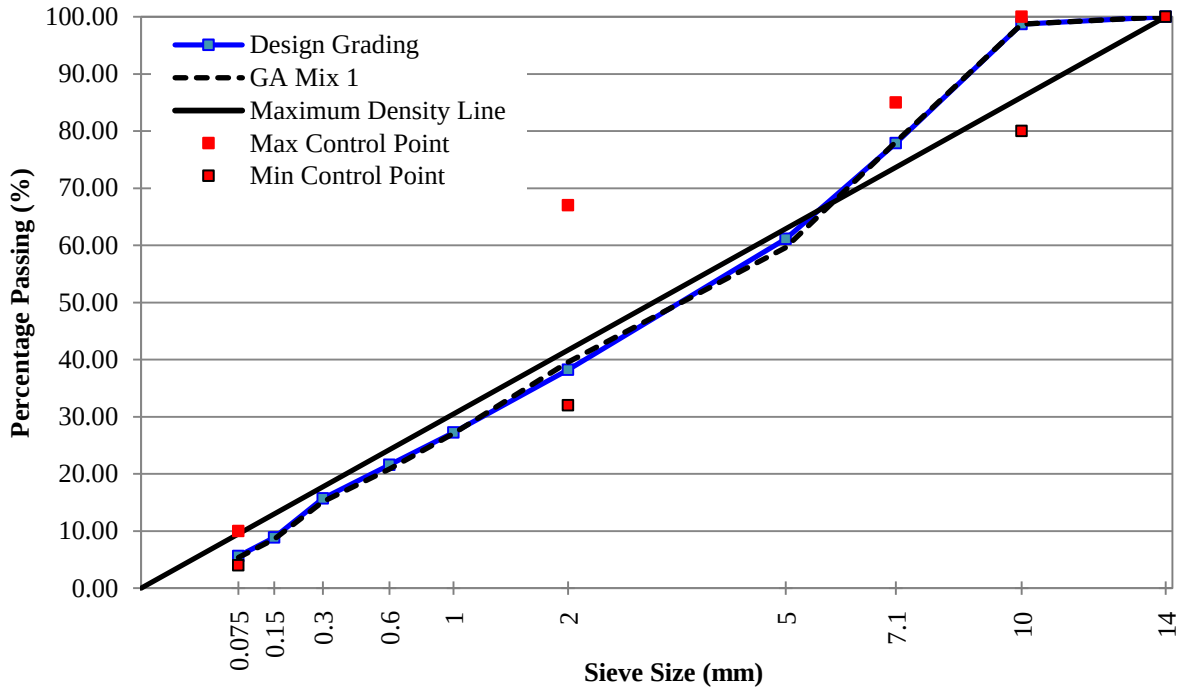

Figure 5-1: Design grading of 10 mm NMPS Reference Mix

5.2.2. Minimum Binder Content

Similar to GA Mix 1; the minimum binder content for the Reference Mix was determined in accordance with Equation 3-1. The minimum binder content was obtained at 4.0% as summarised in Table 5-1.

Table 5-1: Minimum binder content for Reference Mix

	Reference Mix	**GA Mix 1***
Total BD_A in Mix (ton/m^3)	2.765	2.744
Total Surface Area	5.81	5.60
Minimum K Value	2.9	2.9
Minimum Binder Content	$B_{ppc} = 2.9 * \frac{2.65}{2.765} * \sqrt[5]{5.81} = 4.0\%$	$B_{ppc} = 4.0\%$

***Detailed results can be referred to in Section 3.4

5.2.3. Voids in Mix (VIM) and Optimum Binder Content

Similar to GA Mix 1; the laboratory measured MVD values and BD values were used to determine the voids of the compacted specimens at each trial binder content. The specimens were compacted to 150 mm diameter by 115 $\pm$ 5 mm height at 100 gyrations. The results are summarised in Table 5-2 and presented in detail in Appendix C- Table C1 and C2. The voids in the Reference Mix (VIM) were hence plotted against each trial binder content and the optimum binder content of 5% was thus established at 4% air voids, as presented in Figure 5- 2.

Table 5-2: Voids in Reference Mix

Binder Content (%)	BD (ton/m^3)*	Avg. BD (ton/m^3) (A)	MVD (ton/m^3)*	Avg. MVD (ton/m^3) (B)	Voids* (%) (B-A)/(B)
4.0	2.447	2.446	2.645	2.645	7.5
	2.445		2.645		
4.5	2.477	2.479	2.619	2.618	5.3
	2.481		2.618		
5.0	2.506	2.508	2.603	2.604	3.7
	2.510		2.604		
5.5	2.529	2.528	2.582	2.583	2.1
	2.527		2.584		

*Results for GA Mix 1 can be referred to in Section 3.5

As a point of interest, the laboratory measured MVD values were used to determine the percentage of binder absorbed by the Reference Mix using the same approach described in Section 3.5. As expected, the Reference Mix indicated higher binder absorption (B_{ABS} average = 0.8%) than GA Mix 1 (B_{ABS} average = 0.6%). The low absorptive properties of the crushed glass particles in GA Mix 1 may be the primary contributory factor to this observation. The results are summarised in Table 5-3 and presented in detail in Appendix C– Table C3.

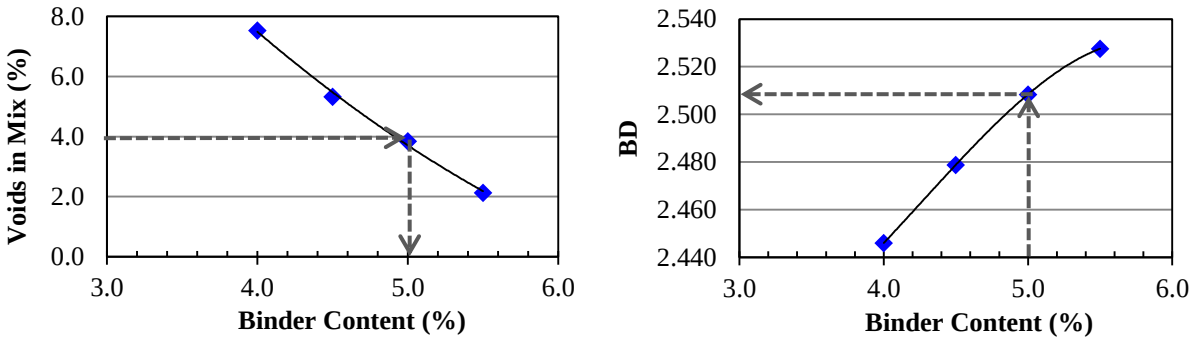

Figure 5-2: Bulk density and voids and in Reference Mix

Table 5-3: Binder absorption in Reference Mix and GA Mix 1

Binder Content (%)	Binder Absorbed by Aggregate in Mix (%)	
	Reference Mix	GA Mix 1
4.0	0.8	0.6
4.5	0.7	0.5
5.0	0.8	0.6
5.5	0.8	0.6

Table 5-4: Aggregate design for Reference Mix

.		AGGREGATE					FILLER	AGGREGATE DESIGN				
		Reference Mix					Ref. Mix	Reference Mix			Grading Spec	
		9.5 Andesite	6.7 Andesite	CD Andesite	CS Granite	Mine Sand	HL	**Design Grading**	**Target Grading (GA Mix 1)**	**Standard Deviation**	Min	Max
% Blend		**28.5%**	**12.5%**	**26%**	**26%**	**6%**	**1%**				(%)	(%)
		PERCENTAGE PASSING (%)										
Sieve Size (mm)	14	100	100	100	100	100	100	100	100	0.0	**100**	
	10	95	100	100	100	100	100	99	99	0.0	**80**	**100**
	7.1	25	94	100	99	100	100	78	78	0.2		**85**
	5	5	28	97	92	100	100	61	60	1.1		
	2	2	3	58	58	100	100	38	40	1.0	**32**	**67**
	1	2	2	38	37	100	100	27	27	0.1		
	0.6	2	2	29	25	99	100	22	21	0.5		
	0.3	1	1	21	13	88	100	16	15	0.4		
	0.15	1	1	15	6	32	100	9	9	0.2		
	0.075	1.0	1.1	11.5	3.1	6.9	99.0	5.6	5.4	0.2	**4**	**10**

5.3. Permanent Deformation Evaluation

Permanent deformation (or rutting) of the asphalt layer is caused by large stresses in the upper layer which is induced by traffic, most especially at increased temperatures, resulting in shear deformation in the asphalt mix. On the surface of a pavement, permanent deformation is apparent in the form of surface depressions in the wheel paths.

In this study, the Flow Number (FN) test was conducted to evaluate the permanent deformation resistance of the optimum glass-asphalt mix (GA Mix 1) and the traditional asphalt mix (Reference Mix). It should be mentioned that previous researchers (Witczak et al., 2002) reported that the FN test results had good correlation with field rutting performance.

The asphalt mixture performance tester (AMPT) permanent deformation test procedure specified in AASHTO TP79 was used to conduct the FN test. The FN test entails the application of a repeated compressive haversine load at 1 Hz (i.e. one cycle with a loading time of 0.1 seconds and a rest period of 0.9 seconds) and a measure of the corresponding cumulative axial permanent strain as a function of load cycles.

In this study, a deviator stress level of 276 kPa with a confining pressure of 69 kPa was applied on the test specimens and conducted at a test temperature of 50°C. The mentioned stress levels were selected in order to generate sufficient number of load cycles, at a test temperature of 50°C, to reasonably compare the FN of the two mixes. Three replicated specimens, each 100 mm diameter by 150 mm high, were gyratory compacted at the obtained optimum binder content to a target air void content of of approximately 7 $\pm$ 0.5% as indicated in Table 5-5.

It should be mentioned that the CSIR is currently investigating the AMPT permanent deformation test parameters such as sample confinement and deviatoric stress levels in order to eliminate any identified test deficiencies. Current investigations entail determining the effects of three deviatoric stress levels of 138 kPa, 276 kPa, and 483 kPa, and a confining pressure of 69 kPa on the flow number, permanent strain at flow and the rate of permanent deformation. The aim is to standardise the test for future use in South Africa (Anochie-Boateng & George, 2016).

Table 5-5: Air voids determination for GA Mix 1 and Reference Mix

Mix Type	Mix	BD (ton/m^3)	MVD (ton/m^3)	Air Voids (%)
Glass-Asphalt Mix	15036-L-C1	2.385	2.570	7.2
	15036-L-C2	2.391		7.0
	15036-L-C5	2.387		7.1
Reference Mix	15036-RB-C6	2.426	2.604	6.8
	15036-RB-C7	2.422		7.0
	15036-RB-C10	2.422		7.0

The typical output parameters generated from the FN test are presented in Figure 5-3. As shown, the permanent strain response is divided into three main stages: primary, secondary and tertiary. The cycle number at which tertiary flow (i.e. tertiary zone) commences is defined as the FN. Thus it is considered that the permanent deformation failure of the asphalt mix occurs at the onset of tertiary flow and is indicative of the resistance of the mix to permanent deformation.

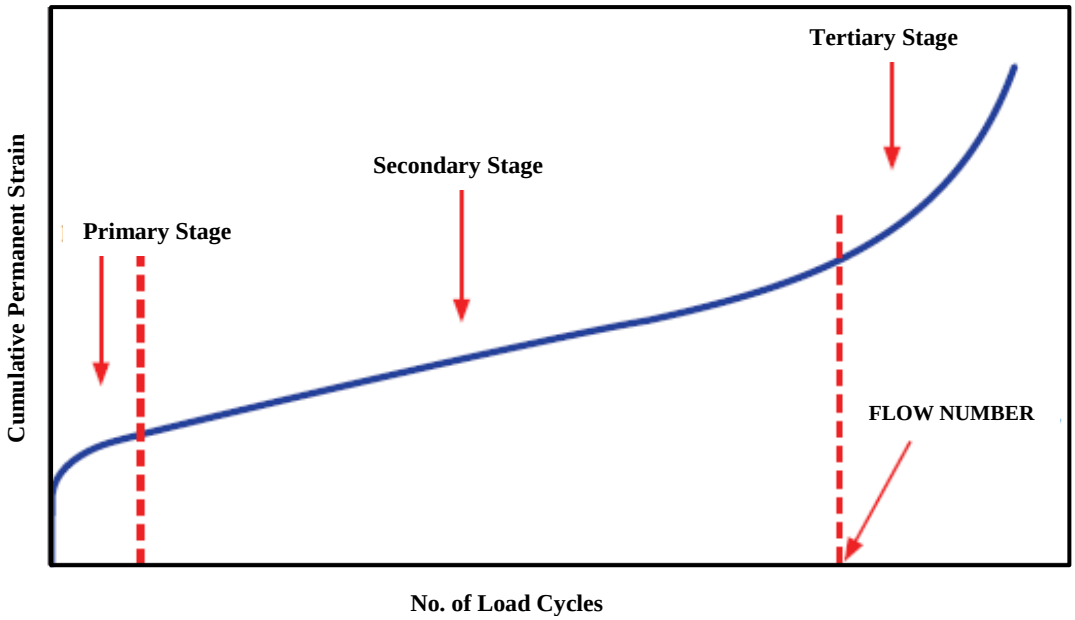

Figure 5-3: Representation of typical output parameters in FN test

Currently there is no standard method for locating the flow number from the permanent deformation curve of the FN test. Inaccuracies may arise when the minimum permanent strain rate is merely obtained directly from the laboratory measured test results. As a result, several mathematical models that describe the permanent deformation curve for determination of the FN value have been proposed by various researchers (Biligiri et al., 2007). An assessment on a selected few of these models, that are known to best describe all three stages of permanent deformation, is discussed below.

5.3.1. Power Model

The mathematical expression that defines the power model is described in Equation 5-1.

$$\varepsilon_p = aN^b \qquad \text{Equation 5-1}$$

Where:

ε_p = permanent strain (%)

N = number of load cycles

a, b = regression coefficients

Figure 5-4 and 5-5 presents the laboratory measured permanent deformation test results for both GA Mix 1 and the Reference Mix which are modelled using the power model. The test results are also provided in Appendix C -Table C4. The coefficients of the power model were obtained from a non-linear least squares regression of the set of measured permanent deformation data. The regression was carried out using the Solver function in Microsoft Excel. The determined coefficients of the power model are given in Table 5-6.

Table 5-6: Determination of power model coefficients

Asphalt Mix	a	b
GA Mix 1	4.4938E-02	6.3581E-01
Reference Mix	2.7427E-02	7.4824E-01

It can be observed that the tertiary stage of permanent deformation is not adequately described by the power model for both mixes. This model may therefore only be effective for asphalt mixes where only the primary and secondary stages of permanent deformation are encountered.

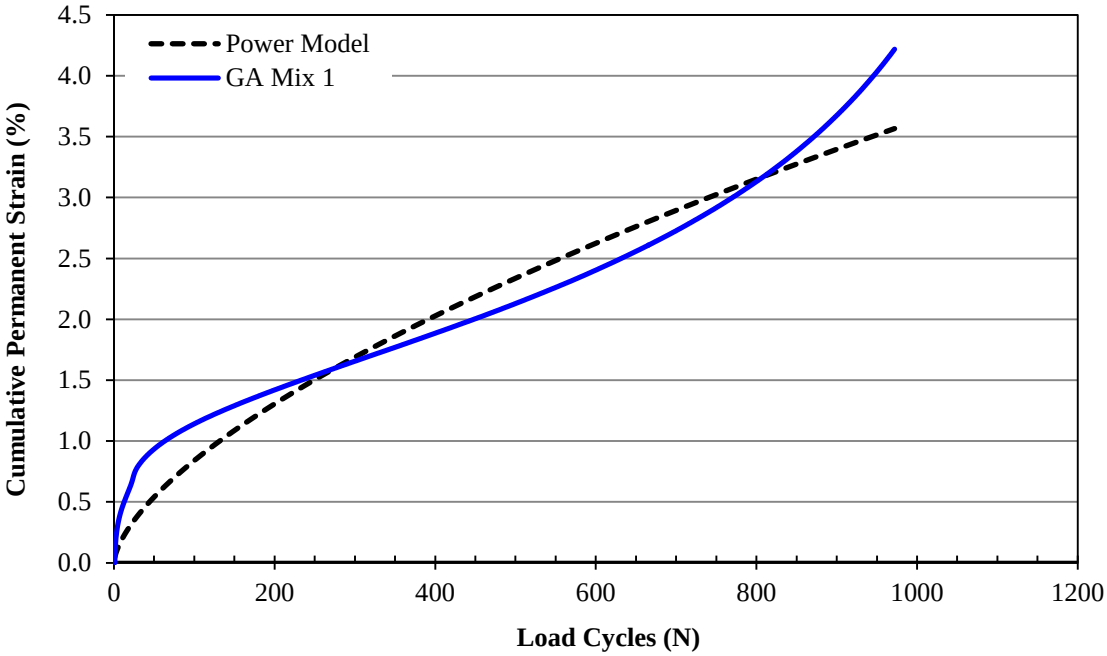

Figure 5-4: Power model describing permanent deformation of GA Mix 1

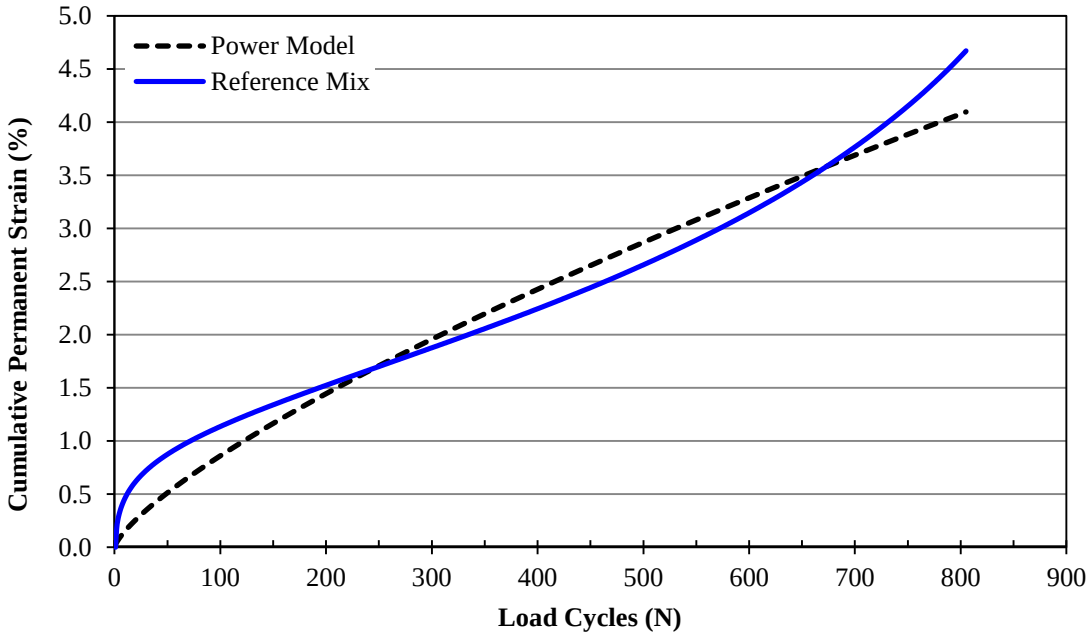

Figure 5-5: Power model describing permanent deformation of Reference Mix

5.3.2. Wilshire and Evans Model

The Wilshire and Evans (WE) model (Wilshire & Evans, 1994) is defined by the following mathematical equation:

$$\boldsymbol{\varepsilon = \theta_1\left(1 - e^{-\theta_2 N}\right) + \theta_3\left(1 - e^{-\theta_4 N}\right)} \qquad \text{Equation 5-2}$$

Where:

$\varepsilon =$ permanent strain (%)

$N =$ number of load cycles

$\theta_1, \theta_2, \theta_3$ and $\theta_4 =$ model parameters, where θ_1 and θ_3 refer to the primary and tertiary strains, while θ_2 and θ_4 refer to the rate parameters quantifying the curvature of the primary and tertiary stages respectively.

Figure 5-6 and 5-7 presents the Wilshire and Evans model which was used to model the permanent deformation behaviour of GA Mix 1 and the Reference Mix. The parameters of the Wilshire and Evans model were obtained from a non-linear least squares regression of the set of measured permanent deformation data. The regression was carried out using the Solver function in Microsoft Excel. The determined parameters of the model are provided in Table 5- 7.

Table 5-7: Determination of Wilshire and Evans model parameters

Asphalt Mix	θ_1	θ_2	θ_3	θ_4
GA Mix 1	1.1389	0.0299	0.7716	-0.0016
Reference Mix	1.0067	0.0315	1.3361	-0.0016

The FN was determined from the Wilshire and Evans model firstly by determining the first derivative (i.e. strain rate of change) of Equation 5-2 as described in Equation 5-3. The strain rate of change (strain slope) is indicated by the secondary axis in Figure 5-8 and 5-9.

$$\boldsymbol{\frac{d\varepsilon}{dN} = (\theta_1\theta_2 e^{-\theta_2 N}) - (\theta_4\theta_3 e^{-\theta_4 N})} \qquad \text{Equation 5-3}$$

The onset of tertiary flow, which is defined as the FN, is represented graphically by the inflection point on the permanent deformation curve or the point at which the curvature changes

from negative to positive. To determine this point, the derivative of Equation 5-3 is determined (or the second derivative of the model) as described in Equation 5-4.

$$\frac{d^2\varepsilon}{d^2N} = (-\theta_1\theta_2{}^2e^{-\theta_2 N}) + (\theta_4{}^2\theta_3 e^{-\theta_4 N}) = 0 \qquad \text{Equation 5-4}$$

The FN value was then determined by solving Equation 5-4 for the load cycle number (N). Using the above approach the FN for GA Mix 1 and the Reference Mix was obtained at 198 and 172 load cycles respectively. It can be seen that these FN values also correspond with the minimum point on the strain slope curve, where commencement of the tertiary stage occurs. From the determined FN values, it is apparent that GA Mix 1 has an increased resistance to permanent deformation than the Reference Mix.

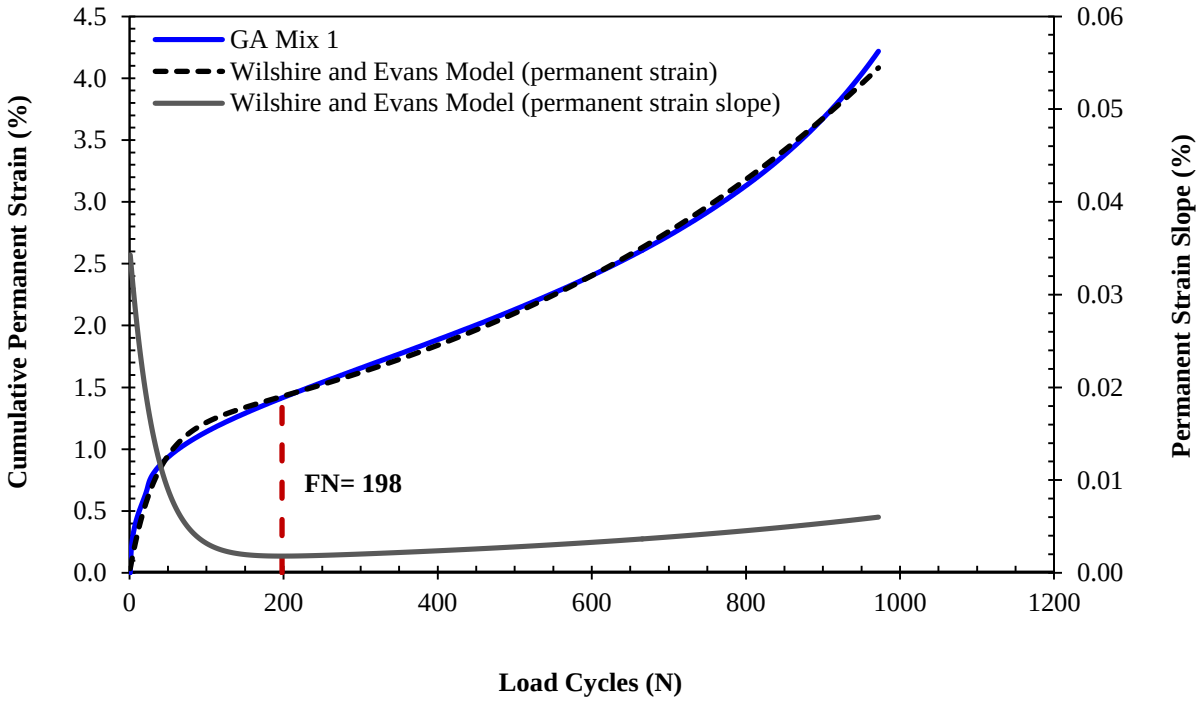

Figure 5-6: Wilshire and Evens model describing permanent deformation of GA Mix 1

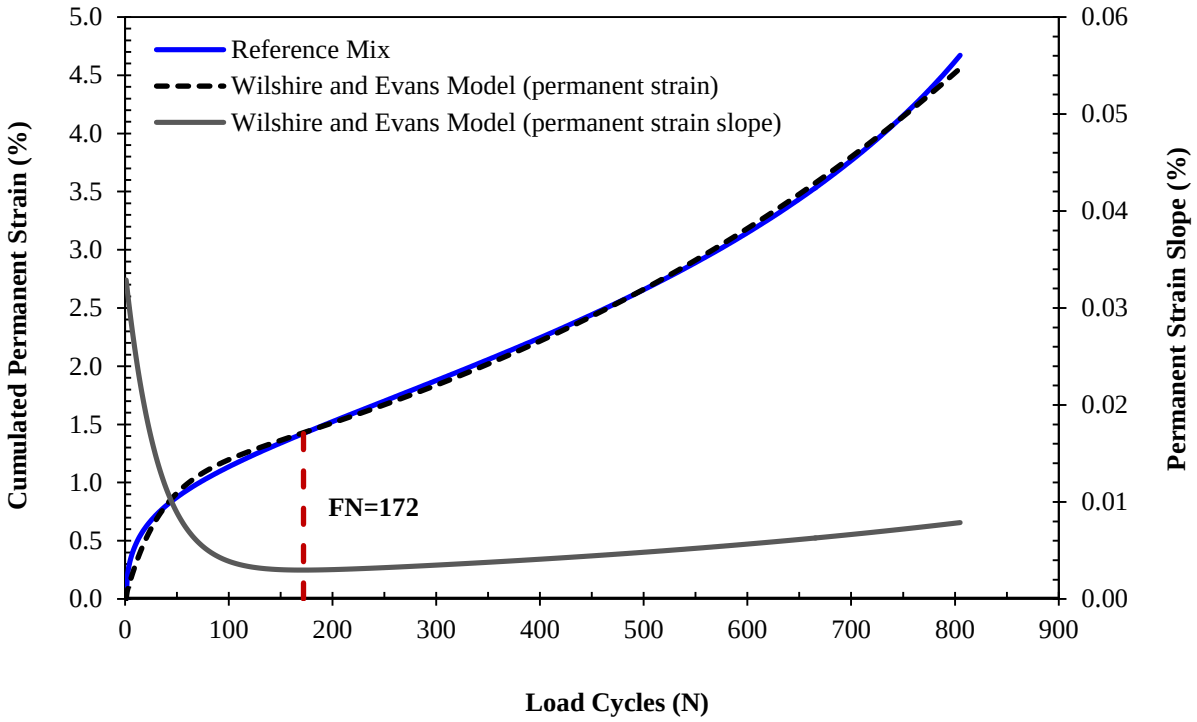

Figure 5-7: Wilshire and Evens model describing permanent deformation of Reference Mix

Unlike the power model, it can be observed that all three stages of permanent deformation are represented by the Wilshire and Evans model for both mixes. Moreover, it can be seen that the measured permanent deformation behaviour for both mixes is described by the model with reasonable accuracy resulting in a coefficient of determination (R^2) of 0.997 (GA Mix 1) and 0.998 (Reference Mix), as indicated in Figure 5-8 and 5-9.

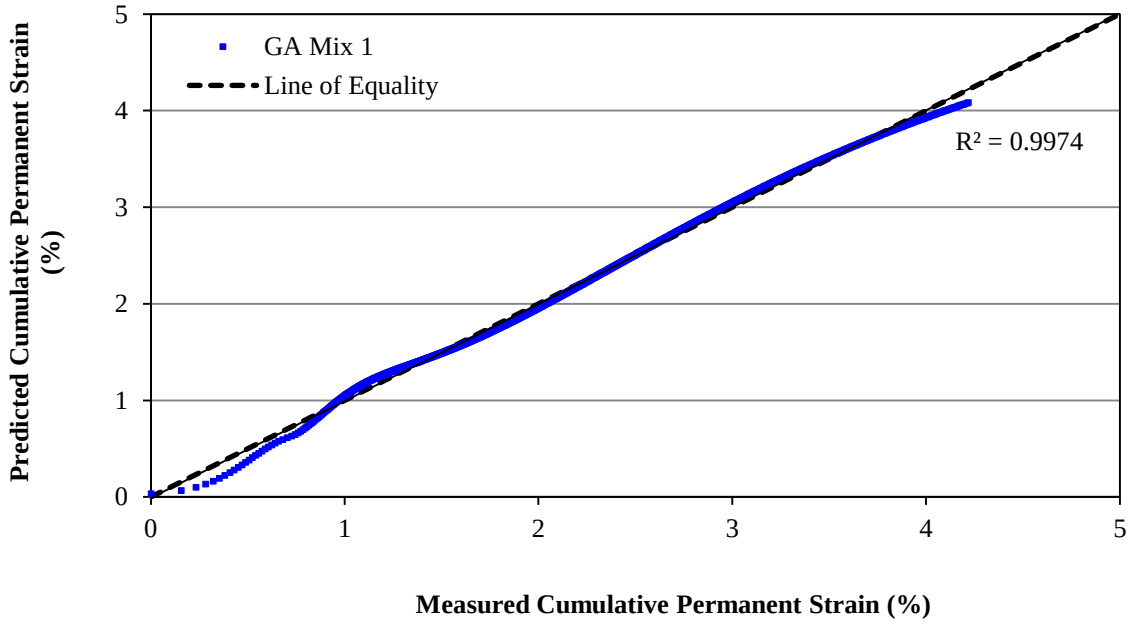

Figure 5-8: Measured vs predicted permanent deformation of GA Mix 1

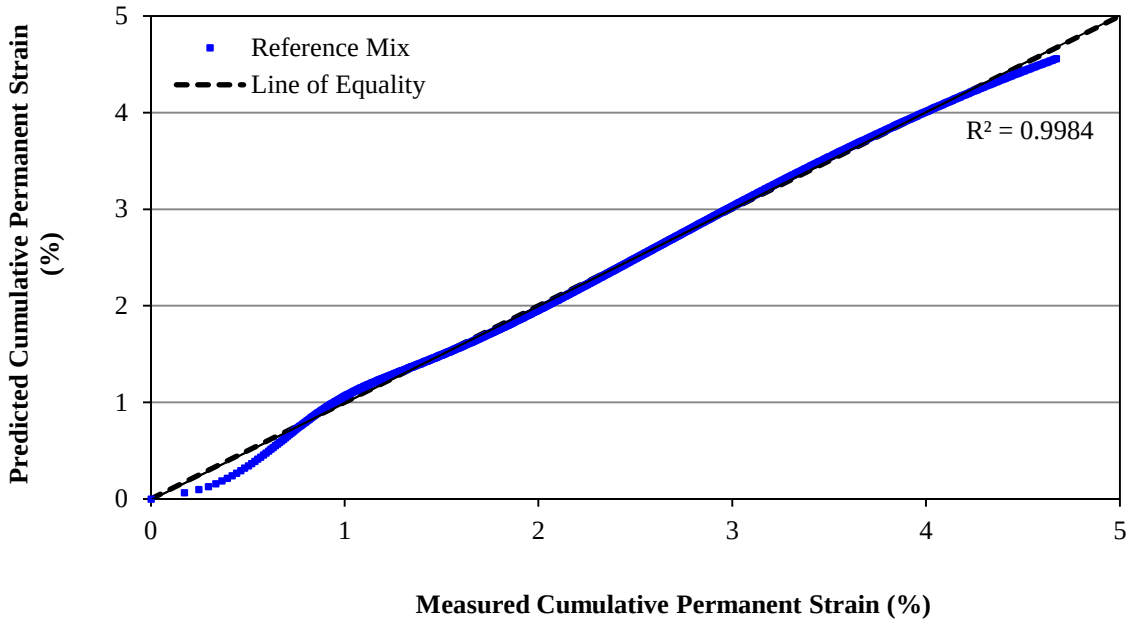

Figure 5-9: Measured vs predicted permanent deformation of Reference Mix

5.3.3. Polynomial Model

During the secondary stage of permanent deformation, the rate of change of strain (strain slope) is considered to reach a minimum after a certain number of loading cycles. The polynomial model is implemented in this region of the permanent deformation curve, whereby a second-degree polynomial curve in the form of Equation 5-5 is used to model the measured rate of change of permanent strain.

$$\boldsymbol{\varepsilon_p = a + bN + cN^2} \qquad \text{Equation 5-5}$$

Where:

ε_p = permanent strain rate

N = load cycle

a, b and c = regression coefficients

The first derivative of Equation 5-5 is then determined and equated to zero to obtain the FN value, as described in Equation 5-6.

$$\boldsymbol{\frac{d\varepsilon_p}{dN} = b + 2cN = 0} \qquad \text{Equation 5-6}$$

Figure 5-10 and 5-11 presents the polynomial model used to describe the measured permanent deformation behaviour of GA Mix 1 and the Reference Mix. The coefficients of the polynomial model were obtained from a non-linear least squares regression of the set of measured permanent deformation data. The regression was carried out using the Solver function in Microsoft Excel. The determined coefficients of the model are provided in Table 5-8.

Table 5-8: Determination of polynomial model parameters

Asphalt Mix	a	b	c
GA Mix 1	3.3020E-03	-6.1095E-06	9.2356E-09
Reference Mix	4.7541E-03	-9.5882E-06	1.8533E-08

The obtained regression coefficients of the polynomial model where then used to determine the FN values using the approach mentioned above. The FN value obtained for GA Mix 1 and the reference mix was determined at 331 and 257 load cycles respectively. Although the same trend in permanent deformation resistance is established, i.e. GA Mix 1 indicating increased resistance to permanent deformation than the Reference Mix, the two models present FN results with a significantly large coefficient of variance (CoV) of 35% (GA Mix 1) and 28% (Reference Mix).

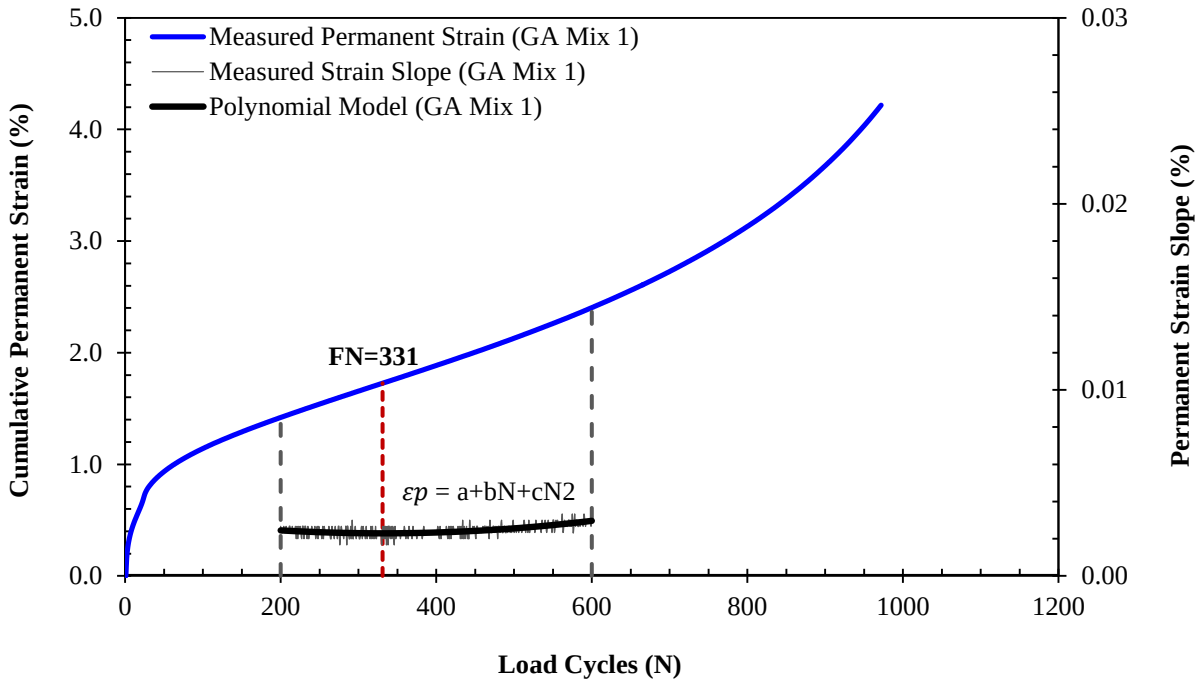

Figure 5-10: Polynomial model describing permanent deformation of GA Mix 1

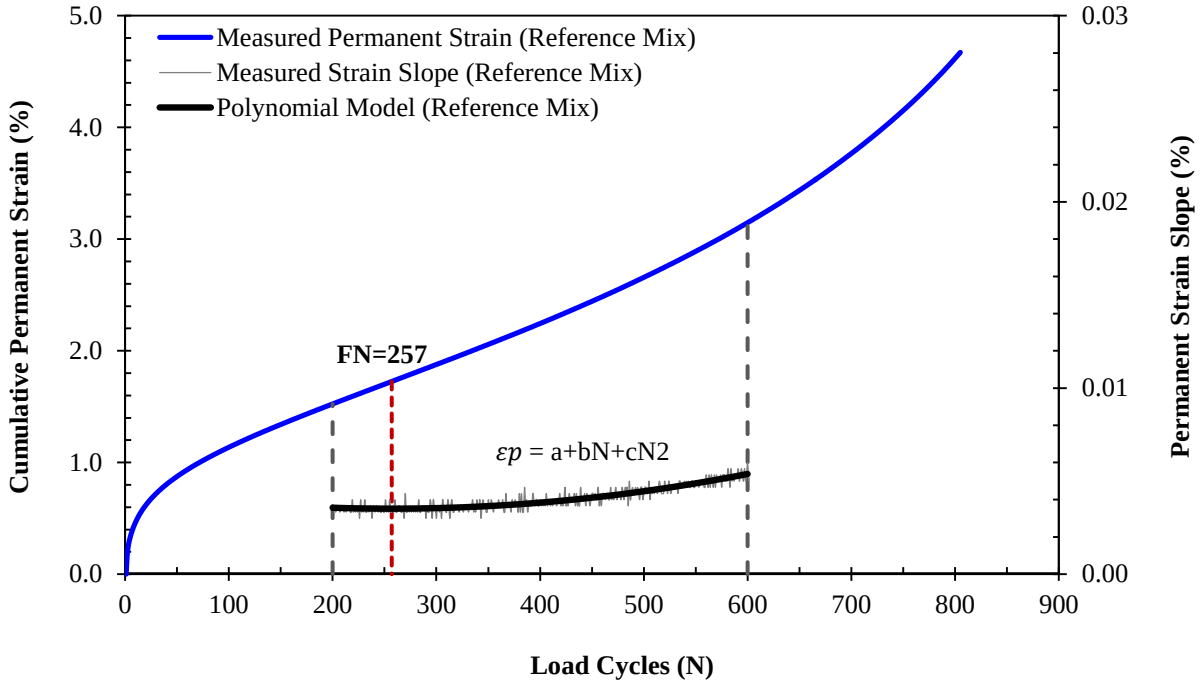

Figure 5-11: Polynomial model describing permanent deformation of Reference Mix

5.3.4. Francken Model

The Francken model (Francken, 1977) is described by the following mathematical equation:

$$\boldsymbol{\varepsilon_p(N) = AN^B + C(e^{DN} - 1)}$$ Equation 5-7

Where:

$\varepsilon_p(N) =$ permanent strain (%)

$N =$ number of load cycles

A, B, C and $D =$ regression coefficients

Figure 5-12 and 5-13 shows the Franken model which was used to model the permanent deformation behaviour of GA Mix 1 and the Reference Mix. The coefficients of the Francken model were obtained from a non-linear least squares regression of the set of measured permanent deformation data. The regression was carried out using the Solver function in Microsoft Excel. The determined coefficients of the model are provided in Table 5-9.

Table 5-9: Determination of Francken model coefficients

Asphalt Mix	A	B	C	D
GA Mix 1	2.5759E-01	3.1425E-01	6.2991E-02	3.5671E-03
Reference Mix	2.0258E-01	3.6032E-01	1.7257E-01	3.3505E-03

Similar to the analysis approach of the Wilshire and Evans model, the FN value is determined from the Franken model by differentiating the model once to obtain the strain slope as per Equation 5-8. The strain slope equation is then differentiated to obtain the gradient of the strain slope (i.e. second derivative of Equation 5-7) as described in Equation 5-9.

$$\frac{d\varepsilon_p}{dN} = \left(ABN^{(B-1)}\right) + \left(CDe^{DN}\right) \qquad \text{Equation 5-8}$$

$$\frac{d^2\varepsilon_p}{dN^2} = \left(AB(B-1)N^{(B-2)}\right) + \left(CD^2e^{DN}\right) \qquad \text{Equation 5-9}$$

The FN is obtained by equating Equation 5-9 to zero and solving for the load cycle number (N).

Using the above approach the FN for GA Mix 1 and the Reference Mix was obtained at 353 and 271 load cycles respectively. Similar to the Wilshire and Evans model and the polynomial model, GA Mix 1 indicates increased resistance to permanent deformation than the Reference Mix.

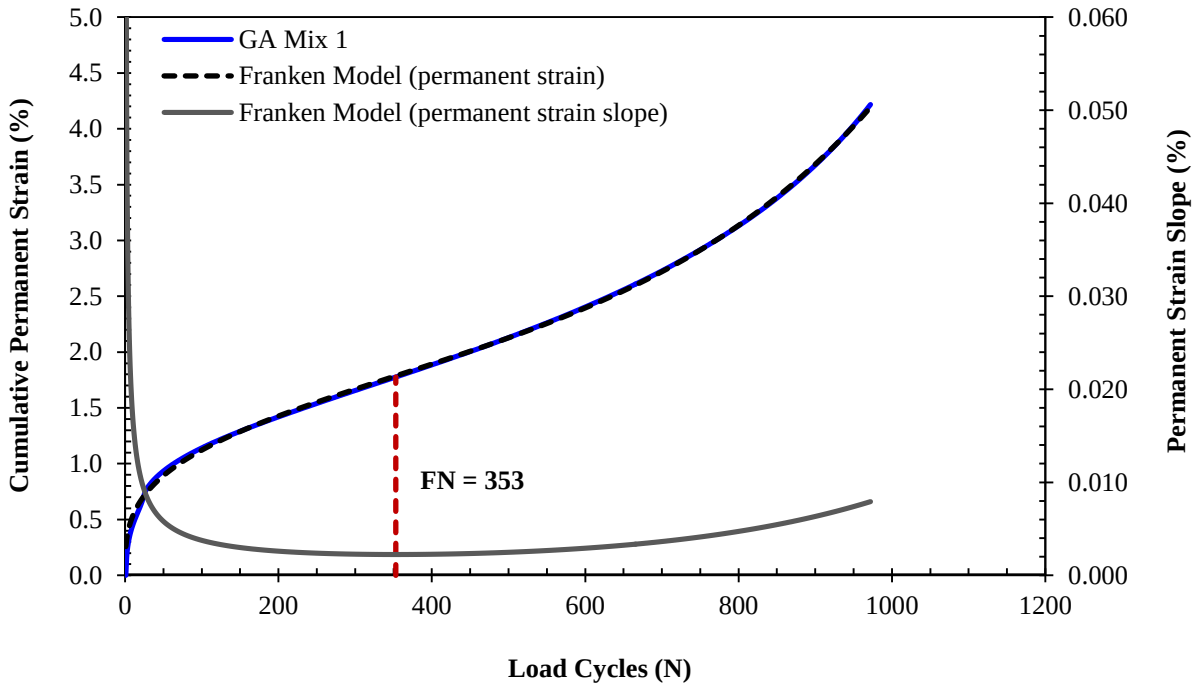

Figure 5-12: Franken model describing permanent deformation of GA Mix 1

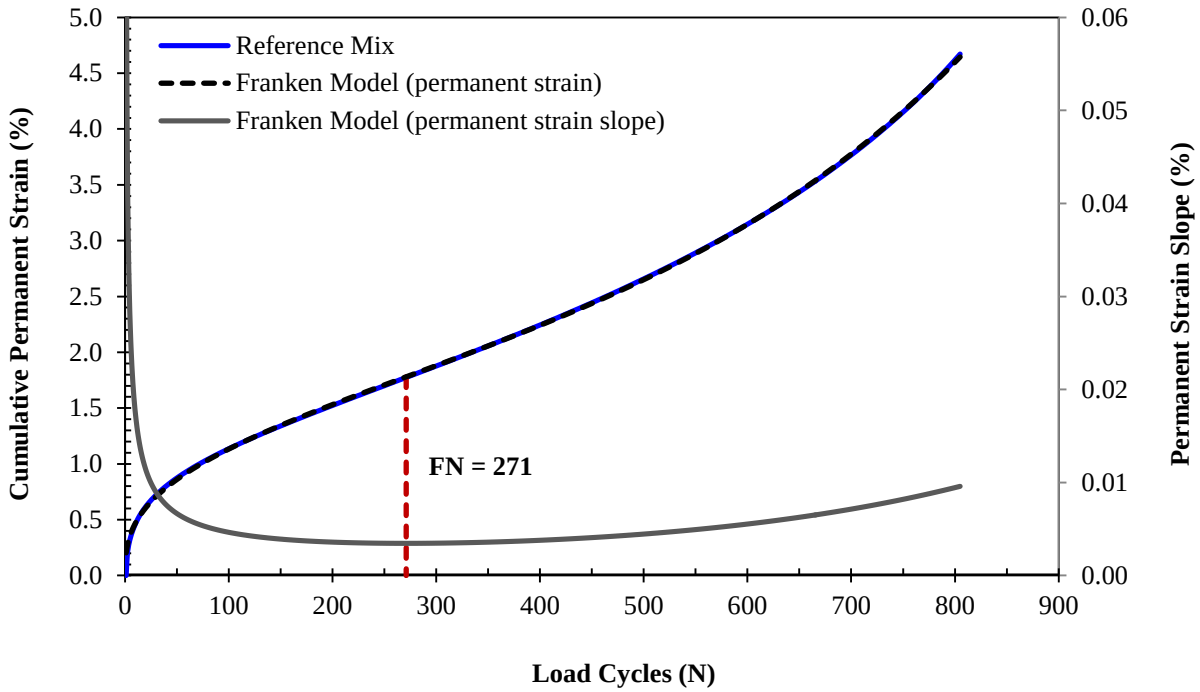

Figure 5-13: Franken model describing permanent deformation of Reference Mix

It can be observed that the Francken model provides a good representation of all three stages of permanent deformation for GA Mix 1 and the Reference Mix. Moreover, from Figure 5-14 and 5-15, it can be seen that the measured permanent deformation behaviour for both mixes is described by the model with significant accuracy resulting in a coefficient of determination (R^2) of 0.9995 (GA Mix 1) and 0.9999 (Reference Mix).

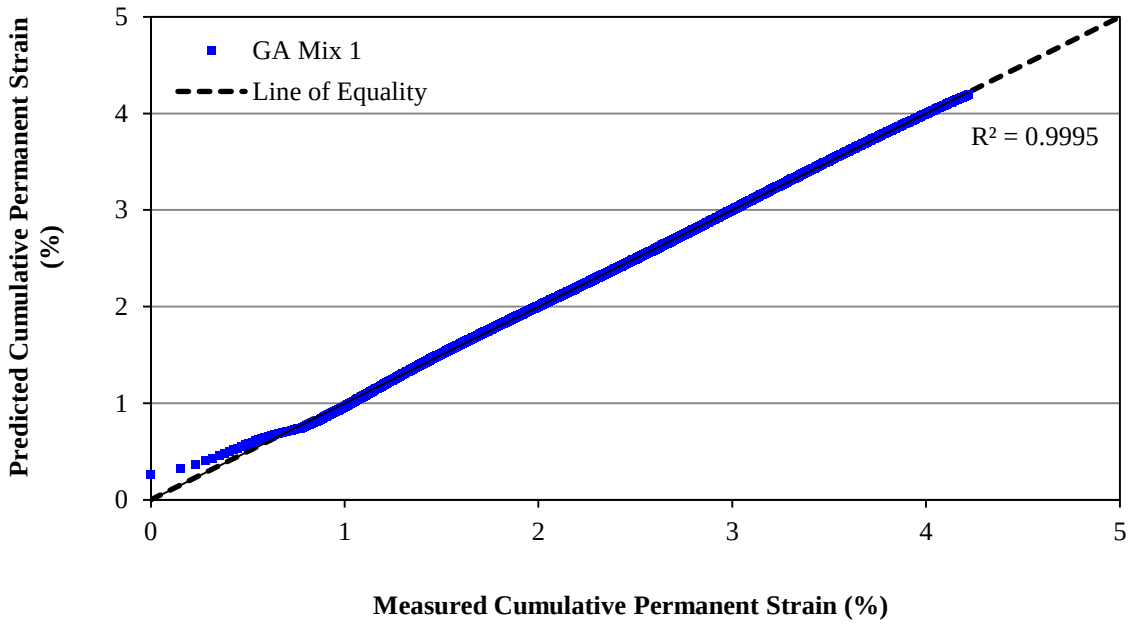

Figure 5-14: Measured vs predicted permanent deformation of GA Mix 1

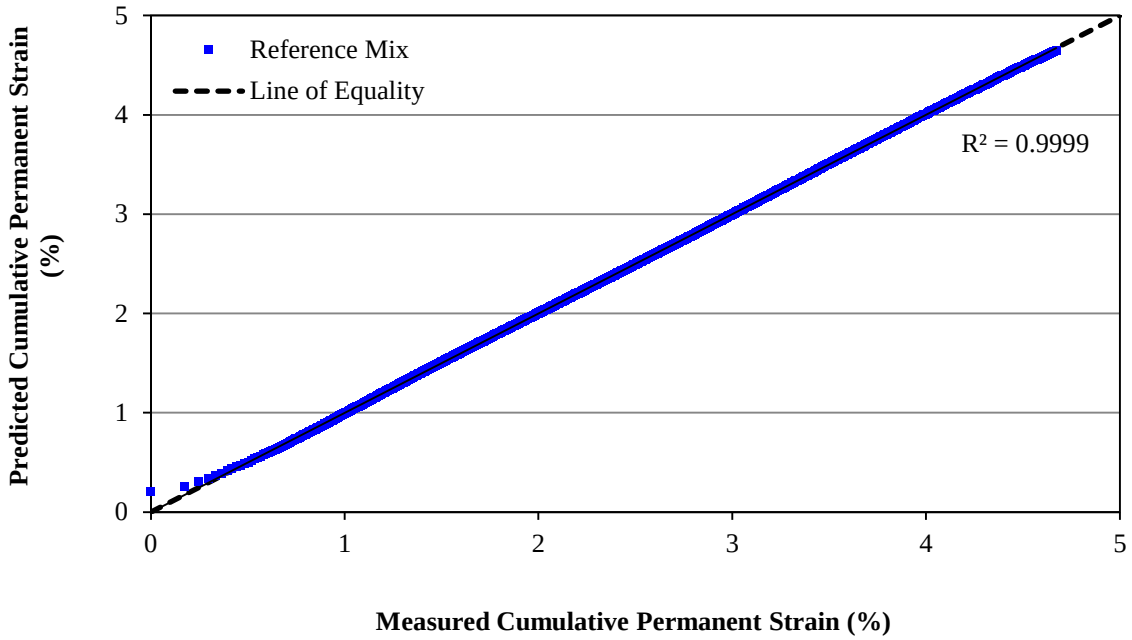

Figure 5-15: Measured vs predicted permanent deformation of Reference Mix

A comparison of the FN results obtained using the first two models with the Franken model reveals the following statistical information:

Table 5-10: Comparison of modelled Flow Number results

Asphalt Mix	W&E (1)	Polynomial (2)	Franken (3)	CoV (1&2)	CoV (1&3)	CoV (2&3)
GA Mix 1	198	331	353	35.6%	39.8%	4.5%
Reference Mix	172	257	271	28.1%	31.6%	3.7%

A similar trend in variance (CoV > ±30%) as with the Wilshire and Evans model (1) and the polynomial model (2) occurs with the Wilshire and Evans model (1) and the Franken model (3) for both mixes. However, very similar FN results are demonstrated with the polynomial model and the Franken model with a CoV less than 5%. It is therefore reasonable to recommend the polynomial model as well as the Franken model for determination of FN values for both glass-asphalt and traditional asphalt mixes.

5.4. Stiffness Evaluation

The dynamic modulus |E*| is currently used to characterise the resilient response (stiffness) of HMA in South Africa. The dynamic modulus test was conducted on the optimum glass-asphalt mix (GA Mix 1) and the Reference Mix in accordance with the CSIR protocol for HMA mixes in South Africa (Anochie-Boateng et al., 2010). A Universal Testing Machine (UTM-25), available at the CSIR Pavement Materials and Testing Laboratory, was used to conduct the dynamic modulus tests on the mixes.

A haversine compressive load pulse was applied on the 100 mm diameter by 150 mm high gyratory compacted specimens at five test temperatures (-5, 5, 20, 40, 55°C) and six loading frequencies (25, 10, 5, 1, 0.5, 0.1 Hz) with no confining pressure. The specimens were compacted at the obtained optimum binder content to a target air void content of approximately 7 $\pm$ 0.5% as indicated in Table 5-11. The vertical deformation of the specimens was determined by recording the average measurements of three axial linear variable displacement transducers (LVDTs). The dynamic modulus of the samples tested were computed by recording the axial stresses and the resulting axial strains for the last five load cycles for each test.

In this study, two specimens, for each mix, were tested at each loading condition to ensure that they are true replicates and provide comparable results. A third specimen was tested only when the test results of the two specimens were not comparable. A strain controlled type of dynamic modulus testing was followed such that the measured strain was limited to approximately 100 microstrains.

Table 5-11: Air voids determination for GA Mix 1 and Reference Mix

Mix Type	Mix	BD (ton/m^3)	MVD (ton/m^3)	Air Voids (%)
Glass-Asphalt Mix	15036-L-C16	2.389	2.570	7.0
	15036-L-C17	2.390		7.0
Reference Mix	15036-RB-C12	2.426	2.604	6.8
	15036-RB-C13	2.422		7.0

5.4.1. Dynamic Modulus Test Results and Analysis

The results of the dynamic modulus test for the two replicate specimens at the test temperatures and frequencies for GA Mix 1 and the Reference Mix are presented in Figure 5-16 and 5-17. The results are also presented in Table 5-12.

As expected, and typical to HMA behaviour, the dynamic modulus of both mixes increased with increasing loading frequency and decreased with increasing test temperature. Thus, the effect of low temperatures and high frequencies on the dynamic modulus of HMA may be similar.

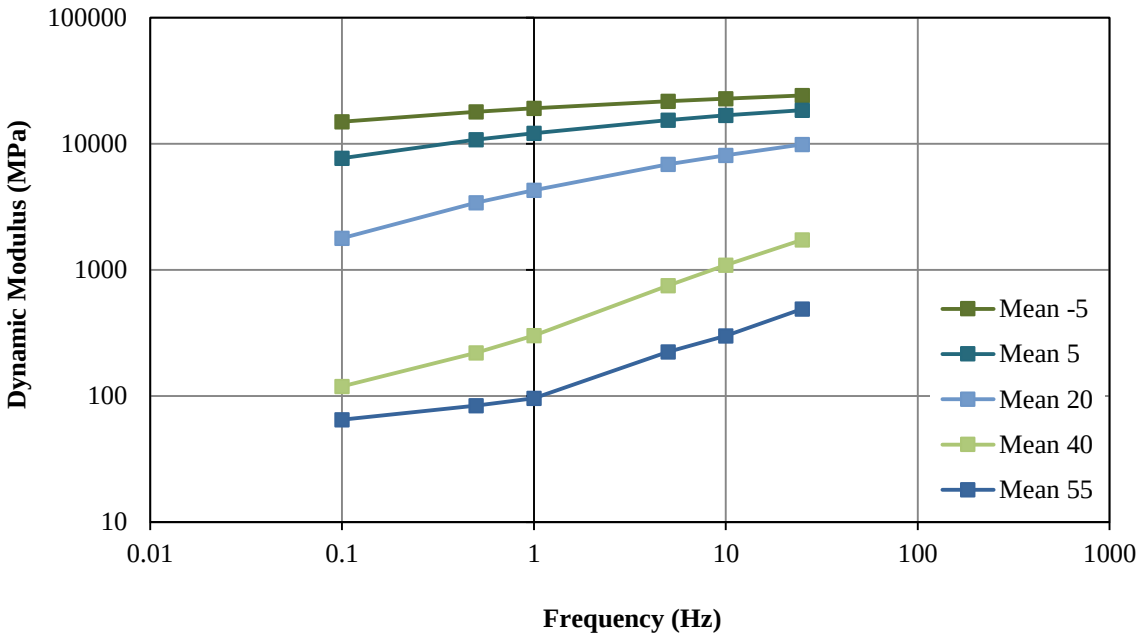

Figure 5-16: Dynamic modulus results for GA Mix 1

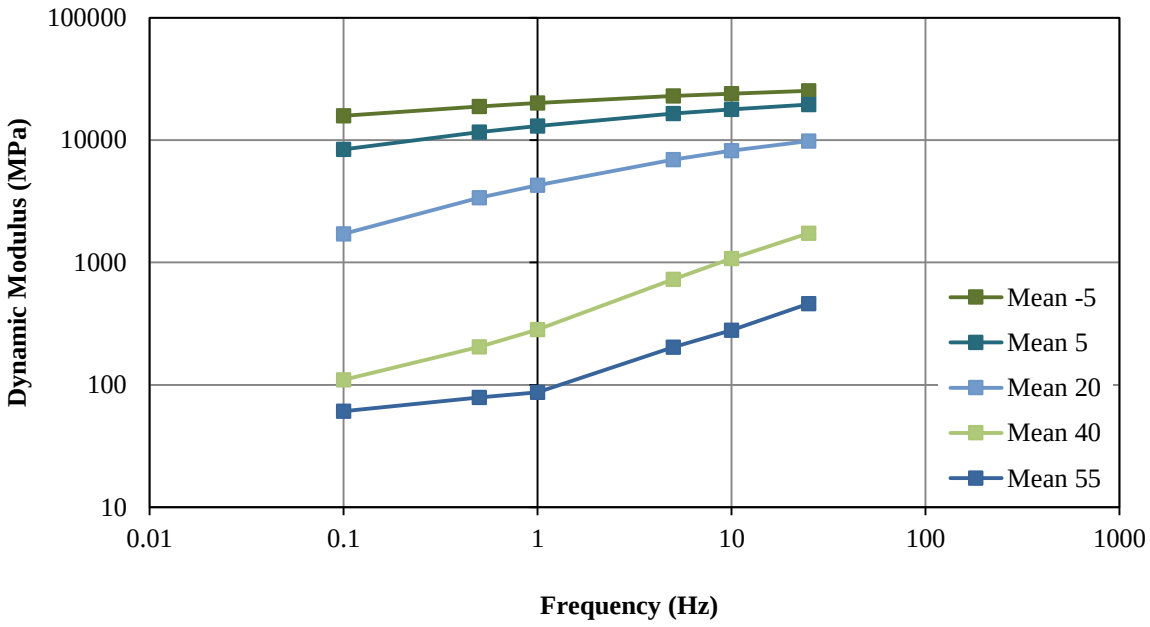

Figure 5-17: Dynamic modulus results for Reference Mix

A comparison of the dynamic modulus for GA Mix 1 and the Reference Mix is presented in Figure 5-18. It can be observed that at the extreme low temperatures, i.e. at -5 and 5°C, the stiffness of the Reference Mix is higher than the glass-asphalt mix while at 20°C the stiffness of both mixes are comparable. At the elevated test temperatures i.e. at 40 and 55°C, it can be observed that GA Mix 1 yields improved stiffness in comparison with the Reference Mix. The improved stiffness behaviour exhibited by the glass-asphalt mix at elevated temperatures indicates that this mix will provide better resistance to permanent deformation than the traditional asphalt mix. This observation is consistent with the improved permanent deformation behaviour indicated by the glass-asphalt mix at 50°C detailed in Section 5.3. In particular, Witczak et al. (2002) reported that both the FN and DM (conducted at 54.4 ^{0}C, 5 Hz) test results had good correlation with field rutting performance.

The improved stiffness behaviour of GA Mix 1 at the elevated temperatures can be further observed in Figure 5-19 which shows a plot of the Black Space diagram for GA Mix 1 and the Reference Mix at 20, 40 and 55°C. The Black diagram presents a plot of the phase angles and the corresponding dynamic moduli at the tested frequencies. For bituminous materials the viscous or elastic properties are indicted by the phase angle. The phase angle for a purely elastic material is 0^0 while for a purely viscous material the phase angle is 90^0. Lower phase angle for GA Mix 1 in comparison with the Reference Mix can be observed at 40 and 55°C. The lower phase angles indicate a tendency towards more elastic behaviour due to the aggregate skeleton taking precedence in the mix.

At elevated temperatures, the binder in the mix becomes more viscous and the load carrying capacity is gradually transferred to the aggregate skeleton, while at low temperatures it is the binder that determines the load carrying capacity of the mix (Nilsson et al., 2002). In this regard, a stable aggregate skeleton with optimal aggregate interlock contributes to increased stiffness at elevated temperatures. As indicated in Section 3-7, the glass particles utilised in this study demonstrate higher angularity than the traditional aggregates. The higher angularity in turn increases the interlock between the crushed glass particles and constituent aggregates in the mix (as observed by Anochie-Boateng and George, 2016 in Section 3-8) and may therefore be a contributory factor towards the increased stiffness observed with GA Mix 1.

It can also be observed that the phase angles for both mixes at 20°C are comparable, reflecting comparable stiffness at intermediate temperatures.

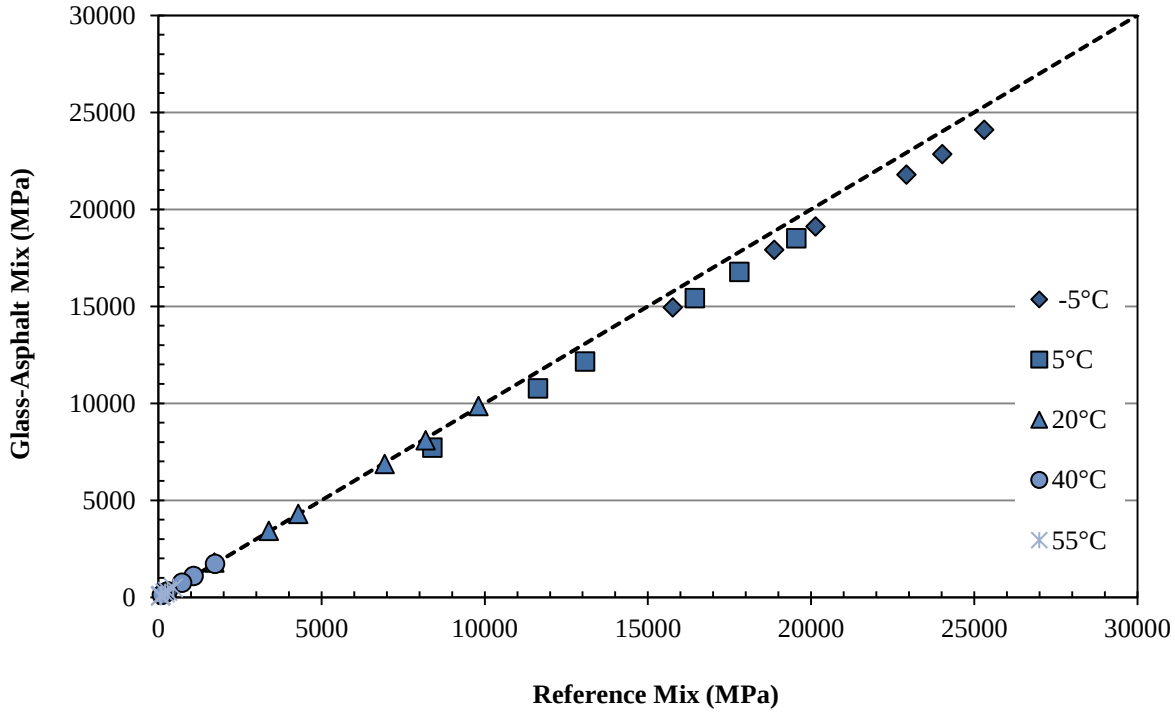

Figure 5-18: Dynamic modulus for GA Mix 1 and Reference Mix

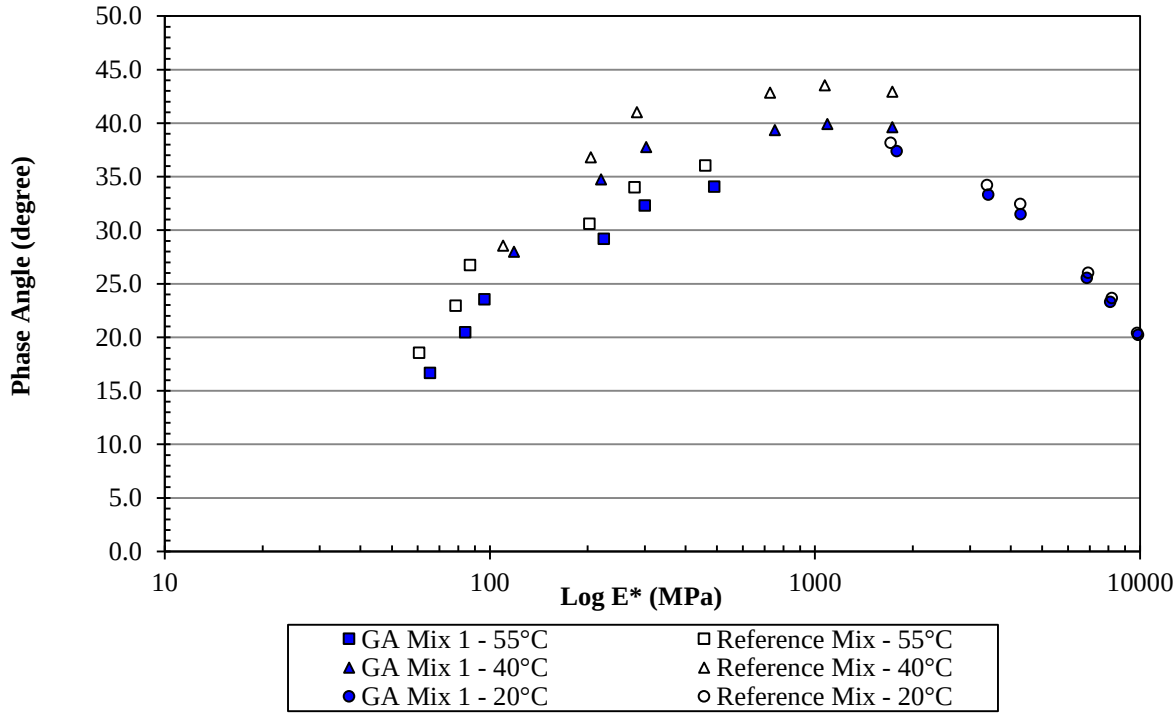

Figure 5-19: Black diagram for GA Mix 1 and Reference Mix

Table 5-12: Dynamic modulus test results for GA Mix 1 and Reference Mix

Temperature	Frequency	Dynamic Modulus for Replicate Specimens (MPa)		Statistic			Phase Angle for Replicate Specimens (MPa)		Statistic
Glass-Asphalt Mix - GA Mix 1									
(ºC)	(Hz)	15036-LC16-5	15036-LC17-5	Mean	STDEV	CoV	15036-LC16-5	15036-LC17-5	Mean
				(MPa)	(MPa)	(%)			(MPa)
-5	25	23788	24419	24104	446.18	1.9	5.2	5.0	5.1
	10	22564	23145	22855	410.83	1.8	6.1	5.9	6.0
	5	21519	22082	21801	398.10	1.8	6.8	6.6	6.7
	1	18858	19383	19121	371.23	1.9	8.7	8.5	8.6
	0.5	17651	18170	17911	366.99	2.0	9.6	9.5	9.6
	0.1	14730	15169	14950	310.42	2.1	12.3	12.2	12.3
5	25	18618	18400	18509	154.15	0.8	9.4	9.6	9.5
	10	16873	16683	16778	134.35	0.8	10.9	11.2	11.0
	5	15534	15304	15419	162.63	1.1	12.1	12.5	12.3
	1	12277	12031	12154	173.95	1.4	15.7	16.2	16.0
	0.5	10886	10639	10763	174.66	1.6	17.5	18.0	17.8
	0.1	7827	7591	7709	166.88	2.2	22.4	23.1	22.8
20	25	9863	9853	9858	7.07	0.1	20.0	20.5	20.2
	10	8081	8124	8103	30.41	0.4	23.0	23.5	23.3
	5	6842	6892	6867	35.36	0.5	25.3	25.8	25.5
	1	4286	4305	4296	13.44	0.3	31.2	31.7	31.5
	0.5	3417	3419	3418	1.41	0.0	33.1	33.5	33.3
	0.1	1796	1774	1785	15.56	0.9	37.4	37.4	37.4
40	25	1756	1707	1732	34.65	2.0	39.8	39.4	39.6
	10	1111	1071	1091	28.28	2.6	40.2	39.6	39.9
	5	769	736	753	23.12	3.1	39.7	39.0	39.3
	1	312	292	302	14.14	4.7	38.1	37.5	37.8
	0.5	227	213	220	9.69	4.4	35.2	34.3	34.7
	0.1	122	115	119	5.23	4.4	28.5	27.4	28.0
55	25	483	498	491	10.57	2.2	32.0	36.1	34.1
	10	306	294	300	8.56	2.9	29.1	35.5	32.3

	5	232	216	224	11.42	5.1	25.8	32.6	29.2
	1	96	96	96	0.14	0.1	19.7	27.3	23.5
	0.5	84	84	84	0.21	0.3	17.1	23.8	20.4
	0.1	66	65	65	1.06	1.6	13.7	19.6	16.7
Reference Mix									
(ºC)	**(Hz)**	**15036-RB12-5**	**15036-RB13-5**	**Mean**	**STDEV**	**CoV**	**15036-RB12-5**	**15036-RB13-5**	**Mean**
				(MPa)	**(MPa)**	**(%)**			**(MPa)**
-5	25	25133	25480	25307	245.36	1.0	5.1	5.0	5.0
	10	23848	24186	24017	239.00	1.0	6.0	5.8	5.9
	5	22775	23074	22925	211.42	0.9	6.7	6.6	6.6
	1	20032	20244	20138	149.90	0.7	8.6	8.4	8.5
	0.5	18771	18967	18869	138.59	0.7	9.5	9.4	9.5
	0.1	15677	15842	15760	116.67	0.7	12.3	12.1	12.2
5	25	19462	19640	19551	125.86	0.6	8.8	8.9	8.8
	10	17749	17850	17800	71.41	0.4	10.3	10.5	10.4
	5	16410	16464	16437	38.18	0.2	11.6	11.7	11.7
	1	13065	13076	13071	7.77	0.1	15.2	15.2	15.2
	0.5	11612	11657	11635	31.81	0.3	17.1	17.0	17.0
	0.1	8367	8412	8390	31.81	0.4	22.2	21.9	22.1
20	25	9736	9880	9808	101.82	1.0	20.2	20.6	20.4
	10	8242	8129	8186	79.90	1.0	23.7	23.6	23.6
	5	6986	6883	6935	72.83	1.1	26.2	25.8	26.0
	1	4321	4256	4289	45.96	1.1	33.0	31.9	32.4
	0.5	3404	3361	3383	30.40	0.9	34.7	33.7	34.2
	0.1	1720	1703	1712	12.02	0.7	38.9	37.4	38.2
40	25	1765	1699	1732	46.66	2.7	46.2	39.6	42.9
	10	1097	1050	1074	33.23	3.1	47.1	40.0	43.5
	5	746.6	707.8	727	27.43	3.8	46.2	39.5	42.8
	1	293.4	273.3	283	14.21	5.0	44.4	37.7	41.0
	0.5	212.9	195.7	204	12.16	6.0	38.8	34.8	36.8
	0.1	114.4	105.1	110	6.57	6.0	29.7	27.4	28.5
55	25	453.2	467.3	460	9.97	2.2	38.5	33.6	36.0

	10	273.9	284.3	279	7.35	2.6	36.3	31.6	34.0
	5	197.3	208.1	203	7.63	3.8	32.6	28.6	30.6
	1	82.3	91.8	87	6.71	7.7	28.8	24.7	26.7
	0.5	74.1	83.1	79	6.36	8.1	24.7	21.2	22.9
	0.1	55.9	65.4	61	6.71	11.1	20.3	16.8	18.5

5.5. Modelling the Linear-Viscoelastic (LVE) Behaviour of Glass-Asphalt

Hot Mix Asphalt (HMA) materials behave as visco-elastic materials, exhibiting properties in between the two extremes of perfectly elastic and viscous. The visco-elastic behaviour of HMA is both temperature and time dependent. At low temperatures and high loading frequencies they behave as elastic materials and at high temperatures and low loading frequencies, they behave as viscous fluid-like materials. In the intermediate temperature and frequency range, HMA materials indicate visco-elastic behaviour.

Various studies have shown that HMA materials exhibit linear visco-elastic behaviour at small strain levels (Olard & Di Benedetto, 2003, Dougan et al., 2003 and Witczak et al., 2002). Since the complex modulus test is performed at small strain levels (limited to an average of 100 microstrain), it is considered as one of the primary performance tests used to characterise the linear visco-elastic properties of HMA materials.

In the complex modulus test, when a haversine stress is applied to the asphalt specimen, the strain response follows a haversine function similar to the applied stress. However, due to the visco-elastic nature of the material, the applied stress and corresponding strain response are out of phase by an angle, δ, as shown in Figure 5-20.

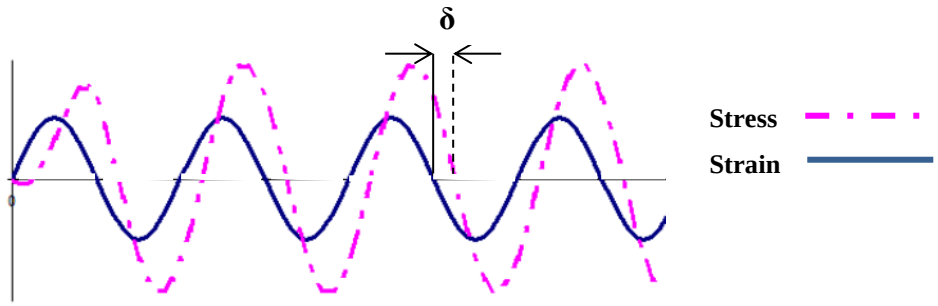

Figure 5-20: Applied stress and strain response

The haversine stress and corresponding haversine strain can be defined in a complex form as per Equation 5-10 and 5-11 (Huang, 2004).

$$\boldsymbol{\sigma = \sigma_0 e^{i\omega t}} \qquad \text{Equation 5-10}$$

$$\boldsymbol{\varepsilon = \varepsilon_0 e^{i(\omega t - \delta)}} \qquad \text{Equation 5-11}$$

Where:

i = imaginary unit, defined by $i^2 = -1$

$\omega =$ angular frequency (Hz), $\omega = 2\pi f$

$\delta =$ phase angle

The complex modulus E^* is determined from Equation 5-10 and 5-11 and is defined by a complex number which consists of real and imaginary parts, as expressed in Equation 5-12. The real part describes the elastic component and is associated with "the energy stored in a sample for every loading cycle", while the imaginary part describes the viscous component and is associated with the "amount of energy lost per cycle" through internal motion and heat. These two components of the complex modulus are illustrated in the Figure 5-21.

$$\boldsymbol{E^*(i\omega) = \frac{\sigma}{\varepsilon} = \frac{\sigma_0}{\varepsilon_0} e^{i\delta} = E' + iE''} \qquad \text{Equation 5-12}$$

Where:

E'= storage modulus (elastic component)

E''=loss modulus (viscous component)

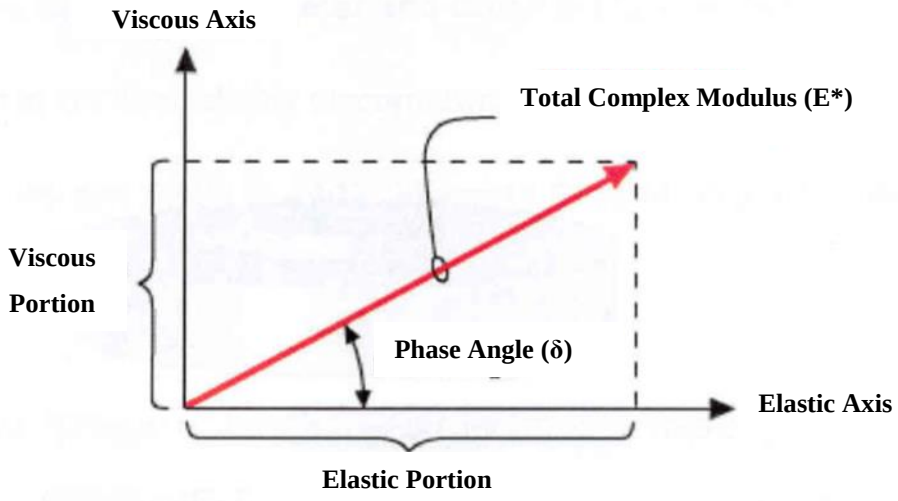

Figure 5-21: Complex modulus components

The absolute value of the complex modulus is defined as the dynamic modulus, as per Equation 5-13.

$$\boldsymbol{|E^*| = \frac{\sigma_0}{\varepsilon_0}} \qquad \text{Equation 5-13}$$

In order to characterise the visco-elastic properties of HMA materials, the modulus over a wide range of frequencies and temperature is required. Since the dynamic modulus laboratory test is conducted within a limited frequency and temperature range, specific models that describe the laboratory measured modulus over a wide range of frequencies and temperature have been proposed.

One such model is the commonly used sigmoidal model which uses the time-temperature superposition principle to model the effects of temperature on the visco-elastic properties of materials. This model is described in more detail in Section 5.5.1.

In addition to the sigmoidal model, various constitutive models which use physical elements to describe the visco-elastic behaviour of materials have also been proposed. Examples of these constitutive models include the Maxwell, Kelvin, Burger, Huet-Sayegh and the 2S2P1D. In Section 5.5.1, a comparison of the Burger and Huet-Sayegh models that best describe the visco-elastic response of the optimum glass-asphalt mix (GA Mix 1) is investigated through the determination of the respective model parameters at a reference temperature of 20°C. The Burger and Huet-Sayegh model parameters are then used to develop the respective master curves for GA Mix 1 at the same temperature.

5.5.1. Constitutive Models

5.5.1.1. Sigmoidal Model

The sigmoidal model can be used to characterise the LVE behaviour of HMA materials through the construction of master curves at different temperatures and loading frequencies using a time-temperature superposition principle. A shift of the dynamic modulus response along the time axis, relative to a reference temperature, results in one master curve. This principle is called time-temperature superposition principle and is used in the Mechanistic-Empirical Pavement Design Guide (MEPDG) (NCHRP 1-37A, 2004), and recommended by SANRAL in the South African Pavement Design Method (SAPDM) (SANRAL, 2007) to model temperature effects on viscoelastic material properties.

The sigmoidal model is defined as per Equation 5-14.

$$\log|E^*| = \delta + \frac{\alpha}{1+e^{\beta+\gamma log f_r}} \qquad \text{Equation 5-14}$$

Where:

$|E^*|$ = dynamic modulus

$\alpha, \beta, \gamma, \delta =$ model parameters, where

$\delta =$ minimum modulus value

$\delta + \alpha =$ maximum modulus value

$\beta, \gamma =$ parameters describing the shape of the sigmoidal model

The temperature dependency of the dynamic modulus is accounted for in the reduced frequency parameter, f_r, which is expressed as the actual loading frequency multiplied by the time-temperature shift factor, a (T) in Equation 5-15.

$$f_r = a(T) * f \qquad \text{Equation 5-15}$$

$$\log(f_r) = \log(f) + \log[a(T)] \qquad \text{Equation 5-16}$$

Where:

f = frequency, Hz

$a(T)$ = shift factor as a function of temperature

T = temperature

In the MEPDG, ageing of the binder over the pavement life is taken into account by the shift factor which is defined as a function of the binder viscosity as expressed in Equation 5-17. This shift factor expression is used in the MEPDG and is implemented in the SAPDM.

$$\log[a(T)] = c[\log(\eta) - \log(\eta_{70_{RTFO}})] \quad \text{Equation 5-17}$$

Where:

$a(T)$ = shift factor as a function of temperature and age

η = viscosity at the age and temperature of interest

$\eta_{70_{RTFO}}$ = viscosity at the reference temperature and RTFO ageing

c = model parameter

As mentioned in Section 3.6.2, loose glass-asphalt mixtures were short-term oven aged for four hours at 135°C (RTFO ageing value) prior to the preparation of GA Mix 1. In this condition, the ASTM viscosity-temperature relationship indicated in Equation 5-18 is used to express the viscosity of the binder as a function of temperature (ASTM D2493 / D2493M-09, 2009).

$$\log[\log(\eta)] = A + VTS\log T_R \quad \text{Equation 5-18}$$

Where:

η = viscosity, cP

T_R = temperature, in Rankine

A, VTS = viscosity-temperature relationship parameters representing RTFO ageing conditions of the binder in the asphalt mix.

The A, VTS parameters for the 50/70 penetration grade binder used in this dissertation were obtained from a combination of the following test results as recommended by NCHRP 1-37A (2004): Brookfield viscosity, penetration and softening point (results indicated in Table 3-2). Dynamic shear rheometer results were, however, not obtained as part of the analysis.

The above mentioned test measurements were first converted into viscosity units. This was achieved as follows:

1. The penetration test data were converted to viscosity units using Equation 5-19 (NCHRP 1-37A, 2004).

$$\boldsymbol{Log\,\eta = 10.5012 - [2.2601 * \log(pen)] + [0.00389 * \log(pen)^2]} \quad \text{Equation 5-19}$$

Where:
$\eta =$ viscosity, in poise
$pen =$ penetration for 100 g, 5 sec loading, 0.1mm

2. The viscosity value at temperature 60ºC was obtained by using the Brookfield Viscometer.

3. Softening point was converted to viscosity units as per the suggested approach by Shell Bitumen U.K. (1990) which indicates that all bitumen at their softening point will yield a penetration of approximately 800 and a viscosity of 13 000 poise (Shell Bitumen U.K., 1990).

The above viscosity data was then used to obtain a viscosity (η) - temperature (T_R) relationship using Equation 5-18.

The VTS term represents the slope of the regression equation, which is also interpreted as the Viscosity Temperature Susceptibility parameter. Thus, a larger (negative) slope value represents a higher temperature susceptibility of the bituminous binder.

Figure 5-22 shows the viscosity-temperature relationship, i.e. Log Log viscosity (centipoise) against Log temperature (Rankine), of the 50/70 binder at the RTFO condition, and Table 5- 13 presents the regression analyses results.

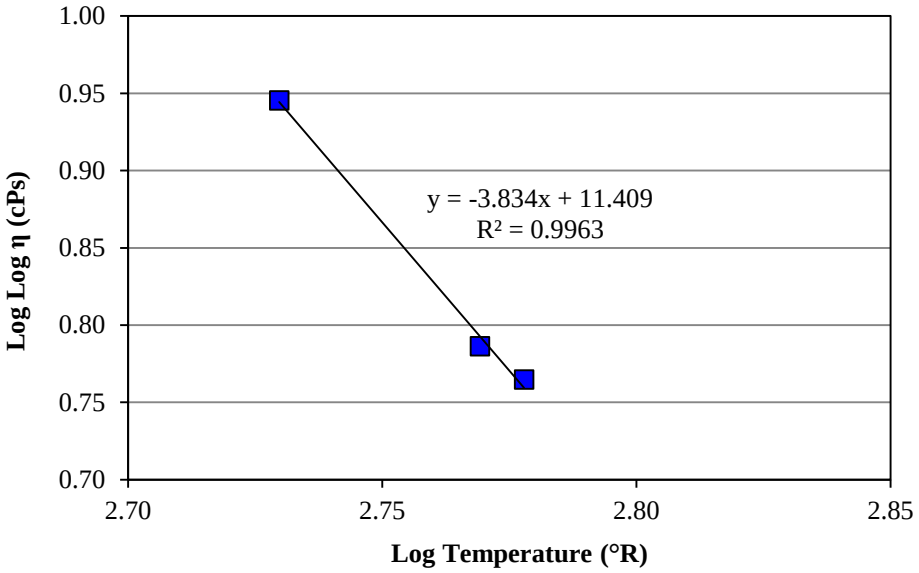

Figure 5-22: Viscosity-temperature relationship for RTFO 50/70 penetration-grade binder

Table 5-13: Summary of viscosity-temperature regression results

Binder	Ageing	Regression Parameters and Coefficients		
		A	VTS	R^2
50/70	RTFO	11.409	-3.834	0.9963

Through the combination of Equations 5-17 and 5-18, the shift factor as a function of A and VTS parameters is presented as per Equation 5-20.

$$\log[a(T)] = c[10^{A+VTSlogT} - 10^{A+VTSlog(527.67)}] \quad \text{Equation 5-20}$$

It should be noted that the T_r value is adjusted according the reference temperature that is used in the construction of the sigmoidal master curve. A reference temperature of 20°C will yield a T_r of 527.67 (1.8*[20+273.15]).

5.5.1.2. Burger's Model

The Burger's Model is represented by a combination of two units connected in series i.e. a spring and dashpot connected in parallel with a spring and a dashpot connected in series, as shown in Figure 5-23. The elastic modulus of the spring is indicated by E and the viscosity of the dashpot is indicated by η.

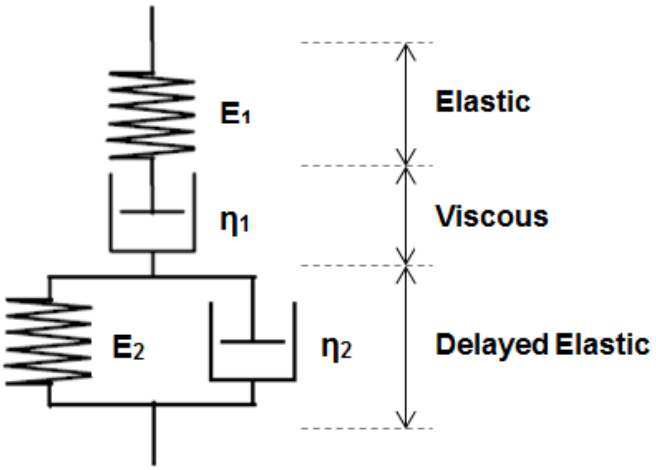

Figure 5-23: Representation of Burger's model

The delayed elastic response of the visco-elastic material is represented by the unit connected in parallel, while the instantaneous elastic response and the linear elastic response/viscous flow of the visco-elastic material is represented by the spring and the dashpot, respectively, of the unit connected in series.

The associated mathematical expression of dynamic modulus for the Burger's Model is determined by Equation 5-21.

$$|\boldsymbol{E^*(i\omega)}| = \frac{1}{\left(\frac{1}{E_1}+\frac{E_2}{{E_2}^2+\omega^2{\eta_2}^2}\right)-\left(\frac{1}{\eta_1}+\frac{\omega\eta_2}{{E_2}^2+\omega^2{\eta_2}^2}\right)i} \qquad \text{Equation 5-21}$$

Where:

$|E^*|$ = dynamic modulus

i^2 = complex number, defined by $i^2 = -1$

ω = angular frequency (Hz), $\omega = 2\pi f$

E_1, E_2, η_1, η_2 = model constants

5.5.1.3. Huet-Sayegh Model

The Huet-Sayegh model is represented by a combination of two units connected in parallel i.e. a spring, E_∞ - E_0, and two bi-parabolic dashpots, h and k, connected in series with a spring, E_0, connected in parallel, as shown in Figure 5-24.

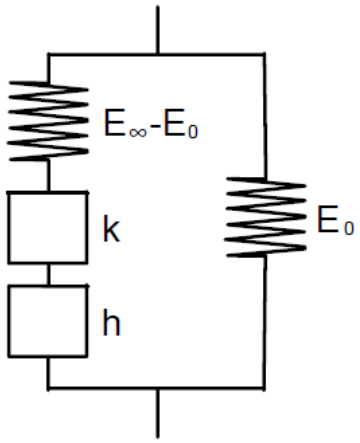

Figure 5-24: Representation of Huet-Sayegh model

The associated mathematical expression of dynamic modulus for the Huet-Sayegh model is determined by Equation 5-22.

$$|\boldsymbol{E^*(i\omega\tau)}| = \boldsymbol{E_0} + \frac{\boldsymbol{E_\infty - E_0}}{\boldsymbol{1+\delta(i\omega\tau)^{-k}+(i\omega\tau)^{-h}}} \qquad \text{Equation 5-22}$$

Where:

$|E^*|$ = dynamic modulus

$i^2 =$ complex number, defined by $i^2 = -1$

$\omega =$ angular frequency (Hz), $\omega = 2\pi f$

$E_0, E_\infty, \delta, k, h, \tau =$ model constants

In Equation 5-22, E_∞ represents the purely elastic component (E^* for the high frequency and low temperature domain) of the complex modulus, while E_0 represents the long-term elastic modulus (residual E^* for the low frequency and high temperature domain). δ, k, and h represent the parameters of the parabolic elements of the Huet-Sayegh model and τ is the retardation time regarding the effect of temperature on the complex modulus, which is defined as per Equation 5-23.

$$\tau = e^{a+bT+cT^2}$$ Equation 5-23

Where:

T = temperature (°C)

a, b, c = regression constants

5.5.2. Analysis of Results

5.5.2.1. Sigmoidal Model

The sigmoidal model master curve for the optimum glass-asphalt mix (GA Mix 1) and the traditional asphalt mix (Reference Mix) was constructed using the dynamic modulus test data presented in Table 5-12. The time-temperature superposition principle was used to shift the test data horizontally along the frequency axis relative to a reference temperature of 20 °C. A non-linear least square regression technique was used to fit the data with the sigmoidal model defined in Equation 5-14. The regression was carried out using the Solver function in Microsoft Excel.

The sigmoidal model master curve and the determined model parameters for the glass-asphalt mix and the traditional asphalt mix are presented in Figure 5-25 and Table 5-14. It can be observed that the dynamic modulus of GA Mix 1 and the Ref Mix at 20 °C is comparable at the wide range of frequencies indicated.

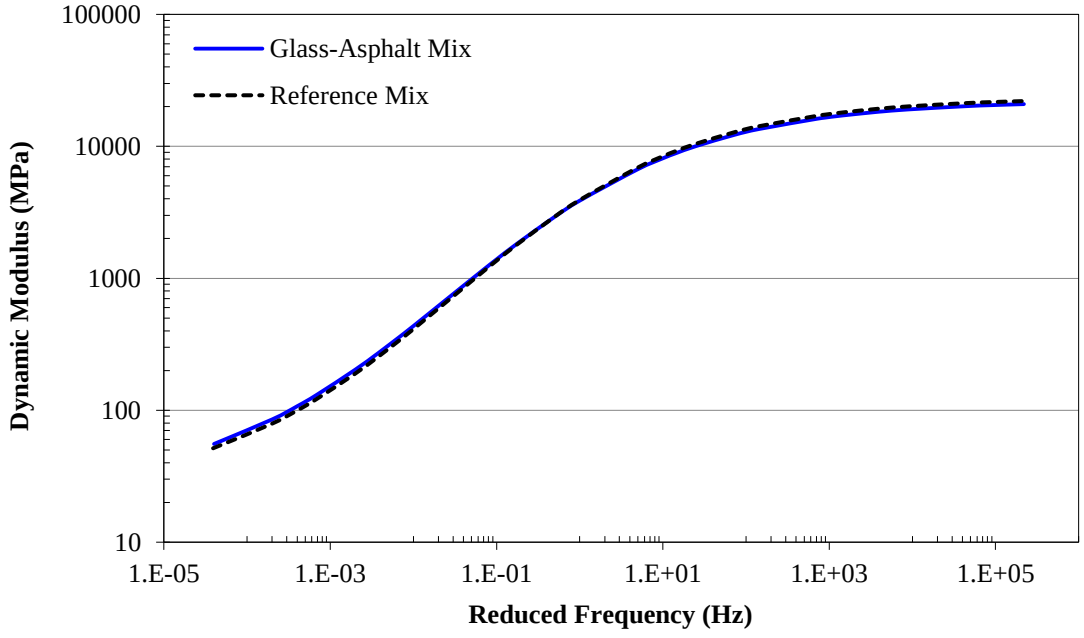

Figure 5-25: Sigmoidal model master curves of GA Mix 1 and Reference Mix at 20°C

Table 5-14: Determination of sigmoidal model parameters

Asphalt Mix	α	β	γ	δ	c
GA Mix 1	2.974	-1.073	-0.687	1.372	1.032
Ref Mix	3.014	-1.061	-0.696	1.354	1.036

Figure 5-26 presents a plot of the measured dynamic modulus versus the predicted dynamic modulus of GA Mix 1 using the sigmoidal model. It can be observed that the measured dynamic modulus of GA Mix 1 is adequately described by the sigmoidal model, resulting in an R-squared value of 0.986. However, it can be observed that the measured values at the extreme low temperatures i.e. -5°C are not well defined. This phenomenon has also been noted for the sigmoidal model by Xu & Solaimanian (2009).

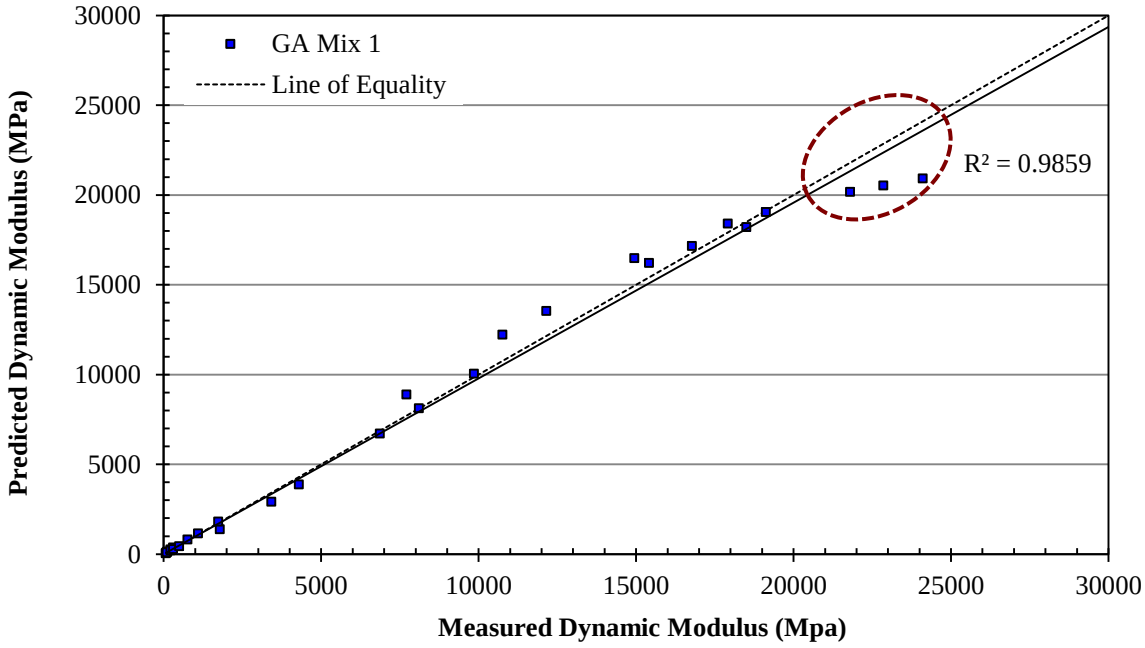

Figure 5-26: Measured versus predicted dynamic modulus for GA Mix 1

5.5.2.2. Burger's Model

The four Burger's parameters representing the dynamic modulus of GA Mix 1 were obtained from a non-linear least squares regression of the set of measured dynamic moduli and phase angles at various frequencies and temperatures presented in Table 5-12. The regression was carried out using the Solver function in Microsoft Excel. Determined values of the Burger's parameters at a reference temperature of 20°C are given in Table 5-15.

Table 5-15: Determination of Burger's model parameters

Asphalt Mix	E_1	E_2	η_1	η_2
GA Mix 1	1.62E+02	1.34E+04	1.53E+06	2.30E+03

The determination of the four parameters, $E_1, E_2, \eta_{1,}, \eta_2$, is obtained such that the measured data is most accurately represented by the model in the Cole-Cole and Black diagrams. A Cole-Cole diagram is a representation of the loss modulus versus the storage modulus. A Black diagram represents the dynamic modulus versus the phase angle. The fitting of the measured values using the Burger's models is illustrated in Figures 5-27 to 5-29.

Figure 5-27 and 5-28 indicates the fitting of the measured data in the Cole-Cole diagram and Black diagram. It can be observed that only the dynamic modulus data at 40°C is adequately described by the Burger's model.

The Burger's model master curve is presented in Figure 5-29. The reduced frequencies obtained by using Equation 5-16 were used to develop the master curve for dynamic modulus of GA Mix 1 at a reference temperature of 20°C. A comparison of the developed master curves from the Burger's model and the sigmoidal model is also presented in Figure 5-29. It can be observed that the dynamic modulus, over the wide frequency range indicated, is not satisfactorily described by the Burger's model.

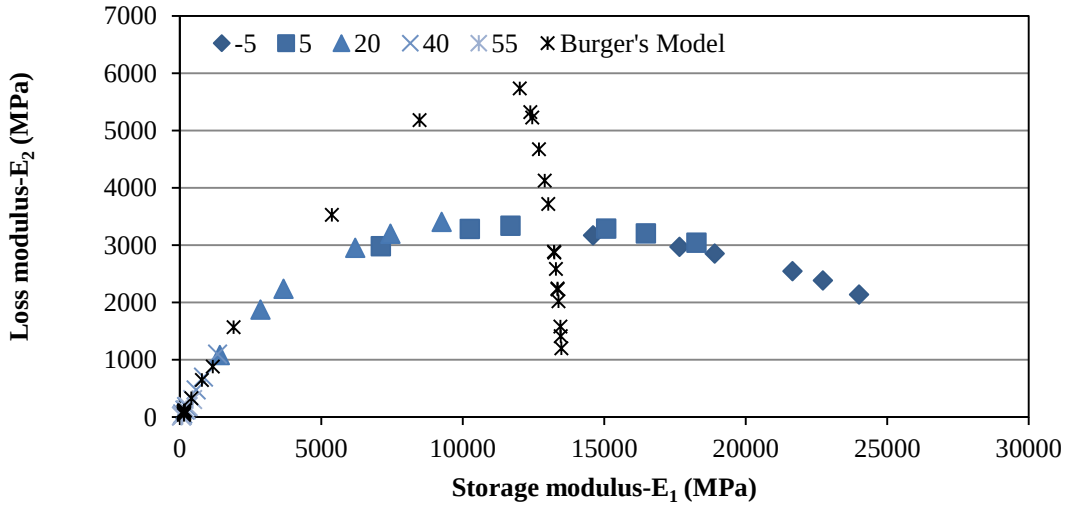

Figure 5-27: Burger's model representation of Cole-Cole diagram for GA Mix 1

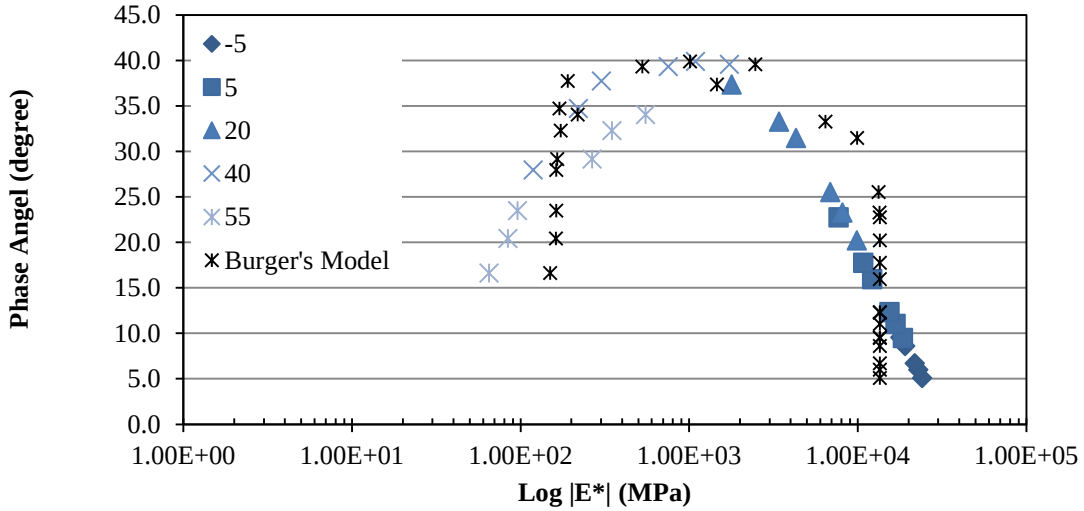

Figure 5-28: Burger's model representation of Black diagram for GA Mix 1

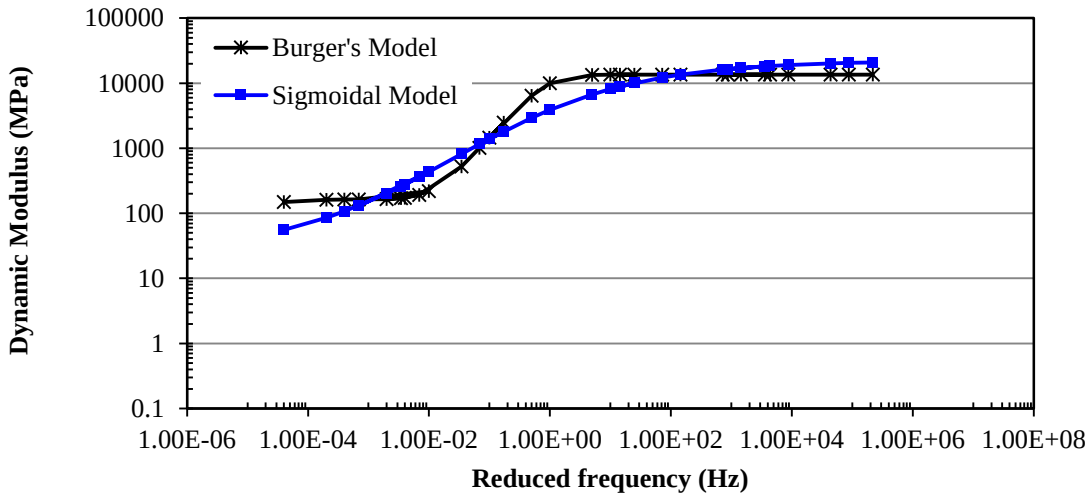

Figure 5-29: Master curves of GA Mix 1 at 20°C

Figure 5-30 presents a plot of the measured dynamic modulus versus the predicted dynamic modulus of GA Mix 1 using the Burger's model. A very poor prediction of the measured dynamic modulus can be observed, with a low R-squared value of 0.687.

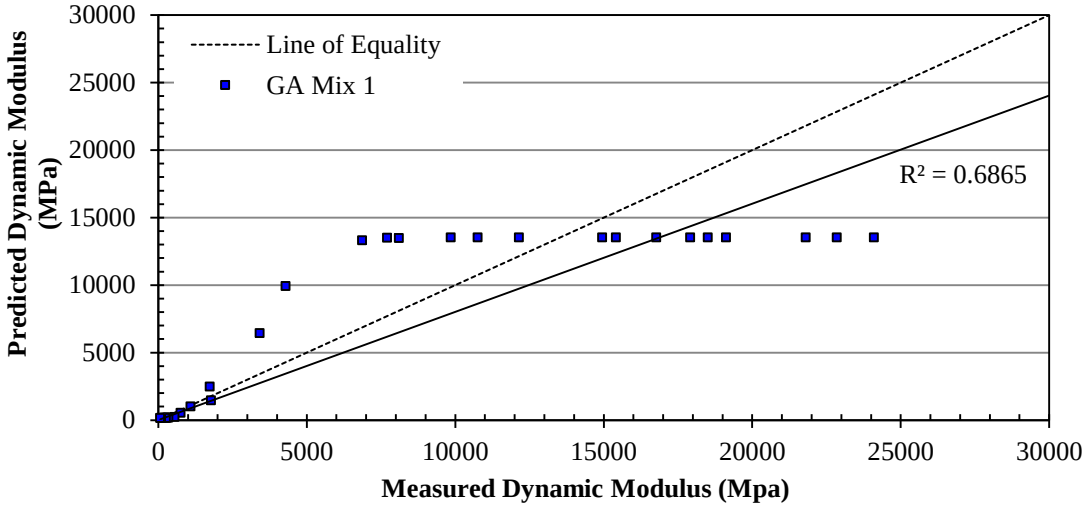

Figure 5-30: Measured versus predicted dynamic modulus for GA Mix 1

5.5.2.3. Huet-Sayegh Model

The purely elastic modulus is obtained when the phase angle approaches zero, resulting in the storage modulus approaching the elastic modulus and the loss modulus approaching zero. The purely elastic parameter,E_∞, is obtained from the Black diagram or the Cole-Cole diagram by extrapolating the curve to zero phase angle or zero loss modulus respectively, as shown in Figure 5-31 and 5-32. The determination of the remaining five parameters, E_0, δ, *k*, *h* and t is performed graphically such that the measured data is most accurately represented by the model in the Cole-Cole and Black diagrams. This was obtained by a non-linear least squares regression of the set of measured dynamic moduli and phase angles at various frequencies and temperatures presented in Table 5-12. The regression was carried out using the Solver function in Microsoft Excel. The obtained Huet-Sayegh model parameters at a reference temperature of 20°C are provided in Table 5-16.

Table 5-16: Determination of Huet-Sayegh model parameters

Asphalt Mix	E_0	E_∞	δ	k	h	τ
GA Mix 1	53	31000	2.3699	0.1932	0.6188	0.01863

Figure 5-31 and Figure 5-32 shows the best fit measured data in the Cole-Cole diagram and the Black diagram. It can be observed that the use of the Huet-Sayegh model provides an excellent fit for the measured dynamic modulus data.

The Huet-Sayegh model master curve is presented in Figure 5-33. Similar to the Burger's model, the reduced frequencies obtained by using Equation 5-16 were used to develop the master curve for dynamic modulus of GA Mix 1 at a reference temperature of 20°C. For

comparative purposes, the sigmoidal model mastercurve is also presented in Figure 5-33. It can be observed that an excellent prediction of the dynamic modulus, over the wide frequency range indicated, is depicted by the Huet-Sayegh model.

The well-defined curve of the Huet–Sayegh model in comparison with the Burger's model illustrates its effectiveness in describing the dynamic modulus over a wide range of frequencies and temperatures.

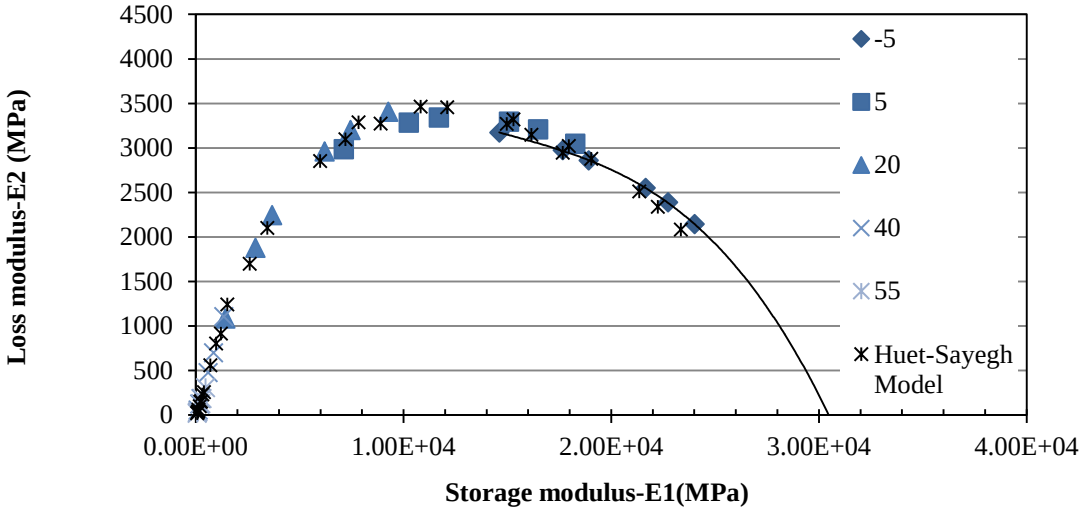

Figure 5-31: Huet-Sayegh model representation of Cole-Cole diagram

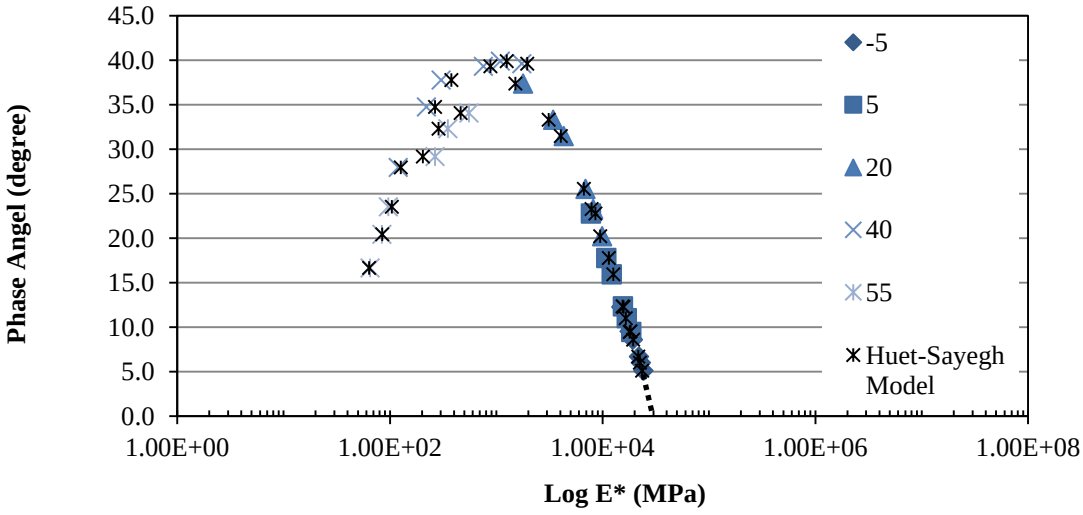

Figure 5-32: Huet-Sayegh model representation of Black diagram

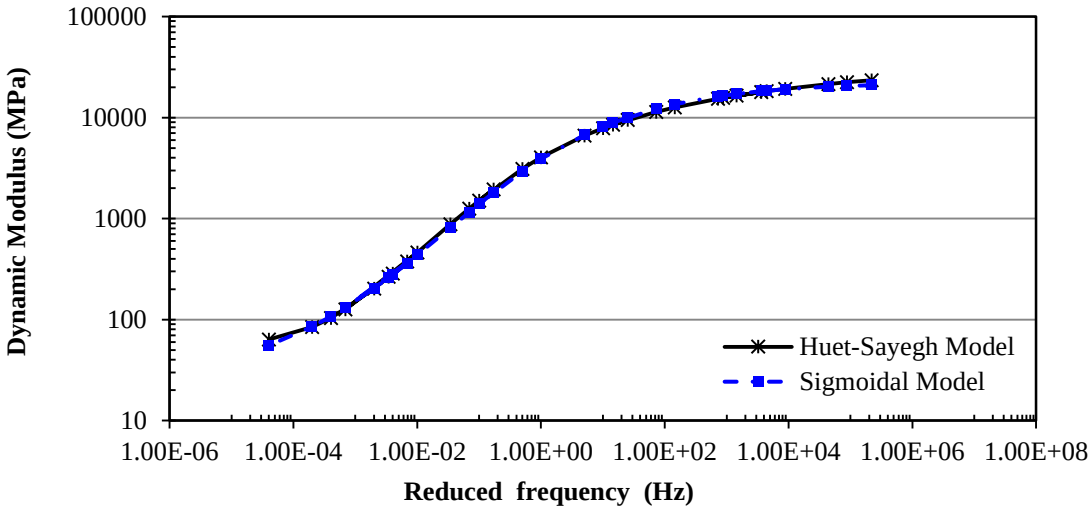

Figure 5-33: Master curves of GA Mix 1 at 20°C

Figure 5-34 presents a plot of the measured dynamic modulus versus the predicted dynamic modulus of GA Mix 1 using the Huet-Sayegh model. Excellent prediction of the measured dynamic modulus can be observed, with a R-squared value of 0.998. Furthermore, unlike the sigmoidal model, the Huet-Sayegh model provides a well-defined prediction of the measured values at the high frequency and low temperature. This may render the Huet-Sayegh model more effective than the sigmoidal model in its ability to characterise the visco-elastic properties of glass-asphalt mixes at cold temperatures.

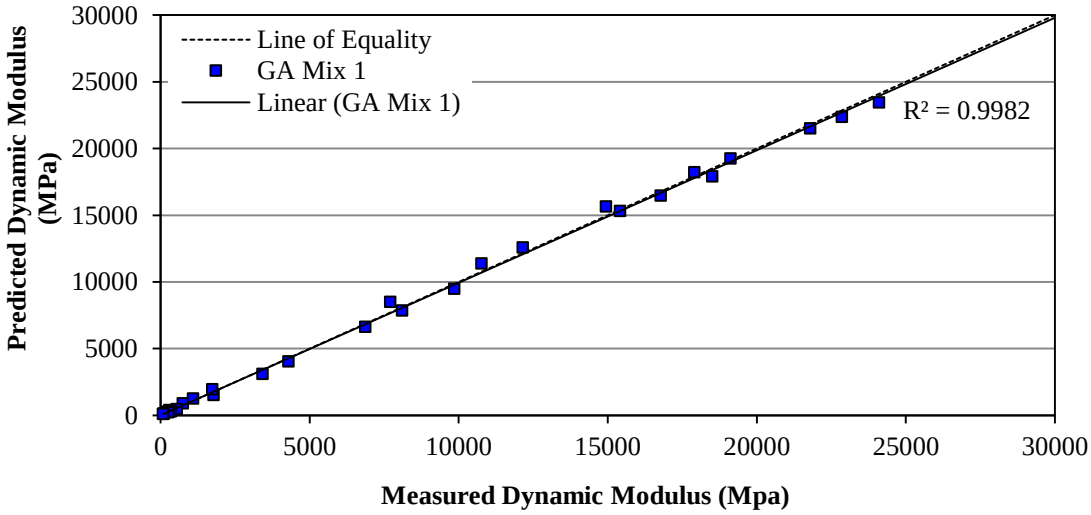

Figure 5-34: Measured versus predicted dynamic modulus for GA Mix 1

5.6. Summary

Chapter 5 presents a comparison of the performance properties i.e. permanent deformation and stiffness of the optimum glass-asphalt mix (GA Mix 1) and a traditional asphalt mix (Reference Mix). Both mixes have been designed to represent a similar design aggregate grading to the standard SANRAL 10 mm NMPS medium continuously-graded asphalt mix using the same component materials (i.e. traditional aggregates, filler (hydrated lime) and binder).

The flow number (FN) test and the dynamic modulus (DM) test were used to conduct the permanent deformation and stiffness performance evaluation respectively. The FN test results reveal a higher FN for GA Mix 1 in comparison with the Reference Mix at a test temperature of 50°C, indicating increased resistance to permanent deformation than the Reference Mix. This behaviour is also consistent with the dynamic modulus test results which show improved stiffness behaviour at elevated test temperatures (i.e. 40°C and 55°C). At low test temperatures (-5°C and 5°C), GA Mix 1 exhibits reduced stiffness behaviour in comparison with the Reference Mix, while at intermediate test temperatures (20°C), GA Mix 1 and the Reference Mix show comparable stiffness behaviour.

From the assessed mathematical models used to compute the tertiary FN value, the Francken model and the polynomial model were considered best suited to calculate the FN value from the laboratory measured data of both GA Mix 1 and the Reference Mix. Furthermore, from the assessed rheological/constitutive models, the Huet-Sayegh model was considered most effective in characterising the visco-elastic properties of GA Mix 1.

6. STRUCTURAL PERFORMANCE EVALUATION OF GLASS-ASPHALT SURFACING PAVEMENTS

6.1. Introduction

As part of current revisions to the South African mechanistic-empirical pavement design method (SAPDM), use of the dynamic modulus (|E*|) as a modulus parameter for HMA materials will be implemented. This is said to involve laboratory testing of HMA samples to obtain the complex modulus of the material (Maina, et al., 2011).

In Chapter 5, the laboratory measured complex modulus (E*) of the glass-asphalt mix (GA Mix 1) and the conventional HMA mix (Reference Mix) was used to describe the linear viscoelastic (LVE) behaviour of both mixes at varying temperatures and load frequencies. The LVE behaviour was best described by the Huet-Sayegh model. The Huet-Sayegh model master curve was hence considered as the most accurate representation of the conventional and glass-asphalt behaviour at any particular reference temperature for a range of load frequencies.

In Chapter 6, a linear-elastic analysis of the glass-asphalt and conventional HMA surfacing layer within a typical pavement structure of ES10 and ES30 design structural capacity is presented. The objective is to analyse the effects of temperature and load frequency variation on the stress-strain behaviour as well as the structural capacity of both surfacing layers, overlying a high and low strength supporting base layer.

The modulus (|E*|) of GA Mix 1 and the Reference Mix is utilised in the analysis and is obtained from the Huet-Sayegh model master curve at two reference temperatures (indicative of intermediate and high temperatures) and two load frequencies (indicative of relatively slow and fast moving traffic).

The analysis is conducted incorporating the latest revisions to the 1996 South African Mechanistic Design Method (SAMDM) using a multi-layer linear-elastic software namely, MeCRAMES.

6.2. Flexible Pavement Analysis

6.2.1. Pavement Structure in accordance with TRH4 (1996)

The Draft TRH4 (1996) catalogue for design of pavements with granular bases in moderate or dry regions was used to select a typical pavement structure for ES10 (3 - 10 million E80s) and ES30 (10 – 30 million E80s) design structural capacity.

Since both asphalt wearing course mixes (i.e. GA Mix 1 and Reference Mix) were designed for a traffic level of 3 to 30 million E80s (with reference to Section 3.1), it is of the understanding that the remaining underlying pavement layers should also have the structural capacity to accommodate the same level of traffic. It is therefore reasonable to select a pavement structure typical to that of a Category A road with ES10 and ES30 structural capacity. Furthermore, since the interest is in the asphalt layer, the effect of a low and high strength supporting base layer is achieved through the selection of Pavement 1 (Category A- ES10) and 2 (Category A-ES30) respectively.

Pavement 1 and 2 are indicated in Figure 6-1 (a) and (b). It should be noted that in order to perform a comparative analysis, the thickness of the asphalt layer in both pavements is 40 mm.

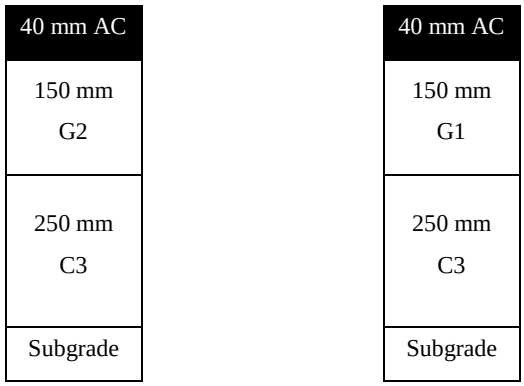

Figure 6-1: Pavement Structure 1 (a) and Pavement Structure 2 (b)

6.2.2. Load Characterisation

The standard design load for South Africa is an 80kN single axle with a dual-wheel configuration at 350 mm spacing between the centre of the two wheels. Revisions to the current SAMDM have, however, considered an increased tyre-contact stress value from 520 kPa to 650 kPa for the standard axle and wheel load configuration (Theyse, et al., 2011).

The linear-elastic analysis performed therefore considers a load of 20kN (per tyre) over an area of radius 99 mm (described by Pressure= Force/Area); assuming a uniformly distributed circular static load.

6.2.3. Material Characterisation

The following material properties were considered in the flexible pavement analysis of Pavement 1 and 2.

6.2.3.1. Glass-Asphalt and Conventional HMA

The modulus (|E*|) of GA Mix 1 and the Reference Mix was obtained from the Huet-Sayegh model master curve at two reference temperatures, i.e. 20ºC and 50ºC, and two load frequencies i.e., 10 Hz and 25 Hz, using Equation 5-22. The master curve model parameters at each reference temperature for the two mixes are presented in Table 6-1. The obtained dynamic moduli is summarised in Table 6-2. The value used for the Poisson's ratio of the conventional and glass-asphalt material is considered to be 0.44 as described by Theyse et al. (1996).

The selected temperatures are indicative of intermediate and high temperatures respectively and the load frequencies translate to approximately 45 km/h and 110 km/h respectively. Equations 6-1 and 6-2 were used to determine the load frequency which is a function of speed and radius of loading area.

$$\boldsymbol{loading\ time} = \frac{\boldsymbol{radius\ of\ loading\ area\ (mm)}*2}{\boldsymbol{speed}\ (\frac{km}{h})} * \frac{1\ (km)}{1*10^6\ (mm)} * \frac{3600\ (sec)}{1\ (h)} \qquad \text{Equation 6-1}$$

$$\boldsymbol{load\ frequency} = \frac{1}{\boldsymbol{loading\ time}} \div (2 * \pi) \qquad \text{Equation 6-2}$$

Table 6-1: Huet-Sayegh model parameters for GA Mix 1 and Reference Mix at reference temperature 20°C and 50°C

Reference Temperature	Asphalt Mix	E_0	E_∞	δ	k	h	t
T_{ref}=20°C	GA Mix 1	53	31000	2.3699	0.1932	0.6188	1.8630E-02
T_{ref}=50°C	GA Mix 1	53	31000	2.3700	0.1931	0.6187	1.7920E-05
T_{ref}=20°C	Ref Mix	53	31000	2.3906	0.2096	0.6494	2.1606E-02
T_{ref}=50°C	Ref Mix	53	31000	2.3878	0.2095	0.6493	2.0283E-05

Table 6-2: Dynamic moduli for GA Mix 1 and Reference Mix

	Mean Asphalt Temperature		Poisson's Ratio
GA Mix 1	**20ºC**	**50 ºC**	0.44
Dynamic Moduli (MPa) at 10 Hz	7837	461	
Dynamic Moduli (MPa) at 25 Hz	9474	710	

Reference Mix			0.44
Dynamic Moduli (MPa) at 10 Hz	8139	411	
Dynamic Moduli (MPa) at 25 Hz	9889	655	

6.2.3.2. Granular and Cement Treated Material

The material properties considered for the cement treated base and granular subbase layers for Pavement 1 and 2 is indicated in Table 6-3. It should be noted that since laboratory or field testing of these materials were not conducted, recommended modulus and Poisson's ratio values as described by Theyse et al. (1996) were utilised to perform the flexible pavement analysis.

Table 6-3: Material properties for base and subbase layers of Pavement 1 and Pavement 2

	Material Code	Elastic Moduli (MPa)	Poisson's Ratio
Pavement 1			
Granular Base	G2	500 [1]	0.35
Cemented Subbase	C3	800 [3]	0.35
Subgrade	G8	180 [4]	0.35
Pavement 2			
Granular Base	G1	1000 [2]	0.35
Cemented Subbase	C3	800 [3]	0.35
Subgrade	**G8**	180 [4]	0.35

[1] Assuming elastic modulus for crushed stone over cemented layer
[2] Assuming elastic modulus for high quality crushed stone over cemented layer
[3] Assuming elastic moduli for cemented material in post-cracked condition (traffic associated cracking)
[4] Assuming elastic moduli for gravel-soil (assuming soaked CBR $\geq$10)

6.2.4. Stress-Strain Behaviour

Since the primary focus is on the asphalt surfacing layer, the stress-strain behaviour of only the glass-asphalt and conventional HMA surfacing layers for the two temperatures and load frequencies is described. It should be noted that in the analysis negative (-) and positive (+) refer to compression and tension respectively.

6.2.4.1. Pavement 1

The stress-strain distribution within the glass-asphalt and the conventional HMA surfacing layers for two load frequencies i.e. 10 Hz and 25 Hz at two temperatures i.e. 20°C and 50°C can be observed in Figure 6-2 and 6-3. It can be seen that a very similar stress-strain profile is obtained for both the surfacing layers. Furthermore, a similar stress-strain profile is obtained for both load frequencies at each temperature. For both surfacing layers, the modular ratio

(MR) is greater than 15 at 20°C and less than 1.5 at 50°C when the elastic modulus (E_2) of the base layer in Pavement 1 is 500 MPa.

At 50°C (i.e. when MR < 1.5), both asphalt surfacing layers are subjected to compressive stresses over its entire depth, as indicated in Figure 6-2 (a), (b), (c) and (d). It can also be seen that the vertical compressive stresses hardly decreases over the surfacing depth and is very close to the tyre-pavement contact stress of 650 kPa at the bottom of the asphalt layer. The asphalt surfacing layer thus appears to be merely transferring the traffic loads to the underlying base layer. It is interesting to note the effect of these large vertical stresses on the horizontal strains at the bottom of the asphalt layer where the horizontal strain changes from compression at the top of the layer (due to the horizontal compressive stresses) to tension at the bottom of the layer (see Figure 6-3 (a) and (b)). This presents an interesting case where the vertical compressive stresses are in fact causing the observed horizontal tensile strains at elevated temperatures, since the horizontal stresses are in compression within the entire asphalt layer. Furthermore, it can be observed that as the MR decreases from greater than 15 to less than 1.5, the horizontal tensile strains at the bottom of the asphalt layer increases. This behaviour can be described by the significantly lower dynamic modulus of the asphalt layer coupled with much larger vertical compressive stresses at the bottom of the asphalt layer, under the given supporting condition.

At 20°C (i.e. when MR > 15), the vertical compressive stresses in both asphalt surfacing layers are reduced by 38% over its entire depth i.e. from 650 kPa at the top to approximately 400 kPa at the bottom. Much of the traffic loading is therefore absorbed within the asphalt layer. It can be observed from Figure 6-2 (c) and (d) that the horizontal stresses changes from compression at the top of the layer to tension at the bottom of the layer where high horizontal tensile stresses are developed. This is due to the high dynamic modulus of both the asphalt layers where the tensile stresses increase with an increase in dynamic modulus. These tensile stresses contribute to the observed horizontal tensile strains at the bottom of the asphalt layer, although not as pronounced as the horizontal tensile strains at elevated temperatures (MR < 1.5).

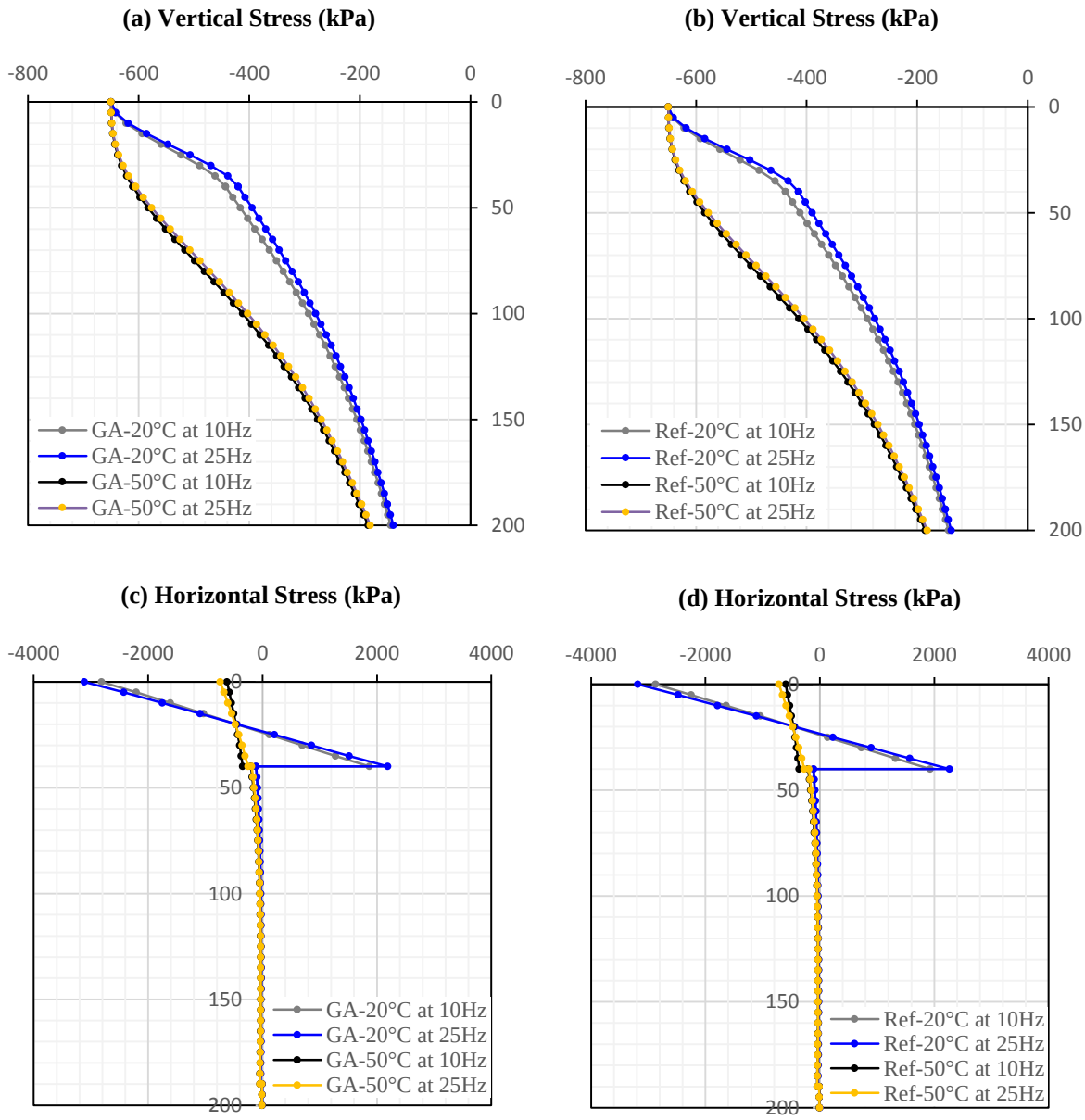

Figure 6-2: Vertical and horizontal stresses in Pavement 1

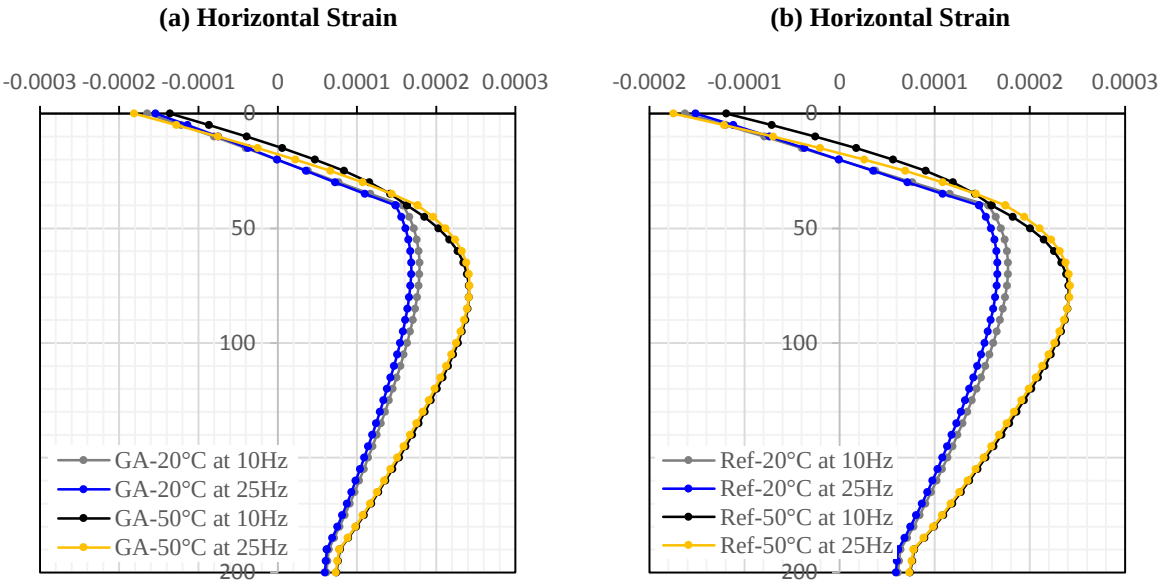

Figure 6-3: Horizontal strains in Pavement 1

6.2.4.2. Pavement 2

Analogous to Pavement 1, a similar stress-strain distribution is obtained for the glass-asphalt and the conventional HMA surfacing layers for the same load frequencies i.e. 10 Hz and 25 Hz at the same asphalt mean temperatures i.e. 20°C and 50°C, as indicated in Figure 6-4 and 6-5. It should be noted that the elastic modulus (E_2) of the base layer in Pavement 2 is 1000 MPa.

The effect of the base layer modulus on the stress-strain response is evident in Figure 6-4. It can be observed that the vertical stresses in Pavement 1 and 2 remain the same even with variation in the modulus of the base layer and only changes when the MR varies, i.e. at 20°C and 50°C (see Figure 6-4 (a) and (b)). This indicates that the vertical stresses in the asphalt layer are independent of the stiffness of the underlying support but is largely sensitive to the modular ratio.

At 50°C, the horizontal tensile strains at the bottom of the asphalt layer shows an opposite behaviour to Pavement 1 and decreases as the MR decreases from greater than 8 (i.e. at 20°C) to less than 0.8 (i.e. at 50°C), while E_2 has increased from 500 MPa to 1000 MPa (see Figure 6- 5 (a) and (b)). The asphalt surfacing layer thus appears to be merely transferring the traffic loads which is sustained by a high strength supporting base layer. Such surfacing layers that rest on high strength support layers may therefore be less inclined to traffic damage than surfacing layers resting on low strength support layers.

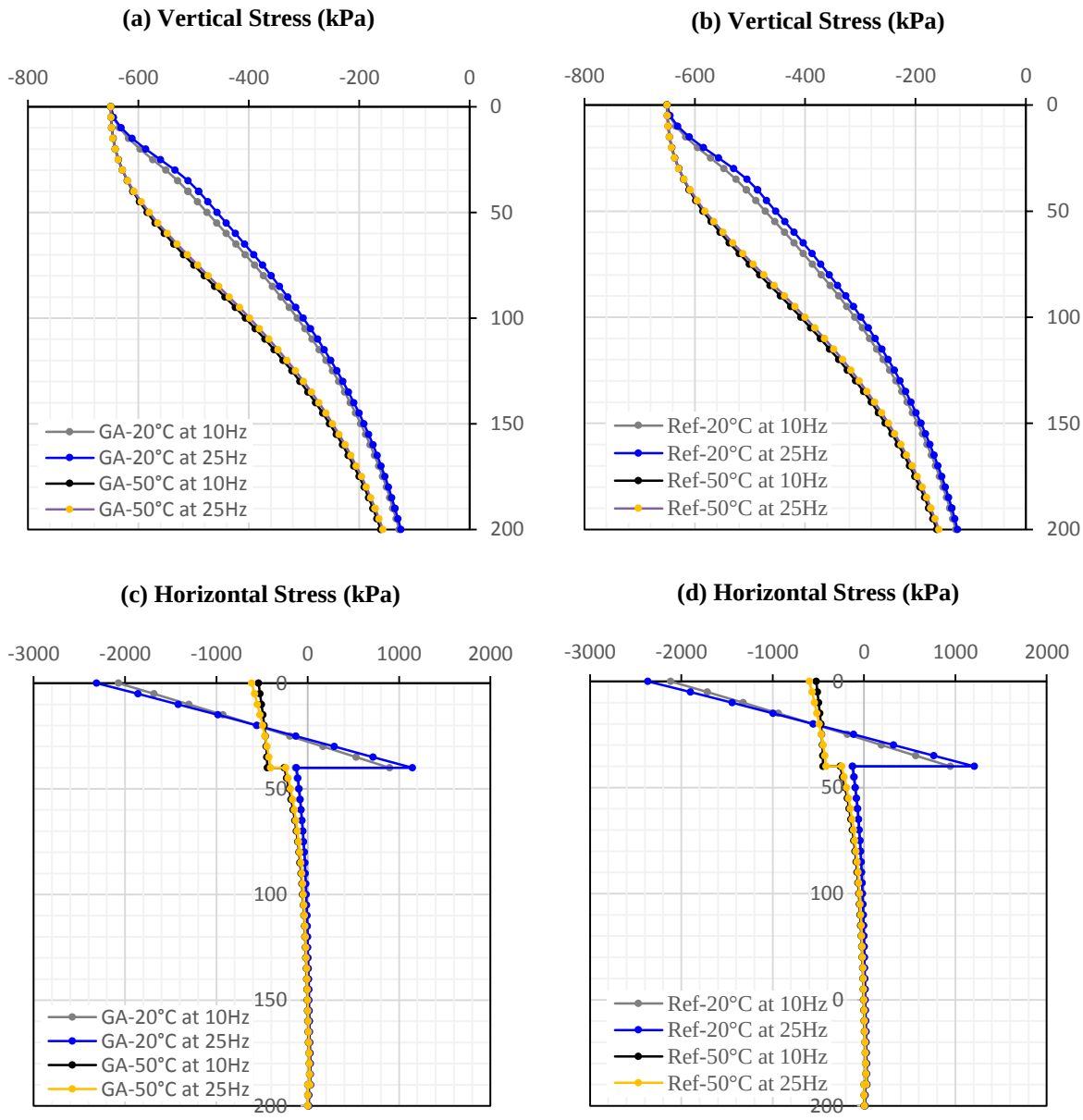

Figure 6-4: Vertical and horizontal stresses in Pavement 2

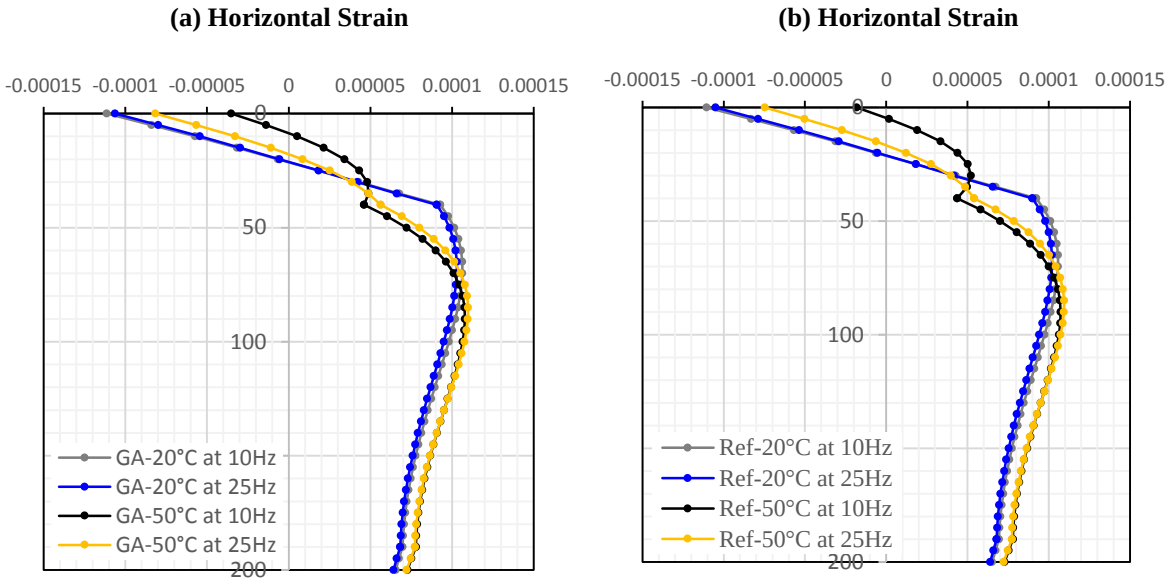

Figure 6-5: Horizontal strains in Pavement 2

6.2.5. Structural Capacity of Asphalt Surfacing Layer

In the SAMDM, the structural capacity of an asphalt layer is determined by its fatigue life (N) which is evaluated using a fatigue damage model described in Equation 6-3. The asphalt layer fails due to fatigue cracking under repeated loading as a result of tensile strain (ε_t) at the bottom or in the layer, which is the critical parameter for fatigue. Equation 6-3 describes the fatigue damage model for continuously-graded thin asphalt surfacing layers (≤ 50 mm) for Category A road (Pavement Modelling Corporation, 2010).

$$\boldsymbol{log\, N = A - B log \varepsilon_1 - offset} \qquad \text{Equation 6-3}$$

Where,

N = number of load repetitions to failure

A, B = model coefficients as a function of asphalt mix stiffness

ε_1 = horizontal tensile strain at the bottom of the asphalt layer

offset = model coefficient related to road category

The fatigue damage model described in Equation 6-3 is a revision to the fatigue crack initiation transfer function described by Theyse et al. (1996). Equation 6-3 was used to assess the structural capacity of the glass-asphalt surfacing layer as well as the conventional HMA surfacing layer for Pavement 1 and 2. It is expected that the variation in stiffness under the same surfacing conditions (i.e. temperature and loading time) and the same supporting

conditions will differentiate the critical horizontal tensile strain parameter (and hence the asphalt layer capacity) of both asphalt surfacing layers. The fatigue damage model coefficients used are indicated in Table 6-4.

Table 6-4: Fatigue damage model coefficients for thin HMA surfacing layers (Pavement Modelling Corporation, 2010)

Aggregate Grading	A	B	Offset – Category A
Continuous	18.114	5.195	0.469

A summary of the asphalt layer capacity for both surfacing layers at each respective temperature and loading condition for Pavement 1 and 2 is presented in Table 6-5. It should be noted that a shift factor that allows for the propagation of the fatigue cracks to the surface of the pavement has been factored into the fatigue capacities indicated in Table 6-5. This was done by multiplying the fatigue capacity with the value of the shift factor. The shift factor was determined based on the thickness of the asphalt layer as described in Equation 6-4.

$$\boldsymbol{Shift\ Factor = 0.048 * thickness\ of\ asphalt\ layer} \qquad \text{Equation 6-4}$$

Table 6-5: Fatigue capacity of asphalt layer in Pavement 1 and 2

	Temperature and Load Frequency	Glass-Asphalt Surfacing	Conventional HMA Surfacing
Pavement 1	20°C at 10 Hz	3.2E+06	3.3E+06
	20°C at 25 Hz	4.4E+06	4.4E+06
	50°C at 10 Hz	2.7E+06	3.1E+06
	50°C at 25 Hz	1.8E+06	2.3E+06
Pavement 2	**Temperature and Load Frequency**	**Glass-Asphalt Surfacing**	**Conventional HMA Surfacing**
	20°C at 10 Hz	5.1E+07	5.2E+07
	20°C at 25 Hz	5.7E+07	5.9E+07
	50°C at 10 Hz	1.9E+09	2.5E+09
	50°C at 25 Hz	6.9E+08	8.3E+08

6.2.5.1. Effect of asphalt mean temperature on fatigue life

For Pavement 1 it can be observed that as the temperature increases from 20°C to 50°C the fatigue life of both asphalt layers decreases, although more pronounced at 25 Hz (55-60% reduction) than at 10 Hz (10-16% reduction). For Pavement 2, the opposite behaviour is observed where the fatigue life increases with an increase in temperature. The increase is clearly more pronounced at 10 Hz than at 25 Hz. The effect of a stiffer supporting layer on the reduced horizontal tensile strains at the bottom of the asphalt layer in Pavement 2, as described

in Section 6.2.4, supports the observation of increased fatigue life in Pavement 2. It can hence be concluded that a high strength supporting base layer is required to improve the fatigue life of both glass-asphalt and conventional HMA surfacing layers at elevated temperatures.

6.2.5.2. Effect of load frequency on fatigue life

Although a similar stress-strain distribution was obtained for both load frequencies at 20°C and 50°C, as described in Section 6.2.4, the effect of load frequency was more pronounced when assessing the fatigue life of the asphalt layer. For Pavement 1 and 2 at 20°C the fatigue life increases with increasing load frequency whereas the opposite behaviour is observed at 50°C, where the fatigue life decreases with increasing load frequency. This trend is similar for both asphalt surfacing layers.

At high temperatures, it is known that the aggregate structure of an asphalt mix contributes to the elastic behaviour of the mix. It is also known that the modulus of an asphalt mix increases at higher load frequencies. As such, at elevated temperatures at higher load frequencies, the modulus of the "aggregate structure" increases making the asphalt mix more prone to tensile cracking than at lower frequencies. The higher tensile strains therefore decrease the fatigue life of the asphalt mix at elevated temperatures, as observed in Pavement 1 and 2.

6.2.5.3. Fatigue life relative to asphalt mix design capacity

For Pavement 1, the glass-asphalt surfacing layer at intermediate temperatures at low and high load frequencies can withstand more than 3 million E80s which is aligned with the mix design traffic capacity of GA Mix 1 (i.e. 3 to 30 million E80s). The same is also true for the glass-asphalt surfacing layer at high temperatures and low frequencies but fails to meet the mix design traffic capacity at 50°C and 25 Hz. For Pavement 2, the fatigue life is the highest at elevated temperatures and is greater than 100 million E80s for both loading conditions, while the fatigue life is greater than 30 million E80s at intermediate temperatures for both loading conditions. A similar trend is observed for the conventional HMA surfacing layer for Pavement 1 and 2.

6.2.5.4. Effect of glass-asphalt surfacing versus conventional HMA surfacing on fatigue life

Both asphalt surfacing layers in Pavement 1 and 2, with the given supporting (base, subbase and subgrade) layers, show comparable fatigue life at intermediate temperatures. At elevated

temperatures however, it can be observed that the fatigue life of the glass-asphalt surfacing layer is lower than the conventional HMA surfacing layer. This behaviour is expected as the complex modulus of the glass-asphalt mix (GA Mix 1) is higher at elevated temperatures and comparable at intermediate temperatures, as determined in Chapter 5. It is also known that at elevated temperatures asphalt material fails due to permanent deformation under repeated loading. The structural capacity of the asphalt layer at elevated temperatures should therefore be evaluated using a permanent deformation damage model rather than a fatigue damage model.

As mentioned in Section 6.2.4, the stresses within the asphalt layer at elevated temperatures are all compressive with highly concentrated vertical compressive stresses prevalent at the top of the surfacing layer. Table 6-6 provides a summary of the resulting vertical compressive strain at the top of the glass-asphalt and conventional HMA surfacing layers for Pavement 1 and 2 at 50°C. It can be seen that the conventional HMA surfacing layer indicates higher vertical compressive strains than the glass-asphalt surfacing layer and is therefore likely to experience more permanent deformation at elevated temperatures. This observation is in line with the GA Mix 1 demonstrating better resistance to permanent deformation than the Reference Mix at elevated temperatures, as determined in Chapter 5. The development of a damage model based on compressive stresses is therefore required to evaluate the structural capacity of the asphalt layer with regard to permanent deformation.

Table 6-6: Vertical compressive strain at top of asphalt layer

	Temperature and Load Frequency	**Glass-Asphalt Surfacing**	**Conventional HMA Surfacing**
Pavement 1	50°C at 10 Hz	-3.73E-04	-4.47E-04
	50°C at 25 Hz	-1.63E-04	-1.96E-04
Pavement 2	**Temperature and Load Frequency**	**Glass-Asphalt Surfacing**	**Conventional HMA Surfacing**
	50°C at 10 Hz	-4.42E-04	-5.17E-04
	50°C at 25 Hz	-2.30E-04	-2.63E-04

6.2.6. Structural Capacity of Subgrade Layer

It is known that the deformation in the surfacing layer can result in permanent deformation failure of the subgrade layer. As such, the effect of deformation in the conventional and glass-asphalt surfacing layers on the subgrade capacity of Pavement 1 and 2 is evaluated under the same variable surfacing conditions.

The vertical compressive strain (ε_v) at the top of the subgrade layer is considered to be the critical parameter for permanent deformation of the subgrade material (Theyse et al., 1996). The transfer function provided in the SAMDM (Theyse et al., 1996) for a terminal rut depth of 10 mm as a function of the vertical compressive strain was therefore used to evaluate the structural capacity of the subgrade layer. Equation 6-5 describes the transfer function for 10 mm subgrade deformation for Category A road.

$$N = 10^{(33.3-10log\,\varepsilon_v)} \qquad \text{Equation 6-5}$$

Where,

N = number of load repetitions to failure

ε_v = vertical compressive strain at top of subgrade layer ($\mu\varepsilon$)

A summary of the vertical compressive strain and subgrade layer capacity for both surfacing layers at each respective temperature and loading condition for Pavement 1 and 2 is presented in Table 6-7. The vertical compressive strains is also presented in Figure 6-6 and 6-7.

Table 6-7: Subgrade layer capacity in Pavement 1 and 2

	Temperature and Load Frequency	**Glass-Asphalt Surfacing**		**Conventional HMA Surfacing**	
		ε_v	**N**	**ε_v**	**N**
Pavement 1	20°C at 10 Hz	-139.90	7.0E+11	-139.60	7.1E+11
	20°C at 25 Hz	-138.20	7.9E+11	-137.80	8.1E+11
	50°C at 10 Hz	-160.20	1.8E+11	-160.80	1.7E+11
	50°C at 25 Hz	-157.80	2.1E+11	-157.80	2.1E+11
	Temperature and Load Frequency	**Glass-Asphalt Surfacing**		**Conventional HMA Surfacing**	
		ε_v	**N**	**ε_v**	**N**
Pavement 2	20°C at 10 Hz	-120.40	3.1E+12	-120.10	3.2E+12
	20°C at 25 Hz	-118.80	3.6E+12	-118.50	3.7E+12
	50°C at 10 Hz	-143.50	5.4E+11	-144.10	5.2E+11
	50°C at 25 Hz	-140.80	6.5E+11	-141.40	6.2E+11

From Table 6-7, it can be observed that at 50°C for Pavement 1 and 2, a similar trend to the vertical compressive strains at the top of the asphalt layer is depicted by the vertical compressive strains at the top of the subgrade layer for both the conventional and glass-asphalt surfacing layers, although the difference in compressive strains between the two surfacing layers is more pronounced at the top of the asphalt layer. In this regard, the subgrade capacities

for both conventional and glass-asphalt surfacing pavements are considered comparable, with a capacity greater than 100 million E80s.

Furthermore and as expected, for Pavement 1 and 2, the vertical strain increases with an increase in temperature and decreases with an increase in load frequency.

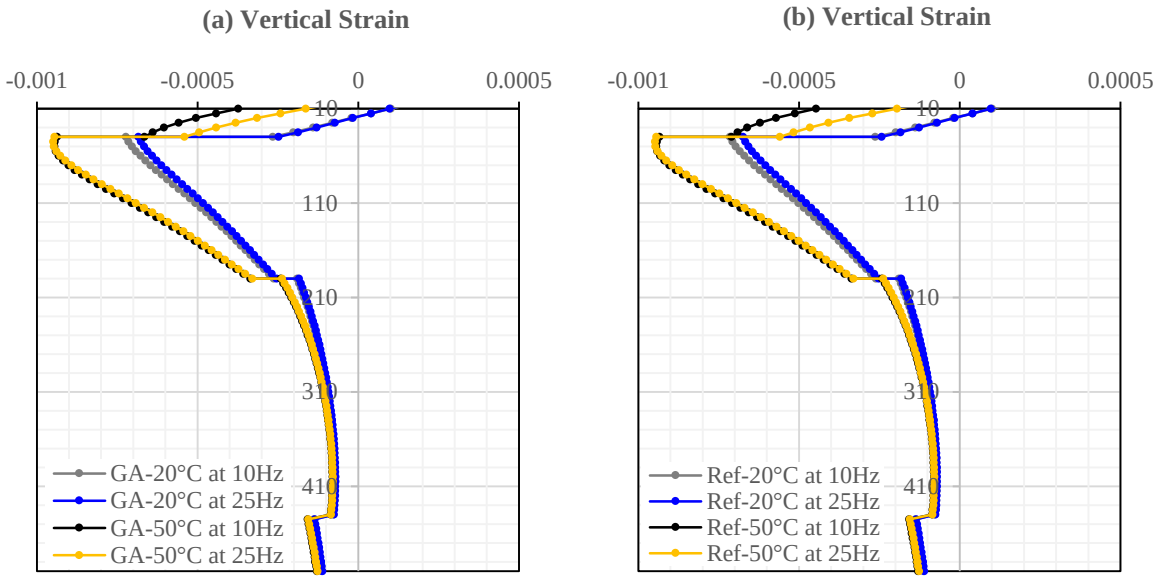

Figure 6-6: Vertical Strains in Pavement 1

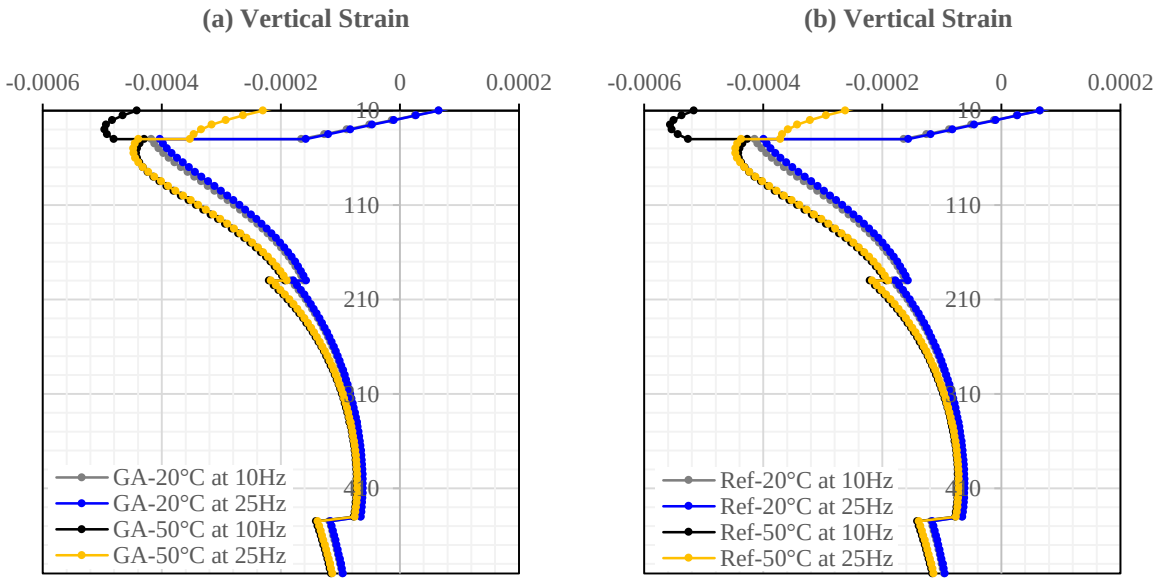

Figure 6-7: Vertical Strains in Pavement 2

6.3. Summary

Chapter 6 presents a linear-elastic analysis of an asphalt layer within a typical pavement structure of ES10 and ES30 design structural capacity. The objective was to analyse the effects of temperature and load frequency variation on the stress-strain behaviour as well as the structural capacity of the glass-asphalt (GA Mix 1) and conventional HMA (Reference Mix) surfacing layers, supported by a high and low strength base layer.

The variables presented in Table 6-7 were considered in the analysis:

Table 6-8: Variable asphalt surfacing parameters

Pavement Type	Temperature and Load Frequency	Asphalt Surfacing Layer
Pavement 1 (500 MPa base)	20°C at 10 Hz	1. Glass-asphalt surfacing layer 2. Conventional HMA surfacing layer
	20°C at 25 Hz	
	50°C at 10 Hz	
	50°C at 25 Hz	
Pavement 2 (1000 MPa base)	20°C at 10 Hz	1. Glass-asphalt surfacing layer 2. Conventional HMA surfacing layer
	20°C at 25 Hz	
	50°C at 10 Hz	
	50°C at 25 Hz	

For Pavement 1 and 2 at 50°C, the vertical compressive stresses in both asphalt surfacing layers hardly decreases over the surfacing depth and is very close to the tyre-pavement contact stress of 650 kPa at the bottom of the asphalt layer. For Pavement 1 and 2 at 20°C, the vertical compressive stresses in both asphalt surfacing layers reduces from 650 kPa at the top to approximately 400 kPa at the bottom. Vertical compressive stresses in Pavement 1 and 2 remain the same and are hence independent of the stiffness of the underlying support.

For Pavement 1 and 2 at 50°C, both asphalt surfacing layers are subjected to compressive stresses over its entire depth. Vertical compressive stresses are therefore causing the horizontal tensile strains at the bottom of the asphalt layer. For Pavement 1 and 2 at 20°C, horizontal stresses at the bottom of both asphalt surfacing layers are tensile. These tensile stresses contribute to the horizontal tensile strains at the bottom of the asphalt layer.

The horizontal tensile strain at the bottom of both asphalt layers increases with an increase in temperature for Pavement 1. The opposite behaviour is observed for both asphalt layers in Pavement 2 where the horizontal tensile strain at the bottom of the asphalt layer decreases with an increase in temperature. The asphalt surfacing layer at elevated temperatures thus appears to be merely transferring the traffic loads which is sustained by a high strength supporting base

layer in Pavement 2. A high strength supporting base layer thus improves the fatigue life of the asphalt layer at elevated temperatures.

For Pavement 1 and 2 at 20°C, the fatigue life of the asphalt layer increases with increasing load frequency whereas the opposite behaviour is observed at 50°C, where the fatigue life decreases with increasing load frequency. This trend is similar for both asphalt surfacing layers.

The glass-asphalt and conventional asphalt surfacing layers in Pavement 1 and 2 show comparable fatigue life at 20°C. At 50°C, however, the fatigue life of the glass-asphalt surfacing layer is lower than the conventional HMA surfacing layer. The structural capacity of the asphalt layer at elevated temperatures should therefore be evaluated using a permanent deformation damage model rather than a fatigue damage model.

For Pavement 1, the glass-asphalt and conventional HMA surfacing layers can withstand more than 3 million E80s which is aligned with the mix design traffic capacity of GA Mix 1 and the Reference Mix (i.e. 3 to 30 million E80s). The glass-asphalt surfacing layer, however, fails to meet the mix design traffic capacity at 50°C and 25 Hz. For Pavement 2, the glass-asphalt and conventional HMA surfacing layers can withstand more than 30 million E80s at 20°C and more than 100 million E80s at 50°C.

The vertical compressive strain at the top of the subgrade for the conventional and glass-asphalt surfacing pavements (Pavement 1 and 2) are comparable resulting in similar subgrade capacities (greater than 100 million E80s), evaluated under the same variable surfacing conditions. The difference in vertical compressive strains at the top of both asphalt layers are however more pronounced than the vertical compressive strains at the top of subgrade, with higher vertical compressive strains observed at the top of the conventional HMA surfacing layer than the glass-asphalt surfacing layer.

7. CONCLUSIONS AND RECOMMENDATIONS

7.1. Conclusions

Based on the information presented in this thesis, the following conclusions are drawn:

- The recycled crushed glass material available at the Consol manufacturing plant in Gauteng is capable of substituting traditional fine aggregates that are typically used in asphalt mixes in South Africa. This conclusion is based on the determined physical properties of the glass material which meets standard criteria for traditional aggregates in South Africa. Additional properties of the recycled crushed glass material, presented in Chapter 2 and 3, render the material favourable for use in asphalt mixes. Such properties include high angularity, high reflectivity, low thermal conductivity, high degree of purity, consistent grading from the same source and no significant health and safety hazards associated with handling of the recycled crushed glass material.

- There is potential to use the optimum glass-asphalt mix in the surfacing course of medium to high volume roads in South Africa (i.e. 3 to 30 million ESALs). This conclusion is based on conformance of the glass-asphalt mix with mix design specifications required for traditional continuously-graded asphalt mixes in South Africa with a design traffic level of 3 to 30 million ESALs, presented in Chapter 3.

- It can be concluded from the findings in Chapter 4 that an antistripping additive for this particular source and grading of glass particles, at a glass content of 15%, is required to meet moisture susceptibility criteria and alleviate stripping in medium continuously-graded glass-asphalt mixes in South Africa. Additionally, it can be concluded that hydrated lime is more effective than the liquid antistripping additive in alleviating stripping. In this regard, the liquid antistripping additive, which is known to be commonly used in HMA production in South Africa, may not be as effective in non-traditional asphalt mixes.

- The proposed new SIP parameter, obtained from the HWTT, is more effective in evaluating mix moisture susceptibility than the current method of evaluation (i.e. AASHTO T324) which demonstrates inconsistency in the calculated SIP value. This is

based on the vague and biased interpretation associated with manually plotting straight lines from the creep and stripping phase during SIP calculations in the current standard method as opposed to the proposed new method which models the HWTT output data to determine the SIP. Unlike the current SIP parameter, the new SIP parameter shows consistency with the degree of moisture damage obtained from the TSR parameter, determined from the Modified Lottman test. It is, however, recommended that future research into the correlation between the proposed new SIP parameter as well as the SIP compliance criterion with glass-asphalt pavements of known stripping performance be conducted. In addition, the image analysis techniques conducted to evaluate mix moisture susceptibility is capable of providing a more accurate representation of the degree of stripping and furthermore eliminates visual judgment and biased interpretation associated with the current standard of visual inspection and reporting (i.e. ASTM D4867M). This method is also suitable to validate the Modified Lottman test results.

- There is potential for the optimum glass-asphalt mix to out-perform the traditional mix as it is expected to demonstrate reduced susceptibility to cracking under low temperatures (thermal cracking), comparable resistance to fatigue cracking and increased resistance to rutting than the same mix without recycled crushed glass. This conclusion is based on the dynamic modulus test results which show reduced stiffness behaviour at low temperatures, comparable stiffness behaviour at intermediate temperatures and increased stiffness behaviour at elevated temperatures of the glass-asphalt mix in comparison with the traditional asphalt mix. The FN test results also show increased resistance to permanent deformation (rutting) of the glass-asphalt mix in comparison with the traditional asphalt mix at elevated temperatures.

- It can be concluded from the assessed mathematical models that the polynomial model and the Franken model are best suited to calculate the tertiary FN value from laboratory measured data using the FN test. These two models show applicability to both traditional and glass-asphalt mixes.

- From the assessed rheological/constitutive models, the Huet-Sayegh model can be concluded as a more effective model than the commonly used sigmoidal model in

characterising the visco-elastic properties of continuously-graded glass-asphalt mixes, particularly at cold temperatures and high frequencies.

- From the multi-layer linear-elastic analysis conducted in Chapter 6, it can be concluded that the fatigue life of the glass-asphalt and HMA surfacing layers are comparable at intermediate temperatures, for both high and low loading frequencies. This is based on comparable horizontal tensile strains obtained at the bottom of the asphalt surfacing layers; which is considered the critical parameter for fatigue life evaluation of asphalt material in the SAMDM. Additionally, higher vertical compressive strains were noted at the top of the HMA surfacing layer, and may therefore experience more permanent deformation than the glass-asphalt surfacing layer at elevated temperatures. This observation is in line with the GA Mix 1 demonstrating better resistance to permanent deformation than the Reference Mix at elevated temperatures, as determined in Chapter 5.

7.2. Recommendations

Based on the information presented in this thesis, the following recommendations for future research are summarised:

- The conclusions presented in this thesis pertain to a 10 mm NMPS medium continuously-graded glass-asphalt surfacing mix. It is recommended, however, that future studies consider other asphalt mix types (e.g. semi-gap graded, gap-graded and fine continuously-graded glass-asphalt) with a larger NMPS (e.g. 14 mm, 20 mm or 28 mm) for surfacing course applications as well as for alternative applications (e.g. bituminous treated base course application) in South African pavements.

- Furthermore, the conclusions drawn are specific to the aggregates, recycled crushed glass material as well as the additional raw materials (antistripping additive, filler and binder) used to manufacture the glass-asphalt mix. It is therefore recommended that future studies consider the use of different types of aggregate as well as recycled crushed glass from different sources in South Africa in order to identify variability in material physical, chemical and mechanical properties which may influence mix

performance. Additionally, the use of more cost-effective antistripping additives that improve moisture susceptibility in glass-asphalt mixes requires consideration.

- The glass-asphalt mix investigated in this thesis contains 15% recycled crushed glass material. Although 10 to 15% glass has been specified in most studies as the optimum glass content, further validation of this optimum content is required. It is therefore recommended that future studies evaluate the glass-asphalt mix performance at higher quantities of recycled crushed glass (i.e. > 15%), with special consideration on mix moisture susceptibility. Additionally, the use of higher quantities of recycled crushed glass in bituminous treated bases should also be considered.

- It is recommended that full-scale accelerated performance testing of glass-asphalt pavement test sections be carried out to form a link with the laboratory performance characterisation of the glass-asphalt mix presented in this study. Additional field investigations into the reflection and glare intensities as well as skid resistance at the quantity of recycled crushed glass investigated in this thesis (i.e. 15% recycled crushed glass) is required. Full-scale construction and testing of glass-asphalt pavement test sections require the support of national and provincial transportation departments. Furthermore, calibration of laboratory performance models for glass-asphalt with full-scale accelerated pavement testing is required for the development of transfer functions for glass-asphalt pavement fatigue cracking and permanent deformation.

- In this thesis, the recycled crushed glass material was utilised as obtained from the Consol manufacturing plant. As such, the material comprises of different colours (i.e. green, amber and flint) of crushed fine glass particles. An avenue for future research into the effect of specific coloured glass on mix performance may be required. However, the extra processing costs (which in turn increases the raw material cost) associated with the colour sorting process should also be taken into consideration.

8. REFERENCES

AASHTO M 323, 2014. *Standard Specification for Superpave Volumetric Mix Design.* American Association of State and Highway Transportation Officials (AASHTO), Washington D.C.

AASHTO T 312, 2015. *Standard method of test for preparing and determining the density of Hot Mix Asphalt (HMA) specimens by means of the Superpave gyratory compactor*. American Association of State and Highway Transportation Officials (AASHTO), Washington D.C.

AASHTO T 324, 2014. *"Method of Test for Hamburg Wheel-Track Testing of Compacted Hot Mix Asphalt (HMA)".* American Association of State Highway and Transportation Officials, Washington D.C.

Andela, C. & Sorge, E.V., n.d. *Handbook of Alternative Uses for Recycled Glass*.

Angelo, J.D. & Anderson, R.M., 2003. Material Production, Mix Design, and Pavement Design Effects on Moisture Damage. In *Moisture Sensitivty of Asphalt Pavements: A National Seminar*. San Diego, California, 2003. Transportation Research Board.

Anochie-Boateng, J., Denneman, E., O'Connell, J. & Ventura, D., 2010. Hot Mix Asphalt testing for the South African pavement design method. *In Proceedings of 29th Southern Africa transportation conference*. Pretoria, 2010.

Anochie-Boateng, K., Denneman, E., O'Connell, J.J. & Ventura, D., 2010. *Test Protocols for determining properties of asphalt materials for SAPDM.* TECHNICAL REPORT No: CSIR/BE/IE/IR/2010/0001/B, Pretoria.

Anochie-Boateng, J.K. & George, T.B., 2016. Use of Waste Crushed Glass for the Manufacturing of Hot Mix Asphalt. In *SCMT 4*. Las Vegas, 2016.

Anochie-Boateng, J.K. & George, T.B., 2016. Laboratory Investigation of the Performance Properties of Hot Mix Asphalt Containing Waste Glass. In *Southern African Transportation Conference (SATC)*. Pretoria, 2016.

Arabani, M., 2010. Effect of glaass cullet on the improvement of the dynamic behaviour of asphalt concrete. *Construction and Building Materials*, 25, pp.1181-85.

Arnold, G., Werkemeister, S. & Alabaster, D., 2008. *The effect of adding recycled glass on the performance of basecourse aggregate*. Research Report 351.40 pp. NZ Transport Agency.

Aschenbrener, T. & Currier, G., 1993. *Influence of Testing Variables on the Result from the Hamburg Wheel-Tracking Device*. Colorado Department of Transportation, Denver.

Aschenbrener, T., 1995. Evaluation of Hamburg Wheel-Tracking Device to Predict moisture Damage in Hot Mix Asphalt. *Transportation Research Record 1492*, pp.193-201.

ASTM D2493 / D2493M-09, 2009. *Standard Viscosity-Temperature Chart for Asphalts*. West Conshohocken, PA: ASTM International.

ASTM D4867M-09, 2009. *Standard Test Method for Effect of Moisture on Asphalt Concrete Paving Mixtures*. West Conshohocken, PA: ASTM International.

Australian Government: Department of Sustainability, Environment, Water, Population and Communities, 2011. *National Wate Policy Case Study*. Commonwealth of Australia.

Bagampadde, U., Isacsson, U. & Kiggundu, B.M., 2004. Classical and Contemporary Aspects of Stripping in Bituminous Mixes. *Road Materials and Pavement Design*, 5(1), pp.7-43.

Belosovie, S. & Zidekova, E., 1996. Adhesion of Bitumen Binders on Aggregates. In *Euroasphalt & Eurobitumen Congress*. Strasbourg, 1996.

Biligiri, K.P., Kaloush, K.E., Mamlouk, M.S. & Witczak, M.W., 2007. Rational Modelling of tertiary Flow for Asphalt Mixtures. *Journal of the Transportation Research Board*, 2001(10.3141), pp.63-72.

Carswell, J., Claxton, M.J. & Green, P.J., 2000. The classification of bitumens and polymer modifed bitumens within the SHRP performance grading system. *In 2nd Eurasphalt & Eurobitumen Congress.* Barcelona, 2000.

Chang, T.C., Chou, W.S. & Huang, C.E., 2001. Practical Technologies and Stategies for Recycling Waste Glass in Taiwan. In Dhir, K., Limbachiya, M.C. & Dyer, T.D., eds. *International Symposium*. Scotland, UK, 2001. Thomas Telford.

Cheng, D., Little, D.N., Lytton, R.L. & Holste, J.C., 2002. Surface Energy Measurements of Asphalt and Its Application to Predicting Fatiue and Healing in Asphalt Mixtures. *Transportation Research Record: Journal of the Transportation Research Board*, 1810, pp.44-53.

Committee of Land Transport Officials, 1996. *Draft TRH4 (1996): Structural Design of Interurban and Rural Roads*. Pretoria, South Africa: Department of Transport

Dames & Moore Inc. , 1993. *Engineering Suitability Evaluation*. Clean Washington Center.

Dane County Department of Public Works, 2003. *Resuse/Recycling of Glass Cullet for Non-Container Uses*. Wisconsin, USA.

Department of Environmental Affairs, 2012. *National Waste Information Baseline Report*.

Dougan, C.E., Stephens, J.E., Mahoney, J. & Hansen, G., 2003. *E* - Dynamic Modulus Test Protocol - Problems and Solutions*. Report No. CT-SPR-0003084-F-03-3. Storrs: University of Connecticut.

Federal Highway Administration, 1998. *User Guidelines for Waste and By-product Materials in Pavement Construction*. FHWA-RD-97-148, Report No. 480017, Guideline Manual.

Francken, L., 1977. Pavement Deformation Law of Bituminous Road Mixes in Repeated Load Triaxial Compression. In *4th International Conference on the Structural Design of Asphalt Pavements*. University of Michigan, Ann Arbor, 1977.

Heindrich, O., Bird, R. & Huang, Y., 2007. The Application of Recycled Waste Materials in the Construction of Asphalt Pavements. In *World Congress*. Amsterdam, Netherlands, 2007.

Huang, Y.H., 2004. *Pavement Analysis and Design*. 2nd ed. Pearson Prentice Hall.

Hughes, C.S., 1990. *Feasibility of Using Recycled Glass in Asphalt*. Richmond, Virginia, USA: Virginia Department of Transportation.

Khatib, J.M., ed., 2009. *Sustainability of Construction Materials*. Cambridge: Woodhead Publishing Limited.

Labib, M.E., 1992. Asphalt-Aggregate Interactions and Mechanisms for Water Stripping. *American Chemical Society*, 37(3), pp.1472-81.

Lachance-Tremblay, E., Vaillancourt, M. & Perraton, D., 2014. Evaluation on the Performance of an Asphalt Mix with Crushed Glass., 2014.

Maina, J.W., Anochie-Boateng, J.K. & Matsui, K., 2011. Application of Visco-Elastic Models to Flexible Pavement Analysis. In *10th Conference on Asphalt Pavements in South Africa*. Sun City, South Africa, 2011

Masson, J.F. & Lacasse, M.A., 2000. Review of Adhesion Mechanisms at the Crack Sealant/Asphalt Concrete Interface. In *RILEM 3rd International Symposium on Durability of Building and Construction Sealants*. Fort Lauderdale, Florida, 2000.

Mertens, E.W. & Wright, J.R., 1959. Cationic Emulsions: How They Differ from Conventional Emulsions in Theory and Practice. *Highway Research Board Proceedings*, 38, pp.386-97.

Moloi, T., 2015. Waste Glass Information. [email].

NCHRP 1-37A, 2004. *Development of the 2002 Guide for the design of New and rehabilitated Pavement Structures: Phase II.*

NCHRP Project 20-07/Task 361, 2015. *Hamburg Wheel-Track Test Equipment Requirements and Improvements to AASHTO T 324.* Washington, D.C: Transportation Research Board.

NCHRP Project Report 589, 2007. *Improved Conditioning and Testing Procedures for HMA Moisture Susceptibility*. Washington, D.C: Transportation Research Board.

Nebraska State Recycling Association, 1997. *Glass Cullet Utilization in Civil Engineering Applications*. Omaha, Nebraska.

Nilsson, R.N., Hopman, C.P. & Isacsson, U., 2002. Influence of Different Rheological Models on Predicted Pavement Responses in Flexible Pavements. *Road Materials Pavement Design*, 3(2), pp.117-49.

Olard, F. & Di Benedetto, H., 2003. General "2S2P1D" model and relation between the linear viscoelastic behavior of bituminous binders and mixes. *International Journal of Road Materials and Pavement Design (RMPD)*, 4(2), pp.185-224.

Pavement Interactive, n.d. [Online] Available at: HYPERLINK "http://pavementinteractive.org" http://pavementinteractive.org [Accessed January 2018].

Pavement Modelling Corporation, 2010. *The Classical South African Mechanistic-Empirical Design Method (SAMDM).* Flexible pavement design course notes.

Petersen, J.C., 2002. Chemistry of Asphalt-Aggregate Interaction. In *Moisture Damage Symposium*. Laramie, Wyo, 2002.

Pioneer Road Services Pty Ltd, n.d. *Recycled Glass in Asphalt*. Project Evaluation Report. Hazelmere WA.

Rice, J.M., 1958. Relationship of Aggregate Characteristics to the Effect of Water on Bituminous Paving Mixtures. *ASTM STP 240*, pp.17-34.

Roberts, F.L. et al., 1996. *Hot Mix Asphalt Materials, Mixture Design and Construction*. 2nd ed. Lanham, Maryland: National Asphalt Pavement Association Research and Education Foundation.

Sabita, 2016. Sabita Manual 35/TRH8: *Design and Use of Asphalt in Road Pavements*. South Africa.

Schram, S. & Williams, R.C., 2014. Reporting Results from the Hamburg Wheel Tracking Device. *In Transportation Research Board.* Washington D.C, 2014.

Shell Bitumen U.K., 1990. *"The Shell Bitumen Handbook"*. Riversdell Hause.

South African Bureau of Standards (SABS), 2011. *SANS 3001-AS10: Civil engineering test methods-Part AS10: Determination of bulk density and void content of compacted asphalt.* Pretoria.

South African Bureau of Standards (SABS), 2011. *SANS 3001-AS11:Civil engineering test methods-Part AS11: Determination of the maximum void-less density of asphalt mixes and the quantity of binder absorbed by the aggregate.* Pretoria.

South African Bureau of Standards (SABS), 2014. *SANS 3001-AG1: Civil engineering test methods-Part AG1: Particle size analysis of aggregates.* Pretoria.

South African Bureau of Standards (SABS), 2014. *SANS 3001-AG20: Civil engineering test methods-Part AG20: Determination of the bulk density, apparent density and water absorption of aggregate particles retained on the 5 mm sieve for road construction materials.* Pretoria.

South African Bureau of Standards (SABS), 2014. *SANS 3001-AG21: Civil engineering test methods-Part AG21: Determination of the bulk density, apparent density and water absorption of aggregate particles passing the 5 mm sieve for road construction materials.* Pretoria.

South African Bureau of Standards (SABS), 2016. *SANS 4001-BT1: Civil engineering specifications-Part BT1: Penetration grade bitumen.* Pretoria.

Su , N. & Chen, J.S., 2002. Engineering properties of asphalt concrete made with recycled glass. *Resources, Conservation and Recycling*, 35, pp.259-74.

Tarrer, A.R. & Wagh, V., 1991. *The Effect of the Physical and Chemical Characteristics of the Aggregate on Bonding*. SHRP Report A/UIR-91-507. Washington, D.C.: Strategic Highway Research Program.

Theyse, H.L., de Beer, M., Maina, J.W. & Kannemeyer, L., 2011. Interim revision of the South African Mechanistic-Empirical Pavement Design Method for Flexble Pavements. In *10th Conference on Asphalt Pavements in South Africa*. Sun City, South Africa, 2011.

Theyse, H.L., de Beer, M. & Rust, F.C., 1996. Overview of the South African Mechanistic Pavement Design Method. *Transportation Research Record 1539*.

Virginia Trasnportation Research Council, 1998. *Effect of Glass Concentration on Stripping of Glasphalt*. Final Report. Virginia, USA.

Washington State Department of Trade and Economic Development, 1993. *Glass Feedstock Evaluation*.

Wilshire, R. & Evans, R., 1994. Acquisition and Analysis of Creep Data. *Journal of Strain Analysis for Engineering Design*, 29(3), pp.159-65.

Witczak, M.W. et al., 2002. *Simple performance test for Superpave mix design*. NCHRP Report 465. National Cooperative Highway Research Program.

Wu , S., Yang, W. & Xue, Y., 2003. Preparation and Properties of Glass-asphalt Concrete. Wuhan, China, 2003. Wuhan University.

Xu, Q. & Solaimanian, M., 2009. Modelling linear viscoelastic properties of asphalt concrete by the Huet-Sayegh model. *International Journal of Pavement Engineering*, 10(6), pp.401-22.

Yamanaka, M., Gotoh, K., Saruwatari, M. & Mochishita, T., 2001. *Thermal and mechanical Properties of Glass Cullet Mixed with Asphalt as Low-Exothermic Pavement Material*. Japan: Nagasaki University.

Yin, F. et al., 2014. Novel Method for Moisture susceptibility and Rutting Evaluation Using Hamburg Wheel Tracking Test. *Transportation Research Board* , (2446), pp.1-7.

APPENDIX A: VOLUMETRIC TEST DATA

Table A1

	BC (%)	Sample no.	Flask Number	Mass of flask (g)	Mass of flask + sample (g)	Mass of flask + sample + water (g)	Mass of flask + water (g)	MVD (ton/m^3)
				A	B	C	D	$\frac{(B-A)}{[(D-A)-(C-B)]}$
GA MIX 1	4.0 %	15036G	3	1318.9	2562.1	4426.7	3658.9	2.615
		15036G	5	1290.9	2525.4	4394.0	3631.3	2.617
		Average		*1304.9*	*2543.8*	*4410.4*	*3645.1*	*2.616*
	4.5 %	15036G	3	1318.8	2572.6	4429.7	3659.8	2.591
		15036G	5	1290.8	2542.3	4400.2	3631.3	2.593
		Average		*1304.8*	*2557.5*	*4415.0*	*3645.6*	*2.592*
	5.0 %	150363G	3	1318.9	2570.0	4424.4	3659.2	2.575
		150363G	5	1290.9	2532.9	4391.3	3631.2	2.577
		Average		*1304.9*	*2551.5*	*4407.9*	*3645.2*	*2.576*
	5.5 %	15036G	S1	1379.4	2647.6	4484.8	3712.0	2.560
		15036G	S2	1367.8	2624.0	4447.8	3683.5	2.554
		Average		*1373.6*	*2635.8*	*4466.3*	*3697.8*	*2.557*
GA MIX 2	3.9 %	15036G AS PF	S1	1379.2	2612.1	4474.5	3712.0	2.621
		15036G AS PF	S2	1367.7	2606.0	4448.7	3683.1	2.620
		Average		*1373.5*	*2609.1*	*4461.6*	*3697.6*	*2.620*
	4.4 %	15036G AS PF	3	1318.6	2552.8	4417.8	3659.5	2.593
		15036G AS PF	5	1290.5	2526.6	4391.4	3631.3	2.597
		Average		*1304.6*	*2539.7*	*4404.6*	*3645.4*	*2.595*
	4.95	15036G AS PF	S1	1379.2	2620.9	4472.3	3712.0	2.579
		15036G AS PF	S2	1367.7	2591.8	4433.1	3682.9	2.583
		Average		*1373.5*	*2606.4*	*4452.7*	*3697.5*	*2.581*
	5.4 %	15036G AS PF	S1	1379.2	2586.1	4446.8	3711.6	2.559
		15036G AS PF	S2	1367.6	2652.5	4466.1	3682.6	2.563

		Average		*1373.4*	*2619.3*	*4456.5*	*3697.1*	*2.561*
GA MIX 3	3.9 %	15036G PF	3	1318.7	2554.9	4423.3	3659.8	2.615
		15036G PF	5	1290.7	2531.1	4398.2	3631.3	2.620
		Average		*1304.7*	*2543.0*	*4410.8*	*3645.6*	*2.617*
	4.4 %	15036G PF	S2	1367.8	2611.3	4448.4	3683.4	2.599
		15036G PF	3	1318.7	2565.8	4426.9	3660.0	2.597
		Average		*1343.3*	*2588.6*	*4437.7*	*3671.7*	*2.598*
	4.95	15036 PF	5	1290.7	2537.1	4394.4	3631.1	2.580
		15036 PF	5	1290.7	2518.9	4382.4	3631.1	2.575
		Average		*1290.7*	*2528.0*	*4388.4*	*3631.1*	*2.578*
	5.4 %	15036G PF	3	1318.7	2577.5	4426.4	3660.0	2.556
		15036G PF	5	1290.7	2548.4	4397.7	3631.1	2.561
		Average		*1304.7*	*2563.0*	*4412.1*	*3645.6*	*2.559*

Table A2

	BC	Sample No.	Dry Mass	Mass in water	Surface Dry Mass	Thickness	Diameter	BD	AVG. BD	MVD	Voids in Mix (VIM)	AVG. VIM	Effective Binder	Volume Effective Binder	VMA	VFB
	(%)		(g)	(g)	(g)	(mm)	(mm)	(ton/m^3)	(ton/m^3)	(ton/m^3)	(%)		(%)	(%)	(%)	(%)
			A	B	C			$D = \frac{A}{(C-B)}$	E	F	$G = \frac{(F-D)}{D}$	L	K	$H = \frac{(K*E)}{1.03}$	$I = H + L$	$J = 100 * \frac{H}{I}$
GA MIX 1	4.0	15036G16	4966.6	2924.6	5015.8	121.3	149.9	2.375	2.378	2.616	9.2	9.1	3.46	7.98	17.08	46.71
		15036G17	4970.4	2928.0	5015.9	121.4	149.9	2.381			9.0					
	4.5	15036G07	4967.2	2932.2	4994.8	119.2	149.9	2.408	2.410	2.592	7.1	7.0	4.00	9.37	16.41	57.09
		15036 gg1	4975.5	2943.6	5007.2	119.5	149.9	2.411			7.0					
	5.0	15036G08	4966.3	2937.3	4976.3	117.6	150.0	2.436	2.438	2.576	5.5	5.4	4.44	10.51	15.88	66.18
		15036G19	4970.1	2939.1	4976.2	116.9	150.0	2.440			5.3					
	5.5	15036G12	4971.0	2955.0	4976.6	116.7	149.9	2.459	2.462	2.557	3.8	3.7	4.93	11.78	15.49	76.07
		15036G13	4973.8	2962.9	4980.5	116.2	150.0	2.465			3.6					

GA MIX 2	3.9	15036G PF AS04	4975.1	2931.4	5016.5	121.3	149.9	2.386	2.385	2.620	8.9	9.0	3.44	7.97	16.95	47.01
		15036G PF AS05	4973.3	2931.1	5017.2	120.9	150.1	2.384			9.0					
	4.4	15036G PF AS07	4972.4	2937.6	4992.7	119.7	149.9	2.420	2.414	2.595	6.8	7.0	4.01	9.40	16.37	57.40
		15036G PF AS09	4975.8	2933.6	4999.4	119.9	149.9	2.409			7.2					
	4.9	15036G PF AS01	4973.8	2955.5	4990.0	117.6	149.8	2.445	2.443	2.581	5.3	5.4	4.41	10.47	15.83	66.12
		15036G PF AS02	4972.3	2950.3	4987.4	118.0	149.8	2.441			5.4					
	5.4	15036G PF AS10	4971.7	2960.8	4980.4	117.4	149.9	2.462	2.467	2.561	3.9	3.7	4.92	11.78	15.44	76.30
		15036G PF AS11	4973.4	2967.1	4980.8	116.5	149.9	2.470			3.5					
		15036G PF AS12	4975.1	2966.0	4980.9	116.4	149.9	2.469			3.6					
GA MIX 3	4.0	15036G PF18	4971.2	2929.1	5015.4	120.7	149.9	2.383	2.380	2.617	9.0	9.1	3.48	8.05	17.12	47.02
		15036G PF20	4974.3	2926.3	5018.9	121.0	150.0	2.377			9.1					
	4.4	15036G PF13	4972.8	2932.6	4997.5	119.6	149.9	2.408	2.410	2.598	7.3	7.2	3.97	9.28	16.53	56.16
		15036G PF14	4972.2	2930.9	4993.2	119.2	149.9	2.411			7.2					
	4.9	15036G PF01	4974.5	2946.3	4984.8	117.6	149.9	2.440	2.439	2.578	5.3	5.4	4.47	10.57	15.99	66.12
		15036G PF02	4971.7	2941.8	4982.0	117.9	149.9	2.437			5.5					
	5.4	15036G PF09	4974.5	2960.4	4983.5	116.7	150.0	2.459	2.462	2.559	3.9	3.8	4.95	11.84	15.62	75.79
		15036G PF10	4973.0	2962.4	4979.8	116.2	150.0	2.465			3.7					

APPENDIX B: MODIFIED LOTTMAN AND HWTT TEST DATA

Table B1: Modified Lottman results for GA Mix 1

Dry Subset					
Sample ID.		Calculation	15036L16	15036L17	15036L18
Diameter (m)	D		0.1	0.0999	0.0999
Height (m)	t		0.0628	0.0630	0.0629
Dry mass in air	A		1144.1	1141.9	1141.6
Mass in water	B		672.1	667.1	669.5
Mass surface dry	C		1148.8	1146.5	1146.2
Volume (cm^3)	E	C-B	476.7	479.4	476.7
BD (ton/m^3)	F	A/E	2.400	2.382	2.395
MVD (ton/m^3)	G		2.570	2.570	2.570
% Air void	H	100*(G*F)/(G)	6.6	7.3	6.8
Volume air void (cm^3)	I	(H*E)/100	31.5	35.1	32.5
Average % air void			6.9		
Load (kN)	P		11.7	10.6	10.45
Dry Strength (kPa)		(2*P')/(π*t'*D)	1186	1072	1059
Average Strength (kPa)			**1106**		
Wet Subset					
Sample ID.		Calculation	15036L19	15036L20	15036L21
Diameter (m)	D		0.0999	0.0998	0.1
Height (m)	t		0.0628	0.0628	0.063
Dry mass in air	A		1142	1142.5	1142.1
Mass in water	B		671	668.8	670.3
Mass surface dry	C		1146.9	1146.7	1146.9
Volume (cm^3)	E	C-B	475.9	477.9	476.6
BD (ton/m^3)	F	A/(C-B)	2.400	2.391	2.396
MVD (ton/m^3)	G		2.57	2.57	2.57
% Air void	H	100*(G*F)/(G)	6.6	7.0	6.8
Volume air void (cm^3)	I	(H*E)/100	31.5	33.3	32.2
Average % air void			6.8		
		Saturated			
Mass surface dry	B`		1163.9	1165	1163.5
Mass in water	C`		690.3	689.4	689.9
Volume (cm^3)	E`	B'-C'	473.6	475.6	473.6
Vol. abs. water (cm^3)	J`	B'-A	21.9	22.5	21.4
% Saturation		100*(J'/I)	69.4	67.5	66.5
		Conditioned at 60°C			
Height (m)	t`		0.0629	0.0628	0.063
Load (kN)	P`		10.32	9.1	9.66
Wet Strength (kPa)		(2*P')/(π*t'*D)	1046	924	976
Average Strength (kPa)			**982**		

Table B2: Modified Lottman results for GA Mix 2

Dry Subset					
Sample ID.		Calculation	15036MA3	15036MA4	15036MA5
Diameter (m)	D		0.09981	0.09984	0.09981
Height (m)	t		0.06278	0.0628	0.0625
Dry mass in air	A		1135.2	1135.8	1135.5
Mass in water	B		664.6	665.2	665.4
Mass surface dry	C		1139.6	1140.9	1140.5
Volume (cm^3)	E	C-B	475	475.7	475.1
BD (ton/m^3)	F	A/(C-B)	2.390	2.388	2.390
MVD (ton/m^3)	G		2.569	2.569	2.569
% Air void	H	100*(G*F)/(G)	7.0	7.1	7.0
Volume air void (cm^3)	I	(H*E)/100	33.1	33.6	33.1
Average % air void			7.0		
Load (kN)	P		8.514	8.003	9.036
Dry Strength (kPa)		(2*P')/(π*t'*D)	865	813	922
Average Strength (kPa)			**867**		
Wet Subset					
Sample ID.		Calculation	15036MA1	15036MA2	15036MA6
Diameter (m)	D		0.0999	0.09977	0.09988
Height (m)	t		0.06265	0.06263	0.06285
Dry mass in air	A		1136.3	1135.9	1135.9
Mass in water	B		665	664.6	665.8
Mass surface dry	C		1140.8	1140.6	1140.9
Volume (cm^3)	E	C-B	475.8	476	475.1
BD (ton/m^3)	F	A/(C-B)	2.388	2.386	2.391
MVD (ton/m^3)	G		2.569	2.569	2.569
% Air void	H	100*(G*F)/(G)	7.0	7.0	6.9
Volume air void (cm^3)	I	(H*E)/100	33.5	33.3	32.9
Average % air void			7.0		
		Saturated			
Mass surface dry	B`		1159.3	1158.9	1158.4
Mass in water	C`		684.4	683.3	684.3
Volume (cm^3)	E`	B'-C'	474.9	475.6	474.1
Vol. abs. water (cm^3)	J`	B'-A	23	23	22.5
% Saturation		100*(J'/I)	68.7	69.0	68.3
		Conditioned @ 60°C			
Height (m)	t`		0.0622	0.0621	0.0618
Load (kN)	P`		6.692	6.811	6.703
Wet Strength (kPa)		(2*P')/(π*t'*D)	686	700	691
Average Strength (kPa)			**692**		

Table B3: Modified Lottman results for GA Mix 3

Dry Subset					
Sample ID.		Calculation	15036M17	15036M18	15036M19
Diameter (m)	D		0.0999	0.0999	0.0999
Height (m)	t		0.0629	0.0632	0.0631
Dry mass in air	A		1141.4	1142.3	1142.4
Mass in water	B		669.6	669	669
Mass surface dry	C		1145.2	1145.7	1146.2
Volume (cm^3)	E	C-B	475.6	476.7	477.2
BD (ton/m^3)	F	A/(C-B)	2.400	2.396	2.394
MVD (ton/m^3)	G		2.566	2.566	2.566
% Air void	H	100*(G*F)/(G)	6.5	6.6	6.7
Volume air void (cm^3)	I	(H*E)/100	30.8	31.5	32.0
Average % air void			6.6		
Load (kN)	P		9.772	9.235	9.195
Dry Strength (kPa)		(2*P')/(π*t'*D)	990	931	929
Average Strength (kPa)			**950**		
Wet Subset					
Sample ID.		Calculation	15036M14	15036M15	15036M16
Diameter (m)	D		0.0999	0.0998	0.0999
Height (m)	t		0.0627	0.0632	0.0629
Dry mass in air	A		1142.3	1142.5	1142.8
Mass in water	B		669.8	669.1	670.1
Mass surface dry	C		1145.9	1146.2	1146.4
Volume (cm^3)	E	C-B	476.1	477.1	476.3
BD (ton/m^3)	F	A/(C-B)	2.399	2.395	2.399
MVD (ton/m^3)	G		2.566	2.566	2.566
% Air void	H	100*(G*F)/(G)	6.5	6.7	6.5
Volume air void (cm^3)	I	(H*E)/100	30.9	32.0	30.9
Average % air void			6.6		
		Saturated			
Mass surface dry	B`		1164.2	1164	1164.3
Mass in water	C`		689.3	687.8	689.1
Volume (cm^3)	E`	B'-C'	474.9	476.2	475.2
Vol. abs. water (cm^3)	J`	B'-A	21.9	21.5	21.5
% Saturation		100*(J'/I)	70.8	67.3	69.5
		Conditioned @ 60°C			
Height (m)	t`		0.0622	0.0621	0.0618
Load (kN)	P`		6.853	6.974	7.24
Wet Strength (kPa)		(2*P')/(π*t'*D)	702	716	747
Average Strength (kPa)			**722**		

Table B4: Hamburg Wheel Tracking Test Results at 50°C – GA Mix 1

Wheel Passes	Measured Maximum Rut Depth	Fitted Maximum Rut Depth: f (x)	f '(x)	f ''(x)
0	0.000	0.415	0.0026	-4.71E-07
100	1.065	0.673	0.0025	-4.60E-07
200	1.065	0.921	0.0024	-4.50E-07
300	1.065	1.160	0.0024	-4.40E-07
400	1.420	1.391	0.0023	-4.30E-07
600	1.775	1.829	0.0021	-4.11E-07
800	2.130	2.236	0.0020	-3.92E-07
1200	3.195	2.966	0.0017	-3.57E-07
1600	3.550	3.598	0.0015	-3.25E-07
2000	4.260	4.145	0.0013	-2.95E-07
2500	4.615	4.730	0.0011	-2.62E-07
3000	4.970	5.224	0.0009	-2.31E-07
3500	5.680	5.644	0.0008	-2.04E-07
4000	6.035	6.008	0.0007	-1.80E-07
5000	6.745	6.612	0.0005	-1.39E-07
6000	7.100	7.118	0.0005	-1.07E-07
7000	7.810	7.582	0.0005	-8.05E-08
8000	7.810	8.053	0.0005	-5.81E-08
9000	8.520	8.579	0.0006	-3.72E-08
10000	9.230	9.221	0.0007	-1.54E-08
12000	11.360	11.238	0.0014	4.07E-08
14000	15.265	15.335	0.0029	1.30E-07
16000	23.785	23.772	0.0059	2.75E-07

Table B5: Hamburg Wheel Tracking Test Results at 50°C – GA Mix 2

Wheel Passes	Measured Maximum Rut Depth	Fitted Maximum Rut Depth: f (x)	f '(x)	f ''(x)
0	0.00	2.52	0.008	-3.56E-06
100	4.62	3.26	0.007	-3.39E-06
200	4.97	3.94	0.006	-3.23E-06
300	4.97	4.56	0.006	-3.07E-06
400	5.68	5.12	0.005	-2.93E-06
600	6.04	6.09	0.004	-2.64E-06
800	6.75	6.87	0.004	-2.38E-06
1200	7.81	8.02	0.002	-1.92E-06
1600	8.52	8.76	0.001	-1.53E-06
2000	8.52	9.23	0.001	-1.20E-06
2500	9.59	9.62	0.001	-8.70E-07
3000	9.94	9.93	0.001	-6.16E-07
3500	10.65	10.26	0.001	-4.27E-07
4000	11.01	10.66	0.001	-2.90E-07
5000	11.72	11.69	0.001	-1.36E-07
6000	12.78	12.90	0.001	-8.35E-08
7000	14.20	14.08	0.001	-7.80E-08
8000	14.56	15.10	0.001	-7.83E-08
9000	15.98	16.03	0.001	-5.84E-08
10000	17.75	17.18	0.001	-6.88E-09
12000	21.66	21.90	0.004	1.62E-07

Table B6: Hamburg Wheel Tracking Test Results at 50°C – GA Mix 3

Wheel Passes	Measured Maximum Rut Depth	Fitted Maximum Rut Depth: f(x)	f '(x)	f ''(x)
0	0.00	0.82	0.0052	-2.00E-06
100	1.42	1.32	0.0048	-1.91E-06
200	2.13	1.78	0.0044	-1.83E-06
300	2.49	2.20	0.0041	-1.75E-06
400	2.84	2.60	0.0038	-1.67E-06
600	3.55	3.29	0.0032	-1.53E-06
800	3.91	3.88	0.0027	-1.39E-06
1200	4.62	4.80	0.0019	-1.15E-06
1600	5.33	5.46	0.0014	-9.38E-07
2000	5.68	5.95	0.0010	-7.57E-07
2500	6.39	6.41	0.0008	-5.70E-07
3000	6.75	6.78	0.0007	-4.21E-07
3500	7.10	7.15	0.0007	-3.04E-07
4000	7.81	7.54	0.0008	-2.14E-07
5000	8.52	8.47	0.0010	-9.96E-08
6000	9.59	9.58	0.0012	-4.56E-08
7000	11.01	10.81	0.0012	-2.59E-08
8000	11.72	12.05	0.0012	-1.98E-08
9000	13.14	13.31	0.0013	-1.22E-08
10000	14.91	14.65	0.0014	6.42E-09
12000	18.46	18.43	0.0025	8.69E-08
14000	25.21	25.26	0.0044	1.86E-07

APPENDIX C: FLOW NUMBER TEST DATA

Table C1

	BC (%)	Sample no.	Flask Number	Mass of flask (g)	Mass of flask + sample (g)	Mass of flask + sample + water (g)	Mass of flask + water (g)	MVD (ton/m^3)
				A	B	C	D	$\frac{(B-A)}{[(D-A)-(C-B)]}$
Reference Mix	4.0%	15036RB	5	1290.5	2522.1	4396.3	3630.3	2.645
		15036RB	S2	1367.7	2613.2	4457.7	3683.0	2.645
		Average		*1329.1*	*2567.65*	*4427.0*	*3656.7*	*2.645*
	4.5%	15036RB	S1	1379.1	2603.3	4468.7	3712.0	2.619
		15036RB	S2	1367.6	2611.3	4451.9	3683.2	2.618
		Average		*1373.4*	*2607.3*	*4460.3*	*3697.6*	*2.618*
	5.0%	150363RB	3	1318.5	2579.7	4435.4	3658.7	2.603
		150363RB	5	1290.5	2526.1	4391.4	3630.3	2.604
		Average		*1304.5*	*2552.9*	*4413.4*	*3644.5*	*2.604*
	5.5%	15036RB	S1	1379.2	2624.4	4474.5	3711.6	2.582
		15036RB	S2	1367.6	2616.0	4459.0	3682.7	2.584
		Average		*1373.4*	*2616.6*	*4459.0*	*3697.2*	*2.583*

Table C2

	BC	Sample No.	Dry Mass	Mass in water	Surface Dry Mass	Thickness	Diameter	BD	AVG. BD	MVD	Voids in Mix (VIM)	AVG. VIM
	(%)		(g)	(g)	(g)	(mm)	(mm)	(ton/m^3)	(ton/m^3)	(ton/m^3)	(%)	
			A	***B***	***C***			$D = \frac{A}{(C-B)}$	***E***	***F***	$G = \frac{(F-D)}{D}$	***L***
Reference Mix	4.0	15036RB 7	4943.2	2957.1	4977.6	118.4	149.9	2.447	2.446	2.645	7.5	7.5
		15036RB8	4945.4	2961.4	4983.7	118.3	149.9	2.445			7.6	
	4.5	15036RB10	4949.1	2968.2	4966.3	116.5	150.0	2.447	2.479	2.618	5.4	5.3
		15036RB11	4946.0	2968.1	4961.8	116.3	150.0	2.481			5.3	
	5.0	15036RB3	4950.8	2982.1	4957.4	114.8	149.9	2.506	2.508	2.604	3.7	3.7
		15036RBt4	4947.4	2983.6	4954.3	114.5	149.9	2.510			3.6	
	5.5	15036RB4	4946.3	2993.2	4949.3	113.3	149.9	2.529	2.528	2.583	2.1	2.1
		15036RBt3	4947.0	2992.9	4950.9	113.5	149.9	2.527			2.2	

Table C3

BC	M_B	M_A	V_B	V_A	V_T	V_{DA}	B_{ABS}
(%)	(g)	(g)	(cm^3)	(cm^3)	(cm^3)	(cm^3)	(%)
4.0	49.54	1189.01	48.10	430.02	478.12	469.56	0.74
4.5	55.53	1178.42	53.91	426.19	480.10	472.62	0.65
5.0	62.42	1185.98	60.60	428.93	489.53	480.89	0.75
5.5	68.38	1174.82	66.38	424.89	491.28	482.75	0.75

Table C4

Reference Mix						
Cycles (N)	**Permanent Strain for Replicate Specimen (%)**			**Statistic**		
	15036-RB-C6	15036-RB-C7	15036-RB-C10	Mean (%)	Stdev (%)	CoV (%)
1	0.000	0.000	0.000	0.000	0.00	0.00
2	0.146	0.170	0.199	0.172	0.03	15.46
3	0.217	0.244	0.280	0.247	0.03	12.80
4	0.266	0.292	0.330	0.296	0.03	10.87
5	0.305	0.330	0.366	0.334	0.03	9.19
6	0.340	0.361	0.397	0.366	0.03	7.88
7	0.371	0.388	0.423	0.394	0.03	6.73
8	0.399	0.412	0.447	0.419	0.02	5.92
9	0.425	0.434	0.468	0.442	0.02	5.13
10	0.449	0.454	0.488	0.464	0.02	4.58
11	0.472	0.472	0.506	0.483	0.02	4.06
12	0.494	0.489	0.523	0.502	0.02	3.66
13	0.514	0.506	0.539	0.520	0.02	3.31
14	0.533	0.521	0.554	0.536	0.02	3.12
15	0.551	0.535	0.568	0.551	0.02	2.99
16	0.568	0.549	0.581	0.566	0.02	2.84
17	0.584	0.562	0.595	0.580	0.02	2.90
18	0.599	0.575	0.607	0.594	0.02	2.81
19	0.613	0.587	0.619	0.606	0.02	2.81
20	0.627	0.599	0.630	0.619	0.02	2.76
21	0.641	0.610	0.641	0.631	0.02	2.84
22	0.653	0.622	0.651	0.642	0.02	2.70
23	0.666	0.632	0.662	0.653	0.02	2.84
24	0.677	0.643	0.671	0.664	0.02	2.73
25	0.689	0.653	0.682	0.675	0.02	2.83
26	0.700	0.663	0.691	0.685	0.02	2.82
27	0.711	0.672	0.700	0.694	0.02	2.90
28	0.722	0.681	0.709	0.704	0.02	2.98
29	0.732	0.691	0.718	0.714	0.02	2.92

30	0.742	0.700	0.727	0.723	0.02	2.94
31	0.752	0.708	0.735	0.732	0.02	3.03
32	0.762	0.717	0.743	0.741	0.02	3.05
33	0.771	0.725	0.752	0.749	0.02	3.08
34	0.780	0.733	0.759	0.757	0.02	3.11
35	0.790	0.741	0.767	0.766	0.02	3.20
36	0.799	0.749	0.775	0.774	0.03	3.23
37	0.807	0.757	0.782	0.782	0.03	3.20
38	0.816	0.764	0.790	0.790	0.03	3.29
39	0.824	0.772	0.797	0.798	0.03	3.26
40	0.832	0.779	0.804	0.805	0.03	3.29
41	0.840	0.787	0.811	0.813	0.03	3.27
42	0.848	0.793	0.818	0.820	0.03	3.36
43	0.856	0.800	0.825	0.827	0.03	3.39
44	0.864	0.807	0.831	0.834	0.03	3.43
45	0.871	0.814	0.838	0.841	0.03	3.40
46	0.878	0.821	0.844	0.848	0.03	3.38
47	0.885	0.828	0.851	0.855	0.03	3.36
48	0.893	0.834	0.857	0.861	0.03	3.45
49	0.900	0.841	0.863	0.868	0.03	3.44
50	0.907	0.847	0.869	0.874	0.03	3.47
51	0.914	0.854	0.875	0.881	0.03	3.46
52	0.921	0.860	0.881	0.887	0.03	3.49
53	0.928	0.866	0.887	0.894	0.03	3.53
54	0.934	0.872	0.893	0.900	0.03	3.50
55	0.941	0.878	0.899	0.906	0.03	3.54
56	0.947	0.885	0.905	0.912	0.03	3.47
57	0.953	0.891	0.910	0.918	0.03	3.46
58	0.960	0.896	0.916	0.924	0.03	3.54
59	0.966	0.902	0.921	0.930	0.03	3.54
60	0.972	0.908	0.927	0.936	0.03	3.51
61	0.978	0.914	0.932	0.941	0.03	3.51
62	0.984	0.920	0.938	0.947	0.03	3.48
63	0.990	0.925	0.943	0.953	0.03	3.52

64	0.996	0.931	0.949	0.959	0.03	3.50
65	1.002	0.937	0.954	0.964	0.03	3.50
66	1.008	0.942	0.960	0.970	0.03	3.52
67	1.013	0.948	0.965	0.975	0.03	3.46
68	1.019	0.953	0.970	0.981	0.03	3.49
69	1.025	0.959	0.975	0.986	0.03	3.49
70	1.030	0.964	0.980	0.991	0.03	3.47
71	1.036	0.969	0.985	0.997	0.03	3.51
72	1.041	0.974	0.990	1.002	0.03	3.49
73	1.047	0.980	0.995	1.007	0.04	3.49
74	1.052	0.985	1.000	1.012	0.04	3.47
75	1.057	0.990	1.005	1.017	0.04	3.46
76	1.062	0.995	1.010	1.022	0.04	3.44
77	1.068	1.001	1.015	1.028	0.04	3.44
78	1.073	1.005	1.020	1.033	0.04	3.46
79	1.078	1.010	1.025	1.038	0.04	3.44
80	1.084	1.015	1.029	1.043	0.04	3.50
81	1.088	1.020	1.034	1.047	0.04	3.43
82	1.093	1.025	1.039	1.052	0.04	3.41
83	1.098	1.030	1.043	1.057	0.04	3.42
84	1.103	1.035	1.048	1.062	0.04	3.40
85	1.108	1.040	1.053	1.067	0.04	3.38
86	1.113	1.045	1.057	1.072	0.04	3.39
87	1.118	1.050	1.062	1.077	0.04	3.37
88	1.123	1.054	1.066	1.081	0.04	3.41
89	1.128	1.059	1.071	1.086	0.04	3.39
90	1.133	1.064	1.075	1.091	0.04	3.40
91	1.138	1.069	1.080	1.096	0.04	3.38
92	1.142	1.073	1.084	1.100	0.04	3.37
93	1.147	1.078	1.089	1.105	0.04	3.36
94	1.152	1.082	1.093	1.109	0.04	3.39
95	1.156	1.087	1.097	1.113	0.04	3.35
96	1.161	1.092	1.102	1.118	0.04	3.33
97	1.166	1.096	1.106	1.123	0.04	3.37

98	1.171	1.101	1.111	1.128	0.04	3.36
99	1.175	1.105	1.115	1.132	0.04	3.35
100	1.180	1.110	1.119	1.136	0.04	3.35
101	1.184	1.115	1.123	1.141	0.04	3.31
102	1.189	1.119	1.128	1.145	0.04	3.33
103	1.194	1.123	1.132	1.150	0.04	3.36
104	1.198	1.128	1.136	1.154	0.04	3.32
105	1.202	1.132	1.140	1.158	0.04	3.31
106	1.207	1.137	1.144	1.163	0.04	3.32
107	1.211	1.141	1.148	1.167	0.04	3.30
108	1.216	1.146	1.152	1.171	0.04	3.31
109	1.220	1.150	1.156	1.175	0.04	3.30
110	1.225	1.154	1.160	1.180	0.04	3.34
111	1.229	1.159	1.164	1.184	0.04	3.30
112	1.234	1.163	1.168	1.188	0.04	3.33
113	1.238	1.167	1.172	1.192	0.04	3.32
114	1.243	1.172	1.176	1.197	0.04	3.33
115	1.247	1.176	1.180	1.201	0.04	3.32
116	1.251	1.180	1.184	1.205	0.04	3.31
117	1.255	1.185	1.188	1.209	0.04	3.27
118	1.260	1.189	1.192	1.214	0.04	3.31
119	1.264	1.193	1.196	1.218	0.04	3.30
120	1.268	1.198	1.199	1.222	0.04	3.28
121	1.272	1.202	1.203	1.226	0.04	3.27
122	1.277	1.206	1.207	1.230	0.04	3.31
123	1.281	1.210	1.211	1.234	0.04	3.30
124	1.285	1.214	1.215	1.238	0.04	3.29
125	1.290	1.218	1.219	1.242	0.04	3.32
126	1.294	1.223	1.223	1.247	0.04	3.29
127	1.298	1.227	1.226	1.250	0.04	3.30
128	1.302	1.231	1.230	1.254	0.04	3.29
129	1.306	1.235	1.234	1.258	0.04	3.28
130	1.310	1.239	1.237	1.262	0.04	3.29
131	1.314	1.244	1.241	1.266	0.04	3.26

132	1.319	1.248	1.245	1.271	0.04	3.30
133	1.323	1.252	1.249	1.275	0.04	3.29
134	1.327	1.256	1.253	1.279	0.04	3.28
135	1.331	1.260	1.256	1.282	0.04	3.29
136	1.335	1.264	1.260	1.286	0.04	3.28
137	1.339	1.268	1.263	1.290	0.04	3.30
138	1.343	1.272	1.267	1.294	0.04	3.29
139	1.346	1.276	1.271	1.298	0.04	3.23
140	1.351	1.280	1.274	1.302	0.04	3.29
141	1.355	1.284	1.278	1.306	0.04	3.28
142	1.359	1.288	1.282	1.310	0.04	3.27
143	1.363	1.292	1.285	1.313	0.04	3.29
144	1.367	1.296	1.289	1.317	0.04	3.28
145	1.371	1.300	1.293	1.321	0.04	3.27
146	1.375	1.304	1.296	1.325	0.04	3.28
147	1.379	1.308	1.300	1.329	0.04	3.27
148	1.383	1.311	1.303	1.332	0.04	3.31
149	1.387	1.315	1.307	1.336	0.04	3.30
150	1.391	1.319	1.311	1.340	0.04	3.29
151	1.394	1.323	1.314	1.344	0.04	3.26
152	1.398	1.327	1.318	1.348	0.04	3.25
153	1.402	1.331	1.321	1.351	0.04	3.27
154	1.406	1.335	1.325	1.355	0.04	3.26
155	1.410	1.339	1.328	1.359	0.04	3.28
156	1.414	1.343	1.332	1.363	0.04	3.27
157	1.418	1.347	1.335	1.367	0.04	3.28
158	1.422	1.350	1.339	1.370	0.05	3.29
159	1.426	1.355	1.343	1.375	0.04	3.26
160	1.430	1.358	1.346	1.378	0.05	3.30
161	1.434	1.362	1.350	1.382	0.05	3.29
162	1.438	1.366	1.353	1.386	0.05	3.30
163	1.442	1.370	1.357	1.390	0.05	3.29
164	1.445	1.374	1.360	1.393	0.05	3.27
165	1.449	1.377	1.363	1.396	0.05	3.30

166	1.453	1.381	1.367	1.400	0.05	3.30
167	1.457	1.385	1.370	1.404	0.05	3.31
168	1.461	1.389	1.374	1.408	0.05	3.30
169	1.465	1.393	1.377	1.412	0.05	3.32
170	1.469	1.397	1.380	1.415	0.05	3.34
171	1.472	1.400	1.384	1.419	0.05	3.30
172	1.476	1.404	1.387	1.422	0.05	3.32
173	1.480	1.408	1.391	1.426	0.05	3.31
174	1.484	1.412	1.394	1.430	0.05	3.33
175	1.488	1.415	1.397	1.433	0.05	3.36
176	1.491	1.420	1.401	1.437	0.05	3.30
177	1.495	1.423	1.404	1.441	0.05	3.33
178	1.499	1.427	1.408	1.445	0.05	3.32
179	1.503	1.431	1.411	1.448	0.05	3.34
180	1.507	1.435	1.414	1.452	0.05	3.36
181	1.510	1.439	1.417	1.455	0.05	3.34
182	1.514	1.442	1.421	1.459	0.05	3.34
183	1.518	1.446	1.424	1.463	0.05	3.36
184	1.522	1.450	1.427	1.466	0.05	3.38
185	1.526	1.454	1.431	1.470	0.05	3.37
186	1.530	1.457	1.434	1.474	0.05	3.40
187	1.533	1.461	1.437	1.477	0.05	3.38
188	1.537	1.465	1.441	1.481	0.05	3.37
189	1.541	1.468	1.444	1.484	0.05	3.40
190	1.545	1.472	1.447	1.488	0.05	3.42
191	1.548	1.476	1.451	1.492	0.05	3.38
192	1.552	1.480	1.454	1.495	0.05	3.40
193	1.556	1.484	1.458	1.499	0.05	3.39
194	1.560	1.487	1.461	1.503	0.05	3.42
195	1.563	1.491	1.464	1.506	0.05	3.40
196	1.567	1.495	1.467	1.510	0.05	3.42
197	1.571	1.499	1.471	1.514	0.05	3.41
198	1.575	1.502	1.474	1.517	0.05	3.44
199	1.578	1.506	1.477	1.520	0.05	3.42

200	1.582	1.510	1.480	1.524	0.05	3.44
201	1.586	1.513	1.484	1.528	0.05	3.44
202	1.590	1.517	1.487	1.531	0.05	3.46
203	1.593	1.521	1.490	1.535	0.05	3.44
204	1.597	1.525	1.493	1.538	0.05	3.46
205	1.601	1.528	1.497	1.542	0.05	3.46
206	1.605	1.532	1.500	1.546	0.05	3.48
207	1.608	1.536	1.503	1.549	0.05	3.47
208	1.612	1.539	1.507	1.553	0.05	3.47
209	1.616	1.543	1.510	1.556	0.05	3.49
210	1.620	1.547	1.513	1.560	0.05	3.50
211	1.623	1.551	1.516	1.563	0.05	3.49
212	1.627	1.554	1.520	1.567	0.05	3.49
213	1.630	1.558	1.523	1.570	0.05	3.47
214	1.634	1.562	1.526	1.574	0.05	3.49
215	1.638	1.565	1.530	1.578	0.06	3.49
216	1.642	1.569	1.533	1.581	0.06	3.51
217	1.645	1.573	1.536	1.585	0.06	3.50
218	1.649	1.576	1.539	1.588	0.06	3.52
219	1.653	1.580	1.543	1.592	0.06	3.52
220	1.656	1.584	1.546	1.595	0.06	3.50
221	1.660	1.588	1.549	1.599	0.06	3.52
222	1.664	1.591	1.552	1.602	0.06	3.55
223	1.667	1.595	1.556	1.606	0.06	3.51
224	1.671	1.598	1.559	1.609	0.06	3.53
225	1.675	1.602	1.562	1.613	0.06	3.55
226	1.678	1.605	1.565	1.616	0.06	3.55
227	1.682	1.609	1.569	1.620	0.06	3.54
228	1.685	1.613	1.572	1.623	0.06	3.52
229	1.689	1.617	1.575	1.627	0.06	3.54
230	1.693	1.620	1.578	1.630	0.06	3.57
231	1.697	1.624	1.582	1.634	0.06	3.56
232	1.700	1.628	1.585	1.638	0.06	3.55
233	1.704	1.631	1.588	1.641	0.06	3.57

234	1.708	1.635	1.591	1.645	0.06	3.59
235	1.711	1.639	1.594	1.648	0.06	3.58
236	1.715	1.642	1.598	1.652	0.06	3.58
237	1.719	1.646	1.601	1.655	0.06	3.60
238	1.722	1.649	1.604	1.658	0.06	3.59
239	1.726	1.653	1.607	1.662	0.06	3.61
240	1.730	1.657	1.610	1.666	0.06	3.63
241	1.733	1.660	1.614	1.669	0.06	3.60
242	1.737	1.664	1.617	1.673	0.06	3.62
243	1.741	1.668	1.620	1.676	0.06	3.63
244	1.745	1.671	1.623	1.680	0.06	3.66
245	1.748	1.675	1.627	1.683	0.06	3.62
246	1.752	1.679	1.629	1.687	0.06	3.67
247	1.755	1.682	1.633	1.690	0.06	3.63
248	1.759	1.686	1.636	1.694	0.06	3.65
249	1.763	1.689	1.639	1.697	0.06	3.68
250	1.766	1.693	1.642	1.700	0.06	3.67
251	1.770	1.697	1.646	1.704	0.06	3.66
252	1.774	1.700	1.649	1.708	0.06	3.68
253	1.778	1.704	1.652	1.711	0.06	3.70
254	1.781	1.708	1.655	1.715	0.06	3.69
255	1.785	1.712	1.659	1.719	0.06	3.68
256	1.789	1.715	1.662	1.722	0.06	3.70
257	1.792	1.719	1.665	1.725	0.06	3.69
258	1.796	1.723	1.668	1.729	0.06	3.71
259	1.800	1.726	1.671	1.732	0.06	3.74
260	1.804	1.730	1.675	1.736	0.06	3.73
261	1.807	1.734	1.678	1.740	0.06	3.72
262	1.811	1.737	1.681	1.743	0.07	3.74
263	1.815	1.741	1.684	1.747	0.07	3.76
264	1.818	1.745	1.688	1.750	0.07	3.72
265	1.822	1.749	1.691	1.754	0.07	3.74
266	1.826	1.752	1.694	1.757	0.07	3.76
267	1.829	1.756	1.697	1.761	0.07	3.76

268	1.833	1.760	1.700	1.764	0.07	3.78
269	1.836	1.763	1.703	1.767	0.07	3.77
270	1.841	1.767	1.707	1.772	0.07	3.79
271	1.844	1.771	1.710	1.775	0.07	3.78
272	1.848	1.774	1.713	1.778	0.07	3.80
273	1.852	1.778	1.716	1.782	0.07	3.82
274	1.855	1.782	1.719	1.785	0.07	3.81
275	1.859	1.786	1.722	1.789	0.07	3.83
276	1.863	1.789	1.725	1.792	0.07	3.85
277	1.866	1.793	1.729	1.796	0.07	3.82
278	1.870	1.796	1.732	1.799	0.07	3.84
279	1.874	1.800	1.735	1.803	0.07	3.86
280	1.877	1.804	1.738	1.806	0.07	3.85
281	1.881	1.808	1.741	1.810	0.07	3.87
282	1.885	1.811	1.744	1.813	0.07	3.89
283	1.889	1.815	1.748	1.817	0.07	3.88
284	1.892	1.819	1.751	1.821	0.07	3.87
285	1.896	1.822	1.754	1.824	0.07	3.89
286	1.900	1.826	1.757	1.828	0.07	3.91
287	1.903	1.830	1.761	1.831	0.07	3.88
288	1.907	1.834	1.764	1.835	0.07	3.90
289	1.911	1.838	1.767	1.839	0.07	3.92
290	1.914	1.841	1.770	1.842	0.07	3.91
291	1.918	1.845	1.773	1.845	0.07	3.93
292	1.921	1.849	1.776	1.849	0.07	3.92
293	1.925	1.852	1.779	1.852	0.07	3.94
294	1.929	1.856	1.783	1.856	0.07	3.93
295	1.933	1.860	1.786	1.860	0.07	3.95
296	1.936	1.863	1.789	1.863	0.07	3.95
297	1.940	1.867	1.793	1.867	0.07	3.94
298	1.944	1.871	1.796	1.870	0.07	3.96
299	1.948	1.875	1.799	1.874	0.07	3.98
300	1.951	1.878	1.802	1.877	0.07	3.97
301	1.955	1.882	1.805	1.881	0.08	3.99

302	1.959	1.885	1.809	1.884	0.08	3.98
303	1.962	1.889	1.812	1.888	0.08	3.97
304	1.966	1.893	1.815	1.891	0.08	3.99
305	1.969	1.896	1.818	1.894	0.08	3.99
306	1.973	1.900	1.822	1.898	0.08	3.98
307	1.977	1.904	1.825	1.902	0.08	4.00
308	1.981	1.908	1.828	1.906	0.08	4.02
309	1.984	1.912	1.831	1.909	0.08	4.01
310	1.988	1.915	1.834	1.912	0.08	4.03
311	1.992	1.919	1.838	1.916	0.08	4.02
312	1.996	1.923	1.841	1.920	0.08	4.04
313	1.999	1.926	1.844	1.923	0.08	4.03
314	2.003	1.930	1.847	1.927	0.08	4.05
315	2.007	1.934	1.851	1.931	0.08	4.04
316	2.011	1.937	1.854	1.934	0.08	4.06
317	2.014	1.941	1.857	1.937	0.08	4.06
318	2.018	1.945	1.860	1.941	0.08	4.07
319	2.022	1.949	1.863	1.945	0.08	4.09
320	2.026	1.952	1.867	1.948	0.08	4.08
321	2.030	1.956	1.870	1.952	0.08	4.10
322	2.033	1.960	1.873	1.955	0.08	4.10
323	2.037	1.964	1.876	1.959	0.08	4.12
324	2.041	1.967	1.880	1.963	0.08	4.11
325	2.045	1.971	1.883	1.966	0.08	4.12
326	2.048	1.975	1.886	1.970	0.08	4.12
327	2.052	1.979	1.889	1.973	0.08	4.14
328	2.056	1.982	1.893	1.977	0.08	4.13
329	2.060	1.986	1.896	1.981	0.08	4.15
330	2.064	1.990	1.899	1.984	0.08	4.16
331	2.067	1.994	1.902	1.988	0.08	4.16
332	2.071	1.997	1.906	1.991	0.08	4.15
333	2.075	2.001	1.909	1.995	0.08	4.17
334	2.079	2.005	1.912	1.999	0.08	4.19
335	2.083	2.009	1.916	2.003	0.08	4.18

336	2.086	2.013	1.919	2.006	0.08	4.17
337	2.090	2.017	1.922	2.010	0.08	4.19
338	2.094	2.020	1.925	2.013	0.08	4.21
339	2.098	2.024	1.929	2.017	0.08	4.20
340	2.102	2.028	1.932	2.021	0.09	4.22
341	2.106	2.032	1.935	2.024	0.09	4.24
342	2.110	2.036	1.939	2.028	0.09	4.23
343	2.113	2.039	1.942	2.031	0.09	4.22
344	2.117	2.043	1.945	2.035	0.09	4.24
345	2.121	2.047	1.949	2.039	0.09	4.23
346	2.125	2.051	1.952	2.043	0.09	4.25
347	2.129	2.055	1.955	2.046	0.09	4.27
348	2.133	2.058	1.958	2.050	0.09	4.28
349	2.136	2.062	1.961	2.053	0.09	4.28
350	2.140	2.066	1.965	2.057	0.09	4.27
351	2.144	2.070	1.968	2.061	0.09	4.29
352	2.148	2.074	1.971	2.064	0.09	4.31
353	2.152	2.078	1.975	2.068	0.09	4.30
354	2.156	2.082	1.978	2.072	0.09	4.32
355	2.160	2.085	1.981	2.075	0.09	4.33
356	2.163	2.089	1.985	2.079	0.09	4.30
357	2.167	2.093	1.988	2.083	0.09	4.32
358	2.171	2.097	1.991	2.086	0.09	4.34
359	2.175	2.101	1.994	2.090	0.09	4.35
360	2.179	2.105	1.998	2.094	0.09	4.35
361	2.183	2.109	2.001	2.098	0.09	4.36
362	2.187	2.113	2.004	2.101	0.09	4.38
363	2.191	2.117	2.007	2.105	0.09	4.40
364	2.195	2.121	2.011	2.109	0.09	4.39
365	2.198	2.125	2.014	2.112	0.09	4.39
366	2.202	2.128	2.017	2.116	0.09	4.40
367	2.206	2.133	2.021	2.120	0.09	4.40
368	2.210	2.137	2.024	2.124	0.09	4.41
369	2.214	2.141	2.027	2.127	0.09	4.43

370	2.218	2.144	2.031	2.131	0.09	4.42
371	2.221	2.149	2.034	2.135	0.09	4.42
372	2.225	2.152	2.037	2.138	0.09	4.43
373	2.229	2.156	2.041	2.142	0.09	4.42
374	2.233	2.160	2.044	2.146	0.10	4.44
375	2.237	2.164	2.047	2.149	0.10	4.46
376	2.241	2.168	2.051	2.153	0.10	4.45
377	2.245	2.172	2.054	2.157	0.10	4.47
378	2.249	2.176	2.057	2.161	0.10	4.49
379	2.253	2.179	2.060	2.164	0.10	4.50
380	2.257	2.184	2.064	2.168	0.10	4.49
381	2.261	2.187	2.067	2.172	0.10	4.51
382	2.265	2.192	2.071	2.176	0.10	4.50
383	2.268	2.196	2.074	2.179	0.10	4.50
384	2.272	2.199	2.077	2.183	0.10	4.51
385	2.277	2.204	2.081	2.187	0.10	4.53
386	2.281	2.208	2.084	2.191	0.10	4.55
387	2.285	2.212	2.088	2.195	0.10	4.54
388	2.288	2.216	2.091	2.198	0.10	4.53
389	2.293	2.219	2.094	2.202	0.10	4.57
390	2.296	2.223	2.098	2.206	0.10	4.54
391	2.300	2.227	2.101	2.209	0.10	4.56
392	2.304	2.231	2.104	2.213	0.10	4.57
393	2.309	2.235	2.108	2.217	0.10	4.58
394	2.313	2.240	2.111	2.221	0.10	4.60
395	2.317	2.243	2.115	2.225	0.10	4.59
396	2.321	2.248	2.118	2.229	0.10	4.61
397	2.325	2.252	2.122	2.233	0.10	4.60
398	2.329	2.256	2.125	2.237	0.10	4.62
399	2.333	2.260	2.128	2.240	0.10	4.64
400	2.337	2.264	2.132	2.244	0.10	4.63
401	2.341	2.268	2.135	2.248	0.10	4.65
402	2.345	2.272	2.139	2.252	0.10	4.64
403	2.349	2.276	2.142	2.256	0.10	4.65

404	2.353	2.280	2.146	2.260	0.10	4.65
405	2.357	2.284	2.149	2.263	0.11	4.66
406	2.361	2.289	2.153	2.268	0.11	4.66
407	2.365	2.293	2.156	2.271	0.11	4.67
408	2.369	2.297	2.160	2.275	0.11	4.67
409	2.374	2.301	2.163	2.279	0.11	4.70
410	2.378	2.305	2.166	2.283	0.11	4.72
411	2.382	2.309	2.170	2.287	0.11	4.71
412	2.386	2.313	2.173	2.291	0.11	4.73
413	2.390	2.317	2.177	2.295	0.11	4.72
414	2.394	2.322	2.180	2.299	0.11	4.74
415	2.398	2.326	2.184	2.303	0.11	4.73
416	2.402	2.330	2.187	2.306	0.11	4.75
417	2.406	2.334	2.191	2.310	0.11	4.74
418	2.411	2.338	2.194	2.314	0.11	4.77
419	2.415	2.343	2.198	2.319	0.11	4.77
420	2.419	2.347	2.201	2.322	0.11	4.78
421	2.423	2.351	2.205	2.326	0.11	4.77
422	2.427	2.355	2.208	2.330	0.11	4.79
423	2.431	2.359	2.212	2.334	0.11	4.78
424	2.436	2.364	2.216	2.339	0.11	4.80
425	2.440	2.368	2.219	2.342	0.11	4.81
426	2.444	2.372	2.223	2.346	0.11	4.80
427	2.448	2.376	2.226	2.350	0.11	4.82
428	2.452	2.381	2.230	2.354	0.11	4.82
429	2.457	2.385	2.233	2.358	0.11	4.85
430	2.461	2.389	2.237	2.362	0.11	4.84
431	2.465	2.393	2.241	2.366	0.11	4.83
432	2.469	2.398	2.244	2.370	0.12	4.85
433	2.474	2.402	2.248	2.375	0.12	4.86
434	2.478	2.406	2.251	2.378	0.12	4.88
435	2.482	2.411	2.255	2.383	0.12	4.87
436	2.486	2.415	2.258	2.386	0.12	4.89
437	2.490	2.419	2.262	2.390	0.12	4.88

438	2.494	2.423	2.265	2.394	0.12	4.90
439	2.499	2.428	2.269	2.399	0.12	4.91
440	2.503	2.432	2.273	2.403	0.12	4.90
441	2.507	2.437	2.276	2.407	0.12	4.92
442	2.511	2.441	2.280	2.411	0.12	4.91
443	2.516	2.445	2.284	2.415	0.12	4.92
444	2.520	2.449	2.287	2.419	0.12	4.94
445	2.525	2.454	2.290	2.423	0.12	4.97
446	2.529	2.458	2.294	2.427	0.12	4.97
447	2.533	2.462	2.298	2.431	0.12	4.96
448	2.537	2.466	2.301	2.435	0.12	4.97
449	2.541	2.470	2.305	2.439	0.12	4.97
450	2.545	2.475	2.309	2.443	0.12	4.96
451	2.550	2.480	2.312	2.447	0.12	5.00
452	2.554	2.484	2.316	2.451	0.12	4.99
453	2.559	2.488	2.320	2.456	0.12	5.00
454	2.563	2.493	2.323	2.460	0.12	5.02
455	2.567	2.497	2.327	2.464	0.12	5.01
456	2.572	2.502	2.331	2.468	0.12	5.02
457	2.576	2.506	2.334	2.472	0.12	5.04
458	2.581	2.510	2.338	2.476	0.12	5.05
459	2.585	2.514	2.341	2.480	0.13	5.06
460	2.589	2.519	2.345	2.484	0.13	5.06
461	2.594	2.523	2.349	2.489	0.13	5.07
462	2.598	2.528	2.353	2.493	0.13	5.06
463	2.603	2.532	2.356	2.497	0.13	5.09
464	2.607	2.537	2.360	2.501	0.13	5.09
465	2.612	2.541	2.364	2.506	0.13	5.10
466	2.616	2.546	2.367	2.510	0.13	5.12
467	2.620	2.550	2.371	2.514	0.13	5.11
468	2.625	2.555	2.375	2.518	0.13	5.12
469	2.629	2.559	2.379	2.522	0.13	5.11
470	2.634	2.564	2.382	2.527	0.13	5.15
471	2.638	2.568	2.386	2.531	0.13	5.14

472	2.642	2.573	2.390	2.535	0.13	5.14
473	2.647	2.578	2.394	2.540	0.13	5.15
474	2.652	2.582	2.397	2.544	0.13	5.18
475	2.656	2.587	2.401	2.548	0.13	5.18
476	2.661	2.591	2.405	2.552	0.13	5.18
477	2.665	2.596	2.409	2.557	0.13	5.18
478	2.669	2.600	2.413	2.561	0.13	5.17
479	2.674	2.605	2.417	2.565	0.13	5.18
480	2.679	2.610	2.420	2.570	0.13	5.22
481	2.683	2.614	2.424	2.574	0.13	5.21
482	2.688	2.619	2.428	2.578	0.13	5.22
483	2.692	2.624	2.432	2.583	0.13	5.22
484	2.697	2.629	2.436	2.587	0.14	5.23
485	2.701	2.633	2.439	2.591	0.14	5.25
486	2.706	2.638	2.444	2.596	0.14	5.24
487	2.710	2.643	2.447	2.600	0.14	5.26
488	2.715	2.647	2.451	2.604	0.14	5.26
489	2.720	2.652	2.455	2.609	0.14	5.28
490	2.724	2.657	2.459	2.613	0.14	5.27
491	2.729	2.661	2.463	2.618	0.14	5.28
492	2.734	2.666	2.467	2.622	0.14	5.29
493	2.738	2.671	2.471	2.627	0.14	5.29
494	2.743	2.676	2.475	2.631	0.14	5.30
495	2.748	2.680	2.479	2.636	0.14	5.31
496	2.752	2.685	2.482	2.640	0.14	5.33
497	2.757	2.690	2.486	2.644	0.14	5.34
498	2.761	2.695	2.491	2.649	0.14	5.31
499	2.766	2.699	2.494	2.653	0.14	5.34
500	2.770	2.704	2.498	2.657	0.14	5.34
501	2.775	2.709	2.502	2.662	0.14	5.35
502	2.780	2.714	2.506	2.667	0.14	5.36
503	2.784	2.719	2.510	2.671	0.14	5.36
504	2.789	2.723	2.514	2.675	0.14	5.37
505	2.794	2.729	2.518	2.680	0.14	5.38

506	2.798	2.733	2.522	2.684	0.14	5.38
507	2.803	2.738	2.526	2.689	0.14	5.39
508	2.808	2.742	2.530	2.693	0.15	5.39
509	2.813	2.747	2.534	2.698	0.15	5.40
510	2.817	2.752	2.538	2.702	0.15	5.40
511	2.822	2.757	2.542	2.707	0.15	5.41
512	2.826	2.762	2.547	2.712	0.15	5.39
513	2.831	2.767	2.550	2.716	0.15	5.42
514	2.836	2.772	2.554	2.721	0.15	5.43
515	2.841	2.777	2.559	2.726	0.15	5.42
516	2.846	2.782	2.563	2.730	0.15	5.44
517	2.850	2.787	2.567	2.735	0.15	5.43
518	2.855	2.792	2.570	2.739	0.15	5.47
519	2.860	2.796	2.574	2.743	0.15	5.47
520	2.864	2.802	2.579	2.748	0.15	5.45
521	2.869	2.807	2.583	2.753	0.15	5.47
522	2.874	2.812	2.587	2.758	0.15	5.48
523	2.879	2.816	2.591	2.762	0.15	5.48
524	2.884	2.822	2.595	2.767	0.15	5.50
525	2.889	2.827	2.599	2.772	0.15	5.51
526	2.893	2.832	2.603	2.776	0.15	5.51
527	2.898	2.837	2.607	2.781	0.15	5.52
528	2.903	2.842	2.611	2.785	0.15	5.53
529	2.908	2.847	2.615	2.790	0.15	5.54
530	2.913	2.852	2.619	2.795	0.16	5.55
531	2.918	2.857	2.623	2.799	0.16	5.56
532	2.923	2.862	2.627	2.804	0.16	5.57
533	2.927	2.867	2.631	2.808	0.16	5.57
534	2.932	2.872	2.636	2.813	0.16	5.56
535	2.937	2.878	2.640	2.818	0.16	5.58
536	2.942	2.883	2.644	2.823	0.16	5.59
537	2.947	2.888	2.648	2.828	0.16	5.60
538	2.952	2.893	2.652	2.832	0.16	5.61
539	2.957	2.898	2.657	2.837	0.16	5.60

540	2.962	2.903	2.661	2.842	0.16	5.61
541	2.967	2.909	2.665	2.847	0.16	5.63
542	2.972	2.914	2.669	2.852	0.16	5.64
543	2.977	2.919	2.674	2.857	0.16	5.63
544	2.982	2.924	2.678	2.861	0.16	5.64
545	2.987	2.929	2.682	2.866	0.16	5.65
546	2.992	2.935	2.686	2.871	0.16	5.67
547	2.997	2.940	2.691	2.876	0.16	5.66
548	3.002	2.945	2.695	2.881	0.16	5.67
549	3.007	2.950	2.699	2.885	0.16	5.68
550	3.012	2.956	2.703	2.890	0.16	5.70
551	3.017	2.961	2.708	2.895	0.16	5.69
552	3.022	2.967	2.712	2.900	0.17	5.70
553	3.027	2.972	2.716	2.905	0.17	5.71
554	3.032	2.977	2.721	2.910	0.17	5.70
555	3.038	2.982	2.725	2.915	0.17	5.73
556	3.043	2.988	2.729	2.920	0.17	5.74
557	3.048	2.993	2.734	2.925	0.17	5.73
558	3.052	2.999	2.738	2.930	0.17	5.74
559	3.057	3.004	2.742	2.934	0.17	5.75
560	3.062	3.010	2.747	2.940	0.17	5.74
561	3.068	3.015	2.751	2.945	0.17	5.77
562	3.073	3.020	2.755	2.949	0.17	5.78
563	3.078	3.026	2.760	2.955	0.17	5.77
564	3.083	3.031	2.764	2.959	0.17	5.78
565	3.088	3.037	2.769	2.965	0.17	5.78
566	3.094	3.042	2.773	2.970	0.17	5.80
567	3.099	3.047	2.777	2.974	0.17	5.81
568	3.104	3.053	2.782	2.980	0.17	5.81
569	3.109	3.058	2.786	2.984	0.17	5.82
570	3.114	3.064	2.791	2.990	0.17	5.82
571	3.119	3.070	2.795	2.995	0.17	5.83
572	3.124	3.075	2.800	3.000	0.17	5.82
573	3.130	3.080	2.804	3.005	0.18	5.84

574	3.135	3.086	2.809	3.010	0.18	5.84
575	3.140	3.091	2.813	3.015	0.18	5.85
576	3.145	3.097	2.818	3.020	0.18	5.85
577	3.150	3.103	2.823	3.025	0.18	5.84
578	3.156	3.109	2.827	3.031	0.18	5.87
579	3.161	3.114	2.832	3.036	0.18	5.86
580	3.166	3.120	2.836	3.041	0.18	5.88
581	3.172	3.126	2.841	3.046	0.18	5.89
582	3.177	3.132	2.846	3.052	0.18	5.88
583	3.182	3.137	2.850	3.056	0.18	5.89
584	3.188	3.143	2.855	3.062	0.18	5.90
585	3.193	3.149	2.859	3.067	0.18	5.92
586	3.199	3.155	2.863	3.072	0.18	5.94
587	3.204	3.160	2.868	3.077	0.18	5.93
588	3.209	3.166	2.873	3.083	0.18	5.93
589	3.215	3.172	2.877	3.088	0.18	5.96
590	3.220	3.178	2.882	3.093	0.18	5.96
591	3.226	3.184	2.887	3.099	0.18	5.96
592	3.231	3.190	2.891	3.104	0.19	5.98
593	3.237	3.195	2.896	3.109	0.19	5.98
594	3.242	3.202	2.901	3.115	0.19	5.98
595	3.248	3.208	2.905	3.120	0.19	6.01
596	3.253	3.213	2.910	3.125	0.19	6.00
597	3.259	3.219	2.915	3.131	0.19	6.01
598	3.264	3.225	2.919	3.136	0.19	6.02
599	3.269	3.231	2.924	3.141	0.19	6.02
600	3.275	3.238	2.929	3.147	0.19	6.04
601	3.280	3.243	2.934	3.152	0.19	6.03
602	3.286	3.250	2.939	3.158	0.19	6.04
603	3.291	3.256	2.943	3.163	0.19	6.06
604	3.297	3.262	2.948	3.169	0.19	6.06
605	3.302	3.268	2.953	3.174	0.19	6.06
606	3.308	3.274	2.958	3.180	0.19	6.07
607	3.314	3.280	2.963	3.186	0.19	6.08

608	3.320	3.286	2.967	3.191	0.19	6.10
609	3.325	3.292	2.972	3.196	0.19	6.10
610	3.331	3.299	2.977	3.202	0.20	6.11
611	3.337	3.305	2.982	3.208	0.20	6.12
612	3.342	3.311	2.987	3.213	0.20	6.12
613	3.348	3.317	2.992	3.219	0.20	6.13
614	3.354	3.323	2.997	3.225	0.20	6.13
615	3.360	3.330	3.002	3.231	0.20	6.15
616	3.365	3.336	3.007	3.236	0.20	6.14
617	3.371	3.342	3.012	3.242	0.20	6.15
618	3.376	3.348	3.017	3.247	0.20	6.15
619	3.382	3.354	3.022	3.253	0.20	6.16
620	3.388	3.361	3.026	3.258	0.20	6.19
621	3.394	3.367	3.032	3.264	0.20	6.18
622	3.399	3.373	3.037	3.270	0.20	6.18
623	3.405	3.379	3.042	3.275	0.20	6.18
624	3.411	3.386	3.047	3.281	0.20	6.20
625	3.417	3.392	3.052	3.287	0.20	6.20
626	3.423	3.399	3.057	3.293	0.20	6.22
627	3.428	3.405	3.062	3.298	0.20	6.22
628	3.435	3.412	3.067	3.305	0.21	6.24
629	3.440	3.418	3.072	3.310	0.21	6.24
630	3.446	3.425	3.077	3.316	0.21	6.25
631	3.452	3.431	3.082	3.322	0.21	6.26
632	3.458	3.438	3.087	3.328	0.21	6.27
633	3.464	3.445	3.092	3.334	0.21	6.28
634	3.470	3.451	3.098	3.340	0.21	6.27
635	3.476	3.458	3.103	3.346	0.21	6.29
636	3.482	3.465	3.108	3.352	0.21	6.30
637	3.488	3.471	3.113	3.357	0.21	6.31
638	3.494	3.478	3.118	3.363	0.21	6.32
639	3.500	3.485	3.124	3.370	0.21	6.32
640	3.507	3.491	3.129	3.376	0.21	6.33
641	3.513	3.498	3.134	3.382	0.21	6.35

642	3.519	3.505	3.139	3.388	0.22	6.36
643	3.525	3.512	3.144	3.394	0.22	6.37
644	3.531	3.519	3.150	3.400	0.22	6.37
645	3.537	3.525	3.155	3.406	0.22	6.38
646	3.543	3.533	3.160	3.412	0.22	6.40
647	3.549	3.540	3.165	3.418	0.22	6.41
648	3.555	3.546	3.170	3.424	0.22	6.42
649	3.561	3.553	3.176	3.430	0.22	6.41
650	3.568	3.560	3.181	3.436	0.22	6.44
651	3.574	3.567	3.186	3.442	0.22	6.45
652	3.580	3.574	3.192	3.449	0.22	6.45
653	3.587	3.581	3.197	3.455	0.22	6.47
654	3.593	3.588	3.202	3.461	0.22	6.48
655	3.599	3.595	3.208	3.467	0.22	6.48
656	3.605	3.602	3.213	3.473	0.23	6.49
657	3.612	3.609	3.218	3.480	0.23	6.51
658	3.618	3.616	3.224	3.486	0.23	6.51
659	3.625	3.623	3.229	3.492	0.23	6.53
660	3.631	3.630	3.235	3.499	0.23	6.53
661	3.637	3.637	3.240	3.505	0.23	6.54
662	3.644	3.645	3.246	3.512	0.23	6.55
663	3.650	3.652	3.251	3.518	0.23	6.57
664	3.656	3.659	3.257	3.524	0.23	6.56
665	3.662	3.666	3.263	3.530	0.23	6.56
666	3.669	3.673	3.268	3.537	0.23	6.58
667	3.676	3.681	3.274	3.544	0.23	6.59
668	3.682	3.688	3.279	3.550	0.23	6.60
669	3.688	3.695	3.285	3.556	0.23	6.60
670	3.695	3.703	3.291	3.563	0.24	6.61
671	3.701	3.710	3.296	3.569	0.24	6.63
672	3.708	3.718	3.302	3.576	0.24	6.64
673	3.715	3.725	3.307	3.582	0.24	6.66
674	3.721	3.732	3.313	3.589	0.24	6.65
675	3.728	3.740	3.319	3.596	0.24	6.67

676	3.735	3.747	3.325	3.602	0.24	6.67
677	3.741	3.755	3.331	3.609	0.24	6.67
678	3.748	3.763	3.336	3.616	0.24	6.70
679	3.754	3.770	3.342	3.622	0.24	6.70
680	3.761	3.778	3.348	3.629	0.24	6.71
681	3.768	3.785	3.354	3.636	0.24	6.71
682	3.775	3.793	3.360	3.643	0.24	6.72
683	3.782	3.801	3.365	3.649	0.25	6.75
684	3.788	3.808	3.371	3.656	0.25	6.75
685	3.795	3.816	3.377	3.663	0.25	6.76
686	3.802	3.824	3.383	3.670	0.25	6.77
687	3.809	3.832	3.388	3.676	0.25	6.80
688	3.816	3.840	3.394	3.683	0.25	6.81
689	3.823	3.847	3.400	3.690	0.25	6.81
690	3.830	3.855	3.406	3.697	0.25	6.83
691	3.837	3.863	3.412	3.704	0.25	6.84
692	3.843	3.871	3.418	3.711	0.25	6.84
693	3.850	3.879	3.424	3.718	0.25	6.85
694	3.857	3.887	3.430	3.725	0.26	6.86
695	3.865	3.895	3.436	3.732	0.26	6.88
696	3.872	3.903	3.442	3.739	0.26	6.89
697	3.879	3.911	3.448	3.746	0.26	6.90
698	3.886	3.919	3.453	3.753	0.26	6.93
699	3.893	3.927	3.459	3.760	0.26	6.94
700	3.900	3.936	3.465	3.767	0.26	6.96
701	3.907	3.943	3.471	3.774	0.26	6.96
702	3.914	3.952	3.477	3.781	0.26	6.98
703	3.921	3.960	3.483	3.788	0.26	6.99
704	3.928	3.968	3.489	3.795	0.27	7.00
705	3.935	3.976	3.495	3.802	0.27	7.01
706	3.942	3.985	3.501	3.809	0.27	7.03
707	3.950	3.993	3.507	3.817	0.27	7.05
708	3.957	4.002	3.514	3.824	0.27	7.05
709	3.964	4.010	3.520	3.831	0.27	7.06

710	3.971	4.018	3.526	3.838	0.27	7.07
711	3.978	4.027	3.532	3.846	0.27	7.09
712	3.986	4.036	3.538	3.853	0.27	7.12
713	3.993	4.044	3.544	3.860	0.28	7.13
714	4.001	4.053	3.551	3.868	0.28	7.14
715	4.008	4.061	3.557	3.875	0.28	7.15
716	4.016	4.070	3.563	3.883	0.28	7.17
717	4.023	4.079	3.570	3.891	0.28	7.17
718	4.031	4.087	3.576	3.898	0.28	7.19
719	4.038	4.096	3.582	3.905	0.28	7.21
720	4.046	4.105	3.589	3.913	0.28	7.22
721	4.053	4.114	3.595	3.921	0.28	7.24
722	4.061	4.122	3.602	3.928	0.28	7.24
723	4.069	4.131	3.608	3.936	0.29	7.26
724	4.076	4.140	3.614	3.943	0.29	7.28
725	4.084	4.149	3.621	3.951	0.29	7.29
726	4.091	4.158	3.628	3.959	0.29	7.29
727	4.099	4.167	3.634	3.967	0.29	7.31
728	4.107	4.176	3.641	3.975	0.29	7.32
729	4.115	4.185	3.647	3.982	0.29	7.35
730	4.123	4.194	3.654	3.990	0.29	7.35
731	4.130	4.203	3.661	3.998	0.29	7.36
732	4.138	4.212	3.667	4.006	0.30	7.38
733	4.146	4.221	3.674	4.014	0.30	7.39
734	4.154	4.230	3.681	4.022	0.30	7.40
735	4.162	4.239	3.687	4.029	0.30	7.42
736	4.170	4.248	3.694	4.037	0.30	7.43
737	4.178	4.257	3.700	4.045	0.30	7.45
738	4.186	4.267	3.707	4.053	0.30	7.47
739	4.194	4.276	3.714	4.061	0.30	7.47
740	4.202	4.285	3.721	4.069	0.30	7.48
741	4.210	4.295	3.728	4.078	0.31	7.50
742	4.218	4.305	3.735	4.086	0.31	7.52
743	4.226	4.314	3.741	4.094	0.31	7.54

744	4.234	4.324	3.748	4.102	0.31	7.55
745	4.242	4.333	3.755	4.110	0.31	7.56
746	4.250	4.343	3.762	4.118	0.31	7.58
747	4.258	4.353	3.769	4.127	0.31	7.59
748	4.266	4.363	3.776	4.135	0.31	7.61
749	4.275	4.372	3.783	4.143	0.32	7.62
750	4.283	4.382	3.790	4.152	0.32	7.64
751	4.291	4.392	3.797	4.160	0.32	7.65
752	4.300	4.401	3.804	4.168	0.32	7.67
753	4.308	4.411	3.811	4.177	0.32	7.68
754	4.316	4.421	3.818	4.185	0.32	7.70
755	4.325	4.432	3.825	4.194	0.32	7.73
756	4.333	4.442	3.832	4.202	0.33	7.74
757	4.342	4.452	3.839	4.211	0.33	7.76
758	4.350	4.462	3.847	4.220	0.33	7.76
759	4.359	4.472	3.854	4.228	0.33	7.78
760	4.367	4.482	3.861	4.237	0.33	7.80
761	4.376	4.492	3.868	4.245	0.33	7.82
762	4.385	4.503	3.876	4.255	0.33	7.83
763	4.394	4.513	3.883	4.263	0.33	7.85
764	4.402	4.523	3.890	4.272	0.34	7.87
765	4.411	4.533	3.898	4.281	0.34	7.87
766	4.420	4.544	3.905	4.290	0.34	7.90
767	4.429	4.555	3.913	4.299	0.34	7.91
768	4.438	4.566	3.920	4.308	0.34	7.94
769	4.447	4.576	3.927	4.317	0.34	7.96
770	4.456	4.587	3.935	4.326	0.34	7.97
771	4.465	4.598	3.942	4.335	0.35	8.00
772	4.474	4.609	3.950	4.344	0.35	8.01
773	4.483	4.620	3.958	4.354	0.35	8.03
774	4.493	4.631	3.965	4.363	0.35	8.06
775	4.501	4.642	3.973	4.372	0.35	8.07
776	4.510	4.653	3.980	4.381	0.35	8.09
777	4.520	4.665	3.988	4.391	0.36	8.12

778	4.529	4.676	3.996	4.400	0.36	8.13
779	4.538	4.687	4.003	4.409	0.36	8.16
780	4.548	4.698	4.011	4.419	0.36	8.17
781	4.557	4.710	4.019	4.429	0.36	8.20
782	4.567	4.721	4.027	4.438	0.36	8.21
783	4.576	4.733	4.034	4.448	0.37	8.25
784	4.586	4.745	4.042	4.458	0.37	8.27
785	4.595	4.756	4.050	4.467	0.37	8.28
786	4.605	4.768	4.058	4.477	0.37	8.31
787	4.615	4.779	4.065	4.486	0.37	8.34
788	4.624	4.791	4.073	4.496	0.38	8.36
789	4.634	4.803	4.081	4.506	0.38	8.38
790	4.644	4.815	4.090	4.516	0.38	8.39
791	4.654	4.827	4.098	4.526	0.38	8.42
792	4.664	4.839	4.106	4.536	0.38	8.44
793	4.674	4.851	4.114	4.546	0.38	8.46
794	4.684	4.864	4.122	4.557	0.39	8.49
795	4.694	4.876	4.130	4.567	0.39	8.52
796	4.704	4.888	4.139	4.577	0.39	8.53
797	4.714	4.901	4.147	4.587	0.39	8.56
798	4.724	4.914	4.155	4.598	0.39	8.59
799	4.735	4.926	4.163	4.608	0.40	8.62
800	4.745	4.939	4.172	4.619	0.40	8.63
801	4.755	4.952	4.180	4.629	0.40	8.67
802	4.766	4.965	4.188	4.640	0.40	8.70
803	4.776	4.977	4.197	4.650	0.40	8.71
804	4.786	4.990	4.206	4.661	0.41	8.73
805	4.797	5.004	4.214	4.672	0.41	8.77

GA Mix 1

Cycles (N)	**Permanent Strain for Replicate Sample**			**Statistic**		
	15036-L-C1	15036-L-C2	15036-L-C5	Mean (%)	Stdev (%)	CoV (%)
1	0	0	0	0.00	0.00	0.00
2	0.161	0.151	0.158	0.16	0.01	3.28

3	0.238	0.23	0.228	0.23	0.01	2.28
4	0.289	0.284	0.273	0.28	0.01	2.90
5	0.33	0.325	0.307	0.32	0.01	3.77
6	0.365	0.359	0.335	0.35	0.02	4.50
7	0.396	0.388	0.36	0.38	0.02	4.96
8	0.424	0.414	0.381	0.41	0.02	5.54
9	0.45	0.436	0.4	0.43	0.03	6.02
10	0.474	0.457	0.418	0.45	0.03	6.38
11	0.498	0.476	0.434	0.47	0.03	6.93
12	0.521	0.494	0.449	0.49	0.04	7.45
13	0.544	0.51	0.463	0.51	0.04	8.04
14	0.566	0.524	0.476	0.52	0.05	8.63
15	0.59	0.539	0.489	0.54	0.05	9.36
16	0.614	0.552	0.501	0.56	0.06	10.18
17	0.638	0.565	0.513	0.57	0.06	10.98
18	0.665	0.577	0.523	0.59	0.07	12.18
19	0.692	0.588	0.534	0.60	0.08	13.28
20	0.722	0.599	0.544	0.62	0.09	14.66
21	0.755	0.61	0.553	0.64	0.10	16.29
22	0.792	0.62	0.563	0.66	0.12	18.11
23	0.836	0.63	0.572	0.68	0.14	20.42
24	0.889	0.64	0.581	0.70	0.16	23.24
25	0.94	0.649	0.589	0.73	0.19	25.86
26	0.978	0.658	0.598	0.74	0.20	27.43
27	1.006	0.666	0.606	0.76	0.22	28.41
28	1.029	0.675	0.613	0.77	0.22	29.06
29	1.048	0.683	0.621	0.78	0.23	29.43
30	1.064	0.691	0.628	0.79	0.24	29.67
31	1.077	0.698	0.636	0.80	0.24	29.71
32	1.089	0.706	0.643	0.81	0.24	29.70
33	1.101	0.713	0.649	0.82	0.24	29.79
34	1.112	0.721	0.656	0.83	0.25	29.73
35	1.123	0.728	0.663	0.84	0.25	29.71
36	1.133	0.734	0.669	0.85	0.25	29.72

37	1.142	0.741	0.676	0.85	0.25	29.59
38	1.151	0.748	0.682	0.86	0.25	29.51
39	1.16	0.754	0.688	0.87	0.26	29.47
40	1.168	0.76	0.694	0.87	0.26	29.38
41	1.176	0.767	0.7	0.88	0.26	29.25
42	1.184	0.772	0.706	0.89	0.26	29.19
43	1.191	0.778	0.711	0.89	0.26	29.10
44	1.199	0.784	0.717	0.90	0.26	29.01
45	1.206	0.79	0.722	0.91	0.26	28.92
46	1.213	0.795	0.727	0.91	0.26	28.87
47	1.219	0.801	0.733	0.92	0.26	28.68
48	1.226	0.806	0.738	0.92	0.26	28.63
49	1.232	0.812	0.743	0.93	0.26	28.49
50	1.239	0.817	0.748	0.93	0.27	28.44
51	1.245	0.822	0.753	0.94	0.27	28.34
52	1.251	0.827	0.758	0.95	0.27	28.24
53	1.257	0.832	0.763	0.95	0.27	28.14
54	1.262	0.838	0.768	0.96	0.27	27.96
55	1.268	0.842	0.773	0.96	0.27	27.90
56	1.274	0.847	0.778	0.97	0.27	27.80
57	1.279	0.852	0.782	0.97	0.27	27.71
58	1.284	0.856	0.787	0.98	0.27	27.60
59	1.289	0.861	0.792	0.98	0.27	27.46
60	1.295	0.865	0.796	0.99	0.27	27.44
61	1.3	0.87	0.801	0.99	0.27	27.30
62	1.305	0.875	0.805	1.00	0.27	27.21
63	1.309	0.879	0.809	1.00	0.27	27.10
64	1.314	0.883	0.814	1.00	0.27	27.00
65	1.319	0.888	0.818	1.01	0.27	26.91
66	1.324	0.892	0.822	1.01	0.27	26.85
67	1.328	0.896	0.826	1.02	0.27	26.74
68	1.333	0.901	0.831	1.02	0.27	26.61
69	1.337	0.905	0.835	1.03	0.27	26.51
70	1.342	0.909	0.839	1.03	0.27	26.45

71	1.346	0.913	0.843	1.03	0.27	26.35
72	1.35	0.917	0.847	1.04	0.27	26.25
73	1.355	0.921	0.851	1.04	0.27	26.19
74	1.359	0.925	0.855	1.05	0.27	26.09
75	1.363	0.929	0.859	1.05	0.27	25.99
76	1.367	0.933	0.863	1.05	0.27	25.90
77	1.372	0.937	0.866	1.06	0.27	25.89
78	1.376	0.941	0.87	1.06	0.27	25.79
79	1.38	0.944	0.874	1.07	0.27	25.72
80	1.384	0.948	0.878	1.07	0.27	25.62
81	1.388	0.952	0.882	1.07	0.27	25.53
82	1.392	0.956	0.885	1.08	0.27	25.47
83	1.396	0.959	0.889	1.08	0.27	25.41
84	1.4	0.963	0.893	1.09	0.27	25.31
85	1.404	0.967	0.896	1.09	0.28	25.26
86	1.408	0.97	0.9	1.09	0.28	25.20
87	1.411	0.974	0.903	1.10	0.28	25.10
88	1.415	0.977	0.907	1.10	0.28	25.04
89	1.419	0.981	0.91	1.10	0.28	24.99
90	1.423	0.984	0.914	1.11	0.28	24.92
91	1.427	0.988	0.917	1.11	0.28	24.87
92	1.43	0.991	0.921	1.11	0.28	24.77
93	1.434	0.995	0.924	1.12	0.28	24.72
94	1.438	0.998	0.928	1.12	0.28	24.66
95	1.441	1.001	0.931	1.12	0.28	24.59
96	1.445	1.005	0.934	1.13	0.28	24.54
97	1.448	1.008	0.938	1.13	0.28	24.44
98	1.452	1.011	0.941	1.13	0.28	24.42
99	1.455	1.015	0.944	1.14	0.28	24.32
100	1.459	1.018	0.948	1.14	0.28	24.27
101	1.462	1.021	0.951	1.14	0.28	24.20
102	1.466	1.024	0.954	1.15	0.28	24.18
103	1.469	1.028	0.958	1.15	0.28	24.06
104	1.473	1.031	0.961	1.16	0.28	24.04

105	1.475	1.034	0.964	1.16	0.28	23.93
106	1.479	1.037	0.967	1.16	0.28	23.91
107	1.483	1.04	0.971	1.16	0.28	23.86
108	1.486	1.043	0.974	1.17	0.28	23.79
109	1.489	1.047	0.977	1.17	0.28	23.71
110	1.492	1.05	0.98	1.17	0.28	23.65
111	1.496	1.052	0.983	1.18	0.28	23.65
112	1.499	1.056	0.987	1.18	0.28	23.53
113	1.502	1.059	0.99	1.18	0.28	23.47
114	1.506	1.062	0.993	1.19	0.28	23.45
115	1.509	1.065	0.996	1.19	0.28	23.40
116	1.511	1.068	0.999	1.19	0.28	23.30
117	1.515	1.071	1.002	1.20	0.28	23.28
118	1.518	1.073	1.005	1.20	0.28	23.25
119	1.521	1.076	1.008	1.20	0.28	23.19
120	1.524	1.079	1.011	1.20	0.28	23.13
121	1.527	1.082	1.014	1.21	0.28	23.07
122	1.53	1.085	1.017	1.21	0.28	23.01
123	1.533	1.088	1.021	1.21	0.28	22.92
124	1.536	1.091	1.024	1.22	0.28	22.87
125	1.539	1.094	1.027	1.22	0.28	22.81
126	1.543	1.096	1.03	1.22	0.28	22.82
127	1.545	1.099	1.033	1.23	0.28	22.72
128	1.548	1.102	1.036	1.23	0.28	22.67
129	1.552	1.105	1.038	1.23	0.28	22.69
130	1.554	1.107	1.042	1.23	0.28	22.58
131	1.557	1.11	1.044	1.24	0.28	22.56
132	1.56	1.113	1.047	1.24	0.28	22.51
133	1.563	1.116	1.05	1.24	0.28	22.45
134	1.566	1.118	1.053	1.25	0.28	22.42
135	1.569	1.121	1.056	1.25	0.28	22.37
136	1.572	1.124	1.059	1.25	0.28	22.32
137	1.575	1.127	1.062	1.25	0.28	22.26
138	1.578	1.129	1.065	1.26	0.28	22.23

139	1.581	1.132	1.068	1.26	0.28	22.18
140	1.584	1.135	1.071	1.26	0.28	22.13
141	1.587	1.137	1.073	1.27	0.28	22.13
142	1.59	1.14	1.076	1.27	0.28	22.08
143	1.592	1.142	1.079	1.27	0.28	22.01
144	1.595	1.145	1.082	1.27	0.28	21.96
145	1.598	1.147	1.085	1.28	0.28	21.93
146	1.601	1.15	1.088	1.28	0.28	21.88
147	1.604	1.153	1.09	1.28	0.28	21.86
148	1.607	1.155	1.093	1.29	0.28	21.83
149	1.609	1.158	1.096	1.29	0.28	21.75
150	1.612	1.16	1.099	1.29	0.28	21.72
151	1.615	1.163	1.102	1.29	0.28	21.67
152	1.618	1.166	1.105	1.30	0.28	21.62
153	1.621	1.168	1.108	1.30	0.28	21.59
154	1.624	1.17	1.11	1.30	0.28	21.60
155	1.626	1.173	1.113	1.30	0.28	21.51
156	1.629	1.176	1.116	1.31	0.28	21.46
157	1.632	1.178	1.119	1.31	0.28	21.43
158	1.635	1.181	1.122	1.31	0.28	21.38
159	1.638	1.183	1.124	1.32	0.28	21.39
160	1.64	1.186	1.127	1.32	0.28	21.30
161	1.643	1.188	1.13	1.32	0.28	21.28
162	1.646	1.191	1.132	1.32	0.28	21.26
163	1.649	1.193	1.135	1.33	0.28	21.24
164	1.651	1.196	1.138	1.33	0.28	21.15
165	1.654	1.198	1.141	1.33	0.28	21.13
166	1.657	1.2	1.143	1.33	0.28	21.13
167	1.659	1.203	1.146	1.34	0.28	21.05
168	1.662	1.205	1.149	1.34	0.28	21.02
169	1.665	1.208	1.151	1.34	0.28	21.01
170	1.668	1.21	1.154	1.34	0.28	20.98
171	1.67	1.212	1.157	1.35	0.28	20.92
172	1.673	1.215	1.159	1.35	0.28	20.90

173	1.675	1.218	1.162	1.35	0.28	20.82
174	1.678	1.22	1.165	1.35	0.28	20.80
175	1.681	1.222	1.167	1.36	0.28	20.80
176	1.683	1.225	1.17	1.36	0.28	20.72
177	1.686	1.227	1.173	1.36	0.28	20.70
178	1.688	1.229	1.176	1.36	0.28	20.64
179	1.691	1.231	1.178	1.37	0.28	20.64
180	1.694	1.234	1.181	1.37	0.28	20.60
181	1.697	1.237	1.184	1.37	0.28	20.55
182	1.699	1.239	1.186	1.37	0.28	20.52
183	1.702	1.241	1.189	1.38	0.28	20.50
184	1.704	1.244	1.192	1.38	0.28	20.42
185	1.707	1.246	1.194	1.38	0.28	20.43
186	1.71	1.248	1.197	1.39	0.28	20.41
187	1.712	1.25	1.2	1.39	0.28	20.35
188	1.715	1.253	1.202	1.39	0.28	20.33
189	1.717	1.255	1.205	1.39	0.28	20.27
190	1.72	1.258	1.207	1.40	0.28	20.26
191	1.723	1.26	1.21	1.40	0.28	20.24
192	1.725	1.262	1.213	1.40	0.28	20.18
193	1.728	1.264	1.215	1.40	0.28	20.19
194	1.73	1.266	1.218	1.40	0.28	20.13
195	1.733	1.269	1.221	1.41	0.28	20.09
196	1.735	1.271	1.223	1.41	0.28	20.06
197	1.738	1.274	1.226	1.41	0.28	20.02
198	1.741	1.276	1.229	1.42	0.28	20.00
199	1.743	1.278	1.231	1.42	0.28	19.97
200	1.746	1.28	1.234	1.42	0.28	19.95
201	1.748	1.283	1.236	1.42	0.28	19.90
202	1.751	1.284	1.239	1.42	0.28	19.90
203	1.753	1.287	1.241	1.43	0.28	19.85
204	1.756	1.289	1.244	1.43	0.28	19.83
205	1.758	1.291	1.247	1.43	0.28	19.78
206	1.76	1.294	1.249	1.43	0.28	19.73

207	1.763	1.296	1.252	1.44	0.28	19.71
208	1.765	1.298	1.255	1.44	0.28	19.65
209	1.768	1.3	1.257	1.44	0.28	19.66
210	1.77	1.302	1.26	1.44	0.28	19.61
211	1.773	1.305	1.262	1.45	0.28	19.59
212	1.776	1.307	1.265	1.45	0.28	19.57
213	1.778	1.309	1.268	1.45	0.28	19.52
214	1.781	1.311	1.27	1.45	0.28	19.53
215	1.783	1.314	1.273	1.46	0.28	19.45
216	1.786	1.316	1.275	1.46	0.28	19.46
217	1.788	1.318	1.278	1.46	0.28	19.41
218	1.791	1.32	1.28	1.46	0.28	19.42
219	1.793	1.323	1.283	1.47	0.28	19.34
220	1.795	1.325	1.285	1.47	0.28	19.31
221	1.798	1.327	1.288	1.47	0.28	19.30
222	1.8	1.329	1.29	1.47	0.28	19.27
223	1.803	1.331	1.293	1.48	0.28	19.25
224	1.805	1.333	1.296	1.48	0.28	19.20
225	1.808	1.336	1.298	1.48	0.28	19.19
226	1.81	1.338	1.301	1.48	0.28	19.14
227	1.812	1.34	1.303	1.49	0.28	19.11
228	1.815	1.342	1.306	1.49	0.28	19.09
229	1.818	1.344	1.309	1.49	0.28	19.08
230	1.82	1.346	1.311	1.49	0.28	19.05
231	1.823	1.348	1.314	1.50	0.28	19.03
232	1.825	1.351	1.317	1.50	0.28	18.96
233	1.828	1.353	1.319	1.50	0.28	18.97
234	1.83	1.355	1.321	1.50	0.28	18.95
235	1.833	1.357	1.324	1.50	0.28	18.93
236	1.835	1.359	1.326	1.51	0.28	18.90
237	1.837	1.361	1.329	1.51	0.28	18.85
238	1.84	1.363	1.331	1.51	0.29	18.86
239	1.842	1.365	1.334	1.51	0.28	18.81
240	1.845	1.368	1.336	1.52	0.29	18.80

241	1.847	1.37	1.339	1.52	0.28	18.75
242	1.85	1.372	1.341	1.52	0.29	18.76
243	1.852	1.374	1.344	1.52	0.29	18.71
244	1.855	1.376	1.347	1.53	0.29	18.70
245	1.857	1.378	1.349	1.53	0.29	18.67
246	1.859	1.38	1.352	1.53	0.28	18.62
247	1.862	1.383	1.354	1.53	0.29	18.61
248	1.864	1.385	1.356	1.54	0.29	18.59
249	1.867	1.387	1.359	1.54	0.29	18.57
250	1.869	1.389	1.362	1.54	0.29	18.52
251	1.872	1.391	1.364	1.54	0.29	18.53
252	1.874	1.393	1.367	1.54	0.29	18.48
253	1.876	1.395	1.369	1.55	0.29	18.46
254	1.879	1.397	1.372	1.55	0.29	18.44
255	1.881	1.399	1.374	1.55	0.29	18.42
256	1.884	1.401	1.377	1.55	0.29	18.41
257	1.886	1.404	1.379	1.56	0.29	18.36
258	1.889	1.405	1.382	1.56	0.29	18.37
259	1.891	1.408	1.384	1.56	0.29	18.32
260	1.893	1.41	1.387	1.56	0.29	18.28
261	1.896	1.412	1.389	1.57	0.29	18.29
262	1.899	1.414	1.392	1.57	0.29	18.27
263	1.901	1.416	1.395	1.57	0.29	18.23
264	1.903	1.418	1.397	1.57	0.29	18.20
265	1.905	1.42	1.399	1.57	0.29	18.18
266	1.908	1.422	1.402	1.58	0.29	18.17
267	1.911	1.424	1.404	1.58	0.29	18.18
268	1.913	1.426	1.407	1.58	0.29	18.13
269	1.915	1.428	1.409	1.58	0.29	18.11
270	1.918	1.43	1.412	1.59	0.29	18.09
271	1.92	1.432	1.415	1.59	0.29	18.05
272	1.923	1.434	1.417	1.59	0.29	18.06
273	1.925	1.436	1.419	1.59	0.29	18.03
274	1.927	1.439	1.422	1.60	0.29	17.97

275	1.93	1.441	1.425	1.60	0.29	17.96
276	1.932	1.442	1.427	1.60	0.29	17.95
277	1.935	1.444	1.429	1.60	0.29	17.96
278	1.937	1.447	1.432	1.61	0.29	17.90
279	1.939	1.449	1.435	1.61	0.29	17.85
280	1.942	1.451	1.437	1.61	0.29	17.86
281	1.945	1.452	1.439	1.61	0.29	17.89
282	1.946	1.455	1.442	1.61	0.29	17.80
283	1.949	1.457	1.444	1.62	0.29	17.81
284	1.952	1.459	1.447	1.62	0.29	17.79
285	1.954	1.46	1.449	1.62	0.29	17.79
286	1.956	1.463	1.452	1.62	0.29	17.73
287	1.959	1.465	1.454	1.63	0.29	17.74
288	1.961	1.466	1.457	1.63	0.29	17.72
289	1.963	1.468	1.459	1.63	0.29	17.69
290	1.966	1.47	1.462	1.63	0.29	17.68
291	1.968	1.472	1.464	1.63	0.29	17.66
292	1.971	1.475	1.467	1.64	0.29	17.63
293	1.973	1.477	1.469	1.64	0.29	17.61
294	1.975	1.479	1.472	1.64	0.29	17.56
295	1.978	1.481	1.474	1.64	0.29	17.57
296	1.981	1.483	1.477	1.65	0.29	17.56
297	1.983	1.485	1.479	1.65	0.29	17.54
298	1.985	1.487	1.482	1.65	0.29	17.50
299	1.988	1.489	1.484	1.65	0.29	17.51
300	1.99	1.491	1.487	1.66	0.29	17.47
301	1.992	1.493	1.489	1.66	0.29	17.45
302	1.995	1.494	1.491	1.66	0.29	17.48
303	1.997	1.496	1.494	1.66	0.29	17.44
304	1.999	1.499	1.497	1.67	0.29	17.37
305	2.001	1.501	1.499	1.67	0.29	17.35
306	2.004	1.503	1.502	1.67	0.29	17.34
307	2.007	1.505	1.504	1.67	0.29	17.35
308	2.009	1.507	1.507	1.67	0.29	17.31

309	2.011	1.509	1.509	1.68	0.29	17.29
310	2.014	1.511	1.512	1.68	0.29	17.28
311	2.016	1.513	1.514	1.68	0.29	17.26
312	2.018	1.515	1.517	1.68	0.29	17.22
313	2.021	1.517	1.519	1.69	0.29	17.23
314	2.023	1.519	1.522	1.69	0.29	17.19
315	2.025	1.521	1.524	1.69	0.29	17.17
316	2.028	1.523	1.527	1.69	0.29	17.16
317	2.03	1.525	1.529	1.69	0.29	17.14
318	2.033	1.527	1.532	1.70	0.29	17.13
319	2.035	1.529	1.534	1.70	0.29	17.11
320	2.037	1.531	1.537	1.70	0.29	17.07
321	2.039	1.533	1.539	1.70	0.29	17.05
322	2.042	1.535	1.542	1.71	0.29	17.04
323	2.044	1.537	1.544	1.71	0.29	17.02
324	2.046	1.539	1.547	1.71	0.29	16.98
325	2.049	1.541	1.549	1.71	0.29	16.99
326	2.051	1.543	1.552	1.72	0.29	16.95
327	2.054	1.545	1.554	1.72	0.29	16.96
328	2.056	1.547	1.557	1.72	0.29	16.92
329	2.059	1.549	1.559	1.72	0.29	16.93
330	2.061	1.55	1.561	1.72	0.29	16.93
331	2.063	1.553	1.564	1.73	0.29	16.87
332	2.065	1.555	1.566	1.73	0.29	16.85
333	2.068	1.557	1.569	1.73	0.29	16.84
334	2.07	1.559	1.571	1.73	0.29	16.82
335	2.073	1.561	1.574	1.74	0.29	16.82
336	2.075	1.562	1.576	1.74	0.29	16.82
337	2.077	1.565	1.579	1.74	0.29	16.76
338	2.079	1.566	1.581	1.74	0.29	16.76
339	2.082	1.568	1.584	1.74	0.29	16.75
340	2.084	1.571	1.586	1.75	0.29	16.71
341	2.086	1.572	1.589	1.75	0.29	16.69
342	2.089	1.575	1.591	1.75	0.29	16.68

343	2.091	1.576	1.594	1.75	0.29	16.67
344	2.094	1.579	1.596	1.76	0.29	16.66
345	2.096	1.581	1.599	1.76	0.29	16.62
346	2.098	1.582	1.601	1.76	0.29	16.62
347	2.101	1.584	1.604	1.76	0.29	16.61
348	2.103	1.586	1.606	1.77	0.29	16.59
349	2.105	1.588	1.609	1.77	0.29	16.56
350	2.108	1.59	1.611	1.77	0.29	16.57
351	2.11	1.592	1.614	1.77	0.29	16.53
352	2.113	1.594	1.616	1.77	0.29	16.54
353	2.115	1.596	1.619	1.78	0.29	16.50
354	2.117	1.598	1.621	1.78	0.29	16.49
355	2.119	1.6	1.624	1.78	0.29	16.45
356	2.122	1.602	1.626	1.78	0.29	16.46
357	2.124	1.604	1.629	1.79	0.29	16.42
358	2.127	1.606	1.631	1.79	0.29	16.43
359	2.13	1.608	1.634	1.79	0.29	16.43
360	2.132	1.61	1.637	1.79	0.29	16.39
361	2.134	1.612	1.639	1.80	0.29	16.37
362	2.137	1.614	1.641	1.80	0.29	16.38
363	2.139	1.616	1.644	1.80	0.29	16.35
364	2.141	1.618	1.646	1.80	0.29	16.33
365	2.144	1.62	1.649	1.80	0.29	16.32
366	2.146	1.622	1.652	1.81	0.29	16.29
367	2.149	1.624	1.654	1.81	0.29	16.30
368	2.151	1.626	1.657	1.81	0.29	16.26
369	2.153	1.628	1.659	1.81	0.29	16.24
370	2.156	1.63	1.662	1.82	0.29	16.24
371	2.158	1.632	1.665	1.82	0.29	16.20
372	2.161	1.634	1.667	1.82	0.30	16.21
373	2.163	1.636	1.67	1.82	0.29	16.18
374	2.166	1.638	1.672	1.83	0.30	16.19
375	2.168	1.64	1.674	1.83	0.30	16.17
376	2.171	1.641	1.677	1.83	0.30	16.19

377	2.173	1.643	1.68	1.83	0.30	16.15
378	2.175	1.645	1.683	1.83	0.30	16.12
379	2.178	1.647	1.685	1.84	0.30	16.13
380	2.18	1.649	1.688	1.84	0.30	16.09
381	2.183	1.651	1.69	1.84	0.30	16.10
382	2.185	1.653	1.692	1.84	0.30	16.09
383	2.187	1.655	1.695	1.85	0.30	16.05
384	2.19	1.657	1.698	1.85	0.30	16.05
385	2.192	1.659	1.701	1.85	0.30	16.01
386	2.195	1.661	1.703	1.85	0.30	16.02
387	2.197	1.663	1.706	1.86	0.30	15.99
388	2.2	1.665	1.708	1.86	0.30	16.00
389	2.202	1.667	1.711	1.86	0.30	15.97
390	2.204	1.669	1.714	1.86	0.30	15.93
391	2.207	1.671	1.716	1.86	0.30	15.95
392	2.209	1.673	1.719	1.87	0.30	15.91
393	2.212	1.675	1.721	1.87	0.30	15.92
394	2.214	1.677	1.724	1.87	0.30	15.89
395	2.217	1.679	1.726	1.87	0.30	15.90
396	2.219	1.681	1.729	1.88	0.30	15.87
397	2.221	1.683	1.732	1.88	0.30	15.83
398	2.224	1.685	1.734	1.88	0.30	15.85
399	2.226	1.687	1.737	1.88	0.30	15.81
400	2.229	1.689	1.739	1.89	0.30	15.82
401	2.231	1.691	1.742	1.89	0.30	15.79
402	2.234	1.693	1.745	1.89	0.30	15.79
403	2.236	1.695	1.748	1.89	0.30	15.75
404	2.238	1.697	1.75	1.90	0.30	15.74
405	2.241	1.699	1.753	1.90	0.30	15.73
406	2.243	1.701	1.755	1.90	0.30	15.72
407	2.246	1.702	1.758	1.90	0.30	15.73
408	2.248	1.704	1.761	1.90	0.30	15.70
409	2.251	1.706	1.763	1.91	0.30	15.71
410	2.253	1.708	1.766	1.91	0.30	15.68

411	2.256	1.71	1.768	1.91	0.30	15.69
412	2.258	1.712	1.771	1.91	0.30	15.66
413	2.261	1.714	1.774	1.92	0.30	15.65
414	2.263	1.716	1.777	1.92	0.30	15.62
415	2.265	1.718	1.779	1.92	0.30	15.61
416	2.268	1.72	1.782	1.92	0.30	15.60
417	2.27	1.722	1.784	1.93	0.30	15.59
418	2.273	1.724	1.787	1.93	0.30	15.58
419	2.275	1.726	1.789	1.93	0.30	15.57
420	2.278	1.728	1.792	1.93	0.30	15.56
421	2.28	1.73	1.795	1.94	0.30	15.53
422	2.283	1.732	1.798	1.94	0.30	15.53
423	2.285	1.734	1.801	1.94	0.30	15.50
424	2.288	1.736	1.803	1.94	0.30	15.51
425	2.29	1.738	1.806	1.94	0.30	15.48
426	2.293	1.74	1.808	1.95	0.30	15.49
427	2.295	1.742	1.811	1.95	0.30	15.46
428	2.298	1.744	1.814	1.95	0.30	15.46
429	2.3	1.746	1.817	1.95	0.30	15.42
430	2.303	1.748	1.82	1.96	0.30	15.42
431	2.305	1.75	1.822	1.96	0.30	15.41
432	2.308	1.752	1.825	1.96	0.30	15.40
433	2.31	1.754	1.827	1.96	0.30	15.39
434	2.313	1.756	1.831	1.97	0.30	15.37
435	2.315	1.758	1.833	1.97	0.30	15.35
436	2.318	1.76	1.836	1.97	0.30	15.35
437	2.32	1.762	1.838	1.97	0.30	15.34
438	2.322	1.764	1.841	1.98	0.30	15.31
439	2.325	1.766	1.844	1.98	0.30	15.30
440	2.327	1.768	1.846	1.98	0.30	15.29
441	2.329	1.77	1.849	1.98	0.30	15.26
442	2.332	1.771	1.851	1.98	0.30	15.29
443	2.335	1.774	1.854	1.99	0.30	15.27
444	2.337	1.776	1.857	1.99	0.30	15.24

445	2.339	1.778	1.86	1.99	0.30	15.21
446	2.342	1.78	1.862	1.99	0.30	15.22
447	2.345	1.782	1.865	2.00	0.30	15.22
448	2.347	1.784	1.868	2.00	0.30	15.19
449	2.35	1.786	1.871	2.00	0.30	15.19
450	2.352	1.788	1.874	2.00	0.30	15.16
451	2.354	1.79	1.876	2.01	0.30	15.14
452	2.357	1.792	1.879	2.01	0.30	15.14
453	2.36	1.794	1.882	2.01	0.30	15.14
454	2.362	1.796	1.885	2.01	0.30	15.11
455	2.365	1.798	1.887	2.02	0.30	15.12
456	2.367	1.8	1.89	2.02	0.30	15.09
457	2.369	1.802	1.893	2.02	0.30	15.06
458	2.372	1.804	1.895	2.02	0.31	15.08
459	2.374	1.806	1.898	2.03	0.30	15.05
460	2.377	1.808	1.901	2.03	0.31	15.05
461	2.379	1.81	1.904	2.03	0.31	15.02
462	2.382	1.812	1.907	2.03	0.31	15.02
463	2.385	1.814	1.91	2.04	0.31	15.01
464	2.387	1.817	1.912	2.04	0.31	14.98
465	2.39	1.819	1.915	2.04	0.31	14.98
466	2.392	1.821	1.918	2.04	0.31	14.95
467	2.395	1.823	1.921	2.05	0.31	14.95
468	2.397	1.824	1.924	2.05	0.31	14.94
469	2.4	1.827	1.927	2.05	0.31	14.92
470	2.403	1.829	1.929	2.05	0.31	14.93
471	2.405	1.831	1.932	2.06	0.31	14.90
472	2.407	1.833	1.935	2.06	0.31	14.88
473	2.41	1.835	1.938	2.06	0.31	14.88
474	2.413	1.837	1.941	2.06	0.31	14.87
475	2.415	1.839	1.944	2.07	0.31	14.85
476	2.418	1.841	1.947	2.07	0.31	14.85
477	2.421	1.843	1.949	2.07	0.31	14.86
478	2.423	1.845	1.953	2.07	0.31	14.82

479	2.425	1.847	1.955	2.08	0.31	14.81
480	2.428	1.849	1.958	2.08	0.31	14.80
481	2.431	1.851	1.961	2.08	0.31	14.80
482	2.433	1.853	1.964	2.08	0.31	14.78
483	2.436	1.855	1.967	2.09	0.31	14.78
484	2.439	1.858	1.97	2.09	0.31	14.76
485	2.441	1.86	1.973	2.09	0.31	14.73
486	2.444	1.862	1.975	2.09	0.31	14.74
487	2.446	1.864	1.979	2.10	0.31	14.70
488	2.449	1.866	1.982	2.10	0.31	14.70
489	2.452	1.868	1.984	2.10	0.31	14.71
490	2.454	1.87	1.987	2.10	0.31	14.69
491	2.457	1.872	1.99	2.11	0.31	14.69
492	2.459	1.874	1.993	2.11	0.31	14.66
493	2.462	1.876	1.996	2.11	0.31	14.66
494	2.465	1.878	1.999	2.11	0.31	14.66
495	2.467	1.88	2.002	2.12	0.31	14.64
496	2.47	1.882	2.005	2.12	0.31	14.64
497	2.472	1.884	2.008	2.12	0.31	14.61
498	2.475	1.886	2.011	2.12	0.31	14.61
499	2.478	1.889	2.014	2.13	0.31	14.59
500	2.48	1.891	2.017	2.13	0.31	14.57
501	2.483	1.893	2.02	2.13	0.31	14.57
502	2.486	1.895	2.023	2.13	0.31	14.57
503	2.488	1.897	2.026	2.14	0.31	14.54
504	2.491	1.899	2.029	2.14	0.31	14.54
505	2.494	1.901	2.032	2.14	0.31	14.54
506	2.496	1.903	2.035	2.14	0.31	14.52
507	2.499	1.905	2.038	2.15	0.31	14.52
508	2.502	1.907	2.041	2.15	0.31	14.52
509	2.504	1.91	2.044	2.15	0.31	14.47
510	2.507	1.911	2.047	2.16	0.31	14.49
511	2.51	1.913	2.05	2.16	0.31	14.49
512	2.512	1.916	2.053	2.16	0.31	14.45

513	2.515	1.918	2.057	2.16	0.31	14.44
514	2.518	1.92	2.06	2.17	0.31	14.44
515	2.521	1.922	2.062	2.17	0.31	14.45
516	2.523	1.924	2.066	2.17	0.31	14.42
517	2.526	1.926	2.069	2.17	0.31	14.42
518	2.528	1.928	2.072	2.18	0.31	14.39
519	2.531	1.931	2.075	2.18	0.31	14.37
520	2.533	1.933	2.078	2.18	0.31	14.35
521	2.536	1.935	2.081	2.18	0.31	14.35
522	2.539	1.937	2.084	2.19	0.31	14.35
523	2.542	1.939	2.087	2.19	0.31	14.35
524	2.545	1.941	2.09	2.19	0.31	14.35
525	2.547	1.943	2.094	2.19	0.31	14.32
526	2.55	1.945	2.097	2.20	0.31	14.32
527	2.552	1.947	2.1	2.20	0.31	14.30
528	2.555	1.95	2.103	2.20	0.31	14.28
529	2.558	1.952	2.106	2.21	0.31	14.28
530	2.561	1.954	2.109	2.21	0.32	14.28
531	2.563	1.956	2.113	2.21	0.32	14.25
532	2.566	1.958	2.116	2.21	0.32	14.25
533	2.569	1.96	2.119	2.22	0.32	14.25
534	2.571	1.963	2.122	2.22	0.32	14.21
535	2.574	1.964	2.125	2.22	0.32	14.23
536	2.577	1.967	2.128	2.22	0.32	14.21
537	2.58	1.969	2.131	2.23	0.32	14.22
538	2.583	1.971	2.134	2.23	0.32	14.22
539	2.585	1.973	2.138	2.23	0.32	14.19
540	2.588	1.976	2.141	2.24	0.32	14.17
541	2.591	1.978	2.144	2.24	0.32	14.17
542	2.593	1.98	2.147	2.24	0.32	14.15
543	2.596	1.982	2.15	2.24	0.32	14.15
544	2.599	1.984	2.154	2.25	0.32	14.14
545	2.602	1.986	2.157	2.25	0.32	14.14
546	2.604	1.988	2.161	2.25	0.32	14.11

547	2.607	1.99	2.164	2.25	0.32	14.12
548	2.61	1.992	2.167	2.26	0.32	14.12
549	2.612	1.994	2.17	2.26	0.32	14.10
550	2.615	1.997	2.173	2.26	0.32	14.08
551	2.618	1.999	2.177	2.26	0.32	14.07
552	2.621	2.001	2.179	2.27	0.32	14.08
553	2.623	2.003	2.183	2.27	0.32	14.05
554	2.627	2.005	2.186	2.27	0.32	14.08
555	2.629	2.007	2.19	2.28	0.32	14.05
556	2.632	2.01	2.193	2.28	0.32	14.03
557	2.635	2.012	2.196	2.28	0.32	14.03
558	2.638	2.014	2.199	2.28	0.32	14.03
559	2.64	2.016	2.203	2.29	0.32	14.01
560	2.643	2.018	2.206	2.29	0.32	14.01
561	2.646	2.02	2.209	2.29	0.32	14.01
562	2.649	2.023	2.213	2.30	0.32	13.98
563	2.652	2.024	2.216	2.30	0.32	14.01
564	2.654	2.026	2.22	2.30	0.32	13.98
565	2.657	2.029	2.223	2.30	0.32	13.96
566	2.66	2.031	2.226	2.31	0.32	13.96
567	2.663	2.033	2.229	2.31	0.32	13.97
568	2.665	2.035	2.233	2.31	0.32	13.94
569	2.668	2.037	2.236	2.31	0.32	13.94
570	2.671	2.04	2.239	2.32	0.32	13.92
571	2.674	2.042	2.243	2.32	0.32	13.92
572	2.677	2.044	2.246	2.32	0.32	13.92
573	2.68	2.046	2.25	2.33	0.32	13.92
574	2.682	2.049	2.253	2.33	0.32	13.88
575	2.686	2.051	2.257	2.33	0.32	13.90
576	2.688	2.053	2.26	2.33	0.32	13.88
577	2.691	2.055	2.263	2.34	0.32	13.88
578	2.694	2.058	2.267	2.34	0.32	13.86
579	2.697	2.06	2.27	2.34	0.32	13.86
580	2.7	2.062	2.274	2.35	0.32	13.85

581	2.703	2.064	2.278	2.35	0.33	13.85
582	2.706	2.066	2.281	2.35	0.33	13.85
583	2.708	2.069	2.284	2.35	0.33	13.81
584	2.711	2.071	2.288	2.36	0.33	13.81
585	2.714	2.073	2.291	2.36	0.33	13.81
586	2.717	2.075	2.295	2.36	0.33	13.81
587	2.72	2.078	2.298	2.37	0.33	13.79
588	2.723	2.08	2.302	2.37	0.33	13.79
589	2.726	2.082	2.305	2.37	0.33	13.79
590	2.729	2.085	2.309	2.37	0.33	13.77
591	2.732	2.087	2.313	2.38	0.33	13.77
592	2.735	2.089	2.316	2.38	0.33	13.77
593	2.738	2.091	2.32	2.38	0.33	13.77
594	2.741	2.094	2.323	2.39	0.33	13.75
595	2.744	2.096	2.327	2.39	0.33	13.75
596	2.747	2.098	2.331	2.39	0.33	13.74
597	2.75	2.101	2.334	2.40	0.33	13.73
598	2.753	2.103	2.338	2.40	0.33	13.73
599	2.756	2.105	2.341	2.40	0.33	13.73
600	2.759	2.107	2.345	2.40	0.33	13.73
601	2.762	2.11	2.348	2.41	0.33	13.71
602	2.764	2.112	2.352	2.41	0.33	13.69
603	2.768	2.114	2.356	2.41	0.33	13.71
604	2.771	2.117	2.36	2.42	0.33	13.68
605	2.774	2.119	2.363	2.42	0.33	13.69
606	2.777	2.121	2.367	2.42	0.33	13.68
607	2.78	2.124	2.371	2.43	0.33	13.66
608	2.783	2.126	2.374	2.43	0.33	13.67
609	2.786	2.128	2.378	2.43	0.33	13.66
610	2.789	2.13	2.382	2.43	0.33	13.66
611	2.792	2.133	2.386	2.44	0.33	13.64
612	2.795	2.135	2.389	2.44	0.33	13.65
613	2.798	2.137	2.393	2.44	0.33	13.64
614	2.801	2.139	2.397	2.45	0.33	13.64

615	2.804	2.142	2.401	2.45	0.33	13.62
616	2.807	2.144	2.404	2.45	0.33	13.63
617	2.81	2.147	2.408	2.46	0.33	13.60
618	2.813	2.149	2.411	2.46	0.33	13.61
619	2.816	2.151	2.415	2.46	0.33	13.61
620	2.819	2.154	2.419	2.46	0.33	13.59
621	2.822	2.156	2.423	2.47	0.34	13.59
622	2.825	2.158	2.426	2.47	0.34	13.59
623	2.828	2.161	2.43	2.47	0.34	13.57
624	2.831	2.163	2.434	2.48	0.34	13.57
625	2.834	2.166	2.438	2.48	0.34	13.55
626	2.837	2.168	2.442	2.48	0.34	13.55
627	2.841	2.17	2.445	2.49	0.34	13.57
628	2.844	2.172	2.449	2.49	0.34	13.57
629	2.847	2.175	2.453	2.49	0.34	13.55
630	2.85	2.177	2.457	2.49	0.34	13.55
631	2.853	2.18	2.461	2.50	0.34	13.53
632	2.856	2.182	2.464	2.50	0.34	13.54
633	2.86	2.184	2.469	2.50	0.34	13.55
634	2.862	2.187	2.473	2.51	0.34	13.51
635	2.866	2.189	2.476	2.51	0.34	13.54
636	2.869	2.192	2.48	2.51	0.34	13.52
637	2.872	2.194	2.484	2.52	0.34	13.52
638	2.875	2.196	2.488	2.52	0.34	13.52
639	2.878	2.199	2.492	2.52	0.34	13.50
640	2.881	2.201	2.496	2.53	0.34	13.50
641	2.884	2.204	2.500	2.53	0.34	13.48
642	2.888	2.206	2.504	2.53	0.34	13.50
643	2.89	2.208	2.508	2.54	0.34	13.48
644	2.894	2.211	2.512	2.54	0.34	13.48
645	2.897	2.213	2.516	2.54	0.34	13.48
646	2.9	2.216	2.520	2.55	0.34	13.46
647	2.903	2.218	2.524	2.55	0.34	13.47
648	2.906	2.221	2.528	2.55	0.34	13.45

649	2.91	2.223	2.532	2.56	0.34	13.47
650	2.913	2.225	2.536	2.56	0.34	13.47
651	2.916	2.228	2.540	2.56	0.34	13.45
652	2.919	2.23	2.544	2.56	0.34	13.45
653	2.922	2.233	2.548	2.57	0.34	13.43
654	2.925	2.235	2.552	2.57	0.35	13.44
655	2.929	2.237	2.556	2.57	0.35	13.46
656	2.932	2.24	2.561	2.58	0.35	13.43
657	2.935	2.243	2.564	2.58	0.35	13.42
658	2.938	2.245	2.569	2.58	0.35	13.42
659	2.941	2.247	2.573	2.59	0.35	13.42
660	2.944	2.25	2.577	2.59	0.35	13.40
661	2.948	2.253	2.581	2.59	0.35	13.40
662	2.951	2.255	2.585	2.60	0.35	13.41
663	2.954	2.257	2.590	2.60	0.35	13.41
664	2.957	2.26	2.594	2.60	0.35	13.39
665	2.961	2.262	2.598	2.61	0.35	13.41
666	2.965	2.265	2.602	2.61	0.35	13.41
667	2.967	2.267	2.607	2.61	0.35	13.39
668	2.971	2.269	2.610	2.62	0.35	13.42
669	2.974	2.272	2.615	2.62	0.35	13.40
670	2.977	2.274	2.619	2.62	0.35	13.40
671	2.981	2.277	2.623	2.63	0.35	13.40
672	2.984	2.279	2.628	2.63	0.35	13.40
673	2.988	2.282	2.632	2.63	0.35	13.40
674	2.991	2.284	2.637	2.64	0.35	13.40
675	2.994	2.287	2.641	2.64	0.35	13.39
676	2.997	2.289	2.645	2.64	0.35	13.39
677	3.001	2.291	2.650	2.65	0.36	13.41
678	3.004	2.294	2.654	2.65	0.36	13.39
679	3.007	2.297	2.658	2.65	0.36	13.38
680	3.011	2.299	2.663	2.66	0.36	13.40
681	3.014	2.302	2.667	2.66	0.36	13.38
682	3.018	2.304	2.671	2.66	0.36	13.40

683	3.021	2.307	2.676	2.67	0.36	13.38
684	3.024	2.309	2.68	2.67	0.36	13.39
685	3.028	2.312	2.685	2.68	0.36	13.39
686	3.031	2.314	2.689	2.68	0.36	13.39
687	3.035	2.317	2.693	2.68	0.36	13.39
688	3.038	2.319	2.698	2.69	0.36	13.40
689	3.041	2.322	2.702	2.69	0.36	13.38
690	3.045	2.324	2.707	2.69	0.36	13.40
691	3.048	2.327	2.711	2.70	0.36	13.38
692	3.052	2.329	2.716	2.70	0.36	13.40
693	3.055	2.332	2.72	2.70	0.36	13.39
694	3.059	2.334	2.725	2.71	0.36	13.41
695	3.062	2.337	2.729	2.71	0.36	13.39
696	3.066	2.34	2.734	2.71	0.36	13.39
697	3.069	2.342	2.739	2.72	0.36	13.40
698	3.072	2.345	2.743	2.72	0.36	13.38
699	3.076	2.347	2.747	2.72	0.37	13.41
700	3.079	2.35	2.752	2.73	0.37	13.39
701	3.083	2.353	2.757	2.73	0.37	13.39
702	3.087	2.355	2.762	2.73	0.37	13.41
703	3.09	2.358	2.766	2.74	0.37	13.40
704	3.094	2.361	2.771	2.74	0.37	13.40
705	3.097	2.363	2.775	2.75	0.37	13.40
706	3.101	2.366	2.78	2.75	0.37	13.40
707	3.104	2.368	2.785	2.75	0.37	13.41
708	3.108	2.371	2.79	2.76	0.37	13.41
709	3.111	2.374	2.795	2.76	0.37	13.40
710	3.115	2.376	2.8	2.76	0.37	13.42
711	3.118	2.379	2.804	2.77	0.37	13.40
712	3.122	2.382	2.809	2.77	0.37	13.41
713	3.126	2.384	2.814	2.77	0.37	13.43
714	3.129	2.387	2.819	2.78	0.37	13.41
715	3.133	2.39	2.823	2.78	0.37	13.41
716	3.137	2.393	2.829	2.79	0.37	13.42

717	3.14	2.395	2.833	2.79	0.37	13.42
718	3.144	2.398	2.838	2.79	0.38	13.42
719	3.147	2.401	2.843	2.80	0.38	13.41
720	3.151	2.403	2.848	2.80	0.38	13.43
721	3.155	2.406	2.853	2.80	0.38	13.44
722	3.158	2.409	2.858	2.81	0.38	13.42
723	3.162	2.412	2.863	2.81	0.38	13.43
724	3.166	2.414	2.868	2.82	0.38	13.45
725	3.169	2.417	2.873	2.82	0.38	13.44
726	3.173	2.419	2.877	2.82	0.38	13.46
727	3.176	2.422	2.883	2.83	0.38	13.45
728	3.18	2.425	2.888	2.83	0.38	13.45
729	3.184	2.428	2.893	2.84	0.38	13.45
730	3.187	2.43	2.898	2.84	0.38	13.46
731	3.191	2.433	2.903	2.84	0.38	13.46
732	3.195	2.436	2.908	2.85	0.38	13.46
733	3.198	2.438	2.913	2.85	0.38	13.47
734	3.202	2.441	2.918	2.85	0.38	13.48
735	3.206	2.444	2.923	2.86	0.39	13.48
736	3.21	2.447	2.928	2.86	0.39	13.48
737	3.214	2.449	2.934	2.87	0.39	13.51
738	3.217	2.452	2.939	2.87	0.39	13.50
739	3.221	2.455	2.944	2.87	0.39	13.50
740	3.224	2.458	2.949	2.88	0.39	13.49
741	3.228	2.461	2.954	2.88	0.39	13.49
742	3.232	2.464	2.959	2.89	0.39	13.49
743	3.236	2.466	2.965	2.89	0.39	13.52
744	3.24	2.469	2.97	2.89	0.39	13.52
745	3.243	2.472	2.975	2.90	0.39	13.51
746	3.247	2.475	2.98	2.90	0.39	13.52
747	3.251	2.477	2.985	2.90	0.39	13.54
748	3.255	2.48	2.991	2.91	0.39	13.55
749	3.259	2.483	2.996	2.91	0.39	13.55
750	3.262	2.486	3.001	2.92	0.39	13.54

751	3.267	2.489	3.007	2.92	0.40	13.56
752	3.271	2.492	3.012	2.93	0.40	13.56
753	3.274	2.494	3.018	2.93	0.40	13.58
754	3.278	2.497	3.023	2.93	0.40	13.58
755	3.282	2.5	3.028	2.94	0.40	13.58
756	3.286	2.503	3.034	2.94	0.40	13.59
757	3.29	2.506	3.039	2.95	0.40	13.59
758	3.294	2.508	3.045	2.95	0.40	13.62
759	3.298	2.512	3.051	2.95	0.40	13.61
760	3.302	2.514	3.056	2.96	0.40	13.63
761	3.305	2.517	3.062	2.96	0.40	13.63
762	3.31	2.52	3.067	2.97	0.40	13.64
763	3.314	2.523	3.073	2.97	0.41	13.65
764	3.318	2.526	3.079	2.97	0.41	13.66
765	3.321	2.529	3.084	2.98	0.41	13.65
766	3.326	2.532	3.09	2.98	0.41	13.67
767	3.329	2.535	3.096	2.99	0.41	13.67
768	3.333	2.537	3.102	2.99	0.41	13.69
769	3.337	2.54	3.107	2.99	0.41	13.70
770	3.341	2.543	3.113	3.00	0.41	13.71
771	3.346	2.546	3.119	3.00	0.41	13.73
772	3.35	2.549	3.125	3.01	0.41	13.73
773	3.353	2.552	3.13	3.01	0.41	13.73
774	3.357	2.554	3.136	3.02	0.41	13.75
775	3.361	2.557	3.142	3.02	0.42	13.76
776	3.365	2.56	3.148	3.02	0.42	13.77
777	3.369	2.563	3.154	3.03	0.42	13.78
778	3.374	2.566	3.16	3.03	0.42	13.80
779	3.378	2.569	3.166	3.04	0.42	13.81
780	3.382	2.572	3.172	3.04	0.42	13.82
781	3.386	2.575	3.178	3.05	0.42	13.83
782	3.39	2.578	3.184	3.05	0.42	13.84
783	3.394	2.581	3.19	3.06	0.42	13.85
784	3.398	2.584	3.196	3.06	0.42	13.85

785	3.402	2.587	3.203	3.06	0.42	13.87
786	3.407	2.59	3.209	3.07	0.43	13.89
787	3.41	2.593	3.215	3.07	0.43	13.89
788	3.415	2.595	3.221	3.08	0.43	13.93
789	3.419	2.598	3.227	3.08	0.43	13.94
790	3.423	2.601	3.233	3.09	0.43	13.95
791	3.427	2.604	3.24	3.09	0.43	13.96
792	3.432	2.607	3.246	3.10	0.43	13.98
793	3.436	2.61	3.252	3.10	0.43	13.99
794	3.44	2.613	3.258	3.10	0.43	14.00
795	3.444	2.616	3.264	3.11	0.44	14.01
796	3.448	2.619	3.271	3.11	0.44	14.03
797	3.453	2.623	3.277	3.12	0.44	14.03
798	3.457	2.625	3.283	3.12	0.44	14.06
799	3.461	2.629	3.29	3.13	0.44	14.05
800	3.465	2.632	3.296	3.13	0.44	14.06
801	3.469	2.634	3.303	3.14	0.44	14.10
802	3.473	2.638	3.308	3.14	0.44	14.08
803	3.478	2.641	3.315	3.14	0.44	14.11
804	3.482	2.644	3.322	3.15	0.44	14.13
805	3.486	2.647	3.328	3.15	0.45	14.14
806	3.491	2.65	3.335	3.16	0.45	14.16
807	3.495	2.653	3.341	3.16	0.45	14.17
808	3.499	2.656	3.348	3.17	0.45	14.19
809	3.504	2.659	3.355	3.17	0.45	14.22
810	3.507	2.662	3.361	3.18	0.45	14.22
811	3.512	2.665	3.368	3.18	0.45	14.24
812	3.516	2.668	3.375	3.19	0.45	14.26
813	3.521	2.672	3.382	3.19	0.46	14.27
814	3.525	2.675	3.388	3.20	0.46	14.28
815	3.529	2.678	3.395	3.20	0.46	14.30
816	3.534	2.681	3.402	3.21	0.46	14.32
817	3.538	2.684	3.409	3.21	0.46	14.34
818	3.543	2.687	3.416	3.22	0.46	14.37

819	3.547	2.691	3.423	3.22	0.46	14.36
820	3.551	2.694	3.43	3.23	0.46	14.38
821	3.556	2.697	3.437	3.23	0.47	14.41
822	3.561	2.7	3.444	3.24	0.47	14.44
823	3.565	2.703	3.451	3.24	0.47	14.45
824	3.569	2.706	3.459	3.24	0.47	14.48
825	3.574	2.709	3.466	3.25	0.47	14.50
826	3.578	2.713	3.473	3.25	0.47	14.50
827	3.583	2.716	3.48	3.26	0.47	14.53
828	3.587	2.719	3.488	3.26	0.48	14.55
829	3.592	2.722	3.495	3.27	0.48	14.58
830	3.596	2.725	3.502	3.27	0.48	14.60
831	3.601	2.729	3.509	3.28	0.48	14.61
832	3.605	2.732	3.517	3.28	0.48	14.63
833	3.61	2.735	3.524	3.29	0.48	14.66
834	3.614	2.738	3.531	3.29	0.48	14.68
835	3.619	2.741	3.539	3.30	0.49	14.71
836	3.624	2.745	3.546	3.31	0.49	14.72
837	3.628	2.748	3.554	3.31	0.49	14.75
838	3.633	2.751	3.561	3.32	0.49	14.77
839	3.638	2.755	3.569	3.32	0.49	14.79
840	3.642	2.758	3.577	3.33	0.49	14.81
841	3.647	2.761	3.584	3.33	0.49	14.84
842	3.652	2.765	3.592	3.34	0.50	14.86
843	3.657	2.768	3.6	3.34	0.50	14.89
844	3.661	2.771	3.608	3.35	0.50	14.92
845	3.666	2.774	3.616	3.35	0.50	14.95
846	3.671	2.778	3.624	3.36	0.50	14.97
847	3.676	2.781	3.631	3.36	0.50	15.00
848	3.68	2.784	3.64	3.37	0.51	15.03
849	3.685	2.788	3.647	3.37	0.51	15.04
850	3.69	2.791	3.656	3.38	0.51	15.08
851	3.694	2.795	3.664	3.38	0.51	15.09
852	3.699	2.798	3.672	3.39	0.51	15.12

853	3.704	2.801	3.68	3.40	0.51	15.16
854	3.709	2.805	3.688	3.40	0.52	15.17
855	3.714	2.808	3.696	3.41	0.52	15.21
856	3.719	2.812	3.705	3.41	0.52	15.23
857	3.724	2.815	3.713	3.42	0.52	15.27
858	3.729	2.818	3.721	3.42	0.52	15.30
859	3.734	2.822	3.73	3.43	0.53	15.32
860	3.739	2.825	3.738	3.43	0.53	15.36
861	3.743	2.829	3.747	3.44	0.53	15.38
862	3.748	2.832	3.755	3.45	0.53	15.41
863	3.753	2.835	3.764	3.45	0.53	15.45
864	3.758	2.838	3.772	3.46	0.54	15.49
865	3.763	2.842	3.781	3.46	0.54	15.51
866	3.768	2.845	3.789	3.47	0.54	15.55
867	3.773	2.849	3.798	3.47	0.54	15.57
868	3.778	2.852	3.807	3.48	0.54	15.61
869	3.783	2.856	3.815	3.48	0.54	15.63
870	3.788	2.859	3.824	3.49	0.55	15.67
871	3.793	2.863	3.833	3.50	0.55	15.70
872	3.799	2.866	3.842	3.50	0.55	15.75
873	3.804	2.87	3.85	3.51	0.55	15.76
874	3.809	2.873	3.86	3.51	0.56	15.81
875	3.814	2.877	3.869	3.52	0.56	15.84
876	3.819	2.88	3.878	3.53	0.56	15.88
877	3.824	2.883	3.887	3.53	0.56	15.92
878	3.829	2.887	3.896	3.54	0.56	15.95
879	3.835	2.89	3.905	3.54	0.57	16.00
880	3.84	2.894	3.914	3.55	0.57	16.02
881	3.845	2.898	3.924	3.56	0.57	16.06
882	3.85	2.901	3.933	3.56	0.57	16.10
883	3.855	2.905	3.942	3.57	0.58	16.13
884	3.861	2.908	3.952	3.57	0.58	16.18
885	3.866	2.912	3.961	3.58	0.58	16.21
886	3.872	2.916	3.971	3.59	0.58	16.25

887	3.877	2.919	3.98	3.59	0.59	16.29
888	3.882	2.923	3.99	3.60	0.59	16.32
889	3.888	2.926	3.999	3.60	0.59	16.37
890	3.893	2.93	4.009	3.61	0.59	16.40
891	3.898	2.934	4.019	3.62	0.59	16.44
892	3.904	2.937	4.029	3.62	0.60	16.49
893	3.909	2.941	4.039	3.63	0.60	16.53
894	3.915	2.945	4.049	3.64	0.60	16.57
895	3.92	2.949	4.058	3.64	0.60	16.59
896	3.926	2.952	4.068	3.65	0.61	16.65
897	3.931	2.956	4.078	3.66	0.61	16.68
898	3.937	2.96	4.088	3.66	0.61	16.72
899	3.942	2.963	4.098	3.67	0.62	16.77
900	3.948	2.967	4.108	3.67	0.62	16.81
901	3.953	2.97	4.118	3.68	0.62	16.86
902	3.959	2.974	4.129	3.69	0.62	16.91
903	3.964	2.978	4.139	3.69	0.63	16.95
904	3.97	2.982	4.149	3.70	0.63	16.98
905	3.976	2.986	4.16	3.71	0.63	17.03
906	3.98	2.989	4.17	3.71	0.63	17.08
907	3.986	2.993	4.181	3.72	0.64	17.13
908	3.992	2.997	4.191	3.73	0.64	17.17
909	3.997	3.001	4.202	3.73	0.64	17.21
910	4.003	3.004	4.213	3.74	0.65	17.27
911	4.009	3.008	4.224	3.75	0.65	17.32
912	4.014	3.012	4.235	3.75	0.65	17.36
913	4.02	3.016	4.245	3.76	0.65	17.40
914	4.026	3.02	4.256	3.77	0.66	17.45
915	4.031	3.024	4.267	3.77	0.66	17.49
916	4.037	3.027	4.278	3.78	0.66	17.56
917	4.042	3.031	4.29	3.79	0.67	17.61
918	4.048	3.035	4.3	3.79	0.67	17.65
919	4.054	3.039	4.312	3.80	0.67	17.70
920	4.06	3.043	4.323	3.81	0.68	17.75

921	4.066	3.047	4.334	3.82	0.68	17.80
922	4.071	3.051	4.345	3.82	0.68	17.84
923	4.077	3.055	4.356	3.83	0.68	17.89
924	4.083	3.059	4.368	3.84	0.69	17.94
925	4.089	3.063	4.38	3.84	0.69	18.00
926	4.095	3.066	4.391	3.85	0.70	18.06
927	4.101	3.071	4.403	3.86	0.70	18.10
928	4.107	3.074	4.414	3.87	0.70	18.16
929	4.113	3.079	4.426	3.87	0.70	18.20
930	4.119	3.083	4.438	3.88	0.71	18.26
931	4.125	3.086	4.45	3.89	0.71	18.33
932	4.131	3.091	4.462	3.89	0.72	18.37
933	4.137	3.095	4.474	3.90	0.72	18.42
934	4.143	3.099	4.487	3.91	0.72	18.49
935	4.149	3.103	4.499	3.92	0.73	18.54
936	4.156	3.107	4.511	3.92	0.73	18.60
937	4.162	3.111	4.524	3.93	0.73	18.66
938	4.168	3.115	4.537	3.94	0.74	18.73
939	4.174	3.119	4.549	3.95	0.74	18.78
940	4.18	3.123	4.562	3.96	0.75	18.85
941	4.187	3.127	4.574	3.96	0.75	18.90
942	4.193	3.131	4.587	3.97	0.75	18.97
943	4.199	3.135	4.6	3.98	0.76	19.03
944	4.205	3.139	4.613	3.99	0.76	19.10
945	4.212	3.143	4.625	3.99	0.76	19.15
946	4.218	3.148	4.638	4.00	0.77	19.20
947	4.224	3.152	4.651	4.01	0.77	19.26
948	4.231	3.156	4.664	4.02	0.78	19.33
949	4.237	3.16	4.677	4.02	0.78	19.39
950	4.243	3.164	4.691	4.03	0.78	19.46
951	4.25	3.168	4.704	4.04	0.79	19.53
952	4.256	3.172	4.718	4.05	0.79	19.60
953	4.262	3.176	4.732	4.06	0.80	19.67
954	4.269	3.181	4.745	4.07	0.80	19.72

955	4.275	3.185	4.759	4.07	0.81	19.79
956	4.282	3.189	4.773	4.08	0.81	19.87
957	4.288	3.193	4.787	4.09	0.82	19.94
958	4.294	3.198	4.801	4.10	0.82	20.00
959	4.301	3.202	4.815	4.11	0.82	20.07
960	4.308	3.206	4.829	4.11	0.83	20.14
961	4.314	3.211	4.843	4.12	0.83	20.20
962	4.321	3.215	4.858	4.13	0.84	20.28
963	4.327	3.219	4.873	4.14	0.84	20.36
964	4.334	3.224	4.887	4.15	0.85	20.42
965	4.341	3.228	4.902	4.16	0.85	20.50
966	4.348	3.232	4.916	4.17	0.86	20.57
967	4.354	3.236	4.931	4.17	0.86	20.65
968	4.361	3.241	4.946	4.18	0.87	20.71
969	4.368	3.245	4.961	4.19	0.87	20.79
970	4.375	3.25	4.976	4.20	0.88	20.86
971	4.382	3.254	4.991	4.21	0.88	20.94
972	4.388	3.259	5.006	4.22	0.89	21.00